ASSESSING SPATIAL AND TEMPORAL IMPACTS OF FOREST MANAGEMENT ON WATER QUALITY

A Dissertation

Presented in Partial Fulfilment of the Requirements for the

Degree of Doctor of Philosophy

with a

Major in Water Resources

in the

College of Graduate Studies

University of Idaho

by

Chinmay Deval

Approved by:

Major Professor: Erin S. Brooks, Ph.D.

Committee Members: Daniel G Strawn, Ph.D.; William J Elliot, Ph.D.;

Mariana Dobre, Ph.D.

Department Administrator: Timothy Link, Ph.D.

May 2022

ABSTRACT

Understanding the nutrient source areas in the forested ecosystems is critical for managing watersheds and protecting downstream water resources. This requires long-term monitoring efforts along with modeling efforts to develop a process-based understanding of the system under different scenarios. Few contemporary models cater to the evaluation of the impacts of various land management strategies and climate scenarios on the water quantity and quality dynamics. Even fewer process-based models serve the outputs in a functional and intuitive format such that it meets the needs of the watershed managers who would want to quickly assess multiple watersheds and management scenarios.

This study: utilizes long term water quality monitoring data to assess the effects of commercial forest management operations on stream water quality; uses laboratory experiments to shed light on the fate and transport of phosphorus in the forest-meadow systems; employs a process-based model to simulate phosphorus transport from a forested watershed and tests its accuracy to model the phosphorus losses; and develops an interactive decision support tool that translates multi-scenario, multi-watershed simulated data from two of the widely used models in the US into information useful for watershed managers. The first study assesses the effect of contemporary forest management activities, including clear-cutting and thinning, on water yield and stream nitrogen and phosphorus (P) dynamics using a quarter-century-long (1992–2016) monitoring data from a paired and nested watershed in the interior Pacific Northwest, US. The study showed that the contemporary forest management activities increased stream nitrate + nitrite ($NO_3 + NO_2$) concentrations and loads following timber harvest activities, but these effects are attenuated due to downstream uptake processes. Interestingly, the $NO_3 + NO_2$ concentration, streamflow, and loads of NO3 + NO2 and orthophosphate (OP) from the undisturbed control watershed also increased. However, these increases were relatively smaller than the harvested watersheds and likely driven by climate variability or subtle forest suc-

cession changes. Furthermore, relative to post-wildfire impacts, these nutrient increases from harvested watersheds are small ($\sim$5 to 20-fold compared to pre-disturbance) and short-lived ($\sim$5 years).

The second study demonstrated that the vertical phosphorus transport through the subsoil in the forest-meadow system soils does occur and it can be significant. However, this pathway is often presumed to be a relatively minor source of phosphorus compared to phosphorus transport through surface runoff and soil erosion. This study showed that phosphorus leaching in the forest-meadow systems of Lake Tahoe Basin does in fact occur and it occurs primarily in organic form. When enriched P source is present leaching from granitic sites is larger than that from andesitic sites and granitic meadows leach the largest amounts of phosphorus. The greatest risk of phosphorus leaching, translocation, and potential loss via subsurface pathways occurs in granitic soils with enriched phosphorus sources. Saturation excess runoff is an important pathway for phosphorus loss from meadow systems as demonstrated by the losses from the exfiltration pathway.

The third study represented one of the first times the WEPP model with water quality algorithms (WEPP-WQ) was tested on forested watersheds. The study demonstrated that the seasonal phosphorus transport from upland sources can be simulated using a process-based watershed model. This study found that the P sorption parameter (PSP), P soil partitioning parameter (PHOSKD), initial labile phosphorus pool in topsoil layer (LabileP), and P uptake distribution parameter (UPB) are some of the relatively important and sensitive parameters for simulating phosphorus loss using the WEPP-WQ model. The relative differences between calibrated values obtained for these parameters in watersheds with differing soil type are well supported by the findings of isotherm experiments in this chapter. Watershed scale modeling study also showed adequate capabilities of the existing phosphorus routines in WEPP to simulate soluble phosphorus losses from the watersheds. While WEPP-WQ does not account for the P contributions associated

with the channel processes, the seasonality and relative trends of particulate phosphorus were correctly predicted. A simple analysis of TP load using a fixed P concentration associated with detached channel sediments, suggested that the absolute magnitude of predicted particulate phosphorus from upland sources is underpredicted by the model. This underprediction may be due to the assumed relative distribution of P in active and stable pools that may not be appropriate for forested soils or due to the underestimation of P enrichment ratio or a combination of both. Further investigation of model structure is needed to identify appropriate soil P pool initialization. Significant development and testing are needed for WEPP-WQ to be fully ready for use. Overall, this study shows that WEPP-WQ, with its current dissolved phosphorus routines, can be an effective, process-based, and yet parsimonious edge-of-the-hillslope effects tool for informing land and water management decisions. Improving the particulate P predictions and making WEPP-WQ a complete water quality prediction tool requires further developments and testing.

In the fourth and final study, a prioritization, interactive visualization, and analysis tool (Pi-VAT) was developed to assist watershed managers with synthesizing multi-scenario, multi-watershed outputs from process-based geospatial models. Pi-VAT was applied to output from multiple watersheds and for multiple management scenarios and treatments from two geospatial models for watershed management: Water Erosion Prediction Project (WEPP) and Soil & Water Assessment Tool (SWAT). This study demonstrated the utility of Pi-VAT to examine simulated hydrologic, sediment, and water quality response at the hillslope/hydrologic response unit (HRU) scale. In a matter of minutes, Pi-VAT can synthesize overwhelming amounts of output from process-based models into information useful for land and water resources managers.

Keywords: *Decision-support, Forest Management, Hydrology, Water Quality, Modeling, WEPP*

Acknowledgements

First of all, I would like to express my deepest gratitude to Dr. Erin S. Brooks for providing me with this research opportunity in his amazing research group at the University of Idaho. My success is due to the Erin's patience, overall support, guidance, and advice. Thank you Erin for pushing me beyond my comfort zone and guiding me along the way in accomplishing my goals.

I am also grateful to my committee members: Dr. Dan G. Strawn, Dr. Mariana Dobre, and Dr. William J. Elliot. Your motivation, insights and perspectives not only steered my research in the right direction but also helped me grow as an individual. Mariana, you are a constant voice of support and encouragement and thank you for always finding time for helping me with my model related queries. Dan thank you for inspiring me to better understand soil chemistry and sharing your expertise. Bill, thanks for sharing your WEPP modeling expertise and guiding me through my research.

Also, thanks to Dr. Anurag Srivastava and Dr. Roger Lew for their guidance with WEPP and WEPPcloud. Thank you to Alex Crump for his patience and guidance as I navigated my experience in the lab.

Thanks to all the the collaborators/co-authors for contributing to my research and inspiring me to improve my work. Thanks to anyone that I may have missed mentioning here but contributed to journey in one or the other way. I am eternally grateful.

Finally, thank you to USDA-NIFA for funding the work in this dissertation.

DEDICATION

This dissertation is dedicated to my friends and family who inspired, encouraged, and supported me during my time at the University of Idaho. Especially my mom (Aboli), brother (Nikhil), sister in law (Kasturi), uncle (Shyam), aunt (Arati) and other amazing people that contributed to this journey.

TABLE OF CONTENTS

List of Tables

LIST OF FIGURES

STATEMENT OF CONTRIBUTION

Chapter 2 and Chapter 5 are based on peer reviewed journal articles that were co-authored by multiple collaborators. The CRediT authorship contribution statement is provide below for both these journal articles.

Chapter 2: C Deval:Methodology,Formal analysis, Visualization, Writing – original draft, Writing – review & editing. Erin S. Brooks: Supervision, Methodology, Writing – review & editing,Resources. J.A.Gravelle: Data curation, Writing – review & editing. T.E.Link: Data curation, Writing – review & editing,Funding acquisition. M.Dobre: Supervision, Writing – review & editing,Funding acquisition. W.J.Elliot: Writing – review & editing

Chapter 5: Chinmay Deval: Conceptualization, Methodology, Software, Formal analysis, Visualization, Writing – original draft, Writing – review & editing, Project administration. Erin S. Brooks: Conceptualization, Methodology, Supervision, Resources, Writing – review & editing. Mariana Dobre: Data curation, Methodology, Supervision, Funding acquisition, Resources, Writing – review & editing. Roger Lew: Data curation, Writing – review & editing. Peter R. Robichaud: Methodology, Supervision, Writing – review & editing. Ames Fowler: Data curation, Writing – review & editing. Jan Boll: Writing – review & editing. Zach M. Easton: Data curation, Writing – review & editing. Amy Collick: Data curation, Writing – review & editing.

CHAPTER 1

Introduction

1.1 Research Context

1.1.1 Nutrient's enrichment of waterbodies –a global challenge

Several prevalent global changes have altered and continue to alter the stocks and flows of biogeochemical elements in the terrestrial and aquatic environments [Teutschbein et al., 2017]. Of these, nutrient enrichment of lakes, reservoirs, rivers, and other water bodies, globally, has drawn particular attention during the last few decades. Mekonnen and Hoekstra [2018] estimated annual anthropogenic P loads to freshwater bodies from both point and nonpoint sources at 1.5 Tg. In the same study, Mekonnen and Hoekstra [2018] also calculated the P-related water pollution level (WPL) metric, defined as the consumed fraction of total waste assimilation capacity of the river basin. The authors found that areas that exceed the river basin's assimilation capacity cover about 38% of the global land area and 37% of the global river discharge. Compared to the pre-industrial levels (12 Mt/yr), the P losses from soils to water have reportedly [Mekonnen and Hoekstra, 2018, Smil, 2000] doubled (27 Mt/yr in the year 2000). Nutrient enrichment is one of the principal causes of impairments in rivers and lakes, and numerous studies report high levels of P as one of the primary causes of impairments of water bodies [Carpenter et al., 1998, Correll, 1998, Kleinman et al., 2011, McDowell et al., 2016, Sharpley et al., 2001]. While P is an indispensable element for primary productivity, excessive amounts in the receiving waters can cause serious problems relating to eutrophication and acidification further threatening the quality of the receiving waters. Increased concentration of phosphorus in the water bodies, can lead to algal bloom and have deleterious effects on the structure and function of the aquatic ecosystem. Impacts of such nutrient enrichment on the water quality of water bodies and the environmental and economic costs have been

widely documented [Antón et al., 2011, Dodds et al., 2009, MacDonald et al., 2016, McDowell et al., 2004, Pretty et al., 2003]. Dodds et al. [2009] estimated potential annual economic losses of approximately $2.2 billion in the U.S. because of the eutrophication of freshwaters. The greatest of these economic losses were associated with the lakefront property value and recreational use of freshwaters.

In the U.S. many streams and water bodies monitored between the period from 1993 to 2003 under the national water quality assessment (NAWQA) program revealed an increasing trend in concentrations of total nitrogen and total phosphorus [Sprague and Lorenz, 2009]. Most of these streams and water bodies were drained by areas dominated by agricultural and urban landscapes [Dubrovsky et al., 2010]. However, Dubrovsky et al. [2010] also acknowledged the evidence of an upward trend in the nutrient concentrations of receiving waters in landscapes covered with significant fractions of forest. Stoddard et al. [2016] embarked on periodic probability surveys of thousands of water bodies across the U.S. and reported increased stream and lake total phosphorus (TP) concentrations at the continental U.S. scale. This study reported 23.8% and 18% decrease in the naturally oligotrophic (TP <0.01 mg/l) stream lengths (between 2004 and 2014) and lakes (between 2007 and 2012), respectively. Interestingly, this pattern of increasing TP concentrations in water bodies was universal in the continental U.S. and was also reported in undeveloped watersheds suggesting factors other than the commonly perceived point and non-point sources must be at the root of this pattern [Stoddard et al., 2016]. For example, in the Lake Coeur d'Alene basin in northern Idaho, where a large fraction of the basin is forested, nutrients are of particular interest to maintain the health of the Lake [Zinsser, 2020]. Compared to 1991–92, Wood and Beckwith [2008] reported statistically significant increases in the total phosphorus concentrations and load in 2004-06 for the streams draining into the Lake Coeur d'Alene. Fernan Lake watershed, which lies in the Lake Coeur d'Alene basin, has also reported algal blooms during late summer and fall.

Total phosphorus concentration reported in Fernan Lake during this time frame was 0.031 mg L^{-1} [Idaho Department of Environmental Quality, 2013]. As such, a significant lack of mechanistic understanding exists about the nutrient variability and transport especially in the relatively undisturbed forested watersheds. This also raises serious questions about the applicability of eco-regional nutrient criteria developed by the US environmental protection agency (EPA) and regional agencies for managing excess nutrient delivery to receiving waters and restoring the health of aquatic ecosystem [Ice and Binkley, 2003].

1.1.2 Nutrient Loading from Forested Landscapes

In addition, an increasing number of studies have demonstrated that the disturbance and forest management practices such as road construction, timber harvest, site preparation, and maintenance can potentially increase the nutrient concentrations in streams draining the area [Anderson and Lockaby, 2011, Gravelle et al., 2009, Kreutzweiser et al., 2008]. Recently, studies have reported elevated nitrogen and phosphorus concentrations of order that exceed the nutrient criteria set by the EPA even in the streams draining the undisturbed forests [Ice and Binkley, 2003, NCASI, 2001]. Such increasing concentrations in the undisturbed watersheds can be partly attributed to the factors like aggressive forest fires suppression strategies which have increased the fire return interval leading to nutrient accumulations. Several studies during the last decade further corroborate this by reporting the elevated nitrogen and phosphorus concentrations in surface runoff and litter inter-flow due to large accumulation of nutrients in the forest litter (O horizon) as a consequence of fire suppression [Miller et al., 2005, 2010, Murphy et al., 2006]. Despite the evidence of increased nutrient loading from minimally disturbed (undeveloped/forest dominated) watersheds, these watersheds are continually perceived as more of a sink than a source of the nutrients. Regardless of the economic and environmental costs that the downstream receiving water bodies might incur, these forest dominated watersheds

attract less attention in terms of nutrient management compared to the agricultural and urban dominated watersheds [Miller et al., 2005, Piatek and Allen, 2001].

Also, it is now becoming widely recognized that the 'do nothing' management strategy will likely have substantially large and long-term consequences on water quantity and quality in an event of a wildfire. Recent studies have reported increased high severity fires in the past few decades with significant post-fire environmental impacts [Schoennagel et al., 2017, Westerling et al., 2006]. Such wildfires alter the soil properties and the hydrologic response of the area by decreasing porosity and infiltration and increasing soil repellency and erosion rates [Certini, 2005, Huffman et al., 2001, Martin and Moody, 2001, Robichaud, 2000] that can lead to potentially large sediment and nutrient loading to the receiving bodies. A recent study suggests that post-fire sediment loads can increase by 1 to 1459 times the unburned conditions Smith et al. [2011]. Similarly, the post-fire nitrogen and phosphorus loads can increase by 3 to 250 and 0.3 to 431 times of unburned conditions, respectively Smith et al. [2011]. This is especially a growing concern for municipalities across the US who are considering strategies to reduce the impact of wildfires on their water supplies Smith et al. [2011], Warziniack and Thompson [2013]. Approximately 80% of the drinking water supply across the US originates from forested areas providing drinking water to more than 68,000 communities [USFS, 2020]. Municipalities are now beginning to weigh the impacts and risks of forest management strategies (e.g., thinning, prescribed burning, etc.) on their water quality and quantity to cataclysmic wildfire events.

In light of these water quality concerns to the water bodies downstream from the forest-dominated watersheds, developing an accurate knowledge about the source areas, fate, and transport of phosphorus is imperative for developing appropriate land and water management strategies. Nutrient generation at the watershed scale is a function of the hydrology of the area and the predominant flow pathway in a landscape can greatly

affect stream nutrient delivery [Green and Wang, 2008]. The hydrology of steep, forested watersheds with highly conductive soils is often dominated by infiltration and subsurface lateral flow whereas the hydrology in flatter, disturbed agricultural dominated landscapes is often dominated by surface runoff leading to erosion. As a result, much of the historic literature and modeling of phosphorus has focused on surface runoff and erosion processes. The exfiltration pathway in landscapes dominated by saturation-excess (variable source area) runoff could be another important mechanism in steep, highly conductive watersheds. A study by Sánchez and Boll [2005] has previously demonstrated the importance of the exfiltration pathway in the release of phosphorus to runoff and interflow. In addition, these unique processes in the hydrological cycle take place at varying spatial and temporal scales (see Figure 1.1). The interaction and feedback among these hydrologic processes at varying spatial and temporal scales eventually combined with the soil and land cover properties lead to an overall integrated nutrient response from the watershed. Representing these flow paths of P adds to the complexity of accounting P and completely changes the understanding of the phosphorus dynamics in a particular area. All these factors together complicate the modeling phosphorus dynamics of the area.

1.2 Problem Statement

Over the years, the understanding of the phosphorus export from land to waterbodies has improved extensively by developing hydrological and nutrient transport models. These models can simulate the phosphorus dynamics at varying degrees of scale and complexities. These complexities are a function of how the model has been structured and parameterized. These models can be categorized as empirical, export coefficient driven, or physically based depending upon the degree of complexity of the model and the level to which the physical processes are incorporated into the model [Beven, 1989, Radcliffe and Cabrera, 2007]. Examples of these models include Hydrologic Simulation Program-Fortran (HSPF)
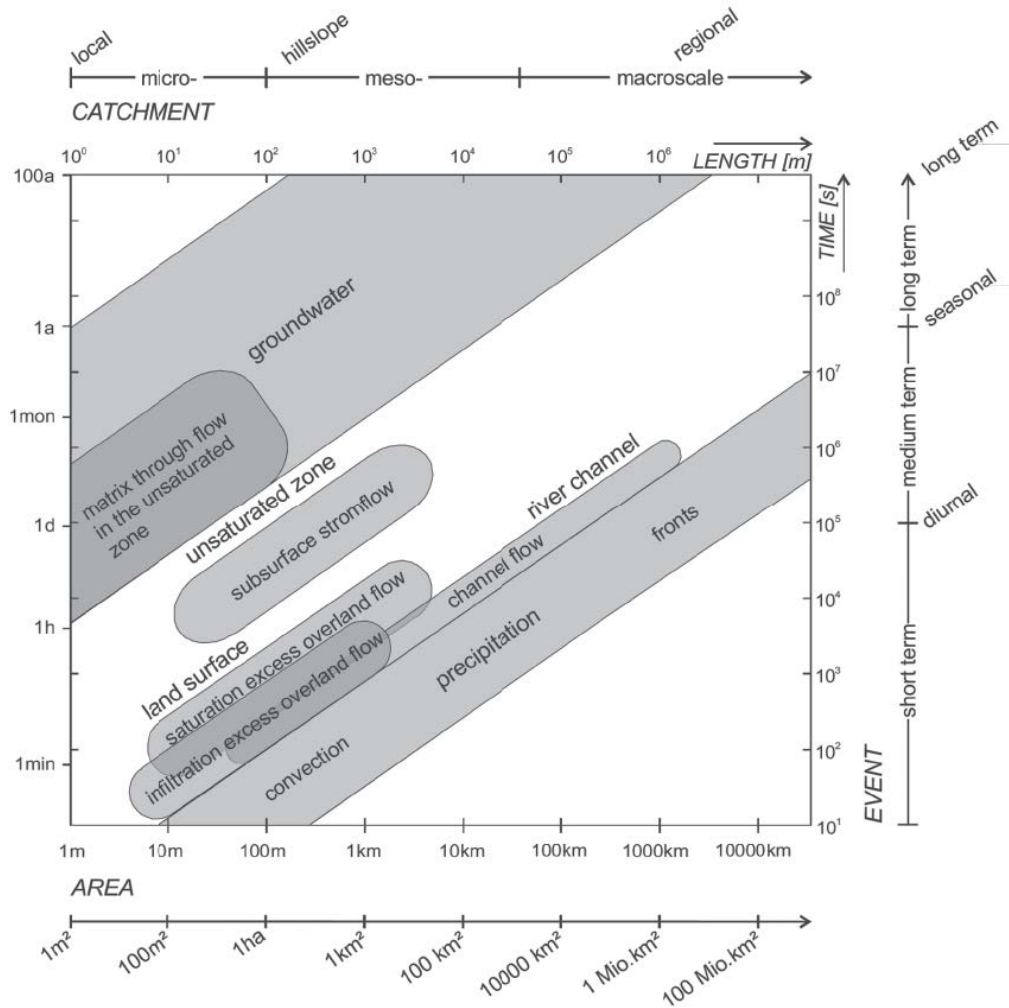
Figure 1.1: The Schematic relationship between spatial and temporal processes for various hydrological processes. Adopted from Bronstert et al., (2005).

[Johanson et al., 1984], Soil and Water Assessment Tool (SWAT) [Neitsch et al., 2011], Annualized Agricultural Non-Point Source (AnnAGNPS) [Young et al., 1989], Generalized Watersheds Loading Functions (GWLF) [Haith and Shoenaker, 1987], Agricultural Policy/Environmental eXtender (APEX) [P. W. Gassman et al., 2010], and Watershed Erosion Prediction Project (WEPP) [Laflen and Forest, 1997] to mention a few.

The field of water quality modeling has progressed substantially over the past few decades. However, several knowledge gaps exist to extend the capabilities and application of water quality models as decision support tools especially in the forest-dominated

watersheds. Although the theoretical mechanisms by which P is transported from land to water bodies is well understood, the insight on the source areas as well as the factors driving the magnitude and variability of phosphorus export from forests to the streams and lakes is limited. Despite the developments in the field of water quality modeling, phosphorus modeling in many of the contemporary models is represented by rudimentary approaches developed in the 1980s [Radcliffe and Cabrera, 2007] and their development tends to stem from agricultural watersheds.

Overland flow and erosion in forest-dominated watersheds are minimal and when present are often related to wildfires [Elliot et al., 2015] and management practices [Binkley and Brown, 1993]. Although in disturbed forests, phosphorus may be transported as soluble reactive P (SRP) in runoff or as particulate P adsorbed to the sediments [Elliot et al., 2015], subsurface lateral flow and base flow are more important flow paths in the undisturbed forest [Srivastava et al., 2013, 2017] and the thick litter layer and soil profile is the major source of P. Studies have shown that a strong linear relationship exists between the soil P and the P in the runoff[Schroeder et al., 2004, Vadas et al., 2005]. A recent study in the forested Sierra Nevada Mountains by Miller et al. [2005] found concentrations of P (as PO_4–P) as high as 24.4 mg/l in the overland/litter interflow. Reducing the P export from land to the streams first requires spatial identification of areas on the landscape that have high P transport potential. Many contemporary models capable of simulating P transport, compute runoff based on the Soil Conservation Services (SCS) curve number (CN) method or Green and Ampt infiltration method (e.g. SWAT, ANSWERS- 2000, Environmental Policy Integrated Climate (EPIC), etc.). Several studies have shown that the saturation excess runoff generation process is a more important mechanism in humid, well-vegetated regions where rainfall intensities seldom exceed infiltration capacity [Beven, 2012, Needelman et al., 2004, Srinivasan et al., 2002]. The spatial and temporal extent of these saturated soils generating runoff is dynamic and a function of soil

properties, topography, and antecedent moisture conditions, therefore termed as variable source area runoff. Incorporating saturation excess runoff in the model and identifying variable source areas is critical for accurate estimation of P export from forest-dominated watersheds. In addition, the knowledge of high concentration P source areas is important for identifying the focus areas for implementing the management practices to minimize the P losses. Schneiderman et al. [2007] in the variable source loading function (VSLF) model modified the GWLF model to explicitly incorporate variable source area hydrology to accurately predict the variable source areas in the landscape. VSLF model, however, retained the SCS curve number-based runoff prediction and export coefficient-based nutrient transport routines from the GWLF model. Easton et al. [2009] argued that estimations based on such routines lack detailed insight on the processes controlling the nutrient export. Also, when the models, using different export coefficients corresponding to the different land uses defined in the model, are calibrated against the observed stream P concentrations the issue of equifinality arises [Beven, 2006, 2012]. It is key to incorporate a more process-driven approach to represent cycling of P within different pools and pathway specific P transport from forest to the streams. These findings spell out a clear need for a process-based P delivery model that more realistically simulates the runoff and erosion generation processes including lateral and base flow components in steep, humid landscapes dominated by variable source area hydrology.

Water Erosion Prediction Project (WEPP) is a process-based hydrology and erosion model that conceptualizes watersheds into a network of hillslopes and channels and has the functionality to simulate surface and subsurface flow paths of water throughout the landscape [Elliot et al., 2015, Srivastava et al., 2013]. Each hillslope can be divided into multiple overland flow elements (OFE) to account for the non-uniformities on a hillslope [Flanagan and Livingston, 1995]. This concept of OFE is similar to the concept of hydrological response units (HRU) used in the SWAT model and each OFE represents a region

on the hillslope with homogeneous soils, cropping, and management. WEPP simulates infiltration using the Green-Ampt infiltration relationship and is also able to compute saturation excess runoff whenever the soil water storage is exceeded [Boll et al., 2015, Dobre et al., 2022, Lew et al., 2022, Saia et al., 2013]. Surface runoff and subsurface lateral flow simulated from each hillslope is routed through the downstream channel network to the watershed outlet [Srivastava et al., 2013]. Recent developments in WEPP included improved algorithms for evapotranspiration, snowmelt, deep percolation, subsurface lateral flow, and channel routing, and have significantly improved the applicability of the WEPP in forestlands. With these model capabilities in combination with the comprehensive soil and climate database, WEPP has all the basic components including the plant growth, senescence, and residue decomposition, necessary to be developed into a P prediction tool and management prioritization tool.

In summary, there is a lack of understanding of phosphorus source areas in the forested ecosystems and few contemporary geospatial models are available to evaluate the impact of various land management strategies on phosphorus dynamics. Some of these aforementioned knowledge gaps and challenges that need to be overcome before such models can reach their full potential include: (i) Better representation of the runoff and erosion generation processes to identify source areas accurately, (ii) Incorporation of different P pathways and physically-based mechanisms by which P mobilizes in soils and is transported out of the watershed, (iii) Incorporation of dissolved P mobilization and export as it relates to shallow subsurface flow and soil chemistry, especially in forested systems and (iv) bridging the gap between the vast information that the process-based water quality models produce and how that is used by land and water managers to inform decisions with regards to the key management questions.

1.3   Research scope and objectives

As identified in the 1.2, there is still a great need for a better understanding of the P sources areas and transport mechanisms in forested watersheds. It is important that this improved understanding is implemented in geospatial water quality models to better assist managers in evaluating impacts of management and climate on P export. This doctoral study, therefore, builds upon the previous modelling efforts but then aims to contribute to the vast research domain of water quality modelling by implementing and validating a process-based P delivery algorithm in forestlands. While large amounts P modelling studies focusing on agriculture dominated watersheds exists, numerous studies as highlighted in section 1.1 have demonstrated increasing P concentrations in water bodies of undeveloped watersheds. Precise identification of the phosphorus source areas and its fate and transport from forested watersheds is therefore imperative. The overall goal of this study is to provide an improved understanding of the source areas and fate and transport of phosphorus in forested watersheds. The main research objectives that will be addressed in the study are listed below:

1. Provide improved understanding of the effects of commercial forest management on nutrient concentration and export dynamics.

   (a) Assess effects of forest management activities on long-term stream nutrient dynamics.

   (b) Quantify the differences between the stream water quality of undisturbed and intensively managed (commercially) forested watershed.

2. Understand the P retention and transport from the volcanic and granitic forest-meadow systems in Lake Tahoe basin.

3. Assess the ability of the WEPP model with process-based P cycling and transport algorithms to simulate the timing of P export from forested watersheds.

4. Develop a post-processing interactive tool for WEPP that can assist land managers identify and characterize pollutant source areas and help managers select, evaluate, and prioritize impacts of management for multiple scenarios and multiple watersheds.

1.4   Outline of the dissertation

This dissertation is organized into six chapters. Chapter 1 is the introduction to the doctoral study that set up the context and provides motivation for the study as well as presents the main goal and specific research objectives. Chapter 2 describes the long-term response in nutrient load from commercial forest management operations in a mountainous watershed. Chapter 3 describes the P retention and transport from forest meadow systems with two different parent materials (volcanic and granitic). Chapter 4 describes the implementation and validation of P algorithm in WEPP and its ability to simulate P export from forested watersheds. Chapter 5 describes the post processing interactive tool developed to support land managers in identifying erosion hotspots in watersheds and planning targeted management. Chapter 6 provides the overall summary of the doctoral dissertation, conclusions, limitations, and future recommendations.

References

C. J. Anderson and B. G. Lockaby. Research gaps related to forest management and stream sediment in the United States. *Environmental Management*, 47(2):303–313, feb 2011. ISSN 0364152X. doi: 10.1007/s00267-010-9604-1. URL `http://link.springer.com/10.1007/s00267-010-9604-1`.

A. Antón, J. Cebrian, K. L. Heck, C. M. Duarte, K. L. Sheehan, M. E. C. Miller, and C. D. Foster. Decoupled effects (positive to negative) of nutrient enrichment on ecosystem services. *Ecological Applications*, 21(3):991–1009, apr 2011. ISSN 10510761. doi: 10.1890/09-0841.1. URL `http://doi.wiley.com/10.1890/09-0841.1`.

K. Beven. Changing ideas in hydrology - The case of physically-based models. *Journal of Hydrology*, 105:157–172, 1989. ISSN 00221694. doi: 10.1016/0022-1694(90)90161-P.

K. Beven. A manifesto for the equifinality thesis. *Journal of Hydrology*, 320(1-2):18–36, 2006. ISSN 00221694. doi: 10.1016/j.jhydrol.2005.07.007.

K. Beven. *Rainfall-Runoff Modelling: The Primer*. John Wiley & Sons, Ltd, Chichester, UK, second edition, jan 2012. ISBN 9781119951001. doi: 10.1002/9781119951001. URL `http://doi.wiley.com/10.1002/9781119951001`.

D. Binkley and T. C. Brown. FOREST PRACTICES AS NONPOINT SOURCES OF POLLUTION IN NORTH AMERICA. *Journal of the American Water Resources Association*, 29(5):729–740, oct 1993. ISSN 17521688. doi: 10.1111/j.1752-1688.1993.tb03233.x. URL `http://doi.wiley.com/10.1111/j.1752-1688.1993.tb03233.x`.

J. Boll, E. S. Brooks, B. Crabtree, S. Dun, and T. S. Steenhuis. Variable Source Area Hydrology Modeling with the Water Erosion Prediction Project Model. *Journal of the American Water Resources Association*, 51(2):330–342, apr 2015. ISSN 1093474X.

doi: 10.1111/1752-1688.12294. URL `http://doi.wiley.com/10.1111/1752-1688.12294http://dx.doi.org/10.1111/1752-1688.12294`.

S. R. Carpenter, V. H. S. N. F. Caraco, D. L. Correll, R. W. Howarth, A. N. Sharpley, N. F. Caracco, D. L. Correll, R. W. Howarth, A. N. Sharpley, and V. H. Smith. Nonpoint pollution of surface waters with phosphorus and nitrogen. *Ecological Applications*, 8(1998):559–568, aug 1998. ISSN 1051-0761. doi: 10.1890/1051-0761(1998)008[0559:NPOSWW]2.0.CO;2. URL `http://onlinelibrary.wiley.com/doi/10.1890/1051-0761(1998)008{\%}5B0559:NPOSWW{\%}5D2.0.CO;2/fullhttp://www.springerlink.com/index/N6N3K6R0163022N1.pdf`.

G. Certini. Effects of fire on properties of forest soils: A review. *Oecologia*, 143(1):1–10, mar 2005. ISSN 00298549. doi: 10.1007/s00442-004-1788-8. URL `https://link.springer.com/article/10.1007/s00442-004-1788-8`.

D. L. Correll. The Role of Phosphorus in the Eutrophication of Receiving Waters: A Review. *Journal of Environment Quality*, 27(2):261, 1998. ISSN 0047-2425. doi: 10.2134/jeq1998.00472425002700020004x. URL `https://www.agronomy.org/publications/jeq/abstracts/27/2/JEQ0270020261`.

M. Dobre, A. Srivastava, R. Lew, C. Deval, E. S. Brooks, W. J. Elliot, and P. Robichaud. WEPPcloud: An online watershed-scale hydrologic modeling tool. Part II. Model performance assessment and applications to forest management and wildfires. *Journal of Hydrology*, (this issue), 2022.

W. K. Dodds, W. W. Bouska, J. L. Eitzmann, T. J. Pilger, K. L. Pitts, A. J. Riley, J. T. Schloesser, and D. J. Thornbrugh. Eutrophication of U. S. freshwaters: Analysis of potential economic damages. *Environmental Science and Technology*, 43(1):12–19, jan 2009. ISSN 0013936X. doi: 10.1021/es801217q.

N. M. Dubrovsky, K. R. Burow, G. M. Clark, J. M. Gronberg, H. P.A., K. J. Hitt, D. K. Mueller, M. D. Munn, B. T. Nolan, L. J. Puckett, M. G. Rupert, T. M. Short, N. E. Spahr, L. A. Sprague, and W. G. Wilber. *The quality of our Nation's waters—Nutrients in the Nation's streams and groundwater, 1992–2004: U.S. Geological Survey Circular 1350.* 2010. ISBN 9781411329041. URL `http://water.usgs.gov/nawqa/nutrients/pubs/circ1350http://pubs.usgs.gov/fs/2010/3078/`.

Z. M. Easton, M. T. Walter, E. M. Schneiderman, M. S. Zion, and T. S. Steenhuis. Including Source-Specific Phosphorus Mobility in a Nonpoint Source Pollution Model for Agricultural Watersheds. *Journal of Environmental Engineering*, 135(1):25–35, jan 2009. ISSN 0733-9372. doi: 10.1061/(ASCE)0733-9372(2009) 135:1(25). URL `http://ascelibrary.org/doi/10.1061/{\%}28ASCE{\%}290733-9372{\%}282009{\%}29135{\%}3A1{\%}2825{\%}29`.

W. Elliot, E. Brooks, D. E. Traeumer, and M. Dobre. Extending WEPP Technology to Predict Fine Sediment and Phosphorus Delivery from Forested Hillslopes. In *SEDHYD 2015 Interagency Conference*, page 12, Reno, NV, 2015. URL `https://www.fs.fed.us/rm/pubs{\_}journals/2015/rmrs{\_}2015{\_}elliot{\_}w002.pdf`.

D. Flanagan and S. Livingston. WEPP Users Guide. Technical report, 1995. URL `https://data.nal.usda.gov/system/files/wepp{\_}usersum.pdf`.

J. A. Gravelle, G. Ice, T. E. Link, and D. L. Cook. Nutrient concentration dynamics in an inland Pacific Northwest watershed before and after timber harvest. *Forest Ecology and Management*, 257(8):1663–1675, 2009. ISSN 03781127. doi: 10.1016/j.foreco.2009. 01.017.

M. B. Green and D. Wang. Watershed flow paths and stream water nitrogen-to-phosphorus ratios under simulated precipitation regimes. *Water Resources Research*,

44(12), dec 2008. ISSN 00431397. doi: 10.1029/2007WR006139. URL `http://doi.wiley.com/10.1029/2007WR006139`.

D. A. Haith and L. L. Shoenaker. GENERALIZED WATERSHED LOADING FUNCTIONS FOR STREAM FLOW NUTRIENTS. *JAWRA Journal of the American Water Resources Association*, 23(3):471–478, jun 1987. ISSN 17521688. doi: 10.1111/j.1752-1688.1987.tb00825.x. URL `http://doi.wiley.com/10.1111/j.1752-1688.1987.tb00825.x`.

E. L. Huffman, L. H. MacDonald, and J. D. Stednick. Strength and persistence of fire-induced soil hydrophobicity under ponderosa and lodgepole pine, Colorado Front Range. *Hydrological Processes*, 15(15):2877–2892, oct 2001. ISSN 08856087. doi: 10.1002/hyp.379. URL `https://onlinelibrary.wiley.com/doi/full/10.1002/hyp.379https://onlinelibrary.wiley.com/doi/abs/10.1002/hyp.379https://onlinelibrary.wiley.com/doi/10.1002/hyp.379`.

G. Ice and D. Binkley. Forest Streamwater Concentrations of Nitrogen and Phosphorus: A Comparison with EPA's Proposed Water Quality Criteria. *Journal of Forestry*, 101(1):21–28, 2003. URL `http://www.ingentaconnect.com/content/saf/jof/2003/00000101/00000001/art00008{\#}`.

Idaho Department of Environmental Quality. Coeur d'Alene Lake and River Subbasin Assessment and Total Maximum Daily Loads 2013. Technical Report October, Idaho Department of Environmental Quality, Coeur d'Alene, 2013.

R. Johanson, J. Imhoff, J. Little, and A. Donigian. Hydrological Simulation Program-Fortran (HSPF): user's manual. Technical report, U.S. Environmental Protection Agency, Athens, GA., 1984.

P. J. A. Kleinman, A. N. Sharpley, R. W. McDowell, D. N. Flaten, A. R. Buda, L. Tao,

L. Bergstrom, and Q. Zhu. Managing agricultural phosphorus for water quality protection: Principles for progress. *Plant and Soil*, 349(1-2):169–182, dec 2011. ISSN 0032079X. doi: 10.1007/s11104-011-0832-9. URL `http://link.springer.com/10.1007/s11104-011-0832-9`.

D. P. Kreutzweiser, P. W. Hazlett, and J. M. Gunn. Logging impacts on the biogeochemistry of boreal forest soils and nutrient export to aquatic systems: A review. *Environmental Reviews*, 16(NA):157–179, dec 2008. ISSN 1208-6053. doi: 10.1139/A08-006. URL `http://www.nrcresearchpress.com/doi/10.1139/A08-006http://www.nrcresearchpress.com/doi/abs/10.1139/A08-006`.

J. M. Laflen and S. Forest. WEPP-Predicting water erosion using a process-based model. *Journal of Soil and Water Conservation*, 52(2):96–102, 1997. URL `http://www.jswconline.org/content/52/2/96.full.pdf+html`.

R. Lew, M. Dobre, A. Srivastava, E. S. Brooks, W. J. Elliot, P. R. Robichaud, and D. C. Flanagan. WEPPcloud: An online watershed-scale hydrologic modeling tool. Part I. Model description. *Journal of Hydrology*, page 127603, feb 2022. ISSN 00221694. doi: 10.1016/j.jhydrol.2022.127603.

G. K. MacDonald, H. P. Jarvie, P. J. A. Withers, D. G. Doody, B. L. Keeler, P. M. Haygarth, L. T. Johnson, R. W. McDowell, M. K. Miyittah, S. M. Powers, A. N. Sharpley, J. Shen, D. R. Smith, M. N. Weintraub, and T. Zhang. Guiding phosphorus stewardship for multiple ecosystem services. *Ecosystem Health and Sustainability*, 2(12):e01251, dec 2016. ISSN 23328878. doi: 10.1002/ehs2.1251. URL `https://www.tandfonline.com/doi/full/10.1002/ehs2.1251http://doi.wiley.com/10.1002/ehs2.1251`.

D. A. Martin and J. A. Moody. Comparison of soil infiltration rates in burned and

unburned mountainous watersheds. *Hydrological Processes*, 15(15):2893–2903, 2001. ISSN 08856087. doi: 10.1002/hyp.380.

R. W. McDowell, B. J. Biggs, A. N. Sharpley, and L. Nguyen. Connecting phosphorus loss from agricultural landscapes to surface water quality. *Chemistry and Ecology*, 20(1):1–40, feb 2004. ISSN 02757540. doi: 10.1080/02757540310001626092. URL `http://www.tandfonline.com/doi/abs/10.1080/02757540310001626092`.

R. W. McDowell, R. M. Dils, A. L. Collins, K. A. Flahive, A. N. Sharpley, and J. Quinn. A review of the policies and implementation of practices to decrease water quality impairment by phosphorus in New Zealand, the UK, and the US. *Nutrient Cycling in Agroecosystems*, 104(3):289–305, apr 2016. ISSN 15730867. doi: 10.1007/s10705-015-9727-0. URL `http://link.springer.com/10.1007/s10705-015-9727-0`.

M. M. Mekonnen and A. Y. Hoekstra. Global Anthropogenic Phosphorus Loads to Freshwater and Associated Grey Water Footprints and Water Pollution Levels: A High-Resolution Global Study. *Water Resources Research*, 54(1):345–358, jan 2018. ISSN 19447973. doi: 10.1002/2017WR020448. URL `https://agupubs.onlinelibrary.wiley.com/doi/full/10.1002/2017WR020448https://agupubs.onlinelibrary.wiley.com/doi/abs/10.1002/2017WR020448https://agupubs.onlinelibrary.wiley.com/doi/10.1002/2017WR020448`.

W. W. Miller, D. W. Johnson, C. Denton, P. S. Verburg, G. L. Dana, and R. F. Walker. Inconspicuous nutrient laden surface runoff from mature forest Sierran watersheds. *Water, Air, and Soil Pollution*, 163(1-4):3–17, may 2005. ISSN 00496979. doi: 10.1007/s11270-005-7473-7. URL `http://link.springer.com/10.1007/s11270-005-7473-7`.

W. W. Miller, D. W. Johnson, S. L. Karam, R. F. Walker, and P. J. Weisberg. A

synthesis of sierran forest biomass management studies and potential effects on water quality. *Forests*, 1(3):131–153, 2010. ISSN 19994907. doi: 10.3390/f1030131.

J. D. Murphy, D. W. Johnson, W. W. Miller, R. F. Walker, E. F. Carroll, and R. R. Blank. Wildfire Effects on Soil Nutrients and Leaching in a Tahoe Basin Watershed. *Journal of Environment Quality*, 35(2):479, 2006. ISSN 1537-2537. doi: 10.2134/jeq2005.0144. URL `https://pubag.nal.usda.gov/download/7327/PDFhttps://www.agronomy.org/publications/jeq/abstracts/35/2/479`.

NCASI. Patterns and processes of variation in nitrogen and phosphorus concentrations in forested streams. Technical report, IMPROVEMENT, NATIONAL COUNCIL FOR AIR AND STREAM (NCASI), INC., Research Triangle Park, NC, 2001.

B. A. Needelman, W. J. Gburek, G. W. Petersen, A. N. Sharpley, and P. J. A. Kleinman. Surface Runoff along Two Agricultural Hillslopes with Contrasting Soils. *Soil Science Society of America Journal*, 68(3):914, 2004. ISSN 1435-0661. doi: 10.2136/sssaj2004.0914. URL `https://pubag.nal.usda.gov/download/9560/PDF`.

S. Neitsch, J. Arnold, J. Kiniry, and J. Williams. Soil & Water Assessment Tool Theoretical Documentation Version 2009, 2011. ISSN 2151-0040. URL `http://oaktrust.library.tamu.edu/bitstream/handle/1969.1/128050/TR-406{\_}SoilandWaterAssessmentToolTheoreticalDocumentation.pdf?sequence=1`.

P. W. Gassman, J. R. Williams, X. Wang, A. Saleh, E. Osei, L. M. Hauck, R. C. Izaurralde, and J. D. Flowers. Invited Review Article: The Agricultural Policy/Environmental eXtender (APEX) Model: An Emerging Tool for Landscape and Watershed Environmental Analyses. *Transactions of the ASABE*, 53(3):711–740, 2010. ISSN 2151-0040. doi: 10.13031/2013.30078. URL `https://ageconsearch.umn.edu/bitstream/49156/2/09-TR49.pdfhttp:`

`//elibrary.asabe.org/abstract.asp??JID=3{\&}AID=30078{\&}CID=t2010{\&`
`}v=53{\&}i=3{\&}T=1.`

K. B. Piatek and H. L. Allen. Are forest floors in mid-rotation stands of loblolly pine (Pinus taeda) a sink for nitrogen and phosphorus? *Canadian Journal of Forest Research*, 31: 1164–1174, 2001. ISSN 00455067. doi: 10.1139/cjfr-31-7-1164. URL `http://www.nrcresearchpress.com/doi/pdfplus/10.1139/x01-049`.

J. N. Pretty, C. F. Mason, D. B. Nedwell, R. E. Hine, S. Leaf, and R. Dils. Environmental costs of freshwater eutrophication in England and Wales. *Environmental Science and Technology*, 37(2):201–208, jan 2003. ISSN 0013936X. doi: 10.1021/es020793k. URL `https://pubmed.ncbi.nlm.nih.gov/12564888/`.

D. E. Radcliffe and M. L. Cabrera. *Modeling phosphorus in the environment*, volume 72. 2007. ISBN 978-0-8493-3777-2. doi: 10.2136/sssaj2007.0025br.

P. R. Robichaud. Fire effects on infiltration rates after prescribed fire in northern Rocky Mountain forests, USA. In *Journal of Hydrology*, volume 231-232, pages 220–229. Elsevier Science B.V., may 2000. doi: 10.1016/S0022-1694(00)00196-7.

S. M. Saia, E. S. Brooks, Z. M. Easton, C. Baffaut, J. Boll, and T. S. Steenhuis. Incorporating pesticide transport into the WEPP model for mulch tillage and no tillage plots with an underlying claypan soil. *Applied Engineering in Agriculture*, 29(3):373–382, 2013. ISSN 08838542. URL `http://elibrary.asabe.org/azdez.asp?AID=42723{\&}T=2`.

M. Sánchez and J. Boll. The Effect of Flow Path and Mixing Layer on Phosphorus Release. *Journal of Environmental Quality*, 34(5):1600–1609, 2005. ISSN 0047-2425. doi: 10.2134/jeq2004.0306.

E. M. Schneiderman, T. S. Steenhuis, D. J. Thongs, Z. M. Easton, M. S. Zion, A. L. Neal, G. F. Mendoza, and M. T. Walter. Incorporating variable source area hydrology into

a curve-number-based watershed model. *Hydrological Processes*, 21(25):3420–3430, dec 2007. ISSN 08856087. doi: 10.1002/hyp.6556. URL `http://doi.wiley.com/10.1002/hyp.6556`.

T. Schoennagel, J. K. Balch, H. Brenkert-Smith, P. E. Dennison, B. J. Harvey, M. A. Krawchuk, N. Mietkiewicz, P. Morgan, M. A. Moritz, R. Rasker, M. G. Turner, and C. Whitlock. Adapt to more wildfire in western North American forests as climate changes. *Proceedings of the National Academy of Sciences*, 114(18):4582–4590, 2017. ISSN 0027-8424. doi: 10.1073/pnas.1617464114. URL `http://www.ncbi.nlm.nih.gov/pubmed/28416662http://www.pubmedcentral.nih.gov/articlerender.fcgi?artid=PMC5422781http://www.pnas.org/lookup/doi/10.1073/pnas.1617464114`.

P. D. Schroeder, D. E. Radcliffe, M. L. Cabrera, and C. D. Belew. Relationship between soil test phosphorus and phosphorus in runoff: effects of soil series variability. *Journal of environmental quality*, 33(4):1452–1463, 2004. ISSN 0047-2425. URL `http://www.ncbi.nlm.nih.gov/pubmed/15254128`.

A. N. Sharpley, R. W. Mcdowell, and P. J. A. Kleinman. Phosphorus loss from land to water: Integrating agricultural and environmental management. *Plant and Soil*, 237(2):287–307, 2001. ISSN 0032079X. doi: 10.1023/A:1013335814593. URL `http://link.springer.com/10.1023/A:1013335814593`.

V. Smil. Phosphorus in the environment: Natural flows and human interferences. *Annual Review of Energy and the Environment*, 25(1):53–88, nov 2000. ISSN 10563466. doi: 10.1146/annurev.energy.25.1.53. URL `http://www.annualreviews.org/doi/10.1146/annurev.energy.25.1.53`.

H. G. Smith, G. J. Sheridan, P. N. Lane, P. Nyman, and S. Haydon. Wildfire effects on water quality in forest catchments: A review with implications for water supply.

Journal of Hydrology, 396(1-2):170–192, jan 2011. ISSN 00221694. doi: 10.1016/j. jhydrol.2010.10.043.

L. A. Sprague and D. L. Lorenz. Regional nutrient trends in streams and rivers of the United States, 1993-2003. *Environmental Science and Technology*, 43(10):3430–3435, 2009. ISSN 0013936X. doi: 10.1021/es803664x. URL `https://pubs.acs.org/doi/pdf/10.1021/es803664x`.

M. S. Srinivasan, W. J. Gburek, and J. M. Hamlett. Dynamics of stormflow generation-A hillslope-scale field study in East-Central Pennsylvania, USA. *Hydrological Processes*, 16(3):649–665, 2002. ISSN 08856087. doi: 10.1002/hyp.311. URL `https://pubag.nal.usda.gov/download/36286/PDF`.

A. Srivastava, M. Dobre, J. Q. Wu, W. J. Elliot, E. A. Bruner, S. Dun, E. S. Brooks, and I. S. Miller. Modifying WEPP to improve streamflow simulation in a pacific northwest watershed. *Trans. ASABE*, 56(2):603–611, 2013. URL `https://www.fs.fed.us/rm/pubs{\_}other/rmrs{\_}2013{\_}srivastava{\_}a001.pdf`.

A. Srivastava, J. Q. Wu, W. J. Elliot, E. S. Brooks, and D. C. Flanagan. MODELING STREAMFLOW IN A SNOW-DOMINATED FOREST WATERSHED USING THE WATER EROSION PREDICTION PROJECT (WEPP) MODEL. *American Society of Agricultural and Biological Engineers*, 60(4):1171–1187, 2017. doi: 10.13031/trans.12035. URL `https://elibrary.asabe.org/azdez.asp?search=0{\&}JID=3{\&}AID=48344{\&}CID=t2017{\&}v=60{\&}i=4{\&}T=2`.

J. L. Stoddard, J. Van Sickle, A. T. Herlihy, J. Brahney, S. Paulsen, D. V. Peck, R. Mitchell, and A. I. Pollard. Continental-Scale Increase in Lake and Stream Phosphorus: Are Oligotrophic Systems Disappearing in the United States? *Environmental Sci-*

ence and Technology, 50(7):3409–3415, apr 2016. ISSN 15205851. doi: 10.1021/acs.est. 5b05950. URL `www.epa.gov/nheerl/arm/designpages/monitdesign/survey{\_}`.

C. Teutschbein, R. A. Sponseller, T. Grabs, M. Blackburn, E. W. Boyer, J. K. Hytteborn, and K. Bishop. Future Riverine Inorganic Nitrogen Load to the Baltic Sea From Sweden: An Ensemble Approach to Assessing Climate Change Effects. *Global Biogeochemical Cycles*, 31(11):1674–1701, nov 2017. ISSN 19449224. doi: 10.1002/2016GB005598. URL `http://doi.wiley.com/10.1002/2016GB005598`.

USFS. Water Facts — US Forest Service, 2020. URL `https://www.fs.usda.gov/managing-land/national-forests-grasslands/water-factshttps://www.fs.fed.us/managing-land/national-forests-grasslands/water-factshttps://www.fs.usda.gov/managing-land/national-forests-grasslands/water-facts{\%}0Ahttps://www.fs.fed.us`.

P. A. Vadas, P. J. A. Kleinman, A. N. Sharpley, and B. L. Turner. Relating Soil Phosphorus to Dissolved Phosphorus in Runoff. *Journal of Environment Quality*, 34(2):572, 2005. ISSN 1537-2537. doi: 10.2134/jeq2005.0572. URL `http://citeseerx.ist.psu.edu/viewdoc/download?doi=10.1.1.168.2218{\&}rep=rep1{\&}type=pdfhttps://www.agronomy.org/publications/jeq/abstracts/34/2/0572`.

T. Warziniack and M. Thompson. Wildfire risk and optimal investments in watershed protection. *Western Economics Forum*, 12(2):19–28, 2013.

A. L. Westerling, H. G. Hidalgo, D. R. Cayan, and T. W. Swetnam. Warming and Earlier Spring Increase Western U.S. Forest Wildfire Activity. *Science*, 313(5789):940 LP – 943, aug 2006. doi: 10.1126/science.1128834. URL `http://science.sciencemag.org/content/313/5789/940.abstract`.

M. S. Wood and M. A. Beckwith. Coeur d ' Alene Lake , Idaho : Insights Gained from

Limnological Studies of 1991 – 92 and 2004 – 06. Technical report, U.S. Geological Survey, 2008. URL `https://pubs.usgs.gov/sir/2008/5168/pdf/sir20085168.pdf`.

R. A. Young, C. A. Onstad, D. D. Bosch, and W. P. Anderson. AGNPS - A Non-Point Source Pollution Model for Evaluating Agricultural Watersheds. *Journal of Soil Water Conservation*, 44(2):168–173, 1989.

L. M. Zinsser. Trends in Concentrations, Loads, and Sources of Trace Metals and Nutrients in the Spokane River Watershed, northern Idaho, water years 1990-2018. Technical report, U.S. Geological Survey Scientific Investigations Report, 2020.

CHAPTER 2

Long-term response in nutrient load from commercial forest management operations in a mountainous watershed

Chapter based on: Deval C, Brooks ES, Gravelle JA, Link TE, Dobre M, Elliot WJ. Long-term response in nutrient load from commercial forest management operations in a mountainous watershed. For Ecol Manage. 2021;494(March):119312. Available from: https://doi.org/10.1016/j.foreco.2021.119312

2.1   Abstract

An increased emphasis on fuel management strategies to mitigate wildfire risks is raising the awareness and need for comprehensive forest management strategies that satisfy long-term water quantity and water quality needs. Forest management activities can alter the soil nutrient pools and affect the timing and magnitude of stream water quantity and quality. We investigated the effect of contemporary forest management activities, including clear-cutting and thinning, on water yield and stream nitrogen and phosphorus dynamics in a quarter-century-long (1992–2016) paired and nested watershed study in the interior Pacific Northwest, US. Monthly water samples were collected and analyzed for total Kjeldhal nitrogen (TKN), total available nitrogen (TAN), nitrate + nitrite (NO_3 + NO_2), total phosphorus (TP), and orthophosphate (OP) concentrations throughout the study period. Five years of pre-disturbance data, 4 years of post-road construction, 6 years of Phase I (PH-I) experimental post-harvest, and 9 years of Phase II (PH-II) operational harvest data were analyzed using a before-after, control-impact paired series (BACIPS) study design. We found statistically significant increases in stream NO_3 + NO_2 loading from the paired and nested watersheds following timber harvest treatments. In the case of OP, any increase in nutrient load was attributed to increases in streamflow, as OP

concentrations remained near minimum detectable concentrations. Streamflow increased the greatest following clear-cut practices (33.4% at W1 during PH-I) with the largest response in stream $NO_3 + NO_2$ concentration (up to 0.33 mg-N L^{-1} at W1). In-stream $NO_3 + NO_2$ and OP concentrations were lower in the downstream cumulative watersheds, which was likely due to dilution and nutrient assimilation effects. Interestingly, the $NO_3 + NO_2$ concentration, streamflow, and loads of $NO_3 + NO_2$ and OP from the undisturbed control watershed also increased. This increase was, however, smaller than the harvested watersheds and likely driven by climate variability or subtle forest succession changes. In summary, we found that contemporary forest management activities increased stream $NO_3 + NO_2$ concentrations and loads following timber harvest activities, but these effects were also attenuated due to downstream uptake processes. Furthermore, relative to post-wildfire impacts, these nutrient increases are small and short-lived.

Keywords: *Forest Management, Nutrient Loads, Timber Harvest, Nitrogen, Phosphorus, Before-After-Control-Impact-Paired Series (BACIPS)*

2.2 Introduction

Upland forested regions provide a wide range of ecosystem services ranging from a valuable source of timber for the forest products industry to drinking and irrigated water supply, to fish and wildlife habitat, and human recreation. Forestland managers have advanced management practices over the last 30 or more years in an effort to minimize the effects of harvest activities on downstream aquatic ecosystems. In older unmanaged forests the increasing threat of wildfire due to long-term fire suppression strategies and forest fuel accumulation [Agee and Skinner, 2005, Schoennagel et al., 2017], climate change [Schoennagel et al., 2017, Westerling et al., 2006], and insect/disease [Bentz et al., 2010, Collins et al., 2012] has elevated the need and consideration for more active forest management involving clear-cutting, thinning, and prescribed burns. In forested landscapes, any forest

management strategy, including the 'do-nothing' option, will likely have long-term consequences on water quantity and quality [Johnson et al., 2011, Miller et al., 2005]. It is becoming more widely recognized that wildfire is a part of natural forest ecosystem development and that the fire suppression strategy coupled with climate change has led to higher severity fires and increased post-fire environmental impacts [Schoennagel et al., 2017, Westerling et al., 2006]. Recent shifts in the wildfire regime have led to increased research , illustrating the effects on the soil properties [Certini, 2005, Huffman et al., 2001, Martin and Moody, 2001, Robichaud, 2000] and the hydrologic response [Hallema et al., 2018, Niemeyer et al., 2020] that can result in potentially large sediment and nutrient loading [Emelko et al., 2016, Kunze and Stednick, 2006, Robinne et al., 2020, Rust et al., 2018] to the receiving waterbodies. To the nearly 180 million people and approximately 2/3 of municipalities across the US that rely on forested lands for drinking water [NRC, 2008], the impact of excessive nutrient and sediment loading following a wildfire is a great concern [Bladon et al., 2014, Jones et al., 2008, NRC, 2008]. Many communities that rely solely on a single reservoir in forested landscapes that are highly vulnerable to wildfires are considering thinning operations to minimize the risk and severity of future wildfires despite the potential for short-term water quality impacts [Gannon et al., 2019]. In recognition of the need to thin forests to reduce the severity and extent of wildfires and to maintain the full range of ecosystem services in commercial forestlands, there is a great need to identify and understand the short- and long-term effects of these forest management strategies on water quantity and quality.

Forested watersheds are often perceived as a sink rather than a source of nutrients, and although they continue to attract less attention in terms of nutrient management as compared to the watersheds dominated by agricultural and urban landscapes [Miller et al., 2005, Piatek and Allen, 2001], significant progress has been made in recent decades to understand nutrient effects in forested streams [Argerich et al., 2013, Binkley et al.,

2004]. While there are studies that have documented increases in nutrient concentrations from streams draining forested watersheds [Dubrovsky et al., 2010, Eddy-Miller et al., 2016], this is also contrasted with other studies that demonstrate decreasing trends in some forestland streams [Argerich et al., 2013]. It is important to note that elevated nitrogen and phosphorus concentrations observed in forestland streams are generally orders of magnitudes lower than nutrient criteria set by the US Environmental Protection Agency (EPA), and any increases from contemporary forest management practices are very small compared to other land uses [Binkley, 2001, Ice and Binkley, 2003]. Stream chemistry in forested landscapes is complex and is subject to considerable geographic and temporal variability [Feller, 2005]. Natural variations in stream nutrient concentrations and loads can occur because of geology [Nagorski et al., 2003], wildfires [Miller et al., 2005, 2006, Murphy et al., 2006], precipitation dynamics, and consequent changes in discharge [Bhangu and Whitfield, 1997] and biological activity [Minshall et al., 2001, Peterson et al., 2001]. Numerous studies have demonstrated that anthropogenic disturbances and forest management practices such as road construction, timber harvest, site preparation, and maintenance, increase nutrient concentrations [Anderson and Lockaby, 2011, Gravelle et al., 2009, Kreutzweiser et al., 2008] and loads [Dahlgren, 1998, Palviainen et al., 2014, 2015] in streams draining forested watersheds, but these increases are typically small in magnitude and limited in duration [Loehle et al., 2014].

This magnitude and duration of such changes in nutrient loads during and after forest management activities is dependent on several factors including topography, soil properties, watershed hydrology, the timing and type of management practices (e.g. broadcast burning of slash, competition release herbicide spraying), harvest intensity, vegetation recovery, climate, atmospheric deposition, mineralization rates, and relative distance of disturbance from streams [Kreutzweiser et al., 2008, Lintern et al., 2017]. For instance, many studies have reported statistically significant changes in the stream water nutrient

concentrations[Baldigo et al., 2005, Boggs et al., 2016, Martin et al., 2000, Tremblay et al., 2009] and loads [Boggs et al., 2016] following both partial and clear-cut harvesting treatments. Palviainen et al. [2014] reported minimal impact on stream nutrient loads from boreal forest watersheds when clear cuts occurred on small scales ($< 10\%$ of the total watershed area) and wider stream buffer zones (between 10 to 454 m) were maintained. But when the clear-cut exceeded 30% of the watershed area, annual loads increased 72% for total nitrogen, 76% for total organic nitrogen, 1056% for nitrate, 35% for phosphate, and 715% for suspended sediments, and this nutrient increase, in general, was sustained for more than 10 years. Siemion et al. [2011] reported that the initial effects and the long-term water quality response were directly related to harvest intensity, defined as the percent of total basal area removed, and the stream water nutrient concentrations declined faster in forests with lower intensity harvests. Regardless of harvest intensity, research compiled from recent decades has also demonstrated that contemporary forestry Best Management Practices (BMPs) appear to reduce water quality impacts by 80-90% compared to impacts from historic legacy practices [Loehle et al., 2014]. While Swank et al. [2001] reported that the nitrate-nitrogen response peaked three years following the clear-cut harvest, Wang et al. [2006] have reported a five-fold increase in the nitrate-nitrogen loads from a catchment draining a hardwood forest one year after the forest was partial-cut. Other studies have also reported elevated nutrient concentrations and loads in streams draining clear-cut forests, especially during large storm events [Dahlgren, 1998, Oda et al., 2011]. Many studies have found that atmospheric deposition and nutrient mineralization rates following management practices coupled with the high stream discharge associated with the storm events govern the variability in stream nutrient concentrations [Akselsson et al., 2004, Dahlgren, 1998, Kortelainen et al., 2006, Palviainen et al., 2014]. All these studies reveal that the response in water quantity and quality to natural and anthropogenic disturbances in forested ecosystems can vary widely both in space and time.

It is therefore imperative to further improve our understanding of the nutrient loads dynamics occurring in both relatively undisturbed as well as commercially managed forested watersheds. Previous work in the watershed focused on experimental treatment impacts of timber harvest on water yield [Hubbart et al., 2007], peak stream temperature [Gravelle et al., 2009], suspended sediment loads [Karwan et al., 2007], and stream nutrient concentrations [Gravelle et al., 2009]. In this study, we explore in greater depth the long-term response in nutrient loads following early vegetation regeneration from the actively managed timber harvest units in the Mica Creek Experimental Watershed (MCEW). The primary objective of this study was to quantify and compare the differences in nitrogen and phosphorus concentrations and loads between the Pre-disturbance period, road construction (Post-road), experimental harvest (PH-I), and operational harvest (PH-II) with simultaneous regeneration. We analyze the extent to which the site management operations and harvesting practices occurring during two distinct time periods, Phase I (PH-I) and Phase II (PH-II), and how these activities affected nutrient yield from both a hydrological yield and nutrient concentration perspective.

2.3   Methods

2.3.1   Study area

This study was carried out in the Mica Creek Experimental Watershed (MCEW) located in Shoshone County in northern Idaho, US (Figure 2.1). MCEW occupies roughly 2700 ha and is located approximately between latitudes 47° 11' 36" N and 47° 08' 13" N and longitudes 116° 18' 42" W and 116° 13' 5" W. It is a paired and nested watershed draining into the St. Joe River and is privately owned by PotlatchDeltic Corporation, a timberland real estate investment trust.

Elevation in the MCEW ranges from 1000 m and 1600 m a.m.s.l. The mountainous wa-
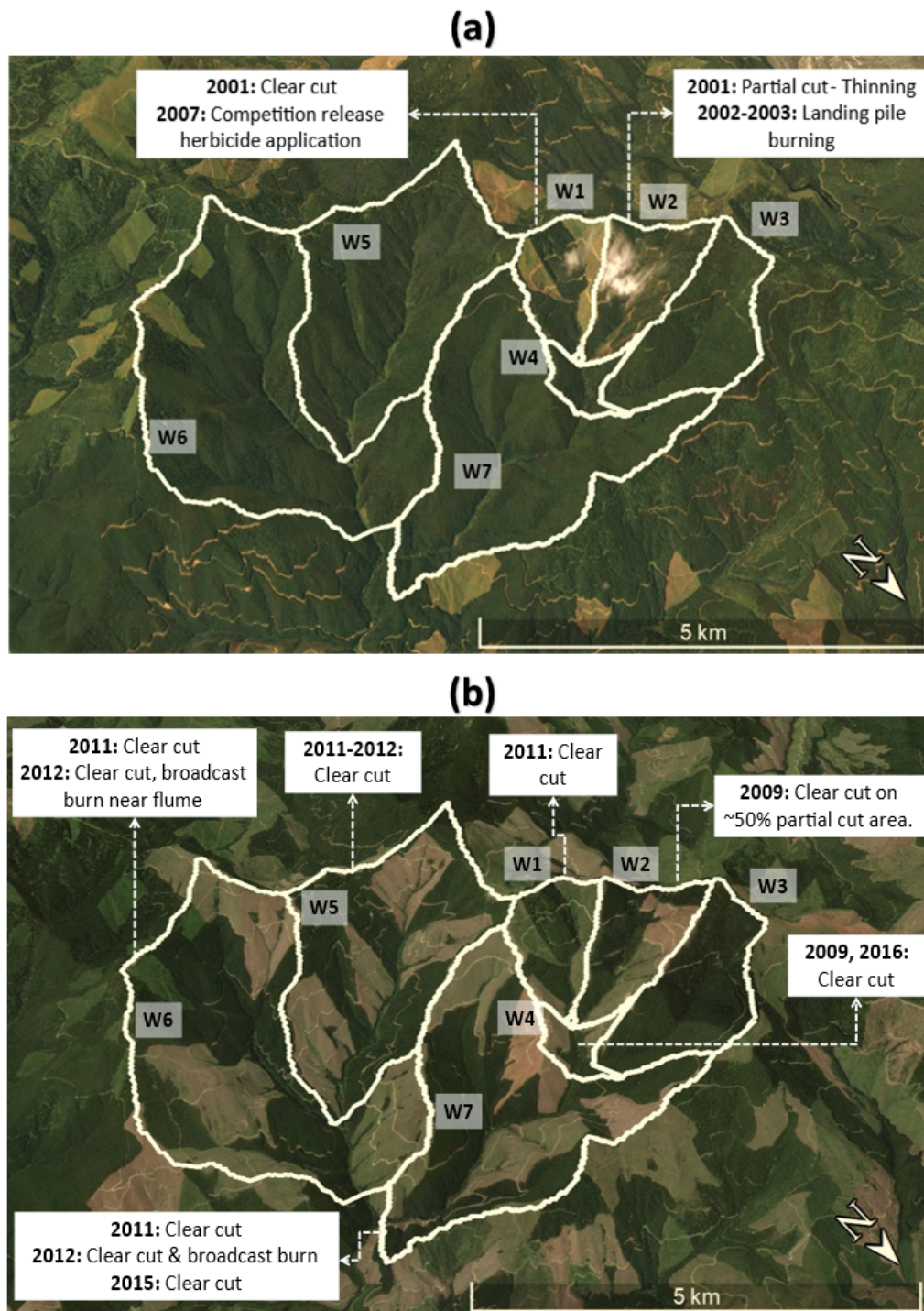
Figure 2.1: (a) MCEW land cover (2005) before PH-II; (b) MCEW land cover (2016) post-PH-II harvest treatment.

tershed has v-shaped valleys with slopes of 15-30% and stream gradients between 5- 20%. The geology of the region is largely dominated by Wallace gneiss/Prichard quartzite parent material, which is overlain by silty soils. Annual mean precipitation is approximately 1450 mm, more than half of which falls primarily as snow from October to March. The average annual temperature in the region is 5 °C with warm and dry summers and cold and wet winters. MCEW was harvested and burned between 1920 and 1930. The current vegetation cover in the watershed consists primarily of 90-100-year-old naturally regenerated second-growth mixed conifer and < 15-year-old replanted mixed conifer stands with majority comprised of Grand fir (Abies grandis), Douglas-fir (Pseudotsuga menziesii), Western red cedar (Thuja plicata) and Western larch (Larix occidentalis), and the under-story cover dominated by grasses, forbs, and shrubs.

2.3.1.1 Treatment sites

For this analysis time periods have been broken into four distinct phases: Pre-disturbance (1992-1997), Post-road (1997-2001), experimental-harvest Phase I (PH-I) (2001-2007), and operational sequential harvest Phase II (PH-II) when the extent and frequency of harvests increased (2007-2016). PH-I represents an experimental treatment phase during which harvest activities were experimentally controlled (only upstream headwater watersheds were harvested and mature vegetation removal ranged between 24%-47%) followed by site management operations including broadcast burning and replanting. PH-II represents the post-experimental phase where the study area transitioned to operational treatments that consisted of additional road construction and timber harvest, with site management operations including pile burning and competition release herbicide application. During this operational phase, the mature vegetation removal in the upstream and cumulative downstream watersheds ranged between 36%-50% and 17-28%, respectively (Table 2.1). No activity occurred for the first 5 years of the study (Pre-disturbance phase)

to provide baseline data. Roads for harvesting timber were constructed in the fall of 1997. This included restoration and slight widening of the existing primary road, which in the early 1930s was a railroad bed used for harvesting, to suit heavy truck traffic. Mid-slope access roads designed for log hauling were constructed in W1 and W2. Harvesting in PH-I occurred in the late summer and fall of 2001 and was completed with a combination of line and tractor skidding. This four-year period between road construction and harvesting provided for the isolation of road construction effects from harvest effects (post-road phase). About 23 ha of north-facing slopes and 43 ha of southeast-facing slopes in a 139-ha Watershed 1 (W1) were clear-cut harvested in 2001 (Figure 2.1a). The lower slopes in this unit were broadcast burned in spring 2003 and replanted with mixed conifer species. The northeast and southeast slopes in a 176-ha Watershed 2 (W2) consisting of 34 and 49 ha, respectively were partial-cut harvested (i.e. 50% of the canopy was removed over 50% of the area) in 2001. Watersheds 4 (W4) and 7 (W7) were considered as the downstream cumulative effect assessment sites and Watersheds 5 (W5) and 6 (W6) were regarded as controls for these cumulative sites, respectively.

Table 2.1: Summary of MCEW characteristics and harvesting activities. CC refers to clear-cut; PC refers to partial-cut and C refers to control sites

Watershed	Area (ha)	Harvest type	% Area harvested (PH-I)	%Area harvested (PH-II)	Mean degree slope	Elevation range (m)
W1	139	CC	47.1%	50.5%	19	1205-1528
W2	177	PC/CC	23.8%	35.8%	18	1201-1612
W3	227	C	0.0%	0.0%	17	1193-1612
W4	597	PC/CC	18.0%	25.7%	18	1169-1612
W5	667	C/CC	0.0%	17.5%	18	1055-1528
W6	1456	C/CC	0.0%	28.2%	18	1017-1594
W7	1226	CC/PC	9.0%	26.1%	18	1008-1612

The PH-II harvesting treatment period began around the 2008 water year (Figure 2.1b). New roads were initially constructed (with subsequent new construction through-

out PH-II) for harvesting the downstream watersheds (W5-W7). In the summer of 2009, a portion of W2 that was partially cut as part of PH-I experimental treatment in 2001 was clear cut. Portions of the unharvested downstream control watersheds W5 and W6 were clear-cut harvested and broadcast burned in 2011 and 2012. A small portion of W1 adjacent to W4 was also clear-cut in 2011 and vegetation near the south side of the W1 flume was removed. Portions of watershed W7 were clear cut during 2011 (southwest of the flume), 2012 (near flume), and 2015 (northeast of the flume), respectively. Competition release herbicide, which generally consisted of some mixture of Oust (sulfometuron methyl); Accord Concentrate (glyphosate); Atrazine 4L; or Arsenal AC (imazapyr), were applied to several post-harvest areas during the PH-II period. Although a herbicide treatment was first applied in W1 in August 2007 at the end of the PH-I period, this treatment was considered part of PH-II since the response from this activity occurred during PH-II. All forest management practices followed the Idaho Forest Practices Act and Stream Protection Zone (SPZ) requirements [Idaho Administrative Procedures Act (IDAPA), 2020, Idaho Department of Lands (IDL), 2000]. This includes maintaining 75 ft (22.86 m) stream protection zones on each side of fish-bearing (Class I) streams. All existing shade in the Class I stream buffer was retained although the regulations before 2014 permitted the removal of 25% of the existing shade. Buffer requirements for non-fish-bearing (Class II) streams include a 30 ft (9.14 m) equipment exclusion zones on each side of the streams, but merchantable timber is allowed to be removed.

2.3.2 Water sampling and chemical analyses

Monthly manual grab samples of stream water were collected at each of the seven flumes in the MCEW using 250 ml high-density polyethylene (HDPE) bottles, starting in June 1992 until September 2016. The sample collection was continuous except in some winter months when harsh weather conditions limited access to the flumes. Although event-

based storm sampling is preferable to fixed monthly grab sampling for capturing event loads, this was not feasible considering minimum holding times and the remote location of the site. The long consistent monthly sampling record (i.e. more than 25 years of data) in this data set however minimizes the risk of short term biases in the data. The collected samples were sent to water quality laboratories at Oregon State University in Corvallis, OR (1992 - 1997), the National Council for Air and Stream Improvement, Inc. (NCASI) in Anacortes, WA (1998 - 1999), and NCASI in Corvallis, OR (2000 - 2016). The samples were analyzed for six parameters, specifically nitrate+nitrite (NO_3+NO_2), total Kjeldhal nitrogen (TKN), total ammonia nitrogen (TAN) containing un-ionized (NH3) and ionized (NH4+) ammonia, total nitrogen (TN), total phosphorus (TP), and orthophosphate (OP). The TAN measurements started from August 1999 and the TP measurements were discontinued after July 2014. A detailed description of the sample collection and the chemical analyses (methods, instrument calibration procedures, and instrument detection limits) is included in Gravelle et al. [2009].

2.3.3   Load estimation

The monthly nutrient concentration data along with the corresponding daily discharge data were used to estimate the daily N and P loads for each of the seven flume sites using the Load Estimator (LOADEST) software [Runkel et al., 2004]. LOADEST has nine predefined regression models to estimate nutrient loads given the measured nutrient concentrations and flows. In this study, the LOADEST model was allowed to automatically select the best regression model based on the lowest Akaike Information Criterion (AIC) value. The specific regression models selected by LOADEST to estimate N and P daily loads for each watershed as well as model performance metrics are presented in appendix A in the supporting information.

2.3.4 Study design and data analyses

A before-after, control-impact paired series (BACIPS) design [Stewart-Oaten et al., 1986, 2001] was used to evaluate both direct and cumulative effects of commercial forest management practices on stream nutrients in paired and nested watersheds that comprise the MCEW. In this study, the paired watershed approach was applied to the upper W1, W2, and W3 watersheds each with areas of approximately 139 ha, 177 ha, and 227 ha, respectively (Figure 2.1). The cumulative effects of management in the upper watersheds during Phase I were assessed using the downstream watersheds W4 and W7, and their paired control watersheds W5 and W6 that occupy 597 ha and 667 ha, and 1456 ha and 1226 ha, respectively.

The nutrient data sample size (n) of 54, 34, 50, and 120 instantaneous measurements were available during the Pre-disturbance, Post-road, PH-I, and PH-II treatment periods, respectively. The nutrient data from the lab analyses were used to establish a linear relationship in stream nutrient concentrations between control and treatment watersheds during the Pre-disturbance phase. Similarly, BACIPS relationships between the control and treatment watersheds during the Pre-disturbance phase were also established for daily streamflow observations as well as nutrient loads. Since portions of the downstream control watersheds (W5 and W6) were harvested during PH-II, all the downstream sites during this treatment period were compared to the remaining control site (W3). To do so, linear relationships between monthly nutrient concentrations, daily streamflow, and daily nutrient load observations at W3 and the downstream control sites (W5 & W6) and the downstream cumulative sites (W4 & W7) were established. The intercept (X control) and slope (a) from these relationships were then used to predict the nutrient concentrations, streamflow, and loads that would have occurred in the treatment watersheds ($C_{treatment, predicted}$) in the absence of management practices (Equation 2.1). $C_{control}$,

observed in Equation 2.1 is the observed nutrient concentration/streamflow/load at the control watershed. Since this method provides control over climate variability [Bari et al., 1996] and can separate the climatic effects from vegetation cover effects [Hewlett et al., 1969], the estimated difference ($\triangle$C) between the observed ($C_{\text{treatment, observed}}$) and predicted ($C_{\text{treatment, predicted}}$) concentrations (Equation 2.2) are assumed to have occurred because of changes in vegetation cover and/or soil disturbance. Such research design using BACIPS approaches has been implemented in several recent studies [Artigas et al., 2013, Boggs et al., 2016, Menberu et al., 2017, Swank et al., 2001] to investigate the relationship between harvesting and water quality across a diverse range of ecosystems.

$$C_{\text{treatment, predicted}} = X_{\text{control}} + a(C_{\text{treatment, observed}}) \tag{2.1}$$

$$\triangle C = C_{\text{treatment, observed}} - C_{\text{treatment, predicted}} \tag{2.2}$$

The difference between the observed and predicted nutrient concentrations, streamflow, and nutrient loads were tested for statistical significance using the Student's t-test at a 0.05 significance level (α). The statistical software R was used for all statistical computations and analyses. All the p-values are based on a comparison of Pre-disturbance (1992-1997) to Post-road (1997-2001), to PH-I (2001-2007), and PH-II (2007-2016) treatment periods except for the TAN. Since TAN (NH_3 + NH_4) data collection started in 1999, Post-road concentrations were compared to post-harvest and PH-II concentrations to determine if significant changes in TAN concentrations occurred following timber harvest.

One challenge with analyzing nutrient data from forested watersheds is that a large portion of the data can vary around the minimum detection limit. A small fraction of the total nitrogen and phosphorus observations were below-detection limits, ranging from

a maximum of 16% to no observations below detection limits within a particular phase. The fraction of samples below these limits decreased in the later treatment phases. In this study, values smaller than the minimum detection limit were assumed to be half the value of the detection limit. Such a substitution of the values below detection limits is a common approach to handle concentrations below detection limits [Huston and Juarez-Colunga, 2009].

The Modified Mann-Kendall trend test [Hamed and Rao, 1998] was used to identify the monotonic trend in the daily as well as seasonal streamflow. The modified Mann-Kendall test corrects for the autocorrelation effects on the Mann-Kendall test statistic and therefore is suitable for detecting statistically significant trends in autocorrelated data [Hamed and Rao, 1998]. The Kendall-Tau statistic (ranges between -1 and 1) provides the strength of ranked correlation between the ordered daily/seasonal streamflow at a certain significance level (α).

Both the length of the water quality record and the multiple paired and nested sub-watershed design provided a very rare opportunity to examine the impacts of two distinct intensities of commercial timber harvest in forested watershed.

2.4 Results

2.4.1 Streamflow

2.4.1.1 Long-term trends in streamflow

Table 2.2 details seasonal trends in the daily mean streamflow across all management phases at the MCEW watersheds. Statistically significant increasing trends in streamflow were identified in all the watersheds during the fall and winter seasons. The relative magnitude of this increasing trend was highest during the fall with Kendal-τ values ranging between 0.30 to 0.48 followed by the magnitudes during winter which ranged

between 0.22 and 0.32. Summer flows increases were significant only at W5 and W6. Spring and summer streamflow showed no significant change at W3.

Table 2.2: Kendall rank correlation coefficient statistics for the daily mean streamflow series for each season (months' abbreviations in parentheses). All Kendal-$\mathcal{T}$ values at a p-value <0.05 indicate a statistically significant trend

	Winter (DJF)		Spring (MAM)		Summer (JJA)		Fall (SON)	
	Kendall-$\mathcal{T}$	p-value	Kendall-$\mathcal{T}$	p-value	Kendall-$\mathcal{T}$	p-value	Kendall-$\mathcal{T}$	p-value
W1	0.265	<0.001	0.125	<0.001	0.070	0.235	0.319	<0.001
W2	0.318	<0.001	0.179	<0.001	0.137	0.050	0.409	<0.001
W3	0.253	<0.001	0.049	0.211	0.106	0.069	0.427	<0.001
W4	0.309	<0.001	0.133	<0.001	0.140	0.054	0.483	<0.001
W5	0.276	0.005	0.167	0.015	0.181	<0.001	0.402	0.001
W6	0.263	0.006	0.155	0.022	0.112	0.049	0.300	<0.001
W7	0.217	0.001	0.120	0.005	0.066	0.246	0.300	<0.001

2.4.1.2   Effects of site treatment on Streamflow

Trends in mean annual streamflow in all the MCEW watersheds, including the control (W3) watershed, are displayed in Figure 2.2. Table 2.3 summarizes the observed streamflow and the estimated change in streamflow for each treatment phase along with the Student's t-test p-values between the treatment-control watershed pairs at MCEW. During the Post-road phase, a statistically significant but relatively small increase in streamflow occurred in the paired watersheds W1 (58 mm/yr, p-value= 0.039) and W2 (66 mm/yr, p-value= 0.012). In all post-harvest watersheds (PH-I or PH-II treated), statistically significant increases in stream flows were observed. For the PH-I period, the largest increase in streamflow was observed in the W1 (248 mm/yr, p-value< 0.001) watershed while the increase at the downstream cumulative sites W4 (p-value< 0.001) and W7 (p-value= 0.002) amounted to 131 mm/yr and 51 mm/yr, respectively. During the PH-II treatment, the highest increase in streamflow occurred at the W2 (252 mm/yr, p-value<0.001) followed by W5 (248 mm/yr, p-value<0.001) watershed. The increase in streamflow at the

downstream cumulative sites (p-value< 0.001) W4 and W7 during this treatment phase amounted to 186 mm/yr and 91 mm/yr, respectively.
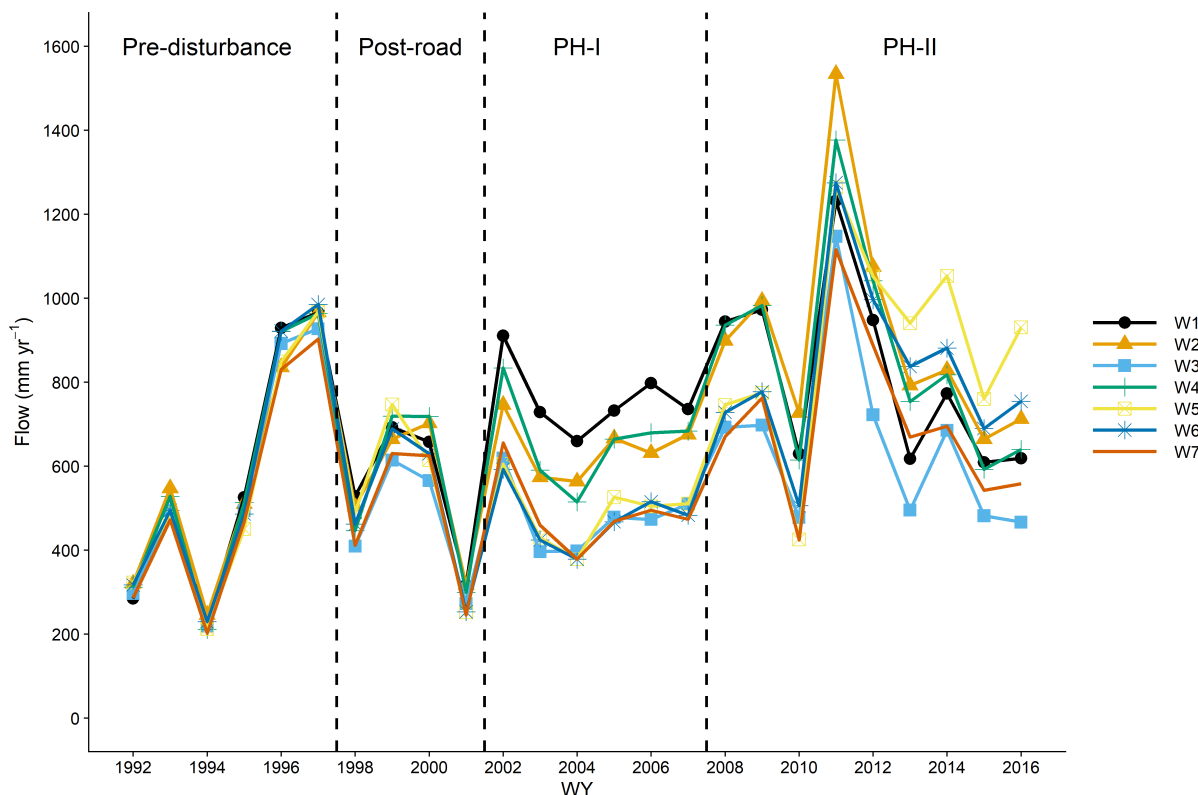
Figure 2.2: Mean annual streamflow from all watersheds in the MCEW.

2.4.2 Nitrogen and Phosphorus concentrations and loads

2.4.2.1 Total Kjeldahl nitrogen (TKN)

There were minimal changes in TKN concentration (Appendix A: Figure 6.1), with a slight observed reduction in long-term TKN loads. Based on Student's t-test results (Table 2.5), significant changes in TKN concentrations only occurred in one of the two paired headwater catchments (W2) during PH-I and PH-II treatment periods, and at the W5, W6, and W7 watersheds during the PH-II treatment period only. The TKN concentration at W2 decreased by 0.018 mg-N.L^{-1} and 0.028 mg-N.L^{-1} during PH-I (p-

Table 2.3: Observed streamflow, estimated change in streamflow due to treatment calculated from relationships with paired control watershed response (equation 2.2), and Student's t-test p-value results. Estimated change at $\alpha < 0.05$ indicates a statistically significant change. Insignificant changes are indicated by an asterisk next to the watershed name.

Treatment	Watershed	Mean Observed (mm/yr)	Estimated Change (mm/yr)	p-value
Post-road	W1	558.45	58.40	0.039
	W2	558.45	65.70	0.012
	W4*	551.15	-21.90	0.472
	W7*	489.10	10.95	0.695
PH-I	W1	740.95	248.20	<0.001
	W2	620.50	131.40	<0.001
	W4	646.05	131.40	<0.001
	W7	474.50	51.10	0.002
PH-II	W1	817.60	146.00	<0.001
	W2	908.85	251.85	<0.001
	W4	865.05	186.15	<0.001
	W7	704.45	91.25	<0.001
	W5	886.95	248.20	<0.001
	W6	828.55	167.90	<0.001

value =0.017) and PH-II (p-value = 0.011) treatment periods, respectively. Despite the reduced concentrations, the TKN load from W2 increased by 0.14 kg ha^{-1} yr^{-1} and 0.09 kg ha^{-1} yr^{-1} during PH-I (p-value < 0.001) and PH-II (p = 0.006) treatment periods, respectively (Table 2.6) due to increasing streamflow. TKN concentration at W7 during the PH-II treatment period decreased by 0.020 mg-N.L^{-1} (p-value =0.034) and TKN load during this period was 0.37 kg ha^{-1} yr^{-1}. The cumulative annual load of TKN from MCEW watersheds is depicted in appendix A, Figure 6.2. Change in the slope of the annual load curve in the cumulative plot indicates the change (increase/decrease) in load whereas the flattening of this slope indicates recovery of load to the background values. Although a statistically significant decline in concentrations occurred only during the PH-I and PH-II treatment periods, the overall steady TKN load from all watersheds is apparent.

Table 2.4: Mean annual load of nitrogen and phosphorus from each watershed per treatment period in kg ha $^{-1}$ yr^{-1}. NA: data not measured/discontinued.

		W1	W2	W3	W4	W5	W6	W7
TKN	Pre-disturbance	0.67	0.82	0.65	0.81	0.80	0.88	0.85
	Post-road	0.86	0.73	0.59	0.75	1.05	0.85	0.95
	PH-I	0.32	0.23	0.10	0.18	0.13	0.11	0.14
	PH-II	NA	0.44	0.29	0.52	0.49	0.42	0.37
TAN	Pre-disturbance	NA	NA	NA	NA	NA	NA	NA
	Post-road	0.07	0.11	0.05	0.26	0.07	0.09	0.07
	PH-I	0.08	0.07	0.05	0.08	0.05	0.05	0.05
	PH-II	0.09	0.11	0.07	0.10	0.12	0.10	0.10
NO_3+NO_2	Pre-disturbance	0.40	0.07	0.07	0.13	0.05	0.08	0.06
	Post-road	0.57	0.42	0.16	0.32	0.14	0.24	0.18
	PH-I	2.99	0.35	0.10	0.69	0.07	0.06	0.24
	PH-II	3.95	1.35	0.33	1.73	0.66	0.77	1.24
TP	Pre-disturbance	0.15	0.16	0.12	0.16	0.16	0.18	0.14
	Post-road	0.25	0.21	0.15	0.22	0.26	0.23	0.23
	PH-I	0.15	0.12	0.11	0.12	0.12	0.09	0.11
	PH-II	0.16	0.19	0.08	0.15	0.19	0.16	0.13
	Pre-disturbance	0.07	0.06	0.04	0.05	0.05	0.05	0.05
OP	Post-road	0.08	0.08	0.05	0.07	0.08	0.08	0.09
	PH-I	0.12	0.10	0.06	0.10	0.08	0.08	0.07
	PH-II	0.11	0.12	0.06	0.11	0.12	0.10	0.09

2.4.2.2 Total ammonia nitrogen (TAN)

Analysis of TAN concentrations (Figure 6.3 in appendix, Table 2.5) showed a statistically significant decrease at W1 (0.002 mg-NH$_3$.L^{-1}, p=0.044) and W2 (0.003 mg- NH$_3$.L^{-1}, p-value=0.042) watersheds during the PH-I treatment period. During PH-II, a similar small decline in the TAN concentration was observed at W1, W6, and W7, which amounted to 0.002 mg- NH$_3$.L^{-1} (p-value = 0.015), 0.008 mg- NH$_3$.L^{-1} (p-value = <0.001), and 0.004 mg-NH$_3$.L^{-1} (p-value < 0.001), respectively. For the same treatment period, the TAN

Table 2.5: Observed nutrient concentrations, estimated change in concentration due to treatment calculated from relationships with paired control watershed response (Equation 2.2), and Student's t-test p-value results. The estimated change at p-value <0.05 indicates a statistically significant change.

		Post-Road				Post-Harvest				Phase-II					
		W1	W2	W4	W7	W1	W2	W4	W7	W1	W2	W4	W5	W6	W7
TKN	Mean Observed (mg-N/L)	0.166	0.145	0.137	0.178	0.048	0.041	0.037	0.041	NA	0.046	0.045	0.045	0.041	0.048
	Estimated Change (mg-N/L)	0.037	0.002	-0.028	0.039	-0.012	-0.018	0.012	-0.012	NA	-0.028	0.008	-0.025	-0.019	-0.020
	p-value	0.218	0.942	0.419	0.287	0.183	0.017	0.176	0.168	NA	0.011	0.454	0.001	0.019	0.034
TAN	Mean Observed (mg-NH3/L)	NA	NA	NA	NA	0.011	0.012	0.015	0.013	0.011	0.013	0.011	0.013	0.012	0.013
	Estimated Change (mg-NH3/L)	NA	NA	NA	NA	-0.002	-0.003	0.002	-0.001	-0.002	-0.001	-0.001	0.000	-0.008	-0.004
	p-value	NA	NA	NA	NA	0.044	0.042	0.443	0.627	0.015	0.470	0.287	0.580	<0.001	<0.001
NO$_3$+NO$_2$	Mean Observed (mg-N/L)	0.060	0.039	0.050	0.037	0.338	0.053	0.101	0.049	0.401	0.157	0.192	0.077	0.086	0.144
	Estimated Change (mg-N/L)	-0.003	0.011	0.003	0.025	0.276	0.034	0.072	0.038	0.334	0.113	0.128	0.046	0.022	0.117
	p-value	0.793	0.414	0.893	0.082	<0.001	<0.001	<0.001	<0.001	<0.001	<0.001	<0.001	<0.001	0.027	<0.001
TP	Mean Observed (mg-P/L)	0.048	0.040	0.040	0.048	0.020	0.019	0.023	0.022	0.018	0.018	0.016	0.020	0.019	0.017
	Estimated Change (mg-P/L)	0.003	-0.009	-0.005	0.009	-0.006	-0.008	-0.003	0.000	0.002	0.003	0.001	0.006	0.004	0.003
	p-value	0.760	0.299	0.560	0.207	0.204	0.118	0.587	0.925	0.146	0.045	0.616	<0.001	0.030	0.048
OP	Mean Observed (mg-P/L)	0.014	0.014	0.011	0.015	0.017	0.016	0.016	0.017	0.014	0.013	0.013	0.014	0.013	0.013
	Estimated Change (mg-P/L)	0.002	0.003	0.000	0.006	0.003	0.003	0.003	0.007	0.003	0.003	0.002	0.004	-0.003	0.003
	p-value	0.152	0.109	0.821	0.021	0.144	0.136	0.120	<0.001	0.002	0.002	0.009	<0.001	0.068	0.018

Table 2.6: Nutrient load (kg ha^{-1} yr^{-1}), the estimated change in load due to treatment calculated from relationships with paired control watershed response (Equation 2.2), and Student's t-test p-value-value results. The estimated change at p-value <0.05 indicates a statistically significant change.

		Post-Road				PH-I				PH-II					
		W1	W2	W4	W7	W1	W2	W4	W7	W1	W2	W4	W5	W6	W7
TKN	Mean Observed	0.859	0.732	0.750	0.365	0.315	0.231	0.177	0.136	NA	0.438	0.524	0.494	0.424	0.366
	Estimated Change	0.243	-0.016	-0.290	-0.141	0.217	0.139	-0.026	0.092	NA	0.088	0.279	0.184	0.079	0.090
	p-value	<0.001	0.665	<0.001	0.004	<0.001	<0.001	<0.001	<0.001	NA	0.006	<0.001	<0.001	0.062	0.010
TAN	Mean Observed	NA	NA	NA	NA	0.075	0.068	0.080	0.053	0.092	0.110	0.096	0.117	0.102	0.098
	Estimated Change	NA	NA	NA	NA	0.004	-0.046	-0.134	0.010	-0.002	-0.032	-0.213	0.029	0.002	0.015
	p-value	NA	NA	NA	NA	0.193	<0.001	<0.001	<0.001	0.649	<0.001	<0.001	<0.001	0.633	<0.001
NO$_3$+NO$_2$	Mean Observed	0.567	0.422	0.321	0.156	2.986	0.352	0.685	0.243	3.952	1.346	1.727	0.664	0.771	1.240
	Estimated Change	-0.302	0.272	-0.059	-0.029	2.396	0.251	0.496	0.196	2.188	1.040	0.931	0.471	0.481	0.882
	p-value	<0.001	<0.001	0.012	0.094	<0.001	<0.001	<0.001	<0.001	<0.001	<0.001	<0.001	<0.001	<0.001	<0.001
TP	Mean Observed	0.246	0.213	0.223	0.109	0.150	0.122	0.123	0.107	0.164	0.185	0.145	0.194	0.159	0.128
	Estimated Change	0.068	0.031	-0.041	-0.020	0.015	-0.016	-0.005	0.033	0.057	0.075	0.041	0.088	0.032	0.027
	p-value	<0.001	<0.001	<0.001	<0.001	0.008	0.002	0.152	<0.001	<0.001	<0.001	<0.001	<0.001	<0.001	<0.001
OP	Mean Observed	0.075	0.085	0.065	0.032	0.117	0.098	0.102	0.073	0.111	0.120	0.106	0.122	0.103	0.088
	Estimated Change	-0.033	-0.003	-0.011	-0.006	-0.007	-0.002	0.027	-0.002	-0.006	0.026	0.018	0.031	0.015	-0.001
	p-value	<0.001	0.607	0.003	0.665	0.173	0.654	<0.001	0.454	0.124	<0.001	<0.001	<0.001	<0.001	0.769

load (Table 2.6) appeared to be relatively stable at the W1 and W6 watersheds. The mean annual TAN load from the W7 watershed during PH-II showed an increase of 0.05 kg.ha^{-1}.yr^{-1} compared to the PH-I period (Table 2.4). Overall, the cumulative mean TAN loads from all watersheds did not show large variations with sequential varying treatments over time (Figure 6.4 in appendix).

2.4.2.3 Nitrate + Nitrite (NO$_3$+NO$_2$)

In contrast to TAN, there was a significant response in NO$_3$+NO$_2$ following timber harvest activities in the MCEW. The response in NO$_3$+NO$_2$ concentrations was negligible at all treatment sites, with W7 showing negligible effects (p-value =0.08), following the road construction activities, however NO$_3$+NO$_2$ concentrations during the PH-I period increased significantly (p-value< 0.001) at all treatment sites (Table 2.5). The largest increase in the mean monthly concentration during the PH-I period was a 0.28 mg-N.L^{-1} increase observed following clear-cut operations at W1. Similar to the PH-I period, all watersheds experienced significant increases in NO$_3$+NO$_2$ concentration during the PH-II treatment period. The greatest response in NO$_3$+NO$_2$ during the PH-II treatment period was a 0.33 mg-N.L^{-1} increase at W1, which is possibly related to the competition release herbicide applied within an original experimental harvest unit. As seen in Figure 2.3, NO$_3$+NO$_2$ concentrations increased at W1 during both phases which were then followed by roughly a 5-year recession back to approximately twice the pre-harvest concentrations. Mean annual NO$_3$+NO$_2$ loads from all watersheds increased considerably, especially, during the PH-I and PH-II treatment periods. Statistically significant increases in NO$_3$+NO$_2$ loads occurred at all the sites (p-value<0.001) during all treatment phases (Table 2.6) with the largest increase of 2.19 kg.ha^{-1}.yr^{-1} and 1.04 kg.ha^{-1}.yr^{-1} occurring at the two headwater sites W1 and W2, respectively. The highest mean annual load of NO$_3$+NO$_2$ occurred at W1 amounting to 3.95 kg.ha^{-1}.yr^{-1} during the PH-II treatment period followed by the

load of 1.73 kg.ha^{-1}.yr^{-1} at W4 during the same treatment period (Table 2.4). Overall, the cumulative mean NO_3+NO_2 load from all the MCEW watersheds followed an increasing trend with initial signs of recovery in W1 after 2014 as indicated by a flattening of the cumulative load curve near the end of the data series (Figure 2.4).
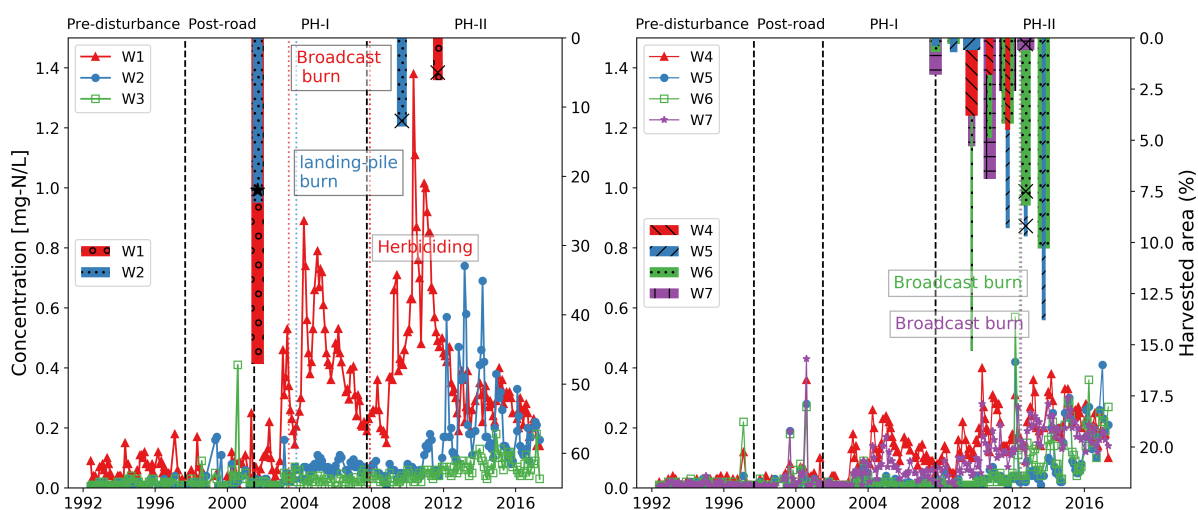
Figure 2.3: Observed monthly stream NO_3+NO_2 concentrations (mg-N.L^{-1}) in MCEW watersheds. The asterisk denotes partial cut and 'x' denotes harvest that includes areas adjacent to the stream harvest.
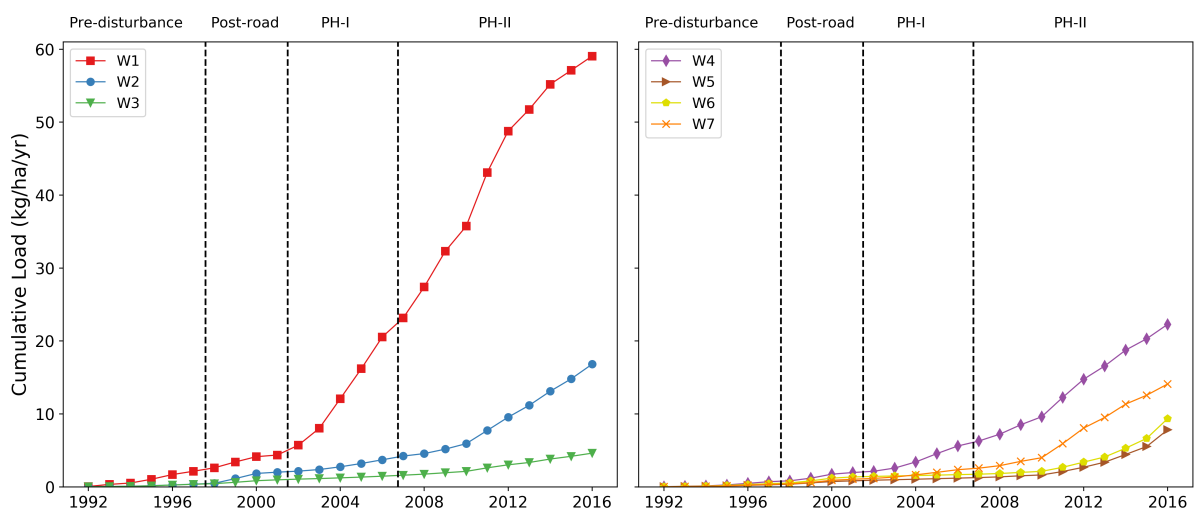
Figure 2.4: Cumulative annual mean NO_3+NO_2 loads from MCEW watersheds.

2.4.2.4   Total Phosphorus (TP)

Mean monthly TP concentrations (Figure 2.5) showed no significant changes in the concentrations during the post-road and PH-I treatment periods. The mean monthly concentration at all treatment sites during the post-road phase was 0.044 mg-P.L^{-1}, which decreased to 0.021 mg-P.L^{-1} during the PH-I phase. However, a statistically significant increase in TP concentrations (0.003 mg-P.L^{-1}, p-value=0.048) and load (0.03 kg.ha^{-1}.yr^{-1}, p-value<0.001) occurred at the downstream cumulative site W7 during PH-II. TP loads increased significantly (p-value<0.001) at all sites during PH-II (Table 2.6). This is also apparent from the cumulative annual mean TP load displayed in Figure 2.6.
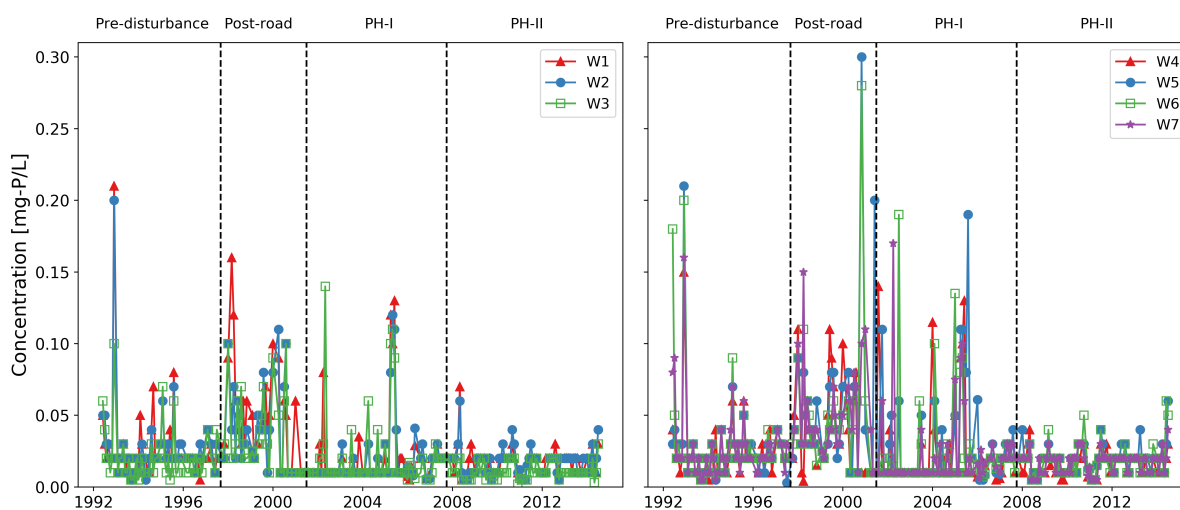
Figure 2.5: Observed monthly stream TP concentrations (mg-P.L^{-1}) in MCEW watersheds.

2.4.2.5   Orthophosphate (OP)

Generally, OP concentrations throughout the study remained near the minimum detectable concentrations (0.01 mg L^{-1}). A statistically significant increase in mean monthly OP concentrations of 0.006 mg-P.L^{-1} and 0.007 mg-P.L^{-1} occurred only at the W7 (cumulative downstream) treatment site during both Post-road (p-value=0.021) and PH-I
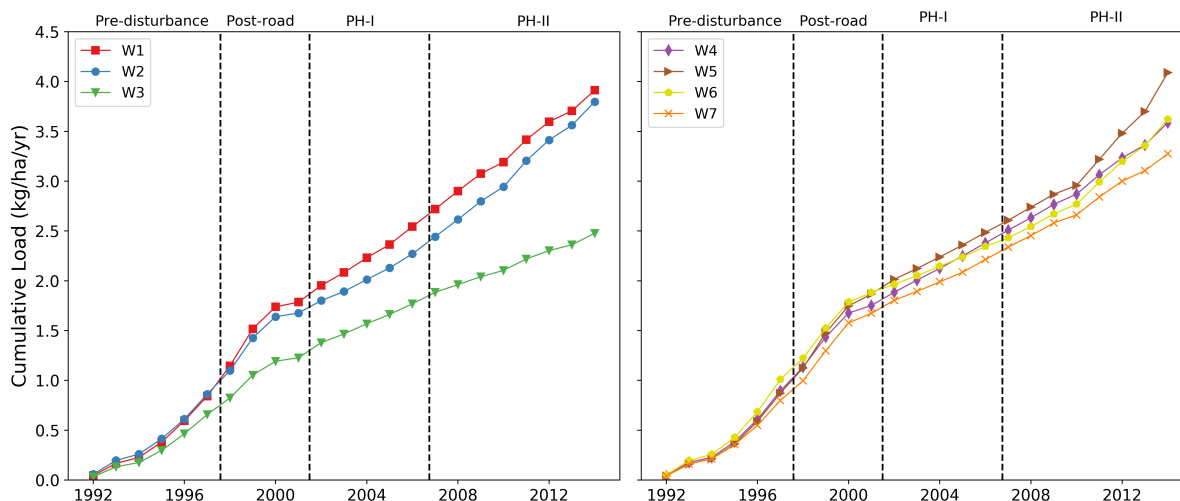
Figure 2.6: Cumulative annual mean TP loads from MCEW watersheds.

(p-value<0.001) treatment periods, respectively. The mean concentrations at all sites were relatively constant at 0.015 mg-P.L^{-1} during both PH-I and PH-II periods. During the PH-II treatment period, however, small but statistically significant, changes in the mean monthly orthophosphate concentrations occurred at all watersheds, except W6 (Table 2.5). A maximum increase of 0.004 mg-P.L^{-1} was observed at the W5 (p-value<0.001) treatment site. Overall, trends in OP concentrations and cumulative annual mean load are shown in Figure 2.7 and Figure 2.8, respectively. Despite relatively small changes in OP concentrations following harvest treatments, the increased streamflow during this time period resulted in increases in OP loads from all of the watersheds, except for W1 and W7, during the PH-II treatment period (Table 2.6). Maximum load of OP occurred at W2 and W5 amounting to 0.12 kg.ha^{-1}.yr^{-1} followed by W4 with 0.11 kg.ha^{-1}.yr^{-1} (Table 2.4). The largest cumulative mean annual loads occurred from the W1 and W5 watersheds (Figure 2.8) and can be largely attributed to the increased flow.
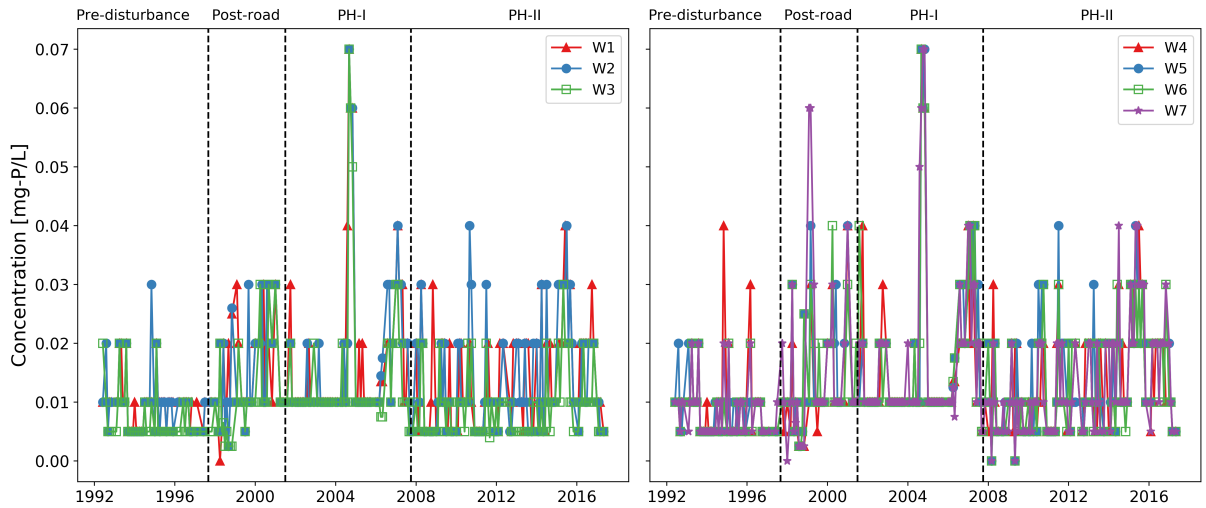
Figure 2.7: Observed monthly stream OP concentrations (mg-P.L^{-1}) in MCEW watersheds.
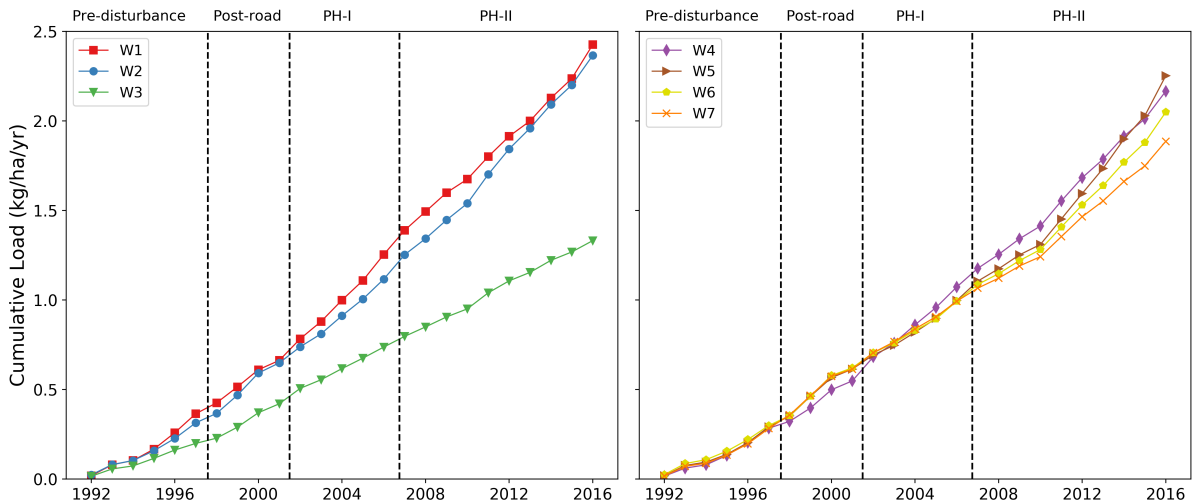
Figure 2.8: Cumulative annual mean OP loads from MCEW watersheds.

2.5 Discussion

The long-term monitoring and assessment of the temporal responses in nutrient concentrations and streamflows from paired and nested watersheds in the MCEW provide important insights into the effects of forest management practices on nutrient loads relative to the response from an undisturbed forest. Through the synthesis of two-and-a-half

decade-long nutrient concentration data in MCEW, we found the greatest response to timber harvest is an increase in NO_3+NO_2 concentrations following clear-cutting and site management operations such as broadcast burning and herbicide application. Although OP concentrations remained near minimum detectable levels, both NO_3+NO_2 and OP loads increased significantly at all locations as a result of the increased streamflows across the MCEW. TP loads observed in this study showed little to no response to the clear-cut harvest and broadcast burning in the MCEW and these findings are consistent with similar findings related to suspended sediment loading [Karwan et al., 2007]. Karwan et al. [2007] reported an increase in sediment loads following the clear-cut harvest for a brief period (1 year) in MCEW which returned to background levels shortly after harvest.

2.5.1 Streamflow

Road construction resulted in a relatively small increase in streamflow in W1 (10.6%) and W2 (11.4%) watersheds as compared to the increase of 33.4% and 21.5% following the PH-I clear cut and partial cut treatments in the respective watersheds. The streamflow in the larger cumulative watersheds W4 and W7 increased by 20.4% and 10.5% during the PH-I phase and by 21.5% and 12.9% during the PH-II phase, respectively. These results are slightly different from the findings of Hubbart et al. [2007] who analyzed data for slightly different treatment periods than the current study and reported similar increases in water yield from W1 and W2 following harvesting. To further identify and separate the impacts of management from annual precipitation on streamflow response, a streamflow index was calculated as the ratio of the annual streamflow at a watershed outlet and the total annual precipitation observed at the Mica Creek SNOTEL station (SNOTEL 623, elevation- 1375 m) (annual Q:P_Mica) (Figure 2.9). No attempt was made to correct the average annual precipitation by elevation or topography and therefore this index should not be used as an absolute predictor of runoff; however, assuming the relative difference

in precipitation across the basin does not differ across years, the efficiency of precipitation capture by the large-volume storage gauge at the SNOTEL site and the accuracy of flow measurements did not change, this index can serve as a reasonable proxy for variability in streamflow response through time. As Figure 2.9 shows, as the percent mature forest cover declines due to timber harvest this streamflow index increases. Interestingly, there is also a small temporal increase in the streamflow index in the control watershed (W3) in MCEW.

To assess whether this increasing trend in streamflow from the control watershed was consistent across the region we also investigated the streamflow from a nearby watershed draining into East Fork Pine Creek (PC) gauge station (USGS 12413370) for the same treatment period. PC is a 72 km^2 watershed located 25 km north of MCEW and is similar in terms of elevation, size, and slope-aspect. The PC streamflow record showed a similar increase in long-term daily streamflow and the streamflow index calculated using MCEW SNOTEL, as observed in W3 in MCEW (see supplemental Figures A.5-A.6). Long-term cumulative outflow plots at each of these stream gauges show an increasing trend in water yield, particularly around 2010, at W3 and W7 in MCEW and PC (see supplemental Figure A.7).

These observations demonstrate the importance of the BACIPS design to account for variations like streamflow through time. Several factors could help explain the relative increase in streamflow observed at W3, and these include: catchments like MCEW and PC are located in the rain-snow transition zone where the hydrologic response is more sensitive to changes in climate; variability caused by El Niño Southern Oscillation (ENSO)/ Pacific Decadal Oscillation (PDO) patterns; changes in the transpiration dynamics of the aging forest [Koch et al., 2004, Naranjo et al., 2012]; observed tree mortality; or minor wind redistribution of snow [Hubbart et al., 2015] from thinned/clear-cut areas adjacent to the mature forest stands. Further data collection and focused research will provide more
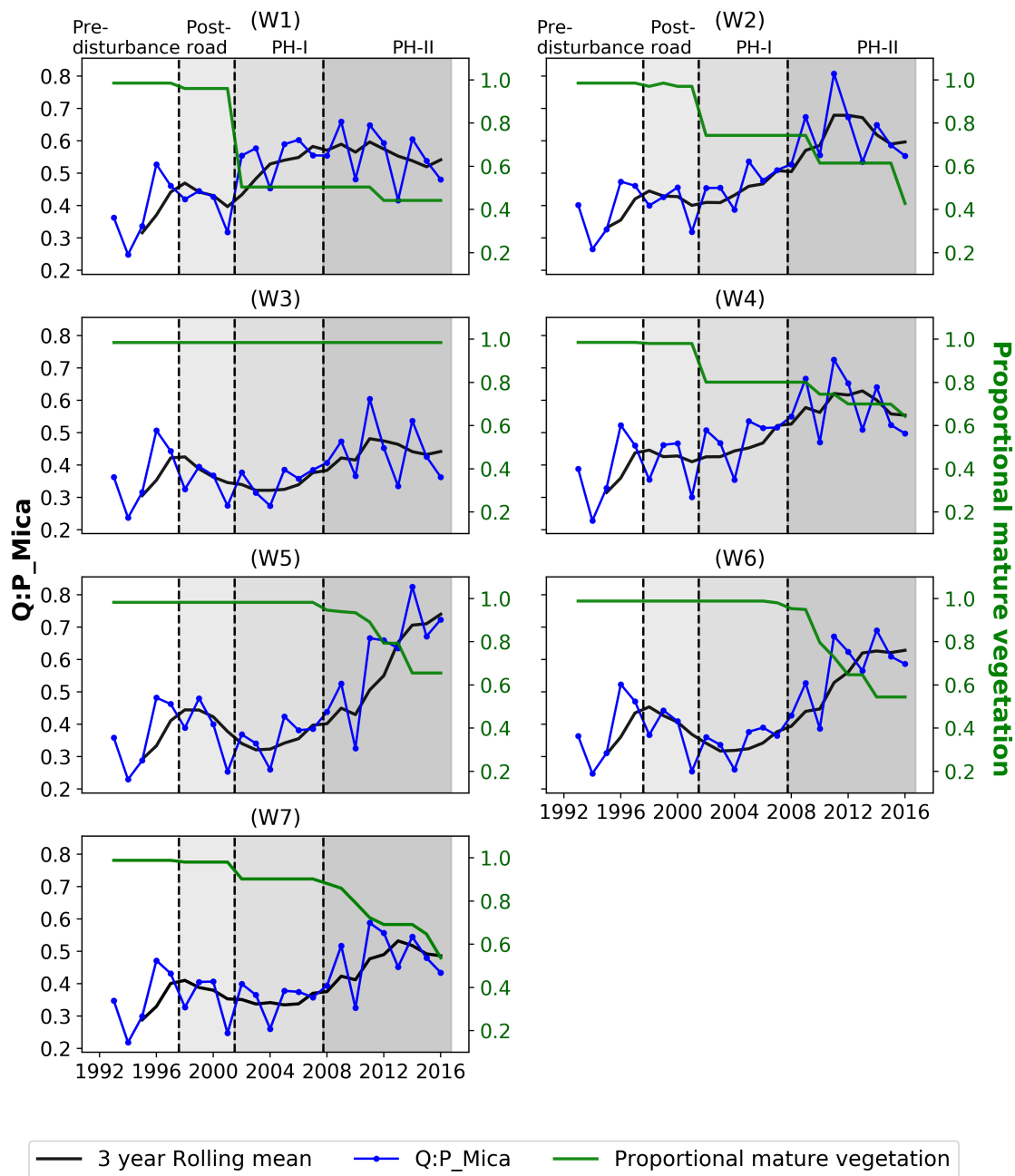
Figure 2.9: Annual streamflow index (ratio of observed annual streamflow to the annual precipitation measured at Mica SNOTEL (623) Q:P_Mica) and percent area covered with mature vegetation in MCEW.

clarity to the causes and persistence of this observed trend of increasing streamflow.

2.5.2 Spatio–temporal dynamics of Nitrogen and Phosphorus

2.5.2.1 Nitrogen

Similar to the streamflow response, forest management activities in MCEW affected the transport of nitrogen from the landscape. During the Pre-disturbance period, NO_3+NO_2 concentrations were low compared to TKN in the MCEW. However, following PH-I and PH-II harvest activities, NO_3+NO_2 became the dominant form of nitrogen in MCEW, with concentrations and loads at some sites more than double the TKN concentrations and loads, respectively (Table 2.5 & Table 2.6). Overall, the observed stream nitrogen concentration in MCEW increased significantly during the different harvest treatment periods. However, there were clear indications of vegetative recovery and decline in NO_3+NO_2 concentration and load particularly at the original experimental PH-I clear-cut sites (e.g. W1).

This increase in stream nitrogen concentration following timber harvest is consistent with other studies that reported increased post-harvest stream nitrogen species. Binkley et al. [2004] reported the mean concentrations of nitrate and dissolved organic nitrogen to be 0.31 mg-N.L^{-1} and 0.32 mg-N.L^{-1}, respectively in forested streams across the United States. Also, mean concentrations of nitrate and dissolved organic nitrogen for the streams draining coniferous forests across the US have been reported to be 0.15 mg-N.L^{-1} and 0.7 mg-N.L^{-1}, respectively [Binkley et al., 2004]. The nitrogen concentrations found in our study were relatively small compared to mean concentrations for forested streams across the US. For example, the TKN concentrations across all the treatment periods and for all watersheds in MCEW were less than 0.18 mg-N.L^{-1}. TAN concentrations during the entire study period, and for all watersheds in MCEW, displayed little variability and were

less than 0.015 mg-N.L^{-1}. These values are consistent with the ammonia concentrations reported by Argerich et al. [2013] who investigated trends in stream nitrogen across the US and found that stream ammonia concentrations in 19 of the 21 study catchments had values of $\leq$ 0.01 mg-N.L^{-1}.

One of the challenges in analyzing long-term water quality data is accounting for changes in the instrumentation used to analyze water samples. Detailed information on the Pre-disturbance ranges and detection limits of methods used for measuring different nutrients are tabulated in Gravelle et al. [2009]. The minimum detection capabilities of instruments in earlier treatment periods appear to have impeded detection of lower concentrations, and therefore small changes in TKN and TAN concentrations. This is evident from the statistically significant changes that occurred during the PH-I and PH-II treatment periods. These changes were captured because during these treatment periods the NCASI laboratory improved the minimum detection capabilities. Similar to TKN and TAN, NO$_3$+NO$_2$ concentrations did not exceed the aforementioned mean nitrate concentration of 0.31 mg-N.L^{-1} except for the W1 watershed where a similar mean concentration of 0.33 mg-N.L^{-1} and 0.4 mg-N.L^{-1} was observed during the PH-I and PH-II treatment periods, respectively. Except for W1 and W4, the observed NO$_3$+NO$_2$ concentrations do not exceed the mean nitrate concentration reported for the forested watersheds in the western United States, 0.18 mg-N.L^{-1} [Binkley et al., 2004].

The naturally consistently high concentrations of nitrogen from the W1 watershed have been largely attributed to the upstream presence of N-fixing alder through additional extensive headwater sampling. Gravelle et al. [2009] have reported the presence of dense alder (*Alnus spp.*) in the riparian areas of MCEW. Several studies have shown a strong relationship between the upstream presence of alder stands, that increase the soil N content, and increased stream nitrogen [Compton et al., 2003, Shaftel et al., 2012]. Atmospheric N deposition is another factor that could contribute to increasing losses of N

especially in the disturbed forest watersheds where the vegetation is unable to utilize the deposited N. A recent study in the Fish Creek watershed in Wyoming reported that 46% of total N input to the watershed was from atmospheric deposition [Eddy-Miller et al., 2016]. In the context of MCEW, to our knowledge, there are no data on atmospheric N deposition that can help elucidate the depositional N contributions to the MCEW watersheds. However, data elsewhere in the region (e.g., National Atmospheric Deposition Program (NADP) site ID02 located in the Priest River Experimental Forest) does suggest increasing trends in total nitrogen deposition largely due to increases in NH_4 deposition. The increased NO_3+NO_2 concentration and loads from all the MCEW could be explained by a reduced uptake of nutrients due to reduced vegetation cover, increased mineralization in the unharvested control watershed due to relatively wetter soils, and nitrification in the litter layer. Many studies have demonstrated that such factors lead to increased nitrogen availability and subsequent transport to the streams [Kreutzweiser et al., 2008, Palviainen et al., 2004, 2005, Piirainen et al., 2007]. However, the elevated NO_3+NO_2 concentration response from W1, following harvest and onset of forest regeneration, appeared to be in a steady recovery (Figure 2.3). The first peak response (PH-I) occurred in 2004 following experimental harvest and broadcast burning, with concentrations receding until late 2008 when increases began to be observed until a second peak (PH-II) occurred in 2010. This second peak exceeded the PH-I peak, and it appears to be associated with the 2007 competition release herbicide application since the PH-II harvest in W1 occurred around 2011. Similar to the PH-I phase, the elevated NO_3+NO_2 concentration receded to about twice the pre-harvest concentration levels within 5 years. This pattern of NO_3+NO_2 response is also reflected at downstream cumulative sites W4 and W7. The stream nitrate recovery observed at MCEW is consistent with previous studies. For example, Oda et al. [2018] reported that nitrate recovery times can range anywhere from 0 to 20 years as a function of both biological processes such as vegetation uptake and hydrological interaction and

transport processes.

Interestingly, similar to streamflow, we also observed a long-term increase in NO_3+NO_2 concentrations at the control watershed (W3) during PH-II. However, much like streamflow, even though there could be factors unique to the catchment, there is also a rationale to believe overall environmental variability is being captured that otherwise would not in a shorter-term, non-BACIPS study design. When looking at mean NO_3+NO_2 concentrations through treatment phases (see Table 2.5), W3 mean NO_3+NO_2 concentrations were 0.07 mg-N.L^{-1} during Pre-disturbance, 0.16 mg-N.L^{-1} during Post-road, 0.10 mg-N.L^{-1} during PH-I, and 0.33 mg-N.L^{-1} during PH-II. What is notable is that the other control watersheds (W5 and W6) showed strikingly similar variability during the first three phases of the study before treatment activities occurred in those watersheds during PH-II. At W5, mean NO_3+NO_2 concentrations were 0.05 mg-N.L^{-1} during Pre-disturbance, 0.14 mg-N.L^{-1} during Post-road, and 0.07 mg-N.L^{-1} during PH-I. At W6, mean NO_3+NO_2 concentrations were 0.08 mg-N.L^{-1} during Pre-disturbance, 0.24 mg-N.L^{-1} during Post-road, and 0.06 mg-N.L^{-1} during PH-I. While it is possible other factors like stand age [Hedin et al., 1994, Vitousek and Reiners, 1975], increased tree mortality, increased decaying downed wood, or increasing alder vegetation could all be contributing factors to the recent W3 increase, further research would be necessary to provide more clarity.

2.5.2.2 Phosphorus

The results of forest management on phosphorus loads were much more subtle than nitrogen. TP concentration in the streams of the MCEW watersheds appeared to be relatively stable during the study period except in the four watersheds (W2, W5, W6 & W7) during PH-II when very small, yet statistically significant, changes occurred. These results are consistent with the findings of a recent study that evaluated long-term regional TP trends across the US and found that a large number of locations in the western US fol-

lowed a general decreasing trend, most of which were statistically insignificant [Sprague and Lorenz, 2009]. The statistically insignificant, yet smaller than reference period, TP concentrations following harvesting are consistent with the TP budgets evaluated before and after logging activities in watersheds of H. J. Andrews Experimental Forest in the western Oregon Cascades [Martin and Harr, 1989]. Martin and Harr [1989] reported OP concentrations from the clear-cut watersheds (0.014 mg/L) comparable to those reported in this study (0.013-0.014 mg/L), but the OP loads were approximately 2-3 times the loads reported in this study. Although these higher loads were irrespective of the harvest and could be related to the consistently higher streamflow reported from the watershed both before and after the clear-cut harvest. Other factors that might explain these higher loads include significantly smaller watershed area ($\sim$ 11 times smaller than the current study) and the OP inputs from precipitation that ranged between 30-43% of the net OP loss from the clear-cut watershed. The inter-annual variability observed in the TP loads during the study periods (Figure 2.6) can be partly associated with the changes in flow and suspended sediment loads. Karwan et al. [2007] assessed the effects of timber harvest on suspended sediment load in MCEW and found that the clear-cut harvesting produced a significantly higher suspended sediment load, but its magnitude returned to that of the pre-treatment sediment load within a year after harvesting. In the case of the partial-cut treatment, no significant differences in monthly sediment load were found between the treatment and control sites. The relatively stable TP concentrations and inter-annual variability of TP loads presented here are congruent with the aforementioned study that evaluated the effects of timber harvests on suspended sediment loads.

The pre-harvest OP concentrations found in MCEW were similar to the mean of 0.014 mg-P.L^{-1} for streams draining forests across the US, the mean of 0.01 mg-P.L^{-1} for the streams draining coniferous forests in general, and the regional mean concentration of 0.008 mg-P.L^{-1} reported for forest streams in the western US [Binkley et al., 2004].

Although OP concentrations from the control watershed W3 also showed a very slight increase, and this could again be related to minimum detectable limits, climatic variation, or some combination of soil mineralization processes. OP concentrations remained similar across the study area irrespective of treatment and time (Figure 2.7). Any calculated increased loads of orthophosphate from MCEW were essentially driven by increases in streamflow.

2.5.2.3 Longitudinal and adjacency effects

Although interesting long-term nutrient responses were observed in both upstream (W1, W2, W3) and downstream cumulative (W4, W7) watersheds, nutrient concentrations were generally lower in the downstream watersheds than the upstream headwater watersheds (Figure 2.10). This attenuating effect at a longitudinal scale can also be seen in mean annual load estimates (Table 2.4), where the loads of NO_3+NO_2 and OP decreases as one moves longitudinally down the stream network (e.g. during PH-II NO_3+NO_2 moves from 3.95 kg.ha^{-1}.yr^{-1} at W1 downstream to 1.73 kg.ha^{-1}.yr^{-1} at W4 to 1.24 kg.ha^{-1}.yr^{-1} at W7). This can be partly attributed to the dilution effect and in-stream processing as the water flows downstream. Studies have shown the magnitude of nutrient concentrations tends to decrease with an increase in the catchment area [Jacobs et al., 2017], and the presence of denitrification and assimilation processes can substantially reduce the nitrate concentrations in streams [Shinozuka et al., 2017]. Bernhardt et al. [2003] noted that the absence of in-stream processing would have increased the loads of nitrate-nitrogen from the Hubbard Brook Experimental Forest by about 80-140%. Furthermore, although the streambed occupies a small fraction of the watershed, generally streambed sediments store significant amounts of phosphorus. For example, a study in a nutrient-impacted catchment by Lannergård et al. [2020] reported high proportions of organic and iron-bound phosphorus in the sediments of forested headwater streams.
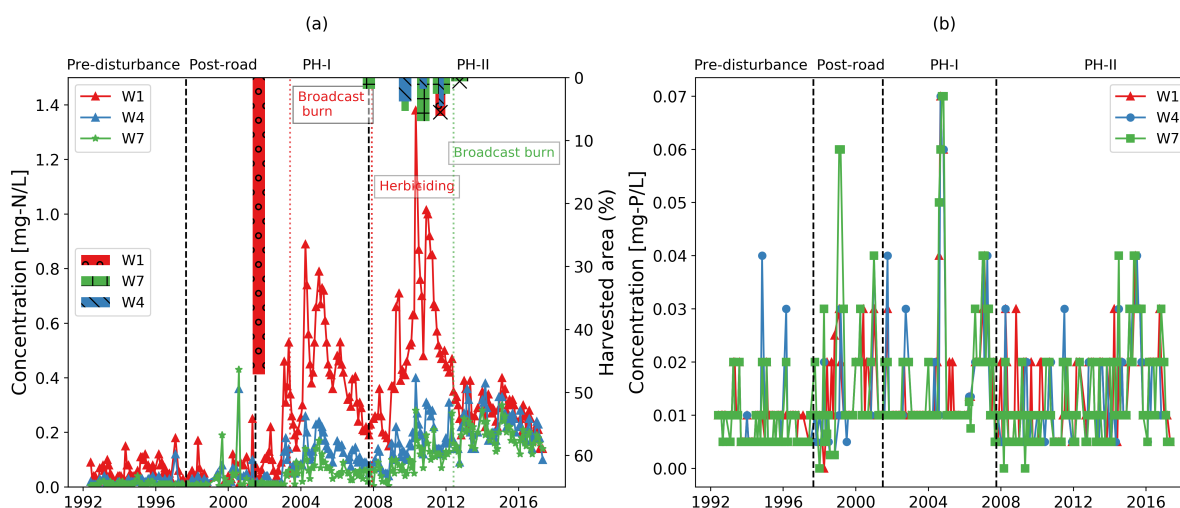
Figure 2.10: Response in space and time of commercial forest management practices on NO3+NO2 (a) and OP (b) concentrations.

It is likely that not only does the harvest intensity, but also the location of the harvest relative to the stream plays a critical role in explaining the nutrient concentration dynamics and recovery in the stream. This is evident in W2 (see Figure 2.3) where the higher intensity coupled with the harvest adjacent to the stream showed relatively strong (albeit slightly delayed) NO_3+NO_2 response and longer recovery times compared to the Phase-I response and recovery. Similarly, in W1 after the competition release herbicide application, the NO_3+NO_2 concentration recession curve was interrupted when a PH-II harvest was conducted near the W1 sampling point. Similar response signals caused by the proximity of the harvest to the flume sampling points can be noticed in the NO_3+NO_2 response from W5, W6, and W7 (see Figure 2.3). However, isolation of these adjacent harvest responses is confounded by the simultaneous PH-II forest management activities occurring further upstream within these watersheds.

2.5.2.4   Land use and nutrient response

Although evaluation of the nutrient response between different land uses is beyond the scope of this study, it is important to put these findings in a larger perspective. Previous studies have all suggested that compared to the forest-dominated watersheds, the magnitude of nitrate-nitrite N, soluble reactive phosphorus, and TP concentrations and loads are higher in urban [Brett et al., 2005, Duan et al., 2012, Poor and McDonnell, 2007] and agriculture[McColl et al., 1977, Poor and McDonnell, 2007, Quinn and Stroud, 2002, Verheyen et al., 2015] dominated watersheds. Comparatively, the nutrient concentrations in the forested MCEW streams are much lower than streams draining agricultural and urban watersheds. However, the slight increase in nutrient loads in this study is similar to the recent observations of nutrient buildup and subsequent loads from undisturbed forests elsewhere in the US [Loupe et al., 2007, Miller et al., 2005]. Due to both a temporary effect and substantial longitudinal nutrient uptake observed in remote forestland streams like MCEW streams, any potential downstream negative effects will depend on proximity to municipalities and other areas of concern (e.g. lakes). A recent survey of undeveloped water bodies across the US indicates that between 2004 and 2014 the percentage of stream length that is naturally oligotrophic (TP $\sim$ 0.01 mg-P/L) has decreased by 23.8% and the percent of naturally oligotrophic lakes has decreased by 18.2% between 2007 and 2012 [Stoddard et al., 2016]. This further emphasizes the need for understanding the sources and processes that affect nutrient dynamics and management approaches for nutrient loads from forested systems. This is becoming an increasing concern for municipalities across the US that are considering localized forest fuel management strategies to lower the risk and impact of wildfire within their municipal water supplies [Smith et al., 2011, Warziniack and Thompson, 2013]. Approximately 80 percent of the drinking water supply across the US originates from forested lands providing drinking water to more than

68,000 communities [USFS, 2020]. Annual costs of eutrophication of US fresh water from excessive nutrient loading is estimated to be \$830 million and it is likely to be significantly higher in regions affected by wildfires [Bladon et al., 2014]. Estimates suggest that after a wildfire the increase in the sediment load can range between 1 to 1459 fold of unburned conditions. Similarly, the increase in the NO_3 and TP loads can range between 3 to 250 fold and 0.3 to 431 fold of unburned conditions respectively [Smith et al., 2011]. In contrast to these wildfire impacts, timber harvesting resulted in a relatively low increase in NO_3+NO_2 (4.9 to 19 fold) and TP (0.66 to 1.25-fold) loads compared to the Pre-disturbance phase. Municipalities must weigh the risk and impact of localized forest thinning strategies on their water quality and quantity relative to the potential impacts of catastrophic wildfire events.

2.6   Conclusions

Understanding stream nutrient concentration dynamics and nutrient loads from watersheds draining relatively undisturbed, as well as actively managed forests using contemporary management practices, is imperative to improve management of land resources and downstream water quality. A quarter-century of monitoring at MCEW provided an important understanding of the background nutrient concentrations in relatively undisturbed forests as well as the effect that contemporary commercial forest management activities have on nutrient response and loads. Overall, the contemporary commercial forest management practices applied in the MCEW resulted in relatively small increases in nutrient loads and suggest that Idaho Forest Practices Act regulations and BMPs are effective in minimizing the delivery of particulate-bound pollutants. Statistically significant increases in stream NO_3+NO_2 concentrations and loads were observed following timber harvest treatments. In the case of OP, concentrations remained near minimum detectable concentrations. Longitudinal evaluation of stream nutrient concentrations indicates in-

stream dilution and nutrient assimilation processes. The unharvested control watershed also displayed increases in concentration, streamflow, and loads of NO_3+NO_2. This increase, however, was smaller than in the harvested watersheds and potentially driven by a combination of climatic variability and subtle forest changes, further demonstrating the effectiveness of employing a BACIPS design for long-term watershed evaluation. In summary, contemporary forest management activities increased stream NO_3+NO_2 concentrations and loads following timber harvest activities, but these effects are also attenuated in downstream reaches. Seasonal effects and factors like instream processes and atmospheric deposition may also influence stream nutrient dynamics. Further research is needed to disaggregate and understand the effects of these processes on the stream nutrient dynamics.

References

J. K. Agee and C. N. Skinner. Basic principles of forest fuel reduction treatments. In *Forest Ecology and Management*, volume 211, pages 83–96. Elsevier, jun 2005. ISBN 0378-1127. doi: 10.1016/j.foreco.2005.01.034. URL `https://www.sciencedirect.com/science/article/pii/S0378112705000411?via{\%}3Dihub{\#}bib13`.

C. Akselsson, O. Westling, and G. Örlander. Regional mapping of nitrogen leaching from clearcuts in southern Sweden. *Forest Ecology and Management*, 202(1-3):235–243, dec 2004. ISSN 03781127. doi: 10.1016/j.foreco.2004.07.025. URL `https://www.sciencedirect.com/science/article/pii/S0378112704005432?via{\%}3Dihub`.

C. J. Anderson and B. G. Lockaby. Research gaps related to forest management and stream sediment in the United States. *Environmental Management*, 47(2):303–313, feb 2011. ISSN 0364152X. doi: 10.1007/s00267-010-9604-1. URL `http://link.springer.com/10.1007/s00267-010-9604-1`.

A. Argerich, S. L. Johnson, S. D. Sebestyen, C. C. Rhoades, E. Greathouse, J. D. Knoepp, M. B. Adams, G. E. Likens, J. L. Campbell, W. H. McDowell, F. N. Scatena, and G. G. Ice. Trends in stream nitrogen concentrations for forested reference catchments across the USA. *Environmental Research Letters*, 8(1):014039, mar 2013. ISSN 17489326. doi: 10.1088/1748-9326/8/1/014039. URL `http://stacks.iop.org/1748-9326/8/i=1/a=014039?key=crossref.3217949ec712e5f36885b6dd262dfebb`.

J. Artigas, E. García-Berthou, D. E. Bauer, M. I. Castro, J. Cochero, D. C. Colautti, A. Cortelezzi, J. C. Donato, A. Elosegi, C. Feijoó, A. Giorgi, N. Gómez, L. Leggieri, I. Muñoz, A. Rodrigues-Capítulo, A. M. Romaní, and S. Sabater. Global pressures, specific responses: Effects of nutrient enrichment in streams from different biomes. *Environmental Research Letters*, 8(1), 2013. ISSN 17489326. doi: 10.1088/1748-9326/

8/1/014002. URL `http://iopscience.iop.org/article/10.1088/1748-9326/8/1/014002/pdf`.

B. P. Baldigo, P. S. Murdoch, and D. A. Burns. Stream acidification and mortality of brook trout (Salvelinus fontinalis) in response to timber harvest in Catskill Mountain watersheds, New York, USA. *Canadian Journal of Fisheries and Aquatic Sciences*, 62(5):1168–1183, 2005. ISSN 0706-652X. doi: 10.1139/f05-022. URL `http://www.nrcresearchpress.com/doi/pdf/10.1139/f05-022http://www.nrcresearchpress.com/doi/abs/10.1139/f05-022`.

M. A. Bari, N. Smith, J. K. Ruprecht, and B. W. Boyd. Changes in streamflow components following logging and regeneration in the southern forest of Western Australia. *Hydrological Processes*, 10(3):447–461, mar 1996. ISSN 08856087. doi: 10.1002/(SICI)1099-1085(199603)10:3⟨447::AID-HYP431⟩3.0.CO;2-1. URL `http://doi.wiley.com/10.1002/{\%}28SICI{\%}291099-1085{\%}28199603{\%}2910{\%}3A3{\%}3C447{\%}3A{\%}3AAID-HYP431{\%}3E3.0.CO{\%}3B2-1`.

B. J. Bentz, J. Régnière, C. J. Fettig, E. M. Hansen, J. L. Hayes, J. A. Hicke, R. G. Kelsey, J. F. Negrón, and S. J. Seybold. Climate Change and Bark Beetles of the Western United States and Canada: Direct and Indirect Effects. *BioScience*, 60(8): 602–613, 2010. doi: 10.1525/bio.2010.60.8.6. URL `www.biosciencemag.org`.

E. S. Bernhardt, G. E. Likens, D. C. Buso, and C. T. Driscoll. In-stream uptake dampens effects of major forest disturbance on watershed nitrogen export. *Proceedings of the National Academy of Sciences*, 100(18):10304–10308, 2003. ISSN 0027-8424. doi: 10.1073/pnas.1233676100. URL `http://www.pnas.org/content/pnas/100/18/10304.full.pdfhttp://www.pnas.org/cgi/doi/10.1073/pnas.1233676100`.

I. Bhangu and P. H. Whitfield. Seasonal and long-term variations in water quality of

the Skeena River at Usk, British Columbia. *Water Research*, 31(9):2187–2194, sep 1997. ISSN 00431354. doi: 10.1016/S0043-1354(97)00063-8. URL `https://www.sciencedirect.com/science/article/pii/S0043135497000638?via{\%}3Dihub`.

D. Binkley. Patterns and processes of variation in nitrogen and phosphorus concentrations in forested streams. *Technical Bulletin of the National Council for Air and Stream Improvement*, 836(836):143, 2001. ISSN 08860882.

D. Binkley, G. G. Ice, J. Kaye, and C. A. Williams. Nitrogen and phosphorus concentrations in forest streams of the United States. *Journal of the American Water Resources Association*, 40(5):1277–1291, oct 2004. ISSN 1093-474X. doi: 10.1111/j.1752-1688.2004.tb01586.x. URL `http://doi.wiley.com/10.1111/j.1752-1688.2004.tb01586.x`.

K. D. Bladon, M. B. Emelko, U. Silins, and M. Stone. Wildfire and the future of water supply. *Environmental Science and Technology*, 48(16):8936–8943, 2014. ISSN 15205851. doi: 10.1021/es500130g. URL `https://pubs.acs.org/sharingguidelines`.

J. Boggs, G. Sun, and S. McNulty. Effects of Timber Harvest on Water Quantity and Quality in Small Watersheds in the Piedmont of North Carolina. *Journal of Forestry*, 114(1):27–40, 2016. ISSN 00221201. doi: 10.5849/jof.14-102. URL `https://www.srs.fs.usda.gov/pubs/ja/2015/ja{\_}2015{\_}boggs{\_}002.pdfhttp://openurl.ingenta.com/content/xref?genre=article{\&}issn=0022-1201{\&}volume=114{\&}issue=1{\&}spage=27`.

M. T. Brett, G. B. Arhonditsis, S. E. Mueller, D. M. Hartley, J. D. Frodge, and D. E. Funke. Non-point-source impacts on stream nutrient concentrations along a forest to urban gradient. *Environmental Management*, 35(3):330–342, 2005. ISSN 0364152X. doi: 10.1007/s00267-003-0311-z.

G. Certini. Effects of fire on properties of forest soils: A review. *Oecologia*, 143(1):1–10, mar 2005. ISSN 00298549. doi: 10.1007/s00442-004-1788-8. URL `https://link.springer.com/article/10.1007/s00442-004-1788-8`.

B. J. Collins, C. C. Rhoades, M. A. Battaglia, and R. M. Hubbard. The effects of bark beetle outbreaks on forest development, fuel loads and potential fire behavior in salvage logged and untreated lodgepole pine forests. *Forest Ecology and Management*, 284:260–268, nov 2012. ISSN 03781127. doi: 10.1016/j.foreco.2012.07.027. URL `https://www.sciencedirect.com/science/article/pii/S037811271200432X`.

J. E. Compton, M. R. Church, S. T. Larned, and W. E. Hogsett. Nitrogen Export from Forested Watersheds in the Oregon Coast Range: The Role of N2-fixing Red Alder. *Ecosystems*, 6(8):773–785, 2003. ISSN 14329840. doi: 10.1007/s10021-002-0207-4. URL `http://www.fsl.orst.edu/rna/Documents/publications/NitrogenexportfromforestedwatershedsintheOregoncoastrangetheroleofN2-fixingRedalder.pdf`.

R. A. Dahlgren. Effects of forest harvest on stream-water quality and nitrogen cycling in the Caspar Creek watershed. *USDA Forest Service General Technical Report PSW*, (8): 45–53, 1998. URL `https://www.fs.fed.us/psw/publications/documents/psw{\_}gtr168/06dahlgren.pdfhttp://search.proquest.com/docview/52461961?accountid=14439`.

S. Duan, S. S. Kaushal, P. M. Groffman, L. E. Band, and K. T. Belt. Phosphorus export across an urban to rural gradient in the Chesapeake Bay watershed. *Journal of Geophysical Research: Biogeosciences*, 117(1):1–12, 2012. ISSN 01480227. doi: 10.1029/2011JG001782.

N. M. Dubrovsky, K. R. Burow, G. M. Clark, J. M. Gronberg, H. P.A., K. J. Hitt, D. K.

Mueller, M. D. Munn, B. T. Nolan, L. J. Puckett, M. G. Rupert, T. M. Short, N. E. Spahr, L. A. Sprague, and W. G. Wilber. *The quality of our Nation's waters—Nutrients in the Nation's streams and groundwater, 1992–2004: U.S. Geological Survey Circular 1350.* 2010. ISBN 9781411329041. URL `http://water.usgs.gov/nawqa/nutrients/pubs/circ1350http://pubs.usgs.gov/fs/2010/3078/`.

C. A. Eddy-Miller, R. Sando, M. J. MacDonald, and C. E. Girard. Prepared in cooperation with Teton Conservation District Estimated Nitrogen and Phosphorus Inputs to the Fish Creek Watershed, Teton County, Wyoming, 2009–15. Technical report, U.S. Geological Survey, 2016. URL `https://pubs.er.usgs.gov/publication/sir20165160`.

M. B. Emelko, M. Stone, U. Silins, D. Allin, A. L. Collins, C. H. Williams, A. M. Martens, and K. D. Bladon. Sediment-phosphorus dynamics can shift aquatic ecology and cause downstream legacy effects after wildfire in large river systems. *Global Change Biology*, 22(3):1168–1184, mar 2016. ISSN 13652486. doi: 10.1111/gcb.13073. URL `http://doi.wiley.com/10.1111/gcb.13073`.

M. C. Feller. Forest harvesting and streamwater inorganic chemistry in western north america: A Review. *Journal of the American Water Resources Association*, 41(4): 785–811, aug 2005. ISSN 1093-474X. doi: 10.1111/j.1752-1688.2005.tb03771.x. URL `http://doi.wiley.com/10.1111/j.1752-1688.2005.tb03771.x`.

B. M. Gannon, Y. Wei, L. H. Macdonald, S. K. Kampf, K. W. Jones, J. B. Cannon, B. H. Wolk, A. S. Cheng, R. N. Addington, and M. P. Thompson. Prioritising fuels reduction for water supply protection. *International Journal of Wildland Fire*, 28(10):785–803, nov 2019. ISSN 10498001. doi: 10.1071/WF18182. URL `http://www.publish.csiro.au/?paper=WF18182`.

J. A. Gravelle, G. Ice, T. E. Link, and D. L. Cook. Nutrient concentration dynamics in

an inland Pacific Northwest watershed before and after timber harvest. *Forest Ecology and Management*, 257(8):1663–1675, 2009. ISSN 03781127. doi: 10.1016/j.foreco.2009. 01.017.

D. W. Hallema, G. Sun, P. V. Caldwell, S. P. Norman, E. C. Cohen, Y. Liu, K. D. Bladon, and S. G. McNulty. Burned forests impact water supplies. *Nature Communications*, 9(1):1–8, dec 2018. ISSN 20411723. doi: 10.1038/s41467-018-03735-6. URL `www.nature.com/naturecommunications`.

K. H. Hamed and R. A. Rao. A modified Mann-Kendall trend test for autocorrelated data. *Journal of Hydrology*, 204(1-4):182–196, jan 1998. ISSN 00221694. doi: 10. 1016/S0022-1694(97)00125-X. URL `http://linkinghub.elsevier.com/retrieve/pii/S002216949700125X`.

L. O. Hedin, L. Granat, G. E. Likens, T. Adri Buishand, J. N. Galloway, T. J. Butler, and H. Rodhe. Steep declines in atmospheric base cations in regions of Europe and North America. *Nature*, 367(6461):351–354, jan 1994. ISSN 0028-0836. doi: 10.1038/367351a0. URL `http://www.nature.com/doifinder/10.1038/367351a0`.

J. D. Hewlett, H. W. Lull, and K. G. Reinhart. In Defense of Experimental Watersheds. *Water Resources Research*, 5(1):306–316, feb 1969. ISSN 19447973. doi: 10.1029/ WR005i001p00306. URL `http://doi.wiley.com/10.1029/WR005i001p00306`.

J. A. Hubbart, T. E. Link, J. A. Gravelle, and W. J. Elliot. Timber harvest impacts on water yield in the continental/maritime hydroclimatic region of the United States. *Forest Science*, 53(2):169–180, apr 2007. ISSN 0015749X. doi: 10.1093/forestscience/53.2.169. URL `https://academic.oup.com/forestscience/article/53/2/169/4604383`.

J. A. Hubbart, T. E. Link, and J. A. Gravelle. Forest canopy reduction and snowpack dynamics in a Northern Idaho watershed of the continental-maritime region, United

States. *Forest Science*, 61(5):882–894, oct 2015. ISSN 0015749X. doi: 10.5849/forsci. 14-025. URL `https://academic.oup.com/forestscience/article/61/5/882-894/4583849`.

E. L. Huffman, L. H. MacDonald, and J. D. Stednick. Strength and persistence of fire-induced soil hydrophobicity under ponderosa and lodgepole pine, Colorado Front Range. *Hydrological Processes*, 15(15):2877–2892, oct 2001. ISSN 08856087. doi: 10.1002/hyp.379. URL `https://onlinelibrary.wiley.com/doi/full/10.1002/hyp.379https://onlinelibrary.wiley.com/doi/abs/10.1002/hyp.379https://onlinelibrary.wiley.com/doi/10.1002/hyp.379`.

C. Huston and E. Juarez-Colunga. Guidelines for computing summary statistics for datasets containing non-detects. Technical report, Bulkley Valley Research Center, 2009. URL `http://bvcentre.ca/files/research{\_}reports/08-03GuidanceDocument.pdf`.

G. Ice and D. Binkley. Forest Streamwater Concentrations of Nitrogen and Phosphorus: A Comparison with EPA's Proposed Water Quality Criteria. *Journal of Forestry*, 101 (1):21–28, 2003. URL `http://www.ingentaconnect.com/content/saf/jof/2003/00000101/00000001/art00008{\#}`.

Idaho Administrative Procedures Act (IDAPA). Rules pertaining to the idaho forest practices act. Technical report, BOISE, ID, 2020. URL `https://adminrules.idaho.gov/rules/2011/20/0201.pdf`.

Idaho Department of Lands (IDL). *Forest practices cumulative watershed effects process for Idaho*. Idaho Department of Lands, Boise, ID, 2000. URL `https://books.google.com/books?id=6PYrAQAAMAAJ`.

S. R. Jacobs, L. Breuer, K. Butterbach-Bahl, D. E. Pelster, and M. C. Rufino. Land

use affects total dissolved nitrogen and nitrate concentrations in tropical montane streams in Kenya. *Science of the Total Environment*, 603-604:519–532, dec 2017. ISSN 18791026. doi: 10.1016/j.scitotenv.2017.06.100. URL `https://www.sciencedirect.com/science/article/pii/S0048969717315048`.

D. W. Johnson, W. W. Miller, B. M. Rau, and M. W. Meadows. The nature and potential causes of nutrient hotspots in a Sierra Nevada forest soil. *Soil Science*, 176(11):596–610, 2011. ISSN 0038075X. doi: 10.1097/SS.0b013e31823120a2.

H. Jones, P. Visoottiviseth, M. K. Bux, R. Födényi, N. Kováts, G. Borbély, and Z. Galbács. Case reports: arsenic pollution in Thailand, Bangladesh, and Hungary. *Reviews of environmental contamination and toxicology*, 197:163–87, jan 2008. ISSN 0179-5953. URL `http://www.ncbi.nlm.nih.gov/pubmed/18983000`.

D. L. Karwan, J. A. Gravelle, and J. A. Hubbart. Effects of timber harvest on suspended sediment loads in Mica Creek, Idaho. *Forest Science*, 53(2):181–188, 2007. ISSN 0015749X.

G. W. Koch, S. C. Stillet, G. M. Jennings, and S. D. Davis. The limits to tree height. *Nature*, 428(6985):851–854, apr 2004. ISSN 00280836. doi: 10.1038/nature02417. URL `http://www.nature.com/articles/nature02417`.

P. Kortelainen, T. Mattsson, L. Finér, M. Ahtiainen, S. Saukkonen, and T. Sallantaus. Controls on the export of C, N, P and Fe from undisturbed boreal catchments, Finland. *Aquatic Sciences*, 68(4):453–468, dec 2006. ISSN 10151621. doi: 10.1007/s00027-006-0833-6. URL `http://link.springer.com/10.1007/s00027-006-0833-6`.

D. P. Kreutzweiser, P. W. Hazlett, and J. M. Gunn. Logging impacts on the biogeochemistry of boreal forest soils and nutrient export to aquatic systems: A review. *Environmental Reviews*, 16(NA):157–179, dec 2008. ISSN 1208-6053. doi: 10.1139/A08-

006. URL `http://www.nrcresearchpress.com/doi/10.1139/A08-006http://www.nrcresearchpress.com/doi/abs/10.1139/A08-006`.

M. D. Kunze and J. D. Stednick. Streamflow and suspended sediment yied following the 2000 Bobcat fire, Colorado. *Hydrological Processes*, 20(8):1661–1681, may 2006. ISSN 08856087. doi: 10.1002/hyp.5954. URL `http://doi.wiley.com/10.1002/hyp.5954`.

E. E. Lannergård, O. Agstam-Norlin, B. J. Huser, S. Sandström, J. Rakovic, and M. N. Futter. New Insights Into Legacy Phosphorus From Fractionation of Streambed Sediment. *Journal of Geophysical Research: Biogeosciences*, 125(9), sep 2020. ISSN 2169-8953. doi: 10.1029/2020JG005763. URL `https://onlinelibrary.wiley.com/doi/10.1029/2020JG005763`.

A. Lintern, J. Webb, D. Ryu, S. Liu, U. Bende-Michl, D. Waters, P. Leahy, P. Wilson, and A. W. Western. Key factors influencing differences in stream water quality across space. *Wiley Interdisciplinary Reviews: Water*, 5(1):e1260, jan 2017. ISSN 20491948. doi: 10.1002/wat2.1260. URL `http://doi.wiley.com/10.1002/wat2.1260`.

C. Loehle, T. B. Wigley, A. Lucier, E. Schilling, R. J. Danehy, and G. Ice. Toward improved water quality in forestry: Opportunities and challenges in a changing regulatory environment. *Journal of Forestry*, 112(1):41–47, jan 2014. ISSN 00221201. doi: 10.5849/jof.12-111. URL `https://academic.oup.com/jof/article/112/1/41-47/4599696`.

T. M. Loupe, W. W. Miller, D. W. Johnson, E. M. Carroll, D. Hanseder, D. Glass, and R. F. Walker. Inorganic nitrogen and phosphorus in Sierran forest O horizon leachate. *Journal of environmental quality*, 36(2):498–507, 2007. ISSN 0047-2425. doi: 10.2134/jeq2005.0465. URL `http://www.ncbi.nlm.nih.gov/pubmed/17332254`.

C. W. Martin and R. D. Harr. Logging of mature Douglas-fir in western Oregon has

little effect on nutrient output budgets. *Canadian Journal of Forest Research*, 19(1): 35–43, 1989. ISSN 0045-5067. doi: 10.1139/x89-005. URL `https://andrewsforest.oregonstate.edu/sites/default/files/lter/pubs/pdf/pub974.pdf`.

C. W. Martin, J. W. Hornbeck, G. E. Likens, and D. C. Buso. Impacts of intensive harvesting on hydrology and nutrient dynamics of northern hardwood forests. *Canadian Journal of Fisheries and Aquatic Sciences*, 57(S2):19–29, sep 2000. ISSN 12057533. doi: 10.1139/cjfas-57-S2-19. URL `http://www.nrcresearchpress.com/doi/10.1139/f00-106`.

D. A. Martin and J. A. Moody. Comparison of soil infiltration rates in burned and unburned mountainous watersheds. *Hydrological Processes*, 15(15):2893–2903, 2001. ISSN 08856087. doi: 10.1002/hyp.380.

R. H. McColl, E. White, and A. R. Gibson. Phosphorus and nitrate run-off in hill pasture and forest catchments, Taita, New Zealand. *New Zealand Journal of Marine and Freshwater Research*, 11(4):729–744, 1977. ISSN 11758805. doi: 10.1080/00288330. 1977.9515709.

M. W. Menberu, H. Marttila, T. Tahvanainen, J. S. Kotiaho, R. Hokkanen, B. Kløve, and A. K. Ronkanen. Changes in Pore Water Quality After Peatland Restoration: Assessment of a Large-Scale, Replicated Before-After-Control-Impact Study in Finland. *Water Resources Research*, 53(10):8327–8343, oct 2017. ISSN 19447973. doi: 10.1002/ 2017WR020630. URL `http://doi.wiley.com/10.1002/2017WR020630`.

W. W. Miller, D. W. Johnson, C. Denton, P. S. Verburg, G. L. Dana, and R. F. Walker. Inconspicuous nutrient laden surface runoff from mature forest Sierran watersheds. *Water, Air, and Soil Pollution*, 163(1-4):3–17, may 2005. ISSN 00496979. doi: 10.1007/ s11270-005-7473-7. URL `http://link.springer.com/10.1007/s11270-005-7473-7`.

W. W. Miller, D. W. Johnson, T. M. Loupe, J. S. Sedinger, E. M. Carroll, J. D. Murphy, R. F. Walker, and D. Glass. Nutrients flow from runoff at burned forest site in Lake Tahoe Basin. *California Agriculture*, 60(2):65–71, 2006. ISSN 0008-0845. doi: 10.3733/ca.v060n02p65.

W. G. Minshall, J. T. Brock, D. A. Andrews, and C. T. Robinson. Water quality, substratum and biotic responses of five central Idaho (USA) streams during the first year following the Mortar Creek fire. *International Journal of Wildland Fire*, 10:185–199, 2001. doi: 10.1071/WF01017. URL `https://www.publish.csiro.au/wf/pdf/WF01017`.

J. D. Murphy, D. W. Johnson, W. W. Miller, R. F. Walker, E. F. Carroll, and R. R. Blank. Wildfire Effects on Soil Nutrients and Leaching in a Tahoe Basin Watershed. *Journal of Environment Quality*, 35(2):479, 2006. ISSN 1537-2537. doi: 10.2134/jeq2005.0144. URL `https://pubag.nal.usda.gov/download/7327/PDFhttps://www.agronomy.org/publications/jeq/abstracts/35/2/479`.

S. A. Nagorski, J. N. Moore, T. E. McKinnon, and D. B. Smith. Geochemical response to variable streamflow conditions in contaminated and uncontaminated streams. *Water Resources Research*, 39(2):1–1, feb 2003. ISSN 00431397. doi: 10.1029/2001WR001247. URL `http://doi.wiley.com/10.1029/2001WR001247`.

J. A. B. Naranjo, K. Stahl, and M. Weiler. Evapotranspiration and land cover transitions: Long-term watershed response in recovering forested ecosystems. *Ecohydrology*, 5(6):721–732, nov 2012. ISSN 19360584. doi: 10.1002/eco.256. URL `http://doi.wiley.com/10.1002/eco.256`.

R. J. Niemeyer, K. D. Bladon, and R. D. Woodsmith. Long-term hydrologic recovery after wildfire and post-fire forest management in the interior Pacific Northwest. *Hydrological*

Processes, 34(5):1182–1197, feb 2020. ISSN 10991085. doi: 10.1002/hyp.13665. URL `https://onlinelibrary.wiley.com/doi/abs/10.1002/hyp.13665`.

NRC. *Hydrologic effects of a changing forest landscape.* National Academies Press, dec 2008. ISBN 0309121094. doi: 10.17226/12223.

T. Oda, N. Ohte, and M. Suzuki. Importance of frequent storm flow data for evaluating changes in stream water chemistry following clear-cutting in Japanese headwater catchments. *Forest Ecology and Management*, 262(7):1305–1317, 2011. ISSN 03781127. doi: 10.1016/j.foreco.2011.06.032. URL `http://www.esf.edu/quest/documents/OdaETAL2011.pdf`.

T. Oda, M. B. Green, R. Urakawa, T. M. Scanlon, S. D. Sebestyen, K. J. McGuire, M. Katsuyama, K. Fukuzawa, M. B. Adams, and N. Ohte. Stream Runoff and Nitrate Recovery Times After Forest Disturbance in the USA and Japan. *Water Resources Research*, 54(9):6042–6054, sep 2018. ISSN 19447973. doi: 10.1029/2017WR021986. URL `http://doi.wiley.com/10.1029/2017WR021986`.

M. Palviainen, L. Finér, A. M. Kurka, H. Mannerkoski, S. Piirainen, and M. Starr. Decomposition and nutrient release from logging residues after clear-cutting of mixed boreal forest. *Plant and Soil*, 263(1-2):53–67, jun 2004. ISSN 0032079X. doi: 10.1023/B:PLSO.0000047718.34805.fb. URL `http://link.springer.com/10.1023/B:PLSO.0000047718.34805.fb`.

M. Palviainen, L. Finér, H. Mannerkoski, S. Piirainen, and M. Starr. Changes in the above- and below-ground biomass and nutrient pools of ground vegetation after clear-cutting of a mixed boreal forest. *Plant and Soil*, 275(1-2):157–167, aug 2005. ISSN 0032079X. doi: 10.1007/s11104-005-1256-1. URL `http://link.springer.com/10.1007/s11104-005-1256-1`.

M. Palviainen, L. Finér, A. Laurén, S. Launiainen, S. Piirainen, T. Mattsson, and M. Starr. Nitrogen, phosphorus, carbon, and suspended solids loads from forest clear-cutting and site preparation: Long-term paired catchment studies from eastern Finland. *Ambio*, 43(2):218–233, mar 2014. ISSN 00447447. doi: 10.1007/ s13280-013-0439-x. URL `http://www.ncbi.nlm.nih.gov/pubmed/24046144http://` `www.pubmedcentral.nih.gov/articlerender.fcgi?artid=PMC3906482`.

M. Palviainen, L. Finér, A. Laurén, T. Mattsson, and L. Högbom. A method to estimate the impact of clear-cutting on nutrient concentrations in boreal headwater streams. *Ambio*, 44(6):521–531, oct 2015. ISSN 00447447. doi: 10.1007/ s13280-015-0635-y. URL `http://www.ncbi.nlm.nih.gov/pubmed/25663527http://` `www.pubmedcentral.nih.gov/articlerender.fcgi?artid=PMC4552712`.

B. J. Peterson, W. M. Wollheim, P. J. Mulholland, J. R. Webster, J. L. Meyer, J. L. Tank, E. Marti, W. B. Bowden, H. M. Valett, A. E. Hershey, W. H. McDowell, W. K. Dodds, S. K. Hamilton, S. Gregory, and D. D. Morrall. Control of nitrogen export from watersheds by headwater streams. *Science*, 292(5514):86–90, apr 2001. ISSN 00368075. doi: 10.1126/science.1056874. URL `http://www.ncbi.nlm.nih.gov/pubmed/11292868`.

K. B. Piatek and H. L. Allen. Are forest floors in mid-rotation stands of loblolly pine (Pinus taeda) a sink for nitrogen and phosphorus? *Canadian Journal of Forest Research*, 31(7):1164–1174, jul 2001. ISSN 0045-5067. doi: 10.1139/x01-049. URL `http://www.nrcresearchpress.com/doi/10.1139/x01-049`.

S. Piirainen, L. Finér, H. Mannerkoski, and M. Starr. Carbon, nitrogen and phosphorus leaching after site preparation at a boreal forest clear-cut area. *Forest Ecology and Management*, 243(1):10–18, may 2007. ISSN 03781127. doi: 10.1016/j. foreco.2007.01.053. URL `https://www.sciencedirect.com/science/article/pii/` `S0378112707000771`.

C. J. Poor and J. J. McDonnell. The effects of land use on stream nitrate dynamics. *Journal of Hydrology*, 332(1-2):54–68, 2007. ISSN 00221694. doi: 10.1016/j.jhydrol. 2006.06.022.

J. M. Quinn and M. J. Stroud. Water quality and sediment and nutrient export from New Zealand hill-land catchments of contrasting land use. *New Zealand Journal of Marine and Freshwater Research*, 36(2):409–429, 2002. ISSN 00288330. doi: 10.1080/00288330. 2002.9517097.

P. R. Robichaud. Fire effects on infiltration rates after prescribed fire in northern Rocky Mountain forests, USA. In *Journal of Hydrology*, volume 231-232, pages 220–229. Elsevier Science B.V., may 2000. doi: 10.1016/S0022-1694(00)00196-7.

F. N. Robinne, D. W. Hallema, K. D. Bladon, and J. M. Buttle. Wildfire impacts on hydrologic ecosystem services in North American high-latitude forests: A scoping review, feb 2020. ISSN 00221694.

R. L. Runkel, C. G. Crawford, and T. A. Cohn. Load Estimator (LOADEST): A FORTRAN program for estimating constituent loads in streams and rivers. *Techniques and Methods. U.S. Geological Survey. U.S. Department of the Interior*, 4:69, 2004. URL https://pubs.usgs.gov/tm/2005/tm4A5/pdf/508final.pdf.

A. J. Rust, T. S. Hogue, S. Saxe, and J. McCray. Post-fire water-quality response in the western United States. *International Journal of Wildland Fire*, 27(3):203–216, apr 2018. ISSN 10498001. doi: 10.1071/WF17115. URL http://www.publish.csiro.au/?paper=WF17115.

T. Schoennagel, J. K. Balch, H. Brenkert-Smith, P. E. Dennison, B. J. Harvey, M. A. Krawchuk, N. Mietkiewicz, P. Morgan, M. A. Moritz, R. Rasker, M. G. Turner, and C. Whitlock. Adapt to more wildfire in western North American forests as climate

changes. *Proceedings of the National Academy of Sciences*, 114(18):4582–4590, 2017. ISSN 0027-8424. doi: 10.1073/pnas.1617464114. URL `http://www.ncbi.nlm.nih.gov/pubmed/28416662http://www.pubmedcentral.nih.gov/articlerender.fcgi?artid=PMC5422781http://www.pnas.org/lookup/doi/10.1073/pnas.1617464114`.

R. S. Shaftel, R. S. King, and J. A. Back. Alder cover drives nitrogen availability in Kenai lowland headwater streams, Alaska. *Biogeochemistry*, 107(1-3):135–148, feb 2012. ISSN 01682563. doi: 10.1007/s10533-010-9541-3. URL `http://link.springer.com/10.1007/s10533-010-9541-3`.

K. Shinozuka, M. Chiwa, K. Otsuki, and A. Kume. Differences in Stream Water Nitrate Concentrations between a Nitrogen-Saturated Upland Forest and a Downstream Mixed Land Use River Basin. *Hydrology*, 4(3):43, sep 2017. ISSN 2306-5338. doi: 10.3390/hydrology4030043. URL `http://www.mdpi.com/2306-5338/4/3/43`.

J. Siemion, D. A. Burns, P. S. Murdoch, and R. H. Germain. The relation of harvesting intensity to changes in soil, soil water, and stream chemistry in a northern hardwood forest, Catskill Mountains, USA. *Forest Ecology and Management*, 261(9):1510–1519, may 2011. ISSN 03781127. doi: 10.1016/j.foreco.2011.01.036. URL `https://www.sciencedirect.com/science/article/pii/S0378112711000685`.

H. G. Smith, G. J. Sheridan, P. N. Lane, P. Nyman, and S. Haydon. Wildfire effects on water quality in forest catchments: A review with implications for water supply. *Journal of Hydrology*, 396(1-2):170–192, jan 2011. ISSN 00221694. doi: 10.1016/j.jhydrol.2010.10.043.

L. A. Sprague and D. L. Lorenz. Regional nutrient trends in streams and rivers of the United States, 1993-2003. *Environmental Science and Technology*, 43(10):3430–3435,

2009. ISSN 0013936X. doi: 10.1021/es803664x. URL `https://pubs.acs.org/doi/pdf/10.1021/es803664x`.

A. Stewart-Oaten, W. W. Murdoch, and K. R. Parker. Environmental impact assessment: 'pseudoreplication' in time? *Ecology*, 67(4):929–940, aug 1986. ISSN 00129658. doi: 10.2307/1939815. URL `http://doi.wiley.com/10.2307/1939815`.

A. Stewart-Oaten, J. Bence, A. L. S. T. Aten, J. A. R. B. Ence, and T. A. Continued. Temporal and spatial variation in environmental impact assessment. *Ecological Monographs*, 71(2):305–339, may 2001. ISSN 1557-7015. doi: 10.1890/0012-9615(2001)071[0305:TASVIE]2.0.CO;2. URL `https://esajournals.onlinelibrary.wiley.com/doi/abs/10.1890/0012-9615{\%}282001{\%}29071{\%}5B0305{\%}3ATASVIE{\%}5D2.0.CO{\%}3B2http://www.esajournals.org/doi/pdf/10.1890/0012-9615(2001)071{\%}5B0305:TASVIE{\%}5D2.0.CO{\%}3B2`.

J. L. Stoddard, J. Van Sickle, A. T. Herlihy, J. Brahney, S. Paulsen, D. V. Peck, R. Mitchell, and A. I. Pollard. Continental-Scale Increase in Lake and Stream Phosphorus: Are Oligotrophic Systems Disappearing in the United States? *Environmental Science and Technology*, 50(7):3409–3415, apr 2016. ISSN 15205851. doi: 10.1021/acs.est.5b05950. URL `www.epa.gov/nheerl/arm/designpages/monitdesign/survey{\_}`.

W. T. Swank, J. M. Vose, and K. J. Elliott. Long-term hydrologic and water quality responses following commercial clearcutting of mixed hardwoods on a southern Appalachian catchment. *Forest Ecology and Management*, 143(1-3):163–178, apr 2001. ISSN 03781127. doi: 10.1016/S0378-1127(00)00515-6. URL `https://www.sciencedirect.com/science/article/pii/S0378112700005156`.

Y. Tremblay, A. N. Rousseau, A. P. Plamondon, D. Lévesque, and M. Prévost. Changes

in stream water quality due to logging of the boreal forest in the Montmorency Forest, Québec. *Hydrological Processes*, 23(5):764–776, feb 2009. ISSN 08856087. doi: 10.1002/ hyp.7175. URL `http://doi.wiley.com/10.1002/hyp.7175`.

USFS. Water Facts — US Forest Service, 2020. URL `https://www.fs.usda. gov/managing-land/national-forests-grasslands/water-factshttps://www. fs.fed.us/managing-land/national-forests-grasslands/water-factshttps: //www.fs.usda.gov/managing-land/national-forests-grasslands/water- facts{\%}0Ahttps://www.fs.fed.us`.

D. Verheyen, N. Van Gaelen, B. Ronchi, O. Batelaan, E. Struyf, G. Govers, R. Merckx, and J. Diels. Dissolved phosphorus transport from soil to surface water in catchments with different land use. *Ambio*, 44(2):228–240, 2015. ISSN 00447447. doi: 10.1007/ s13280-014-0617-5.

P. M. Vitousek and W. A. Reiners. Ecosystem Succession and Nutrient Retention: A Hypothesis. *BioScience*, 25(6):376–381, 1975. ISSN 00063568. doi: 10.2307/1297148. URL `https://academic.oup.com/bioscience/article-lookup/doi/10.2307/1297148`.

X. Wang, D. A. Burns, R. D. Yanai, R. D. Briggs, and R. H. Germain. Changes in stream chemistry and nutrient export following a partial harvest in the Catskill Mountains, New York, USA. *Forest Ecology and Management*, 223(1-3):103–112, 2006. ISSN 03781127. doi: 10.1016/j.foreco.2005.10.060. URL `http://citeseerx.ist.psu.edu/viewdoc/ download?doi=10.1.1.484.510{\&}rep=rep1{\&}type=pdf`.

T. Warziniack and M. Thompson. Wildfire risk and optimal investments in watershed protection. *Western Economics Forum*, 12(2):19–28, 2013.

A. L. Westerling, H. G. Hidalgo, D. R. Cayan, and T. W. Swetnam. Warming and Earlier Spring Increase Western U.S. Forest Wildfire Activity. *Science*, 313(5789):940 LP –

943, aug 2006. doi: 10.1126/science.1128834. URL `http://science.sciencemag.org/content/313/5789/940.abstract`.

CHAPTER 3

Phosphorus retention and transport in forest-meadow systems of Lake Tahoe basin, California

3.1 Abstract

Phosphorus loading from undisturbed forests has the potential to impair downstream water bodies. Phosphorus distribution in the forest soils in the Lake Tahoe basin varies significantly and the legacy effects from the long-term fire suppression have caused P hotspots in the forest-meadow systems of the basin. The primary goal of this study was to better understand the retention and transport of phosphorus from the granitic and andesitic forest meadow systems in the basin. Intact soil cores and soil samples were collected from andesitic and granitic forest meadow systems along a hillslope at contrasting topographic positions (hillslope vs meadows) within the Lake Tahoe basin. Phosphorus retention characteristics and adsorption potential of each soil type was evaluated through isotherm analysis. A sequential constant head flow experiment was designed which exposed the undisturbed soil cores to varying concentrations of inorganic and organic forms of dissolved phosphorus and evaluated the effects of flow direction (infiltration vs exfiltration flow path) on phosphorus transport. The experiment indicated that dissolved organic phosphorus transport can be highly mobile in these soils. The parent material type and the ecosystem type influence the amount of phosphorus leached. Andesitic soils retain large amounts of phosphorus whereas granitic soils are more susceptible to phosphorus leaching to the deeper soil layers. As found in other studies, the dissolved phosphorus concentration in exfiltrating water was much greater than dissolved phosphorous concentration in water leached vertically out of the soil cores. This suggests exfiltration (e.g., spring saturation excess runoff) in the meadow systems could be an important pathway of phosphorus loading in the Tahoe basin which has significant implications for management

where such systems are in close proximity to a downstream water body.

Keywords: *Phosphorus, Forest management, Sorption, Leaching, Exfiltration, Andesitic soils, Granitic soils.*

3.2 Introduction

Despite the long-held perception of forests as nutrient sinks, they constitute an important source of nonpoint Phosphorus (P) loading to the surface waters in the United States, contributing 30% of annual loads from non-point sources alone and 25% from point and non-point sources combined [Carpenter et al., 1998]. Impacts of forest management practices such as timber harvest, road construction, etc. on nutrient concentrations and loads to the streams are widely recognized [Anderson and Lockaby, 2011, Dahlgren, 1998, Deval et al., 2021, Gravelle et al., 2009, Palviainen et al., 2014, 2015]. However, phosphorus increases have also been associated with the streams draining undisturbed forests [Binkley, 2001, Binkley et al., 2004, Dubrovsky et al., 2010, Eddy-Miller et al., 2016]. Yet, the quantitative information on P losses via either infiltration and leaching, or exfiltration and runoff from such forested ecosystem is limited. A considerable amount of P in forest ecosystems is accumulated in the litter layer on top of the mineral soil. This P can be potentially mobilized by the water moving through the layer and either translocated into the mineral soil layer with the percolating water or lost to runoff through the shallow litter interflows in soluble or colloidal forms [Bol et al., 2016]. The classical view on the P distribution in soils is that it decreases with increasing soil depth and the P losses are generally controlled by the hydrologic pathways and the physical-chemical properties of the soil, particularly pH and mineralogy. In acidic soils phosphorus will bind to aluminum and iron oxides whereas in basic soils phosphorus predominantly binds with calcium. Organic soil carbon can also affect the P dynamics in soils [Achat et al., 2016, Bol et al., 2016]. Previous studies have emphasized the importance of identifying hydro-

logic and topographic thresholds at which P losses are triggered via the shifting balance between the matrix to macropore flow, or when pathways shift from surface to subsurface, or the factors that lead to infiltration-excess runoff rather than saturation-excess runoff [Heathwaite and Dils, 2000, Sánchez and Boll, 2005]. There have been extensive studies which have shown using O-18 isotopes that the source of water in streamflow from steep forested landscapes is pre-event storage groundwater rather than runoff generated from rainfall during the event as may be expected from a more disturbed agriculture dominated landscape [Goller et al., 2005, McDonnell, 1990, McGuire and McDonnell, 2010]. The P export can therefore vary in time depending upon the source of P, the dominant hydrologic pathway, and the factors driving its mobility and transport. Generally, it is suggested that P leaching not only drives the redistribution of P within the landscape but can also be a major P loss (dissolved or colloidal) pathway from forest ecosystems [Bol et al., 2016]. Estimates suggest that near-surface runoff events from the forested ecosystem are relatively small and often deemed to have minimal impact on P export from the watershed [Sohrt et al., 2019]. However, the runoff from disturbed watersheds (e.g. post wildfire or post harvesting) can be very large [Hallema et al., 2018]. Furthermore, recent studies have observed the presence of nutrient-enriched litter interflow from the forested watershed [Boy et al., 2008, Miller et al., 2005]. When such P enriched litter interflow comes in contact with the mineral soil, depending on the soil properties and position in the landscape (e.g., toe slope or a meadow), P can either can either get adsorbed to the soil or leach to the bottom layers and form hotspots or get exported via the exfiltration pathway. Runoff generated in toe slopes or meadows, particularly in forested watersheds, often occurs as saturated excess runoff or variable source area runoff [Dunne et al., 1975]. These variable source areas are often saturated for long periods of time and experience exfiltrating water. These variable source areas of runoff can transport P. Importance of the exfiltration pathway in the release of phosphorus to runoff and interflow has been demon-

strated by Sánchez and Boll [2005]. The flow pathways (e.g., infiltration or exfiltration) can therefore be an important factor determining the P export.

An increasing number of lakes in forest-dominated watersheds are experiencing seasonal algal blooms due to long-term accumulation of P loading [Elliot et al., 2015, Jones et al., 2007, Willén, 2003]. One of the primary concerns in the Lake Tahoe basin, which at present maintains its ultra-oligotrophic state [Coats et al., 2008, Hatch et al., 2001], is its declining lake water clarity. Land managers in the Lake Tahoe basin are currently facing several environmental challenges that include, but are not limited to, frequent wildfires, nutrient and fine sediment loading from contributing areas that threaten the clarity of the lake. It has been reported that the primary productivity of the lake has been increasing by about 5% per year [Coats et al., 2008] and in the last five decades, the Secchi depth of the Lake Tahoe has decreased by about 10 meters [Kerlin, 2017]. Fire suppression during the 20th century in the Lake Tahoe basin has resulted in excessive accumulation of both standing and forest floor biomass rich in nutrients. Such accumulation has not only increased the risk of frequent and more intense wildfires [McKelvey and Busse, 1996] that can have consequent downstream water quality problems but has also created nutrient hotspots in the landscape that have the potential to increase the nutrient loading to the downstream water bodies. Several previous studies [Johnson et al., 2010, 2011, Woodward, 2012, Woodward et al., 2013] in the Lake Tahoe basin have identified the presence of nutrient hotspots in the surface soils. While reasons for the formation of such hotspot formation are inconsistent [Johnson et al., 2014], nutrient-rich litter (O-horizon) interflow in the Lake Tahoe basin has been reported by previous studies [Loupe et al., 2007, Miller et al., 2005]. One mechanism driving such high nutrient concentrations in the litter interflow is the uncoupled processes of nutrient mineralization and vegetation uptake due to lack of rooting in the O horizons of these systems [Johnson et al., 2011]. As such, the mineralized nutrients are solubilized by litter interflow that is then believed

to be a contributing factor to the formation of some of the hotspots. Furthermore, it is estimated that the groundwater source areas, alone, contribute 61% of the total dissolved P load to Lake Tahoe and about 65% of the total groundwater P contributions come from the west shore of Lake Tahoe basin [USACE, 2003]. In addition, currently implemented approaches to manage fuel load and reduce fire severity in the Lake Tahoe basin, such as mechanical thinning and prescribed fires may also cause fine sediment loading to the lake [Brooks et al., 2016] which has been previously reported to contribute to the decline of in lake clarity [Sahoo et al., 2013, Swift et al., 2006]. Thus, the soils in the forested hillslopes of the basin, and meadows which act as a transitioning zone between the terrestrial and aquatic system in the basin, can play a crucial role serving as either a sink or source of P transport to the lake via either infiltration and leaching, or exfiltration and runoff.

In this paper, using the intact soil cores and soil samples we investigate the role of parent material (andesitic vs. granitic), ecosystem type (forest vs. meadow), the hydrologic pathway (infiltration vs. exfiltration), and the form of dissolved phosphorus (inorganic vs organic) on the retention and transport of dissolved phosphorus in the andesitic and granitic forest-meadow systems in the wetter west shore of Lake Tahoe basin. Hereafter, andesitic meadow, and andesitic forest are referred to as VM and VF while the granitic meadow and granitic forest are referred to as GM and GF respectively.

The experimental design of this research utilized intact soil cores to investigate the effects of infiltration and exfiltration on P mobilization out of the soil profile. The simulation was designed to examine the leaching and storage of P from litter layers followed by subsequent groundwater infiltration and exfiltration of the stored soil P for potential runoff. First, the columns were leached with water to measure how much native P can be leached to groundwater and potentially transferred to streams and lakes through the subsurface. Next, the cores were spiked with a solution containing phosphate at concentrations that represent typical forest litter leaching concentrations to investigate how

much of the litter-sourced P is sequestered in the soil when it infiltrates, and how much can be leached. To account for the behavior of organic P leached from the litter layer, the cores were subjected to a leaching treatment of organic P (phytic acid) solution at the same concentration as the phosphate solution from the previous step. Lastly, the columns that now have simulated P loading from forest litter leaching are subjected to exfiltration to measure the effects of the saturation excess runoff process that occurs in meadows and toe slopes. The exfiltrated inorganic and organic P represents the potential runoff of stored P. Saturation excess runoff is observed in the toe slopes and meadow areas of the Lake Tahoe watersheds during spring snowmelt, and thus represents a unique pathway that may mobilize the stored P.

3.3   Materials and Methods

3.3.1   Site Description

Lake Tahoe is an alpine, ultra-oligotrophic lake situated at an altitude of 1898 m.a.s.l. along the state boundary between California and Nevada, the US with a basin area of 812 km^2 [Brooks et al., 2016, Hatch et al., 2001]. Granitic geology and soils dominate major parts of the basin except for the north and northwestern parts of the basin where volcanic geology and soils prevail [Brooks et al., 2016, USDA-NRCS, 2007]. The basin experiences snow-dominated hydrology with rain-on-snow events at lower elevations. Vegetation is comprised of mixed conifer forests of Jeffrey pine, lodgepole pine, white fir, and red fir with significant areas of the basin covered by meadows and riparian areas, or bare granite outcrops [Brooks et al., 2016, Coats et al., 2008]. Soil samples and intact soil cores were collected from two subalpine forest-meadow systems, Paige Meadow and Meeks Meadow, located on the west shore of the Lake Tahoe basin (Figure 3.1). Paige Meadow is an alluvial floodplain surrounded by forested hillslopes of terminal moraines at elevation $\sim$

2115 m [Heron et al., 2021]. Meeks Meadow is situated in an elongated glacial valley trough floodplain (elevation $\sim$ 1905 m), with steep forested hillslopes of lateral moraines and volcanic rocks from Miocene- through Pleistocene-age volcanic activity [Heron et al., 2021, Kortemeier et al., 2018]. The geologic substrate of the Meeks Meadow watershed is primarily granodiorite eroded from a glacial drift of till and outwash [Saucedo et al., 2005]. Both meadows contain perennial grasses mixed with sedges, rushes, and forbs [USDA-NRCS, 2007]. The forest surrounding Paige Meadow is a red fir forest association, while the forest next to Meeks Meadow consists of a yellow pine association [USDA-NRCS, 2007]. The Meeks gravelly loamy coarse sand with rubbly to extremely bouldery textured soil was predominant in the Meeks meadow area and the surrounding forest [USDA-NRCS]. The Paige medial (having andic properties and water content between 12% [air-dried] and 100% [undried] at 1500 kPa) sandy loam and Jorge-Tahoma complex soils were dominant in the Paige meadow and the surrounding forest [USDA-NRCS]. More information on the soil characteristics can be found in Heron [2019], Heron et al. [2021].

3.3.2 Site sample and soil core collection

Soil samples and six intact cores (3 soil cores from each meadow and adjacent forest locations respectively) were sampled in each type of forest-meadow system in June of 2018. Samples were taken from the top 15 cm of the soil below the O horizon using a 10-cm diameter soil auger. Soil samples and cores were kept on ice during the sampling campaign and later stored (undried) at 4°C until analysis. Soil samples were passed through a 2-mm sieve before analysis. Description of the methods used in the laboratory analyses to characterize physical and chemical properties of soil, as well as the available P extractions, are detailed in Heron et al. [2021].
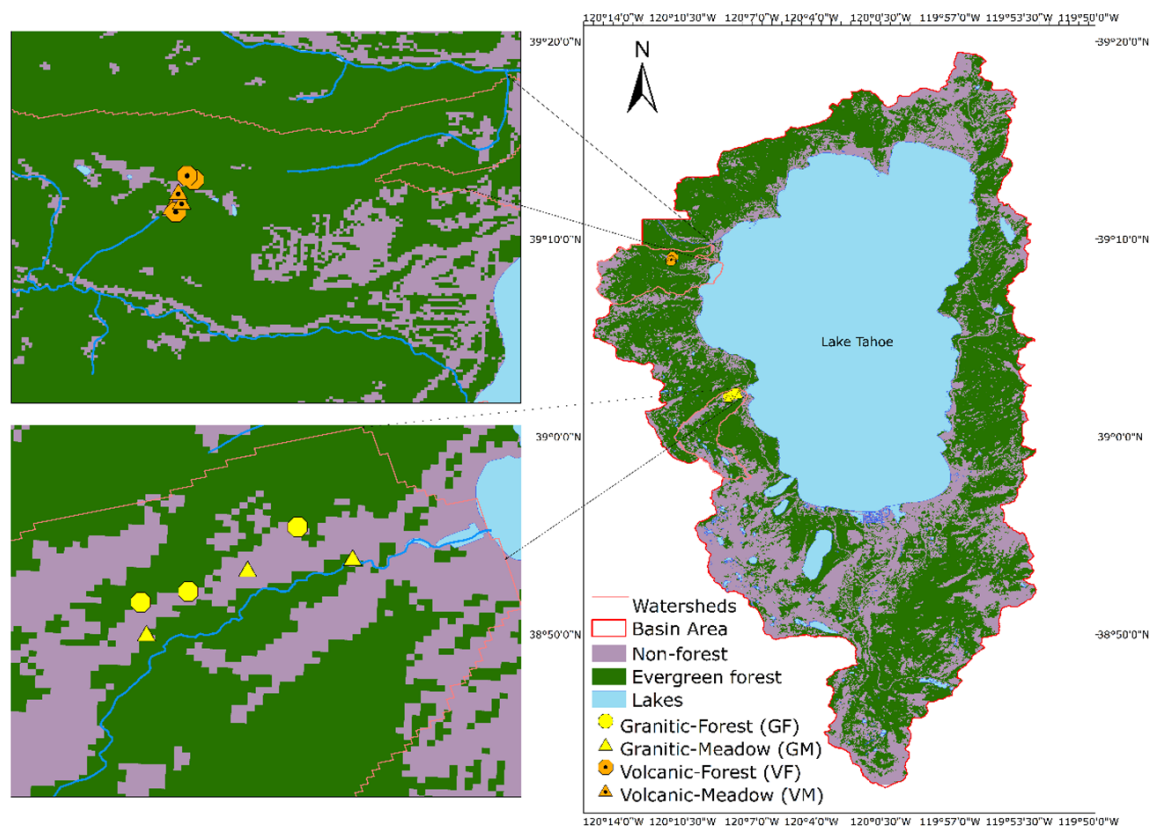
Figure 3.1: The map on the right shows the location of the watersheds within the Lake Tahoe basin settings from which soils were sampled. The figures on the left show the zoomed-in perspective of the sampling sites and the corresponding forest-meadow systems. Top left are the locations in the Paige forest-meadow system and the bottom left are the Meeks forest-meadow system

3.3.3 Experimental Setup

Soil column flow through experiments were set up to quantify the P transport through the soil cores and specifically examine the impacts of flow direction, soil type, P type and the topographic position. To investigate whether the P leaching results can be explained by the sorption properties of the soil P isotherms were determined for each soil. The correlations between the soil chemical properties obtained from Heron et al. [2021] and the P leached during the soil core experiments were evaluated.

3.3.3.1 Soil column flow-through experiment setup

Six intact field wetted soil cores (3 cores from each meadow and adjacent forest locations respectively) representing the top 15 cm of mineral soil from each forest meadow system were used to characterize the effect of P-type (organic vs inorganic) and direction of flow (infiltration and exfiltration) on the transport of P. Soil core setup consisted of the plastic soil core liners in which the intact cores were collected. The plastic caps of these liners were perforated to allow the water flow and lined with 2 mm nylon-mesh to avoid particulate material leaching out. Custom made ceramic caps with openings for connecting silicone tubes for applying water/spiking solution were fitted on top of these plastic lined and capped cores. These ceramic caps were lined with 3 mm dia. glass balls to avoid any displacement of soil particles due to the direct application of water/ spiking solution. Table 3.1 described the sequence in which these experiments were carried out on each core. In each experiment, consisting of four sequences tabulated in Table 3.1 performed on the same soil core, 6.6 cm (300 ml) of DI water/spiking solutions (at pH 6.5) were applied mimicking typical spring precipitation totals. Three infiltration and one exfiltration water flow experiments were conducted on each intact soil core (dia: 7.6 cm; L: 15 cm). To mimic the field conditions where the P enriched litter interflow might get accumulated into the soil or leached to the bottom soil layers depending on the soil properties or get exported via the exfiltration pathway depending upon the topographic position in the landscape the experiments were sequenced in this following specific order: (i) quantify P leaching from mineral soil when water moves through the soil, (ii) quantify P retention and leaching when enriched inorganic P source exists (e.g. substantially high P concentrations in the litter interflow as observed by Miller et al. [2005]), (iii) quantify P retention and leaching when enriched organic P source exists, and (iv) quantify P leaching via exfiltration pathway mimicking the saturation excess runoff events that can

occur at the toe slopes or meadow areas of the watershed. During all four sequences in an experiment 8 leachate samples of approximately 5 ml were collected and filtered through 0.45-μm diameter PES membrane filters analyzed for total dissolved P and molybdate reactive P.

Table 3.1: Description of the soil column flow-through experiment setup.

Sequence No.	Name	Flow direction	Spike solution	Objective
1	No-Spike-Infil	Infiltration	No-spiking	Quantify P leaching from mineral soil
2	25ppm-phosphate-spike	Infiltration	25ppm Potassium Phosphate	Quantify P retention and leaching when enriched inorganic P source exists
3	10ppm-organic-spike	Infiltration	10 ppm Phytic acid	Quantify P retention and leaching when enriched organic P source exists
4	No-Spike-Exfil	Exfiltration	No-spiking	Quantify P leaching from mineral soil via exfiltration pathway mimicking the saturation excess runoff

The first experiment in this sequence was application of pH adjusted DI water (pH $\sim$ 6.5) to simulate infiltration without any P spike in the infiltrating DI water to quantify P leaching from the mineral soils (Table 3.1). This was followed by introduction of a 25-ppm potassium phosphate spiking solution simulating the P in the litter interflow that may be infiltrated vertically through the soil. The concentration of 25 mg L^{-1} was chosen based on the findings of Miller et al. [2005] who reported concentrations of P (as PO$_4$-P) as high as 24.4 mg L^{-1} in the overland/litter interflow in the Lake Tahoe Basin. This was followed by the phytic acid spike to quantify retention and transport of organic P. Finally, the flow directions were reversed and flow through experiments were conducted without any spike in pH adjusted DI water to quantify P transport via the exfiltration pathway mimicking water saturation excess runoff situations. Bromide (KBr$^-$) was introduced in the system along with the potassium phosphate spiking (Sequence 2) as indicator to determine when complete flushing of the core occurred. These Bromide breakthrough curves (C/C$_0$) for each core used in the experiment are displayed in appendix B, Figure 6.8.The C/C$_0$ of the conservative tracer (Bromide) increased for all the cores throughout the experiment and reached a complete breakthrough for most soil cores indicating that the pore water

was being flushed.

3.3.3.2 P sorption isotherms

Phosphate sorption isotherms were measured on all collected soil samples using 1g of air-dried, homogenized soil treated with 25ml of 0.01M KCl solution containing 0, 0.5, 1.0, 2.5, 10.0, 25.0, and 50.0 mg L^{-1} added as KH_2PO_4 in 50mL centrifuge tubes (Southern Cooperative Series Bulletin, 2000). Tubes were placed on a mechanical shaker for a 24-h equilibration period, centrifuged at 6000 rpm for 10 minutes and filtered through a 0.45-µm membrane filter.

3.3.3.2.1 Isotherm Parameters

P bonding strength or the K_L of the Langmuir model [Langmuir, 1918] was calculated using the nonlinear Langmuir isotherm model [Strawn et al., 2020] (Eq. 3.1) as:

$$Q = \frac{Q_{\max}K_L C}{1 + K_L C} \tag{3.1}$$

Eq. 3.1 can be rearranged in the linear form:

$$\frac{C}{Q} = \frac{1}{K_L Q_{\max}} + \frac{C}{Q_{\max}} \tag{3.2}$$

Where,

Q is the total amount of P sorbed to the soil (mg kg^{-1}),

C is the Concentration of P after 24 h equilibration (mg L^{-1}),

$Q_{\max}$ is the P sorption maximum (mg kg^{-1}),

K_L is a constant related to bonding energy (L mg^{-1}).

When the value of C equals $1/K_L$, the total amount of P adsorbed to the soil is

approximately half the Q_{max} meaning half the total P adsorption potential has been achieved [Akhtar et al., 2003].

The Freundlich adsorption coefficient or K_F was calculated from the non-linear Freundlich isotherm model [Freundlich, 1922] (Eq. 3.3) as:

$$Q = K_F C^n \tag{3.3}$$

Where, Q is the amount of P adsorbed per unit mass of soil (mg kg^{-1}),

C is the equilibrium solution concentration of the adsorbate (mg L^{-1}),

K_F is the Freundlich coefficient,

n = empirical constant.

3.3.3.2.2 Phosphorus Saturation Ratio (PSR)

The phosphorus saturation ratio (PSR) of soil from the P, Fe, and Al concentrations reported by Heron et al. [2021] was calculated using Eq. 3.4 [Dari et al., 2015].

$$PSR = \frac{\frac{P_{ex}}{31}}{\frac{Fe_{ex}}{56} + \frac{Al_{ex}}{27}} \tag{3.4}$$

P_{ex}, Fe_{ex}, and Al_{ex} in Eq. 3.4 are extractable phosphorus, iron, and aluminum respectively, and are expressed in moles [Nair and Harris, 2014, Sims et al., 2002]. The extracting reagent can be an acid ammonium oxalate extractant or a soil test solution such as Mehlich 1 or Mehlich 3. In this study, the PSR has been calculated using an acid ammonium oxalate (Ox) extractant (Eq. 3.4).

3.3.3.2.3 Soil P Storage Capacity (SPSC)

SPSC determines the concentration of P that the measured soil horizon can hold

before releasing P at environmentally unacceptable levels [Nair and Harris, 2014]. Nair and Harris [2014] revisited the SPSC concept they developed earlier [Nair and Harris, 2004] (Nair and Harris, 2004) and demonstrated the benefits of using SPSC method for environmental P risk assessment. SPSC was calculated using Eq. 3.5 where the threshold PSR of 0.10 was assumed as defined by Nair and Harris [2014].

$$SPSC = (0.10 - SoilPSR)[(\frac{ox - Fe}{56}) + (\frac{ox - Al}{27})]31 \qquad (3.5)$$

The value for the threshold PSR (0.10; 95% confidence interval of 0.05–0.15) used in equation 3.5 was obtained as the 'changepoint' in a water-soluble P vs. PSR relationship [Nair and Harris, 2014].

3.3.4 Dissolved Reactive P and Total Dissolved P analyses

The filtrate from the isotherms experiments as well as the soil column experiments was analyzed for dissolved reactive P (DRP) by molybdate blue colorimetric method [Murphy and Riley, 1962] using Genesis 10S UV-vis spectrophotometer; Thermo Scientific (Detection limit: 0.001 mg L^{-1}). The total dissolved P in the leachate was analyzed by inductively coupled plasma-atomic emission spectrometry (ICP-AES; Detection limit: 0.05 mg L^{-1}). The difference between the total dissolved P and DRP concentrations is defined as molybdate-unreactive (MU) P. It primarily consists of P associated with organic, non-hydrolyzable, and colloidal forms [Haygarth and Sharpley, 2000, Haygarth et al., 1998]. All the determinations were done at room temperature (23± 1°C). In this study we refer to total dissolved P (Pt), which we define to be the summation of the dissolved reactive P and the dissolved unreactive P. Hereafter in this study the dissolved reactive phosphorus will be referred to as dissolved inorganic P (Pi) and dissolved molybdate unreactive P as dissolved organic P (Po).

3.3.5 Statistical Analyses

Data were analyzed with a two-way analysis of variance (ANOVA). Landscape and parent material type, and their interaction were evaluated for their impact on the average concentration of dissolved phosphorus leached during each experiment. The model fit was assessed by examining the residual plots and log-likelihood. All analyses were performed in R version 4.0 [R Core Team, 2021] using 'car' [Fox and Weisberg, 2019] for building model and, ANOVA and 'emmeans' [Lenth, 2021] for obtaining the estimated marginal means and conducting comparisons. Tukey honest significance difference (HSD) test ($p <$ 0.05) was used to test significance for the parent material type and ecosystem type pairs. The mean P concentrations from the eight leachate samples per treatment were calculated, then the mean for three cores in one each landscape-parent material type (GM, GF, VM, VF) was calculated. Pearson's correlation coefficients were used to evaluate the strength of relationships between soil properties, isotherm parameters, and P leached during different experiments.

3.4 Results

3.4.1 Phosphorus Adsorption Isotherms

The fitted Langmuir and Freundlich adsorption isotherm data for the analyzed soil samples are listed in Table 3.2. In general, both Langmuir and Freundlich's isotherms across all the sites fit the data well. The Langmuir isotherm model had a relatively smaller RMSE range ($\sim$24 to 66 mg/kg) than the Freundlich isotherm ($\sim$8 to 105 mg/kg) across the study sites (see Table 3.2). Figure 3.2 depicts the range of dissolved phosphorus concentrations in the leachate and the corresponding concentrations of P adsorbed to the soil along with the fitted Langmuir isotherm. Similarly, Freundlich isotherms are depicted in Figure 3.3.

Largely, andesitic soils retained more P than the granitic soils. The highest average Q_{max} of 1301 mg/kg was observed in the VF systems while the GM systems showed a relatively lower affinity to P (average Q_{max}: 1145 mg/kg). As can be seen from Figures 3.2 and 3.3, VF retained substantially large concentrations of P compared to all other groups of parent material-ecosystem type.

Table 3.2: Phosphorus sorption properties derived by fitting the Langmuir and Freundlich models to the isotherms data and the goodness-of-fit statistics for the fitted models. Location type is a combination of parent material and ecosystem type (GM, GF, VM, an VF where V: andesitic; G: Granitic; F: forest; and M: meadow). Qmax is the P sorption maximum and K_L and K_F are Langmuir and Freundlich bonding energy constants. RMSE is the Root Mean Squared Error (mg/kg) and AIC is the Akaike information criteria that indicates the relative measure of the quality of a model for a given data set. Smaller the AIC value better the model fit for a given data.

Location Type	Location ID	Langmuir				Freundlich			
		Q_{max} (mg/kg)	K_L (L/kg)	RMSE	AIC	K_F (L/kg)	n	RMSE	AIC
GM	G1	1088	0.25	66	183	286	0.42	20	145
	G7	1147	0.05	24	151	88.	0.62	8	117
	GM2	1202	6.35	35	153	317	0.31	13	123
GF	GN1	916	0.15	47	172	178	0.46	17	132
	GN4	1421	0.07	46	172	148	0.59	28	156
	GN7	1173	0.07	38	166	119	0.59	24	152
VM	V5	1313	0.06	26	153	116	0.62	13	131
	V6	1148	0.15	52	176	204	0.51	22	148
	VM1	1023	6.15	39	167	185	0.49	14	134
VF	V8	1352	0.15	42	169	1142	0.4	77	188
	VN2	1212	11.45	63	182	1004	0.31	105	198
	VN3	1340	5.05	51.68	175.51	1027.12	0.39	88.65	193

3.4.2 P leaching dynamics

For the No-Spike-Infil simulations (Sequence 1), the mean Pt concentration in the leachate was 0.07 mg L^{-1} for GF, 0.20 mg L^{-1} for GM, 0.02 mg L^{-1} for VF, and 0.08 for VM (Figure 3.4). In general, 75-95% of this Pt was in the organic form (Po) with relatively larger proportions from meadow sites (Figure 3.5). The anova analysis of the difference in P concentration leached showed statistically significant interactions with the main effects (parent material and ecosystem type). This means that the concentration of P leached
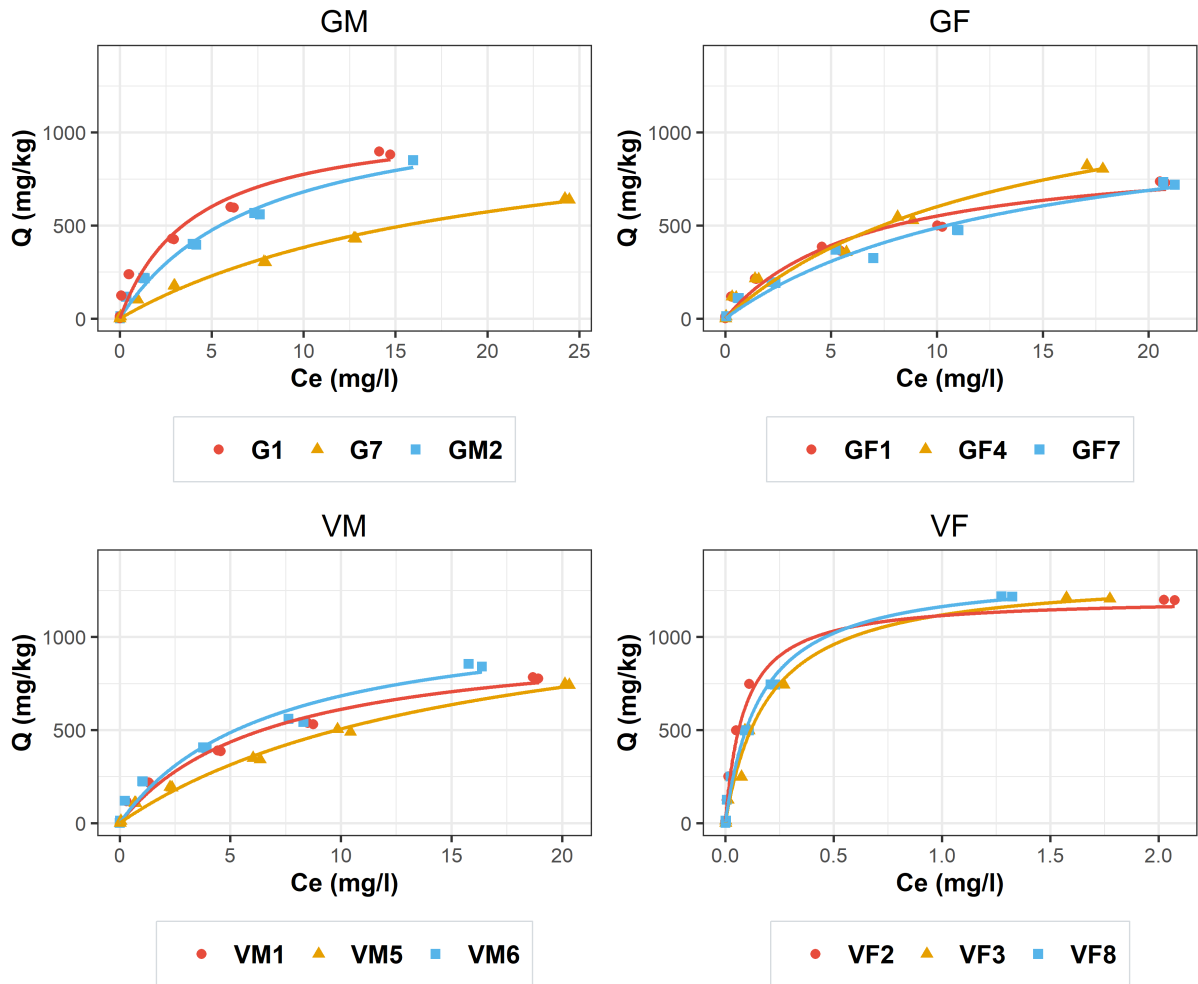
Figure 3.2: Soil P Langmuir adsorption isotherms grouped by the combination of patent material and ecosystem type (GM, GF, VM, VF). Symbols represent the duplicate isotherm measurements that were used to fit the isotherm. Lines are fitted Langmuir isotherms. Ce is concentration of P at equilibrium and Q is the concentration of P adsorbed to the soil.

by a type of parent material was also dependent on the ecosystem type and vice versa (Table 3.3). The effect of parent material on P leaching should therefore be interpreted in the context of ecosystem type and vice versa. Total dissolved phosphorus concentration leached during the No-Spike-Infil experiment was significantly different between all pairs except the granitic forest- andesitic forest pair (p-value = 0.086) (see Table 3.3). For the same experiment, the leached Pi concentration was significantly different (p-value < 0.001)
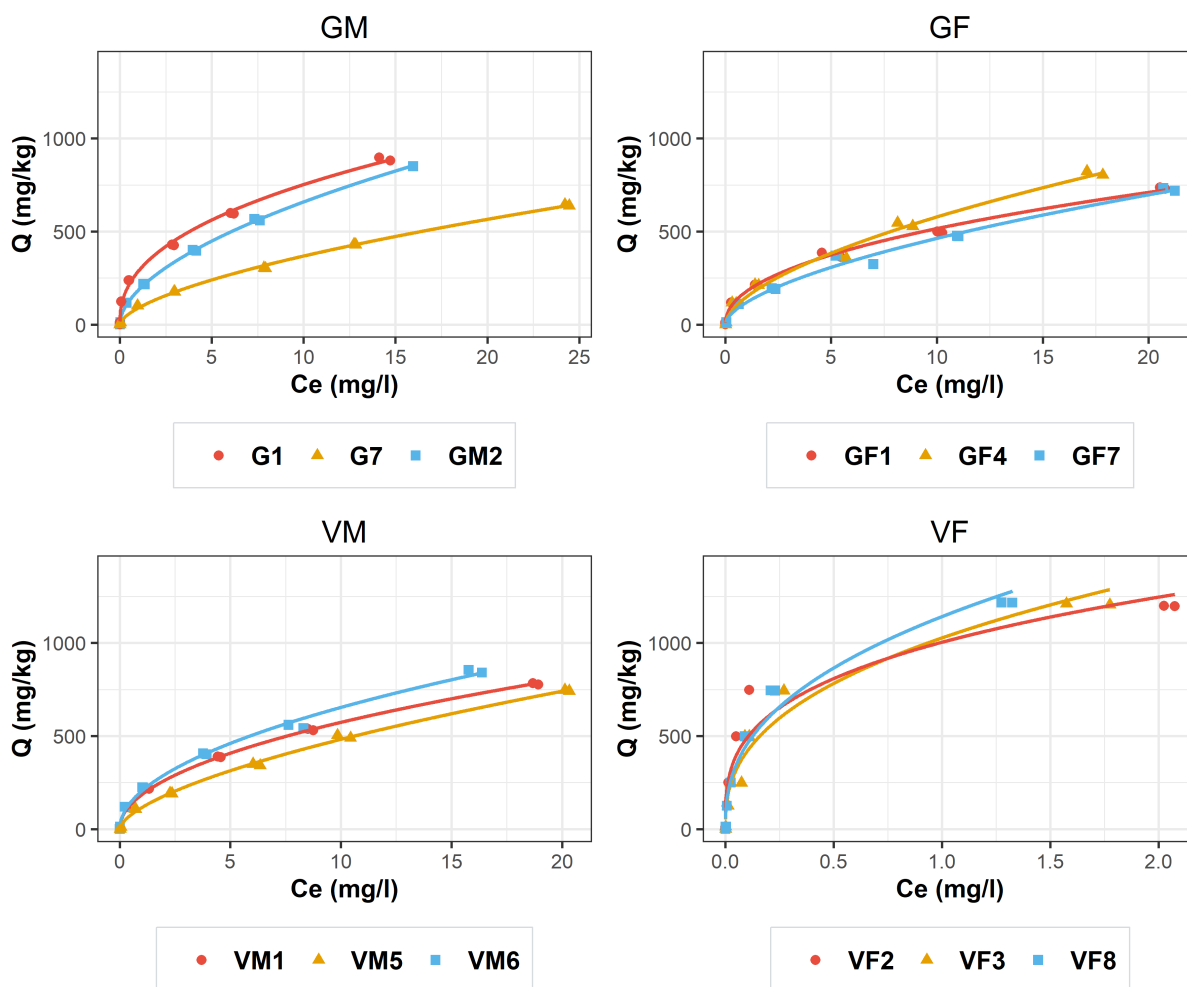
Figure 3.3: Soil P Freundlich adsorption isotherms grouped by the combination of patent material and ecosystem type (GM, GF, VM, VF). Symbols represent the duplicate isotherm measurements that were used to fit the isotherm. Lines are fitted Freundlich isotherms. Ce is concentration of P at equilibrium and Q is the concentration of P adsorbed to the soil.

for the granitic forest-meadow pair and the granitic-andesitic forest pair. Similarly, the leached Po concentration was significantly different between all pairs except the granitic-andesitic forest pair (p-value = 0.3).

For the 25ppm-phosphate-spike simulation (Sequence 2), the mean Pt concentration in the leachate was 10.16 mg L^{-1} for GF, 10.48 mg L^{-1} for GM, 6.7 mg L^{-1} for VF, and 3.25 for VM (Figure 3.4). Generally, 65-90% of the phosphorus from the applied 25 mg
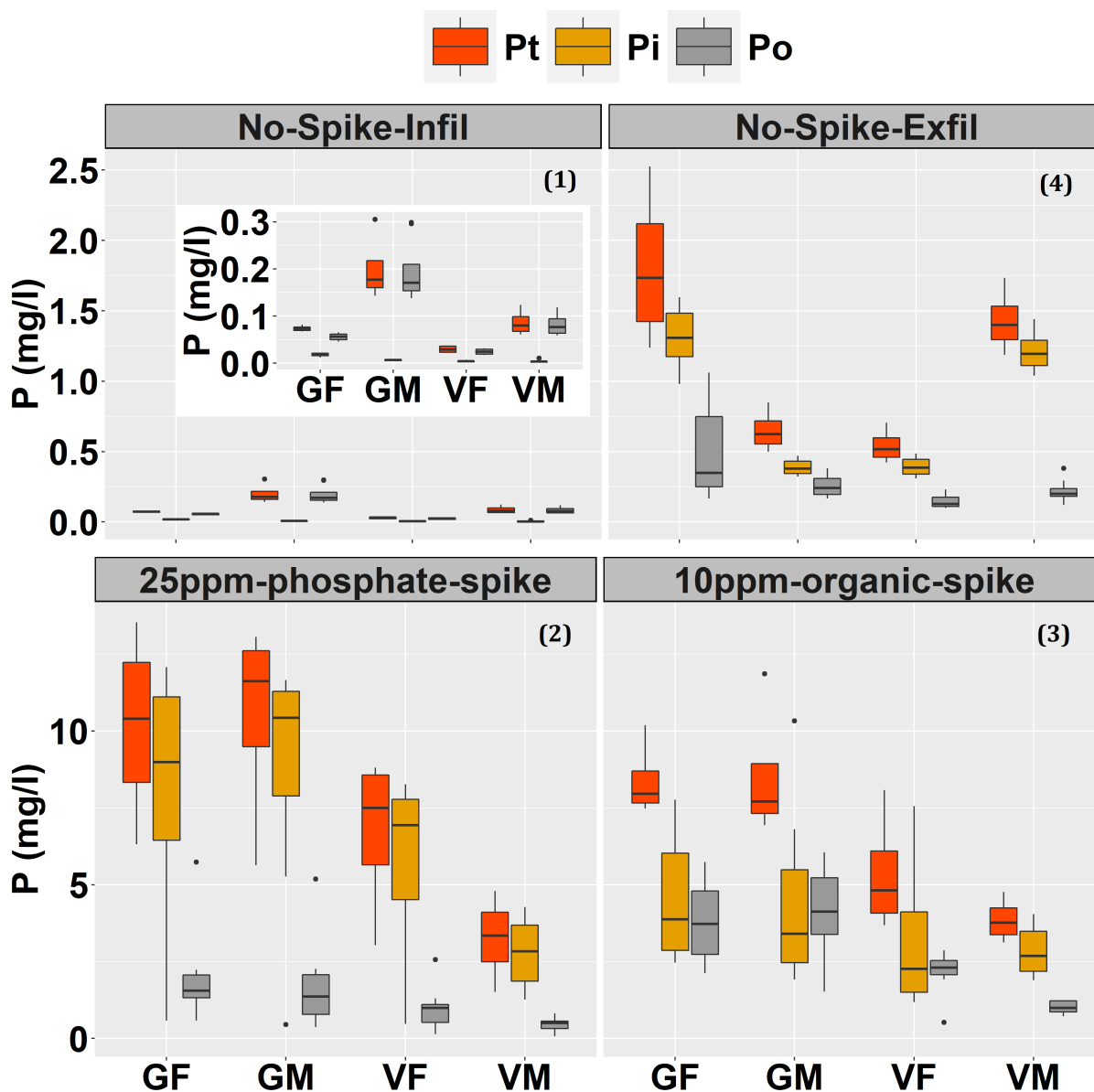
Figure 3.4: Phosphorus concentrations leached during each experiment from the andesitic (V) and Granitic (G) forest (F)-meadow (M) sites. Numbers in parenthesis on the plot indicate the sequence of the spiking experiment. Plot in the inset provides a zoomed in perspective of the data in that panel (No-Spike-Infil). Boxes are the interquartile range (IQR; middle 50% of data), whiskers are upper and lower 25% quartiles, middle lines are medians,and outliers are those points falling beyond 1.5 times the upper/lower IQR limits.

L[-1] enriched inorganic spiking solution was retained by the soils. Andesitic soils retained

a larger amount of phosphorus than granitic soils (Figure 3.5). Statistically significant
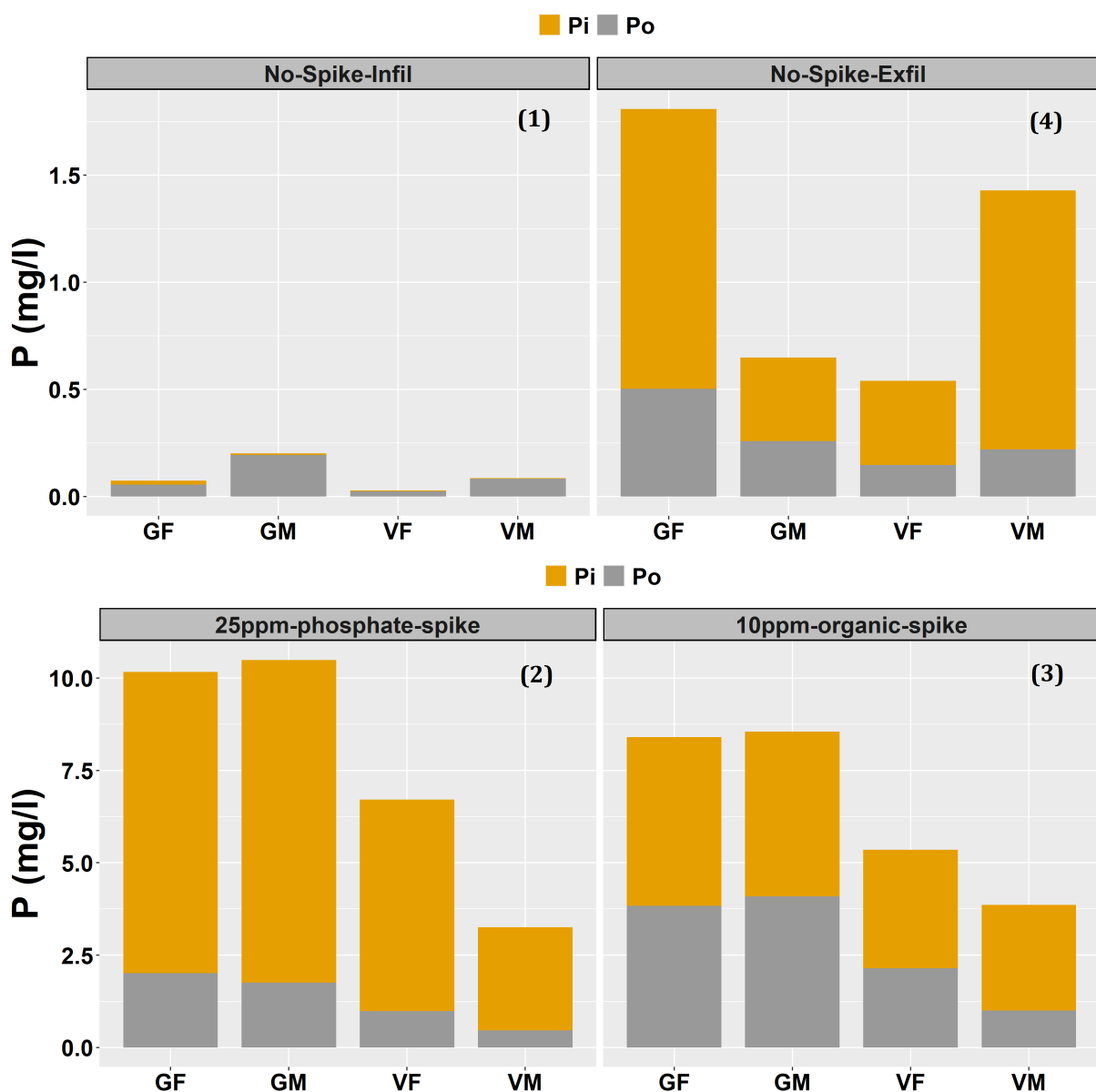
Figure 3.5: Leachate concentrations of inorganic (Pi) and organic (Po) phosphorus for all four experiments from the andesitic (V) and Granitic (G) forest (F)-meadow (M) sites. Numbers in parenthesis on the plot indicate the sequence of the spiking experiment.

differences in leached Pt occurred between the granitic-andesitic meadow pair (p-value < 0.001) and the forest-meadow pair for andesitic soil (p-value $= 0.005$). There were no statistically significant differences in the concentrations of Pi leached between the main effects and their interactions. In the case of Po leaching during the 25ppm-phosphate-spike

experiment statistical differences were observed between the granitic-andesitic meadow pair (p-value = 0.018).

Table 3.3: Estimated marginal means for total dissolved P (Pt), dissolved inorganic P (Pi), and dissolved organic P (Po) concentration (mg/L) in leachate during each experiment in the forest-meadow systems. Values in parenthesis are standard errors. p-values < 0.05 are statistically significant at a 95% confidence interval. Main effects indicated by superscript letters are statistically not different at a 95% confidence interval.

Interactions	No-spike-Infil			25ppm-phosphate-spike			10ppm-organic-spike			No-Spike-Exfil		
	Pt	Pi	Po	Pt	Pi	Po	Pt	Pi	Po	Pt	Pi	Po
Granitic Meadow (GM)	0.20 (0.01)	0.01 (0.00)	0.19 (0.02)	9.97 (1.43)	6.56 (2.16)	1.32 (0.37)	8.36 (0.66)	3.81 (0.71)	3.77 (0.56)	0.64 (0.05)	0.39 (0.05)	0.26 (0.07)
Granitic Forest (GF)	0.07 (0.01)	0.02 (0.00)	0.06 (0.02)	9.76 (1.40)	6.3 (2.07)	1.63 (0.46)	8.33 (0.66)	4.16 (0.77)	3.62 (0.54)	1.74 (0.14)	1.31 (0.05)	0.5 (0.07)
Andesitic Meadow (AM)	0.09 (0.01)	0.004 (0.00)	0.08 (0.02)	2.98 (0.43)	2.55 (0.84)	0.38 (0.11)	3.81 (0.30)	2.75 (0.51)	0.98 (0.15)	1.42 (0.11)	1.21 (0.05)	0.22 (0.07)
Andesitic Forest (AF)	0.03 (0.01)	0.004 (0.00)	0.02 (0.02)	6.2 (0.89)	4.4 (1.45)	0.71 (0.20)	5.11 (0.40)	2.58 (0.48)	1.96 (0.29)	0.53 (0.04)	0.39 (0.05)	0.15 (0.07)
	ANOVA p >F											
GF x GM	<.0001	<.0001	<.0001	1.000	0.999	0.975	1.000	0.995	1.000	<.0001	<.0001	0.053
AF x AM	0.016	0.997	0.011	0.005	0.683	0.433	0.053	0.999	0.011	<.0001	<.0001	0.904
GF x AF	0.086	<.0001	0.300	0.125	0.907	0.181	0.001	0.282	0.026	<.0001	<.0001	0.003
GM x AM	<.0001	0.183	<.0001	<.0001	0.191	0.018	<.0001	0.645	<.0001	<.0001	<.0001	0.988
Main Effects Parent Material												
Granitic	0.14 (0.01)	0.01 (0.00)	0.13 (0.01)	9.87 (1.0)	6.43[A] (1.50)	1.47 (0.29)	8.35 (0.46)	3.98[B] (0.52)	3.69 (0.39)	1.05 (0.06)	0.85 (0.04)	0.32 (0.04)
Andesitic	0.06 (0.01)	0.004 (0.00)	0.05 (0.01)	4.3 (0.44)	3.35[A] (0.78)	0.52 (0.11)	4.41 (0.25)	2.66[B] (0.35)	1.39 (0.15)	0.87 (0.05)	0.8 (0.04)	0.17 (0.02)
Ecosystem												
Meadow	0.14 (0.01)	0.005 (0.00)	0.14 (0.01)	5.45[C] (0.55)	4.09[D] (0.95)	0.71[E] (0.14)	5.64[F] (0.31)	3.24[G] (0.43)	1.93[H] (0.20)	0.95 (0.05)	0.8 (0.04)	0.23 (0.03)
Forest	0.05 (0.01)	0.01 (0.00)	0.04 (0.01)	7.78[C] (0.79)	5.27[D] (1.23)	1.08[E] (0.22)	6.52[F] (0.36)	3.27[G] (0.43)	2.66[H] (0.28)	0.96 (0.05)	0.85 (0.04)	0.24 (0.03)

In the case of 10ppm-organic-spike simulation (Sequence 4), the mean Pt concentration in the leachate was 8.40 mg L^{-1} for GF, 8.55 mg L^{-1} for GM, 5.34 mg L^{-1} for VF, and 3.85 for VM (Figure 3.4). About 60-90% of applied organic phosphorus was retained by the soils. Like the 25ppm-phosphate-spike, andesitic soils in this experiment also retained a relatively larger proportion of phosphorus than granitic soils (Figure 3.5). Differences in total phosphorus, as well as the dissolved organic phosphorus leached during this experiment, were statistically different for all pairs except for the granitic forest-

meadow pair. The differences in dissolved inorganic phosphorus were not statistically different for all main effects and their interactions.

During the No-Spike-Exfil simulation (Sequence 4), the mean total dissolved phosphorus in the leachate was 1.81 mg L^{-1} for GF, 0.65 mg L^{-1} for GM, 0.54 mg L^{-1} for VF, and 1.43 mg L^{-1} for VM (Figure 3.4). Generally, there were much higher phosphorus losses via the exfiltration pathway, compared to the leachate concentrations observed during the No-spike-Infil experiment (Sequence 1) (Figure 3.5). Differences in the Pt and Pi leached during this experiment were statistically significant (p-value < 0.001) for all main effects and their interactions. In the case of Po, only the differences between the granitic forest-meadow pair (p-value = 0.05) and the granitic-andesitic forest pair (0.003) were statistically significant.

3.4.3 Relationship between the soil properties and phosphorus retention and leaching

The soil chemical properties averaged by the ecosystem and parent material type are presented in table 3.4. The soil chemical properties and the average dissolved phosphorus concentrations in the leachate were strongly correlated (Figure 3.6). Total (r = 0.54) and dissolved organic P (r = 0.56) in leachate during the No-spiking-Infil (Sequence 1) experiment were strongly correlated with the total organic carbon content of the soil. Similarly, the total (r= -0.78) and dissolved organic P (r = -0.79) leached during this experiment exhibited statistically significant indirect correlations with the maximum P sorption capacity of the soils (Qmax). Leaching of Pi indicated a strong, statistically significant, positive correlation with soil test phosphorus status represented by the inorganic Bray extractable P (0.75). Pt and Po concentration of the leachate during the phosphate-spiking-infil and organic-spiking-infil were strongly correlated with the soil test phosphorus (Bray extractable P in soils). Sand content (%) of the soils was positively

correlated (r = 0.57) with the total phosphorus lost during No-spike-exfil experiments. During this exfiltration experiment, the phosphorus loss was negatively correlated with the iron oxides (r = -0.53). Similar to the experiments with phosphorus spiking solutions, phosphorus loss during this experiment was highly correlated with the water and Bray extractable P in the soil. Total phosphorus loss from the exfiltration pathway was also positively correlated (r = 0.52) with the phosphorus saturation ratio (PSR).

Table 3.4: Average selected soil chemical properties for the andesitic (V) and Granitic (G) forest (F)-meadow (M) sites [Heron, 2019]. TN is Total Nitrogen, TOC is total organic carbon, WSPt is water-extractable total P, BrayPt is Bray extractable Pt. Al (ox), Fe (ox), P (ox), Si (ox) are aluminum oxide, iron oxide, phosphorus oxide, and silica oxide respectively.

Locations	GM	GF	VM	VF
pH	5.41	5.95	5.27	5.47
TN (%)	0.30	0.06	0.53	0.15
TOC (%)	6.29	2.59	5.56	5.45
% Sand	0.85	0.89	0.89	0.75
% Al (ox)	0.19	0.17	0.27	1.67
% Fe (ox)	0.24	0.20	0.28	0.77
% P (ox)	0.01	0.03	0.02	0.07
% Si (ox)	0.04	0.02	0.05	0.42
WSPt (mg/kg)	0.80	1.67	4.66	0.27
BrayPt (mg/kg)	7.19	73.02	8.99	7.43
PSR	0.17	0.41	0.30	0.28
SPSC	0.00	-0.01	0.00	-0.02
Qmax (mg/kg)	1145.66	1169.93	1161.33	1301.33

3.5   Discussion

As seen in this study subsurface transport of P occurs from both the forest-meadow systems of Lake Tahoe Basin. About 75%-95% of Pt leached from the No-spike-Infil experiment was of dissolved organic form (dissolved molybdate unreactive P). About 10%-40% of the applied P was being transported out of the 15 cm core. This is well below the typical 'mixing layer' and could be reasonable leaching losses of a spring period in the
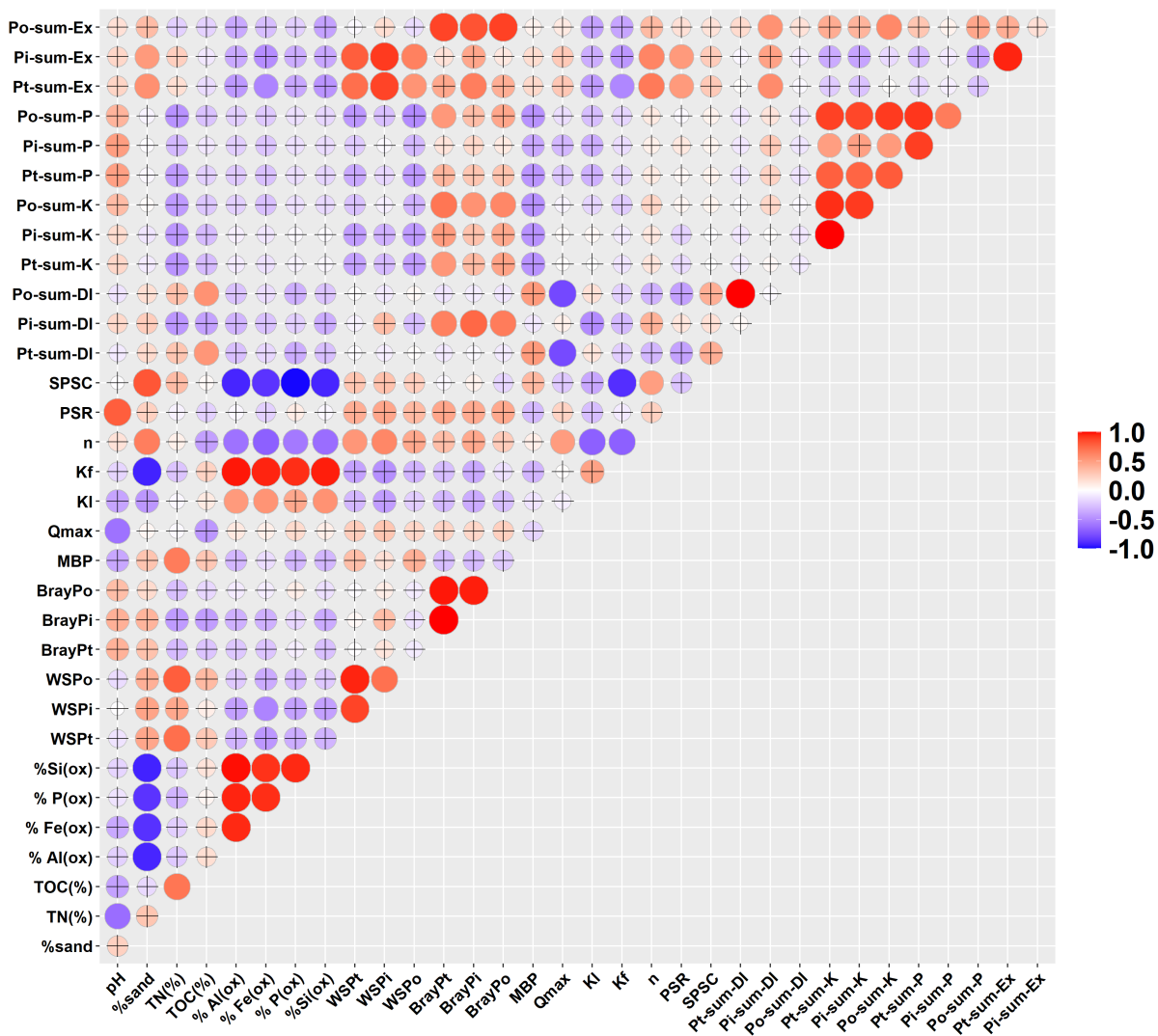
Figure 3.6: Pearson's correlations between the soil physical-chemical properties, soil phosphorus status, and phosphorus concentrations in the leachate. (circles without '+' are statistically significant at 90% confidence intervals). Pt, Pi, Po in the axes labels refers dissolved total P, dissolved inorganic P, dissolve organic P respectively. 'sum' in the axes label refers to the total concentration leached. And DI, K, P and Ex refer to the sequence 1 to 4 respectively in the core flow through experiment. MBP is microbial biomass P.

Tahoe Basin for soils with enriched P litter layer source. This pathway has been largely neglected in other studies particularly those assessing the impact of a disturbance or management scenario on P transport due to the large P adsorption potential of the soils. This study indicates that this pathway could be an important mechanism of phosphorus losses in the Lake Tahoe Basin.

3.5.1 Organic (MU) forms dominate leachate phosphorus fractions

From the No-spike-Infil leaching experiment, granitic soils leached relatively larger dissolved phosphorus concentrations than the andesitic soils and this was related to the sorption properties and the chemical properties of the soils. Andesitic soils which have higher sorption capacity associated with the poorly crystalline iron and aluminum oxides leached smaller amounts of phosphorus compared to the granitic soils with smaller sorption capacity. Heron et al. [2021] reported that concentrations of water-extractable phosphorus from granitic soils in the Lake Tahoe basin were 10-fold higher than the andesitic soils. Our results showing a relatively large phosphorus leaching from granitic soils are in agreement with these findings. This suggests that the translocation of phosphorus into the soil layers below or losses via the subsurface pathways could be an important source of phosphorus in the granitic soils. Further, it is evident that irrespective of the parent material type or the ecosystem type, a large proportion of phosphorus leached was in dissolved organic form. The proportion of organic phosphorus loss was relatively higher in the meadow sites compared to the forest sites. Dissolved organic (MU) phosphorus concentrations leached from the granitic meadow sites were approximately 2 times higher than that from the andesitic meadow sites. This is consistent with Heron et al. [2021] who reported a large fraction (79%-92%) of total phosphorus in the meadow soil of the basin was in organic form compared to a relatively smaller fraction (13%-47%) in

the forest soils. Several other studies [Blackwell et al., 2010, Gerhard et al., 2021, Turner and Haygarth, 2000, 2003] have reported similar trends where organic phosphorus was the dominant fraction of the total phosphorus in the leachate.

3.5.2 Parent material and ecosystem type influence phosphorus retention

When spiked with inorganic and organic phosphorus, the differences in the retention and transport of phosphorus were influenced by the parent material type and the ecosystem type. Relatively larger proportions of the applied phosphorus were retained by the andesitic soils. This is consistent with the expected response from soils with high concentrations of poorly crystalline Al and Fe oxides, which then drive the phosphorus sorption capacity of the soil [Gérard, 2016]. Brödlin et al. [2019] have also reported that phosphorus leaching from sandy soils derived from glacial till parent materials were higher than the soils derived from volcanic rock. While there was no statistical difference between the granitic and andesitic meadow sites during the inorganic spiking experiment, these differences were significant for organic spiking experiments. All these findings are important in the context of century-long fire suppression strategies that have resulted in a very thick organic horizon [Loupe et al., 2007]. Previous studies [Loupe et al., 2007, Miller et al., 2005] have observed very high levels of soluble phosphorus in litter interflow (up to 24 mg L^{-1}) in these thick organic horizons in the Lake Tahoe Basin suggesting it can be a potential source of phosphorus loading via surface or subsurface pathways. Laboratory leaching experiments from this study indicate that the phosphorus from the organic horizons on granitic soils could leach into the deeper soil layers due to their lower sorption capacity resulting in phosphorus hotspots and potentially also act as a subsurface phosphorus loading source. Previous studies have indicated the presence of such hotspots in the Lake Tahoe Basin [Johnson et al., 2011, 2014].

3.5.3 Saturation excess runoff pathway- an important potential source of phosphorus

Runoff generated in toe slopes or meadows, particularly in forested landscapes, often occurs as saturated excess runoff or variable source area runoff [Dunne et al., 1975]. These variable source areas will often be saturated for long periods of time and experience exfiltrating water. These source areas of runoff can also be source areas for phosphorus export. Soils experiencing saturated conditions over extended periods of time will often lead to anaerobic conditions which lead to rapid release of phosphorus [Scott and Weiler, 2001]. Although the experiments in this study did not generate anaerobic conditions it is important to recognize that meadow soils could be susceptible to this process. In addition, as demonstrated in this study the exfiltration of water in these meadow soils can also provide enriched phosphorus concentrations. Similarly, [Sánchez and Boll, 2005] demonstrated the importance of the exfiltration pathway in the release of phosphorus to runoff and interflow. The results of this study show that the phosphorus in the leachate via the exfiltration pathway was much larger than dissolved phosphorus leaching directly out the bottom of the soil core. The high dissolved phosphorus concentration in the exfiltration experiments were directly related to the soil phosphorus status, sand content of the soil, and the phosphorus saturation ratio. Andesitic forest sites released the lowest amount of phosphorus via the exfiltration pathway. In general, saturation excess runoff will rarely occur in steep upland forested sites and the loss of phosphorus via this pathway from these sites should be expected to be minor. In contrast, saturation excess runoff is expected in the meadow sites and in this study andesitic meadows generated more phosphorus loss via the exfiltration pathway than granitic sites. This is partly attributed to the available soil phosphorus and is consistent with [Heron et al., 2021] that reported more total phosphorus in andesitic meadow site compared to the granitic meadow sites

with no major differences in labile phosphorus between the two.

3.5.4   Implications for management

This study indicates that P leaching from forest soils can occur and can be a key pathway for P losses from a specific source area. The results of these sorption isotherms and flow-through experiments show that the soil type, parent material, and the hydrologic pathway are important factors affecting phosphorus retention and transport. One of the important findings is that the subsurface transport of dissolved organic phosphorus is an important pathway in forested soils, particularly granitic soils. The simulation of leachate from a phosphorus-rich thick organic horizon showed that the greatest risk of phosphorus leaching will occur when the enriched phosphorus sources (e.g., thick litter layer after logging, or one developed over the years from lack of management) are left on the granitic forest soils. In the meadow systems, if the water moves via the exfiltration pathway (e.g., spring saturation excess) a potentially large phosphorus export may occur. This has serious implications for meadows in the Lake Tahoe Basin that are in close proximity to the lake and drain directly into the lake with no downstream assimilation potential. While andesitic soils generally retain high P and are less susceptible to subsurface P transport, they can become a greater risk of particulate P transport during the erosion events. From erosion perspective meadows are likely a good sink of particulate P reducing the P export during the erosion events. But they could become source areas of dissolved P later during the runoff events. It is therefore important to think of these areas from a systems perspective when designing management plans for these areas.

3.6 Conclusions

This study exposed undisturbed soil cores from two different parent materials (andesitic and granitic) in the forest-meadow systems of Lake Tahoe basin to a sequential saturated flow experiment. The study was designed to evaluate and identify critical P transport and retention mechanisms as well as identify P source areas. Flow rates were based on typical seasonal spring melt totals. The water was spiked with both inorganic and organic forms of phosphorus. This study evaluated the role of soil parent material, ecosystem type, P type and flow direction on P retention and transport. The study showed that the phosphorus leaching in the forest-meadow systems of Lake Tahoe Basin occurs primarily in organic form. Leaching from granitic sites is larger than that from andesitic sites with granitic meadows leaching the largest amounts of phosphorus. During the spiking experiments, the differences in retention of phosphorus were influenced by the parent material type and the ecosystem type. The greatest risk of phosphorus leaching, translocation, and potential loss via subsurface pathways occurs in granitic soils with enriched phosphorus sources. Saturation excess runoff can be an important pathway for phosphorus loss from meadow systems as demonstrated by the exfiltration pathways. Watershed management decisions and water quality models typically neglect subsurface P transport, and this study emphasizes that subsurface P transport can be a significant pathway of P transport. Subsurface P transport pathway should therefore be considered a major flow path in forested soils and should be accounted for in water quality modeling and recognized in watershed management decision making.

References

D. L. Achat, N. Pousse, M. Nicolas, F. Brédoire, and L. Augusto. Soil properties controlling inorganic phosphorus availability: general results from a national forest network and a global compilation of the literature. *Biogeochemistry*, 127(2-3):255–272, 2016. ISSN 1573515X. doi: 10.1007/s10533-015-0178-0.

M. S. Akhtar, B. K. Richards, P. A. Medrano, M. DeGroot, and T. S. Steenhuis. Dissolved phosphorus from undisturbed soil cores: Related to adsorption strength, flow rate, or soil structure? *Soil Science Society of America Journal*, 67(2):458–470, 2003. ISSN 1435-0661. doi: 10.2136/sssaj2003.0458.

C. J. Anderson and B. G. Lockaby. Research gaps related to forest management and stream sediment in the United States. *Environmental Management*, 47(2):303–313, feb 2011. ISSN 0364152X. doi: 10.1007/s00267-010-9604-1. URL http://link.springer.com/10.1007/s00267-010-9604-1.

D. Binkley. Patterns and processes of variation in nitrogen and phosphorus concentrations in forested streams. *Technical Bulletin of the National Council for Air and Stream Improvement*, 836(836):143, 2001. ISSN 08860882.

D. Binkley, G. G. Ice, J. Kaye, and C. A. Williams. Nitrogen and phosphorus concentrations in forest streams of the United States. *Journal of the American Water Resources Association*, 40(5):1277–1291, oct 2004. ISSN 1093-474X. doi: 10.1111/j.1752-1688.2004.tb01586.x. URL http://doi.wiley.com/10.1111/j.1752-1688.2004.tb01586.x.

M. S. Blackwell, P. C. Brookes, N. de la Fuente-Martinez, H. Gordon, P. J. Murray, K. E. Snars, J. K. Williams, R. Bol, and P. M. Haygarth. Phosphorus Solubilization and Potential Transfer to Surface Waters from the Soil Microbial Biomass Following

Drying–Rewetting and Freezing–Thawing. *Advances in Agronomy*, 106:1–35, jan 2010. ISSN 0065-2113. doi: 10.1016/S0065-2113(10)06001-3.

R. Bol, D. Julich, D. Brödlin, J. Siemens, K. Kaiser, M. A. Dippold, S. Spielvogel, T. Zilla, D. Mewes, F. von Blanckenburg, H. Puhlmann, S. Holzmann, M. Weiler, W. Amelung, F. Lang, Y. Kuzyakov, K. H. Feger, N. Gottselig, E. Klumpp, A. Missong, C. Winkelmann, D. Uhlig, J. Sohrt, K. von Wilpert, B. Wu, and F. Hagedorn. Dissolved and colloidal phosphorus fluxes in forest ecosystems—an almost blind spot in ecosystem research. *Journal of Plant Nutrition and Soil Science*, 179(4):425–438, aug 2016. ISSN 15222624. doi: 10.1002/jpln.201600079.

J. Boy, C. Valarezo, and W. Wilcke. Water flow paths in soil control element exports in an Andean tropical montane forest. *European Journal of Soil Science*, 59(6):1209–1227, dec 2008. ISSN 13510754. doi: 10.1111/j.1365-2389.2008.01063.x. URL `http://doi.wiley.com/10.1111/j.1365-2389.2008.01063.x`.

D. Brödlin, K. Kaiser, A. Kessler, and F. Hagedorn. Drying and rewetting foster phosphorus depletion of forest soils. *Soil Biology and Biochemistry*, 128:22–34, jan 2019. ISSN 00380717. doi: 10.1016/j.soilbio.2018.10.001.

E. S. Brooks, M. Dobre, W. J. Elliot, J. Q. Wu, and J. Boll. Watershed-scale evaluation of the Water Erosion Prediction Project (WEPP) model in the Lake Tahoe basin. *Journal of Hydrology*, 533:389–402, feb 2016. ISSN 00221694. doi: 10.1016/j.jhydrol.2015.12.004.

S. R. Carpenter, V. H. S. N. F. Caraco, D. L. Correll, R. W. Howarth, A. N. Sharpley, N. F. Caracco, D. L. Correll, R. W. Howarth, A. N. Sharpley, and V. H. Smith. Nonpoint pollution of surface waters with phosphorus and nitrogen. *Ecological Applications*, 8(1998):559–568, aug 1998. ISSN 1051-0761. doi: 10.1890/1051-

0761(1998)008[0559:NPOSWW]2.0.CO;2. URL `http://onlinelibrary.wiley.com/` `doi/10.1890/1051-0761(1998)008{\%}5B0559:NPOSWW{\%}5D2.0.CO;2/fullhttp:` `//www.springerlink.com/index/N6N3K6R0163022N1.pdf`.

R. Coats, M. Larsen, A. Heyvaert, J. Thomas, M. Luck, and J. Reuter. Nutrient and sediment production, watershed characteristics, and land use in the Tahoe Basin, California-Nevada. *Journal of the American Water Resources Association*, 44(3):754–770, jun 2008. ISSN 1093474X. doi: 10.1111/j.1752-1688.2008.00203.x.

R. A. Dahlgren. Effects of forest harvest on stream-water quality and nitrogen cycling in the Caspar Creek watershed. *USDA Forest Service General Technical Report PSW*, (8): 45–53, 1998. URL `https://www.fs.fed.us/psw/publications/documents/psw{\_` `}gtr168/06dahlgren.pdfhttp://search.proquest.com/docview/52461961?` `accountid=14439`.

B. Dari, V. D. Nair, J. Colee, W. G. Harris, and R. Mylavarapu. Estimation of phosphorus isotherm parameters: A simple and cost-effective procedure. *Frontiers in Environmental Science*, 3(OCT):70, oct 2015. ISSN 2296665X. doi: 10.3389/fenvs.2015.00070.

C. Deval, E. S. Brooks, J. A. Gravelle, T. E. Link, M. Dobre, and W. J. Elliot. Long-term response in nutrient load from commercial forest management operations in a mountainous watershed. *Forest Ecology and Management*, 494(March):119312, 2021. ISSN 03781127. doi: 10.1016/j.foreco.2021.119312. URL `https://doi.org/10.1016/` `j.foreco.2021.119312`.

N. M. Dubrovsky, K. R. Burow, G. M. Clark, J. M. Gronberg, H. P.A., K. J. Hitt, D. K. Mueller, M. D. Munn, B. T. Nolan, L. J. Puckett, M. G. Rupert, T. M. Short, N. E. Spahr, L. A. Sprague, and W. G. Wilber. *The quality of our Nation's waters—Nutrients in the Nation's streams and groundwater, 1992–2004: U.S. Geological Survey Circular*

1350. 2010. ISBN 9781411329041. URL `http://water.usgs.gov/nawqa/nutrients/pubs/circ1350http://pubs.usgs.gov/fs/2010/3078/`.

T. Dunne, T. R. Moore, and C. H. Taylor. Recognition and prediction of runoff producing zones in humid regions. *Hydrol sci Bull*, 20(3):305–327, 1975. URL `https://www.researchgate.net/publication/240465201{\_}Recognition{\_}and{\_}Prediction{\_}of{\_}Runoff-Producing{\_}Zones{\_}in{\_}Humid{\_}Regions`.

C. A. Eddy-Miller, R. Sando, M. J. MacDonald, and C. E. Girard. Prepared in cooperation with Teton Conservation District Estimated Nitrogen and Phosphorus Inputs to the Fish Creek Watershed, Teton County, Wyoming, 2009–15. Technical report, U.S. Geological Survey, 2016. URL `https://pubs.er.usgs.gov/publication/sir20165160`.

W. Elliot, E. Brooks, D. E. Traeumer, and M. Dobre. Extending WEPP Technology to Predict Fine Sediment and Phosphorus Delivery from Forested Hillslopes. In *SEDHYD 2015 Interagency Conference*, page 12, Reno, NV, 2015. URL `https://www.fs.fed.us/rm/pubs{\_}journals/2015/rmrs{\_}2015{\_}elliot{\_}w002.pdf`.

J. Fox and S. Weisberg. *An {R} Companion to Applied Regression*. Sage, Thousand Oaks {CA}, third edition, 2019. URL `https://socialsciences.mcmaster.ca/jfox/Books/Companion/`.

H. Freundlich. *Colloid \& capillary chemistry*. EP Dutton \& Company, 1922.

F. Gérard. Clay minerals, iron/aluminum oxides, and their contribution to phosphate sorption in soils — A myth revisited. *Geoderma*, 262:213–226, jan 2016. ISSN 0016-7061. doi: 10.1016/J.GEODERMA.2015.08.036.

L. Gerhard, H. Puhlmann, M. Vogt, and J. Luster. Phosphorus Leaching From Naturally Structured Forest Soils Is More Affected by Soil Properties Than by Drying and

Rewetting. *Frontiers in Forests and Global Change*, 4:49, may 2021. ISSN 2624893X. doi: 10.3389/FFGC.2021.543037/BIBTEX.

R. Goller, W. Wilcke, M. J. Leng, H. J. Tobschall, K. Wagner, C. Valarezo, and W. Zech. Tracing water paths through small catchments under a tropical montane rain forest in south Ecuador by an oxygen isotope approach. *Journal of Hydrology*, 308(1-4):67–80, jul 2005. ISSN 00221694. doi: 10.1016/j.jhydrol.2004.10.022.

J. A. Gravelle, G. Ice, T. E. Link, and D. L. Cook. Nutrient concentration dynamics in an inland Pacific Northwest watershed before and after timber harvest. *Forest Ecology and Management*, 257(8):1663–1675, 2009. ISSN 03781127. doi: 10.1016/j.foreco.2009.01.017.

D. W. Hallema, G. Sun, P. V. Caldwell, S. P. Norman, E. C. Cohen, Y. Liu, K. D. Bladon, and S. G. McNulty. Burned forests impact water supplies. *Nature Communications*, 9(1):1–8, dec 2018. ISSN 20411723. doi: 10.1038/s41467-018-03735-6. URL `www.nature.com/naturecommunications`.

L. K. Hatch, J. E. Reuter, and C. R. Goldman. Stream phosphorus transport in the Lake Tahoe basin, 1989-1996. *Environmental Monitoring and Assessment*, 69(1):63–83, 2001. ISSN 01676369. doi: 10.1023/A:1010752628576.

P. M. Haygarth and A. N. Sharpley. Terminology for Phosphorus Transfer. *Journal of Environmental Quality*, 29(1):10–15, jan 2000. ISSN 0047-2425. doi: 10.2134/jeq2000.00472425002900010002x. URL `https://onlinelibrary.wiley.com/doi/full/10.2134/jeq2000.00472425002900010002xhttps://onlinelibrary.wiley.com/doi/abs/10.2134/jeq2000.00472425002900010002xhttps://acsess.onlinelibrary.wiley.com/doi/10.2134/jeq2000.00472425002900010002x`.

P. M. Haygarth, L. Hepworth, and S. C. Jarvis. Forms of phosphorus transfer in hydro-

logical pathways from soil under grazed grassland. *European Journal of Soil Science*, 49(1):65–72, mar 1998. ISSN 13510754. doi: 10.1046/j.1365-2389.1998.00131.x. URL https://onlinelibrary.wiley.com/doi/full/10.1046/j.1365-2389. 1998.00131.xhttps://onlinelibrary.wiley.com/doi/abs/10.1046/j.1365- 2389.1998.00131.xhttps://onlinelibrary.wiley.com/doi/10.1046/j.1365- 2389.1998.00131.x.

A. L. Heathwaite and R. M. Dils. Characterising phosphorus loss in surface and subsurface hydrological pathways. *Science of the Total Environment*, 251-252:523–538, may 2000. ISSN 00489697. doi: 10.1016/S0048-9697(00)00393-4.

T. Heron. *Environmental Factors Influencing Phosphorus Availability and Speciation in Forest and Meadow Soils of the Lake Tahoe Basin.* PhD thesis, University of Idaho, 2019.

T. Heron, D. G. Strawn, M. Dobre, B. J. Cade-Menun, C. Deval, E. S. Brooks, J. Piaskowski, C. Gasch, and A. Crump. Soil Phosphorus Speciation and Availability in Meadows and Forests in Alpine Lake Watersheds With Different Parent Materials. *Frontiers in Forests and Global Change*, 3:159, feb 2021. ISSN 2624893X. doi: 10.3389/ffgc.2020.604200.

D. W. Johnson, D. W. Glass, J. D. Murphy, C. M. Stein, and W. W. Miller. Nutrient hot spots in some sierra Nevada forest soils. *Biogeochemistry*, 101(1):93–103, 2010. ISSN 01682563. doi: 10.1007/s10533-010-9423-8.

D. W. Johnson, W. W. Miller, B. M. Rau, and M. W. Meadows. The nature and potential causes of nutrient hotspots in a Sierra Nevada forest soil. *Soil Science*, 176(11):596–610, 2011. ISSN 0038075X. doi: 10.1097/SS.0b013e31823120a2.

D. W. Johnson, C. Woodward, and M. W. Meadows. A three-Dimensional view of nutrient

hotspots in a Sierra Nevada forest soil. *Soil Science Society of America Journal*, 78: S225–S236, 2014. ISSN 14350661. doi: 10.2136/sssaj2013.08.0348nafsc.

M. Jones, J. Eilers, and J. Kann. Water Quality Effects of Blue-Green Algal Blooms in Diamond Lake, Oregon. In *Advancing the fundamental sciences: Proceedings of the Forest Service National Earth Sciences Conference*, San Diego, CA, 2007. Citeseer.

K. Kerlin. Climate and Ecology Linked to Lake Tahoe Clarity Decline in 2016, 2017. URL `https://www.ucdavis.edu/news/climate-and-ecology-linked-lake-tahoe-clarity-decline-2016https://tahoe.ucdavis.eduresearch/SecchiData.pdf`.

W. Kortemeier, A. Calvert, J. G. Moore, and R. Schweickert. Pleistocene volcanism and shifting shorelines at Lake Tahoe, California. *Geosphere*, 14(2):812–834, apr 2018. ISSN 1553040X. doi: 10.1130/GES01551.1. URL `http://pubs.geoscienceworld.org/gsa/geosphere/article-pdf/14/2/812/4101497/812.pdf`.

I. Langmuir. The adsorption of gases on plane surfaces of glass, mica and platinum. *Journal of the American Chemical society*, 40(9):1361–1403, 1918.

R. V. Lenth. *emmeans: Estimated Marginal Means, aka Least-Squares Means*, 2021. URL `https://cran.r-project.org/package=emmeans`.

T. M. Loupe, W. W. Miller, D. W. Johnson, E. M. Carroll, D. Hanseder, D. Glass, and R. F. Walker. Inorganic nitrogen and phosphorus in Sierran forest O horizon leachate. *Journal of environmental quality*, 36(2):498–507, 2007. ISSN 0047-2425. doi: 10.2134/jeq2005.0465. URL `http://www.ncbi.nlm.nih.gov/pubmed/17332254`.

J. J. McDonnell. A Rationale for Old Water Discharge Through Macropores in a Steep, Humid Catchment. *Water Resources Research*, 26(11):2821–2832, nov 1990. ISSN 19447973. doi: 10.1029/WR026i011p02821. URL `https://onlinelibrary.wiley.com/doi/full/10.1029/WR026i011p02821https:`

//onlinelibrary.wiley.com/doi/abs/10.1029/WR026i011p02821https:
//agupubs.onlinelibrary.wiley.com/doi/10.1029/WR026i011p02821.

K. J. McGuire and J. J. McDonnell. Hydrological connectivity of hillslopes and streams: Characteristic time scales and nonlinearities. *Water Resources Research*, 46(10):10543, oct 2010. ISSN 00431397. doi: 10.1029/2010WR009341. URL https://onlinelibrary.wiley.com/doi/full/10.1029/2010WR009341https:
//onlinelibrary.wiley.com/doi/abs/10.1029/2010WR009341https://agupubs.
onlinelibrary.wiley.com/doi/10.1029/2010WR009341.

K. S. McKelvey and K. K. Busse. Twentieth-century fire patterns on Forest Service lands. Technical report, Davis: University of California, Centers for Water and Wildland Resources, 1996.

W. W. Miller, D. W. Johnson, C. Denton, P. S. Verburg, G. L. Dana, and R. F. Walker. Inconspicuous nutrient laden surface runoff from mature forest Sierran watersheds. *Water, Air, and Soil Pollution*, 163(1-4):3–17, may 2005. ISSN 00496979. doi: 10.1007/s11270-005-7473-7. URL http://link.springer.com/10.1007/s11270-005-7473-7.

J. Murphy and J. P. Riley. A modified single solution method for the determination of phosphate in natural waters. *Analytica Chimica Acta*, 27(C):31–36, 1962. ISSN 00032670. doi: 10.1016/S0003-2670(00)88444-5. URL https://linkinghub.
elsevier.com/retrieve/pii/S0003267000884445.

V. D. Nair and W. G. Harris. A capacity factor as an alternative to soil test phosphorus in phosphorus risk assessment. *New Zealand Journal of Agricultural Research*, 47(4):491–497, 2004. ISSN 11758775. doi: 10.1080/00288233.2004.9513616.

V. D. Nair and W. G. Harris. Soil Phosphorus Storage Capacity for Environmental Risk

Assessment. *Advances in Agriculture*, 2014:9, 2014. ISSN 23147539. doi: 10.1155/2014/723064.

M. Palviainen, L. Finér, A. Laurén, S. Launiainen, S. Piirainen, T. Mattsson, and M. Starr. Nitrogen, phosphorus, carbon, and suspended solids loads from forest clear-cutting and site preparation: Long-term paired catchment studies from eastern Finland. *Ambio*, 43(2):218–233, mar 2014. ISSN 00447447. doi: 10.1007/s13280-013-0439-x. URL `http://www.ncbi.nlm.nih.gov/pubmed/24046144http://www.pubmedcentral.nih.gov/articlerender.fcgi?artid=PMC3906482`.

M. Palviainen, L. Finér, A. Laurén, T. Mattsson, and L. Högbom. A method to estimate the impact of clear-cutting on nutrient concentrations in boreal headwater streams. *Ambio*, 44(6):521–531, oct 2015. ISSN 00447447. doi: 10.1007/s13280-015-0635-y. URL `http://www.ncbi.nlm.nih.gov/pubmed/25663527http://www.pubmedcentral.nih.gov/articlerender.fcgi?artid=PMC4552712`.

R Core Team. The R Project for Statistical Computing, 2021. URL `https://www.r-project.org/`.

G. B. Sahoo, D. M. Nover, J. E. Reuter, A. C. Heyvaert, J. Riverson, and S. G. Schladow. Nutrient and particle load estimates to Lake Tahoe (CA-NV, USA) for Total Maximum Daily Load establishment. *Science of the Total Environment*, 444:579–590, feb 2013. ISSN 00489697. doi: 10.1016/j.scitotenv.2012.12.019. URL `https://www.sciencedirect.com/science/article/pii/S0048969712015628{\#}!`

M. Sánchez and J. Boll. The Effect of Flow Path and Mixing Layer on Phosphorus Release. *Journal of Environmental Quality*, 34(5):1600–1609, 2005. ISSN 0047-2425. doi: 10.2134/jeq2004.0306.

G. J. Saucedo, J. D. Little, S. E. Watkins, J. R. Davis, M. T. Mascorro, V. D. Walker,

and E. W. Ford. *Geologic map of the Lake Tahoe basin, California and Nevada*. State of California, The Resources Agency, Department of Conservation˜..., 2005.

C. A. Scott and K. W. Weiler. Modeling Soluble Phosphorus Desorption Kinetics in Tile Drainage. *Journal of Irrigation and Drainage Engineering*, 127 (2):70–76, apr 2001. ISSN 0733-9437. doi: 10.1061/(asce)0733-9437(2001)127: 2(70). URL `https://ascelibrary.org/doi/abs/10.1061/{\%}28ASCE{\%}290733-9437{\%}282001{\%}29127{\%}3A2{\%}2870{\%}29`.

J. T. Sims, R. O. Maguire, A. B. Leytem, K. L. Gartley, and M. C. Pautler. Evaluation of Mehlich 3 as an Agri-Environmental Soil Phosphorus Test for the Mid-Atlantic United States of America. *Soil Science Society of America Journal*, 66(6):2016–2032, nov 2002. ISSN 0361-5995. doi: 10.2136/sssaj2002.2016. URL `https://onlinelibrary.wiley.com/doi/full/10.2136/sssaj2002.2016https://onlinelibrary.wiley.com/doi/abs/10.2136/sssaj2002.2016https://acsess.onlinelibrary.wiley.com/doi/10.2136/sssaj2002.2016`.

J. Sohrt, D. Uhlig, K. Kaiser, F. von Blanckenburg, J. Siemens, S. Seeger, D. A. Frick, J. Krüger, F. Lang, and M. Weiler. Phosphorus Fluxes in a Temperate Forested Watershed: Canopy Leaching, Runoff Sources, and In-Stream Transformation. *Frontiers in Forests and Global Change*, 2:85, dec 2019. ISSN 2624-893X. doi: 10.3389/ffgc.2019.00085.

D. G. Strawn, H. L. Bohn, and G. A. O'Connor. *Soil chemistry*. John Wiley \& Sons, 2020.

T. J. Swift, J. Perez-Losada, S. G. Schladow, J. E. Reuter, A. D. Jassby, and C. R. Goldman. Water clarity modeling in Lake Tahoe: Linking suspended matter characteristics

to Secchi depth. *Aquatic Sciences*, 68(1):1–15, mar 2006. ISSN 10151621. doi: 10.1007/ s00027-005-0798-x. URL `http://link.springer.com/10.1007/s00027-005-0798-x`.

B. L. Turner and P. M. Haygarth. Phosphorus Forms and Concentrations in Leachate under Four Grassland Soil Types. *Soil Science Society of America Journal*, 64(3):1090–1099, may 2000. ISSN 1435-0661. doi: 10.2136/SSSAJ2000.6431090X. URL `https://onlinelibrary.wiley.com/doi/full/10.2136/sssaj2000.6431090xhttps://onlinelibrary.wiley.com/doi/abs/10.2136/sssaj2000.6431090xhttps://acsess.onlinelibrary.wiley.com/doi/10.2136/sssaj2000.6431090x`.

B. L. Turner and P. M. Haygarth. Changes in Bicarbonate-extractable Inorganic and Organic Phosphorus by Drying Pasture Soils. *Soil Science Society of America Journal*, 67(1):344–350, jan 2003. ISSN 1435-0661. doi: 10.2136/SSSAJ2003.3440. URL `https://onlinelibrary.wiley.com/doi/full/10.2136/sssaj2003.3440https://onlinelibrary.wiley.com/doi/abs/10.2136/sssaj2003.3440https://acsess.onlinelibrary.wiley.com/doi/10.2136/sssaj2003.3440`.

USACE. Lake Tahoe Basin framework study: Groundwater evaluation. Technical Report October, U.S. Army Corps of Engineers, Sacramento, CA, 2003. URL `https://www.waterboards.ca.gov/rwqcb6/water{\_}issues/programs/tmdl/lake{\_}tahoe/docs/peer{\_}review/usace2003.pdf`.

USDA-NRCS. Web Soil Survey. URL `https://websoilsurvey.sc.egov.usda.gov/App/WebSoilSurvey.aspxhttps://websoilsurvey.sc.egov.usda.gov/App/HomePage.htm`.

USDA-NRCS. Soil survey of the Tahoe Basin Area, California and Nevada. Technical report, United States Department of Agriculture, Natural Resources Conservation Service., 2007. URL `http://soils.usda.gov/survey/printed{\_}surveys/`.

E. Willén. Dominance patterns of planktonic algae in Swedish forest lakes. In *Hydrobiologia*, volume 502, pages 315–324, 2003. doi: 10.1023/B:HYDR.0000004289.92343.39.

C. Woodward. *Nutrient Hot Spots in a Sierra Nevada Soil: Physical Assessments and Contributing Factors*. PhD thesis, University Of Nevada, Reno, 2012.

C. Woodward, D. W. Johnson, M. W. Meadows, W. W. Miller, M. M. Hynes, and C. M. Robertson. Nutrient hot spots in a sierra nevada forest soil: Temporal characteristics and relations to microbial communities. *Soil Science*, 178(11):585–595, nov 2013. ISSN 15389243. doi: 10.1097/SS.0000000000000023. URL `https://insights.ovid.com/crossref?an=00010694-201311000-00001`.

CHAPTER 4

Upland Phosphorus Transport in Forested Landscapes with Water Erosion Prediction Project- Water Quality (WEPP-WQ) model

4.1 Abstract

Nutrient loading from forested watersheds in response to forest management practices can be a major threat to the health of the water bodies directly downstream. Land and water managers often rely on hydrologic and water quality models to accurately inform their management decisions. In this study, the parameter sensitivity of the WEPP-WQ model to simulate phosphorus (P) losses was analyzed using a single hillslope. Following that we assessed the ability of the minimally calibrated WEPP-WQ model to simulate P losses from two large, and relatively undisturbed, forested watersheds in the Lake Tahoe Basin. The performance of WEPP-WQ was evaluated by comparing simulated streamflow, sediments, and P values from the model with the observed streamflow and flow-weighted P and suspended sediment concentrations. Analysis revealed that P sorption parameter (PSP), P soil partitioning parameter (PHOSKD), initial labile phosphorus pool in topsoil layer (LabileP), and P uptake distribution parameter (UPB) were some of the relatively important and sensitive parameters for simulating P loss. At the watershed scale, model prediction results suggest the adequate ability of WEPP-WQ to simulate soluble P losses. The future developments on the incorporation of P attached to the channel sediment in the P calculations and P routing as well as better representation of soil P pools in the model will likely improve the model prediction ability at the watershed outlet. Overall, this study shows that WEPP-WQ, with its current dissolved phosphorus routines, can be an effective, process-based, and yet parsimonious edge-of-the-hillslope effects tool for informing land and water management decisions.

Keywords: *Process-based models, WEPP-WQ, Forested watersheds, Water quality, Phosphorus.*

4.2   Introduction

Increasing threat of wildfire due to climate change and long-term fire suppression practices have resulted in an increasing need for more active forest management strategies. Increased active forest management can lead to an increased risk of short-term nutrient and sediment loading. A few examples of forested watersheds where managers struggle with the benefits and risks associated with active forest management include Lake Tahoe Basin spanning parts of California and Nevada, Big Bear Lake watershed in California, and the Cedar River watershed in Washington. Land and water managers are increasingly confronted with complex and evolving forest management challenges due to the increased wildfire risks from compounded effects of century-long fire suppressions [Agee and Skinner, 2005, Schoennagel et al., 2017], climate change [Schoennagel et al., 2017, Westerling et al., 2006], and disease/insect infestation [Bentz et al., 2010, Collins et al., 2012]. Nutrient loading varies as a function of landscape and ecosystem properties as well as management. In the Lake Tahoe Basin, soils are developed on granitic, andesitic, or mixed parent materials [Coats et al., 2016] and P availability is partly controlled by ecosystem and parent material [Heron et al., 2021]. Heron et al. [2021] reported approximately twice the total P in the soils that were developed from andesitic parent material compared to the soils of granitic origin. Studies have also reported that the forest soils developed from granitic parent material have significantly large extractable P compared to those developed on andesitic soils [Coats et al., 2016, Heron et al., 2021, Johnston et al., 1995]. P can be transported to downstream water bodies in dissolved and particulate forms. Land and water managers often rely on the predictive models to understand the impacts of forest management practices on nutrient loading and to inform their short-

and long-term watershed management decisions.

Many such predictive models exist, and they range from simple lumped parameter-driven to physically based complex models. These models can simulate hydrology and water quality from watersheds under several management practices and at varying temporal and spatial scales. Examples of these models include Hydrologic Simulation Program-Fortran (HSPF) [Johanson et al., 1984], Soil and Water Assessment Tool (SWAT) [Neitsch et al., 2011], Annualized Agricultural Non-Point Source (AnnAGNPS) [Young et al., 1989], Generalized Watersheds Loading Functions (GWLF) [Haith and Shoenaker, 1987], Agricultural Policy/Environmental eXtender (APEX) [P. W. Gassman et al., 2010], and Integrated Catchment Model (INCA) [Wade et al., 2002], Hydrologiska Byrans Vattenbalansavdelning (HBV)[Andersson et al., 2005], and Watershed Erosion Prediction Project (WEPP) [Laflen and Forest, 1997] to mention a few.

The development of many of these nutrient delivery models stems from the research and understanding acquired from agricultural watersheds. Such models, therefore, tend to focus on simulating the effects of agricultural management practices and fertilizer applications on the availability of soluble and particulate phosphorus and their delivery pathways [Collick et al., 2016, Sharpley et al., 1994]. However, research in the forested watersheds has shown that the concepts of antecedent moisture conditions, infiltration, and variable source area are critically important to runoff generation mechanisms and directly pertain to the linkages between the soils and water quality at the watershed scale [Neary et al., 2009]. It is also important to capture the effects of elevation and topography on precipitation, temperature, and snow accumulation and melt to simulate accurate hydrologic response from the watershed [Brooks et al., 2016, Srivastava et al., 2013, 2017, 2020]. Many of the aforementioned models do not account for these effects particularly when simulating large, forested watersheds. Predicting P load requires a model that can accurately simulate erosion and sediment transport as well as the water

flow through a landscape. Particulate P is linked with erosion and sediment transport whereas soluble P is linked with water transport and available P in the soil. Therefore to develop a predictive model of phosphorus delivery from forested watersheds, a process-based hydrologic and sediment delivery model that incorporates these concepts is needed [Elliot et al., 2015]. Few if any model has been developed to simulate vertical subsurface P transport described in chapter 3. WEPP is one such physically-based hydrology and erosion model that simulates shallow lateral flow, runoff and sediment detachment and delivery from a hillslope/watershed [Boll et al., 2015, Brooks et al., 2016, Dun et al., 2009, Elliot et al., 2015, Srivastava et al., 2013]. WEPP has a large management database specifically parameterized and assessed based on field studies to mimic the effects of managements such as timber harvest, thinning, skid trails, and burning on vegetative and soil properties. This database, along with the multiple climate forcing options in the newly developed [Lew et al., 2022] and evaluated [Dobre et al., 2022] WEPPcloud interface, sets WEPP apart from all the aforementioned models. The WEPP model has been successfully applied across small and large forest watersheds to predict flow and sediments [Brooks et al., 2016, Covert et al., 2005, Dobre et al., 2022, Lew et al., 2022, Pandey et al., 2009, Singh et al., 2011, Srivastava et al., 2020].

There have been two approaches developed to simulate the transport of pollutants, particularly P, with the WEPP model. The first is a simplistic approach that uses fixed P concentrations in different flow pathways to simulate P transport and has been presented in Dobre et al. [2022], Elliot et al. [2015], Lew et al. [2022]. The approach simulates P transport based on known concentrations of P in runoff, lateral flow, baseflow, and attached to sediments that would be typically measured at the watershed outlet [Dobre et al., 2022, Lew et al., 2022]. Dobre et al. [2022] demonstrated, using existing observed Total P, dissolved reactive P, and total sediment concentration at the outlet of a watershed, a simple approach to assign these fixed P concentrations. The limitation for

using historic observed data at the outlet of the watershed is that it is difficult to address targeted management-oriented questions with the model that might require understand P cycling processes and sources at the scale of management unit rather than the outlet and it is unable to represent changes in the soil P concentrations with time following any disturbance to the primary soil pools.

The second approach uses a more detailed, process-based approach to P cycling between multiple P pools within a hillslope with a recently developed water quality (WQ) module for WEPP, based on the SWAT nutrient delivery algorithms. This approach couples the hydrologic and soil erosion components of WEPP with the Water Quality (WQ) algorithms that were developed[Savabi et al., 2011] and updated [Wang, 2015]. However, this WEPP-WQ model has undergone limited testing to assess its accuracy in predicting phosphorus delivery [Wang, 2015], particularly in the forested watersheds. This testing included small field-scale plots in the relatively flat topography of mid-western states of the United States with no known testing and application to the forested watersheds. Due to a lack of information on soil P pools in forested watersheds such water quality models are often initialized to default settings. These pools are then calibrated to represent the P export observed at watershed outlet. However, from chapter 3 and the soil P availability assessment by Heron et al. [2021], we have information to evaluate this calibration of P pools. Furthermore, although the nutrient delivery routines are based on the widely applied SWAT 2012 algorithms, little is documented about the sensitivity of the parameters for simulating phosphorus after coupling with the WEPP model. In contrast to the simpler Dobre et al. [2022] approach, the WEPP-WQ approach is based on cycling of P through various P pools in the soil profile and its interaction with vegetation and hydrologic flow paths. A key limitation with WEPP is that the model currently does not predict instream P transport and cycling.

The goal of this study was threefold: (i) Understand the importance and sensitivity of

parameters and processes that drive the phosphorus cycling and transport in the WEPP-WQ model, (ii) Apply WEPP-WQ to large watersheds where the forest is dominant land use and test its phosphorus prediction ability (soil P pools as well as P export), and (iii) Use the calibrated model to identify P hot spots in two watersheds in Lake Tahoe Basin with varying dominant soil types. Since the model does not capture instream P channel loading most of the analysis will focus on the ability of the model to represent dissolved reactive P transport. The timing and relative magnitude of simulated particulate P transport from hillslopes will be compared to observed particulate P at the outlet of two watersheds. The WEPP-WQ model used in the study is based on the previous work of Savabi et al. [2011], Wang [2015], but incorporates baseflow components based on Srivastava et al. [2013], establishes an R workflow for parallel simulation of multiple hillslopes, and tests WEPP-WQ's application to large forested watersheds. Here the first objective is to identify the importance and sensitivity of parameters related to phosphorus using a single hillslope represented by a single Overland Flow Element (OFE). Then the second objective is to apply a minimally calibrated WEPP-WQ to the forested watersheds and test its ability to predict phosphorus losses from two watersheds with soils originating from different parent materials (granitic and andesitic) by comparing the model results with the observed data.

4.3   Methods

4.3.1   WEPP-WQ model and Phosphorus cycling

The WEPP model is a physically-based, distributed-parameter, continuous-simulation model developed by the USDA and is designed for predicting runoff, erosion, and sediment yield along the hillslope profile [Flanagan et al., 2007, 2012]. The WEPP-WQ model, initially developed by Savabi et al. [2011] and then further revised by Wang [2015], couples

the hydrologic and soil erosion components of WEPP with the Water Quality (WQ) algorithms based on Soil and Water Assessment Tool (SWAT) [Arnold et al., 1998]. It was developed to apply within a hillslope having a single overland flow element (OFE), the smallest spatial unit used by the WEPP model. Specifically, a hillslope composed of a single OFE is limited to only representing the hydrology through a hillslope profile with single land use and single soil type. For a more detailed discussion of the impacts of OFEs in WEPP see [Boll et al., 2015]. The hydrologic component of the WEPP-WQ lacked the baseflow developments by Srivastava et al. [2013] which were, in this study, incorporated in the WEPP-WQ to make the hydrologic component consistent with the latest developmental version of WEPP for forested watersheds.

Phosphorus cycling in WEPP-WQ is represented by six phosphorus pools, three each for the inorganic and organic pools (Figure 4.1). Phosphorus can be introduced into the model via fertilizer application and from the plant harvest residue or decomposing forest floor. The total soil phosphorus pool is composed of stable, active, and labile pools. Labile P represents the phosphorus that is in the solution and the amount that is adsorbed onto the soil but can easily get into solution form during the growing season. The active and stable pools represent phosphorus that is more tightly adsorbed to the soil. Phosphorus from harvest residues is redistributed to the active and stable P pools through decay and decomposition processes, respectively. A key assumption in the model is that the inorganic labile, active, and stable pools tend to approach a fixed equilibrium based on key soil P parameters described below. The active pool is in equilibrium with the labile pool and is initialized using a relationship between the soluble pool and phosphorus sorption parameter (PSP) as:

$$ActiveP = LabileP[\frac{(1 - PSP)}{PSP}] \qquad (4.1)$$

Where PSP is the phosphorus sorption parameter and represents the amount of inor-
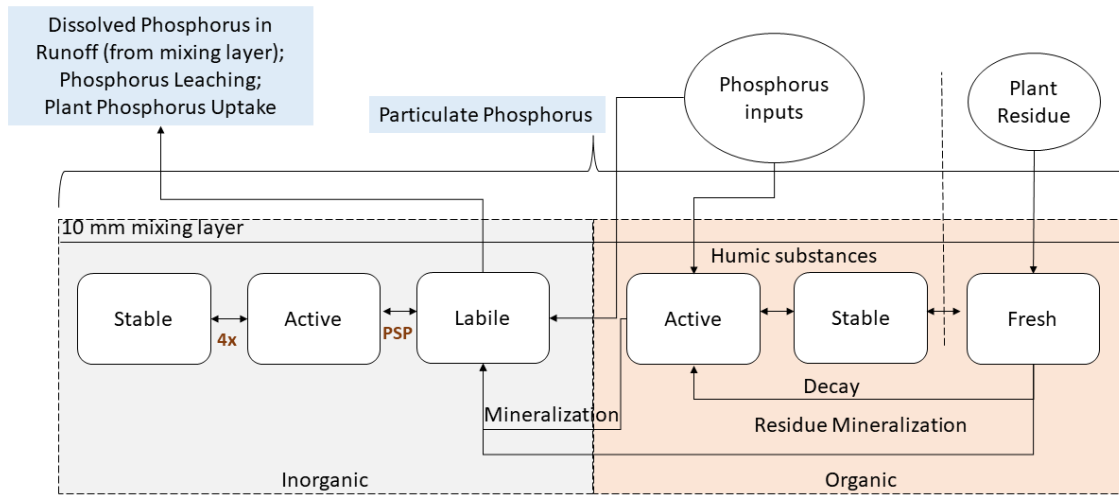
Figure 4.1: Phosphorus processes and cycling in the WEPP-WQ model. Adapted from [Arnold et al., 1998].

ganic phosphorus added to the soil that remains labile on reaching relative equilibrium [Vadas et al., 2006]. The stable pool is initialized as four times the active pool [Neitsch et al., 2011]. This factor of four is a fixed parameter in the model and cannot be calibrated by the user. Organic phosphorus pools are initialized based on the organic carbon content of the soil. The equilibrium between the active and labile pool is maintained by transferring phosphorus from the relatively larger pool of phosphorus. When inorganic P is added to the labile pool it causes an imbalance in the equilibrium with the active pool, then the amount of phosphorus moved from the labile pool to the active pool each day is calculated as:

$$P_{\text{Moved}} = 0.1(LabileP - (ActiveP)[\frac{PSP}{1 - PSP}]) \qquad (4.2)$$

Where the term '(Active P) [PSP/ (1- PSP)]' represents the required amount of phosphorus in the labile pool relative to the unchanged active pool as defined by Eq. 4.1.

PMoved is the mass of imbalance between the labile and active pools [Vadas et al., 2006]. Whenever the active pool is too large relative to the labile pool, P is moved from active to Labile P at a fixed 0.1 day^{-1} rate until the equilibrium is reestablished. This 0.1 day^{-1} rate is informed from the P adsorption study on three different soils by Rájan and Fox [1972] who observed that 100% sorption occurred in 10 days and a subsequent average of 0.1 day^{-1} [Vadas et al., 2006]. In the Environmental Policy Integrated Climate (EPIC) model, P moves from Active to Labile P at the same 0.1 rate when Active P is too large relative to Labile P. However, there is no documented justification for this desorption rate [Vadas et al., 2006]

The model assumes phosphorus can be lost through plant uptake, leaching, and as dissolved phosphorus or particulate phosphorus bound to the soil. The first three pathways are fed by the labile phosphorus pool and the particulate phosphorus pathway is fed by the total soil phosphorus pool. Plant uptake of phosphorus is linked with the plant growth module of WEPP. Phosphorus uptake is governed by the plant's potential phosphorus demand and labile P in soil. Dissolved phosphorus load via the surface runoff is estimated using Eq. 4.3.

$$P_{\text{dissolved}} = \frac{Q_{\text{surf}} * P_{\text{labile,surf}}}{\rho_{\text{b}} * PHOSKD * depth_{\text{surf}}} \tag{4.3}$$

Where P$_{\text{dissolved}}$ is the mass of dissolved phosphorus (kg.ha^{-1}) exported in surface runoffP$_{\text{labile,surf}}$ is the amount of labile phosphorus in the top 10 mm of the soil profile (mixing layer). Q$_{\text{surf}}$ is the depth of surface runoff on a given day, ρ_{b} is the bulk density of the top 10 mm of soil, depthsurf is the depth of surface soil layer, and PHOSKD is the phosphorus soil partitioning coefficient (m^3 Mg^{-1}). PHOSKD is defined as the ratio of labile P concentration in the top 10 mm of soil to the concentration of soluble P in surface runoff [Neitsch et al., 2011] and represents a linear partitioning coefficient.

Sediment-bound phosphorus in surface runoff is calculated using Eq. 4.4.

$$ParticulateP = 0.001 * Conc_{\text{sedP}} * \epsilon_{\text{P:sed}} * \frac{Sed}{area} \qquad (4.4)$$

Where ParticulateP is the mass of phosphorus transported with sediment to the main channel in surface runoff (kg ha^{-1}), Sed/area is the sediment erosion rate on a given day (kg/ha), and conc$_{\text{sedP}}$ is calculated using Eq. 4.5 and is the concentration of phosphorus attached to the sediment in the top 10 mm of soil (g P/ metric ton soil).

$$conc_{\text{sedP}} = 100 * \frac{minP_{\text{act,surf}} + minP_{\text{sta,surf}} + orgP_{\text{hum,surf}} + orgP_{\text{frsh,surf}}}{\rho_{\text{b}} * depth_{\text{surf}}} \qquad (4.5)$$

where minP$_{\text{act,surf}}$, minP$_{\text{sta,surf}}$, orgP$_{\text{hum,surf}}$, and orgP$_{\text{frsh,surf}}$ are the amount of phosphorus (kg P/ha) in the active mineral, stable mineral, humic organic, and fresh organic pools respectively.

The $\epsilon_{\text{P:sed}}$ from Equation 4.4 is P enrichment ratio and is defined as the ratio of concentration of the concentration of P transported with the sediment to the concentration of P in the soil surface layer. WEPP-WQ calculates $\epsilon_{\text{P:sed}}$ for each storm event using equation 4.6.

$$\epsilon_{\text{P:sed}} = 0.078 * Conc_{\text{sed,surq}}^{-0.2468} \qquad (4.6)$$

where Conc$_{\text{sed,surq}}$ is the concentration of sediments in surface runoff (Mg m^3) and is calculated using Eq. 4.7

$$Conc_{\text{sed,surq}} = \frac{sed}{10 * area_{\text{ofe}} * Q_{\text{surf}}} \qquad (4.7)$$

where sed is the sediment yield on a given day (metric tons), and Q$_{\text{surf}}$ is the surface runoff on a given day (mm).

4.3.2   Parameter sensitivity analyses

The sensitivity analysis focused on a single hillslope having a single OFE. This hillslope received mean annual precipitation of 1637 mm. The mean annual sediment eroded from the hillslope was 1100 kg ha^{-1} and the mean annual sediment delivered to the outlet was 530 kg ha^{-1}. The sensitivity analysis focused on the following parameters: two biomass parameters namely the maximum leaf area index (laimx)and the biomass energy ratio (beinp), initialization levels for the labile (laibileP) and organic phosphorus in the topsoil layer (orgP_L1), initialization values for organic nitrogen in the topsoil layer (orgN_L1) and the following four phosphorus parameters percolation coefficient (PPERCO), partitioning coefficient (PHOSKD), plant uptake distribution parameter (UPB) and phosphorus sorption parameter (PSP). The baseline/default values for these parameters along with the range within which the parameters were varied for sensitivity analysis are listed in Table 4.1. The sensitivity of each parameter was assessed using a classical one-factor-at-a-time (OAT) approach. As the name suggests, the effect on output is determined by varying one input parameter at a time while keeping the rest of the parameters constant [Devak and Dhanya, 2017]. Parameter sensitivity was assessed by ranking parameters based on the sensitivity index (SI) calculated using equation 4.8, where X_{max} and X_{min} are maximum and minimum changes in input parameter and Y_{max} and Y_{min} are corresponding changes in output.

$$SI = \frac{Y_{max} - Y_{min}}{X_{max} - X_{min}} \tag{4.8}$$

Table 4.1: Parameters considered for sensitivity analysis, their value for the sensitivity baseline scenario and the range over which they were varied.

Parameter Name	Baseline Value	Range	Units
Maximum leaf area index potential (laimx)	4.5	0.225-9.0	
Biomass energy ratio (beinp)	15	0.75-30	kg MJ^{-1}
Labile P in layer 1 (labileP)	50	2.5-100	mg P kg^{-1}
Organic P in layer 1 (orgP_L1)	50	2.5-100	mg P kg^{-1}
P percolation coefficient (PPERCO)	13.9	10-17.8	m3 Mg^{-1}
P soil partitioning parameter (PHOSKD)	100	5-200	m3 Mg^{-1}
P sorption parameter (PSP)	0.35	0.0175-0.7	-
P uptake distribution parameter (UPB)	50	2.5-100	-
Organic N in layer 1 (orgN_L1)	50	2.5-100	mg N kg^{-1}

4.3.3 Watershed-scale model setup

4.3.3.1 Study area description

Figure 4.2 shows the location of the Blackwood Creek watershed and General Creek watershed in the Lake Tahoe Basin. Lake Tahoe is an alpine, ultra-oligotrophic lake situated at an altitude of 1898 m.a.s.l. along the state boundary between California and Nevada, US [Brooks et al., 2016, Hatch et al., 2001]. Figure 4.3 shows the spatial variation in the land cover, soil parent material, and soil sand content in the Lake Tahoe basin. As can be seen from Figure 4.3, geology and soils across the basin are predominantly granitic except for the volcanic geology and soils in the north and northwestern of the basin. Throughout the Basin, soils have high sand content. The lake Tahoe basin experiences wet winters and dry summers and the orographic effects coupled with the influences from the Pacific ocean causes precipitation differences between the west and the east sides of the basin. Generally, the west shore is five times wetter than the east shore of the basin. Hydrology is largely dominated by snow accumulation and melt, especially at higher elevations, and rain-on-snow events, at lower elevations [Brooks et al., 2016]. Vegetation is comprised of mixed conifer forest of Jeffrey pine (*Pinus jeffreyi Balf.*), lodgepole pine

(*Pinus contorta*), white fir (*Abies concolor*), and red fir (*Abies magnifica*) with significant areas of the basin covered by meadows and riparian areas, shrubs, or bare granite outcrops [Brooks et al., 2016, Coats et al., 2008]. Because particulate P is linked with erosion and soluble P with water transport and available P in the soil, watersheds in the Lake Tahoe Basin with its differences in soil types are good for this type of analysis.

4.3.3.2 Model Setup, calibration, and performance evaluation

Using the WEPPcloud interface [Dobre et al., 2022, Lew et al., 2022] watersheds and hillslopes were delineated with the TOPAZ model and a 30m USGS National Elevation Dataset (NED). Soil files for each hillslope were populated using the SSURGO database and the management files were populated using the 2016 National Land Cover Database (NLCD). Weather files were created using the Daymet dataset. Other weather characteristics such as duration of the storm, dew point temperature, wind speed, etc. were generated with CLIGEN v5.3.2 [Srivastava et al., 2019]. The models were already minimally calibrated in both watersheds by Dobre et al. [2022] for the parameters related to sediment and water yield. These runs were downloaded from WEPPcloud [Lew et al., 2022] and used in this study to simulate phosphorus yield. All simulations were performed using R parallel hillslope processing scripts developed in this study for running WEPP-WQ locally. Detailed information on the calibration methods for the parameters related to streamflow, water yield, and sediment can be found in Dobre et al. [2022]. The key model parameters related to phosphorus yield that were identified with sensitivity analysis were calibrated in both watersheds using the parameter estimation (PEST) tool [Doherty, 2015]. Since in the current version of WEPP-WQ, nutrients are not routed through the channels and any instream P cycling or detachment, deposition, or transport is not simulated, the model performance was evaluated by comparing the relative timing and magnitude of the simulated TP, PP, and SRP leaving the hillslope as the edge of the field
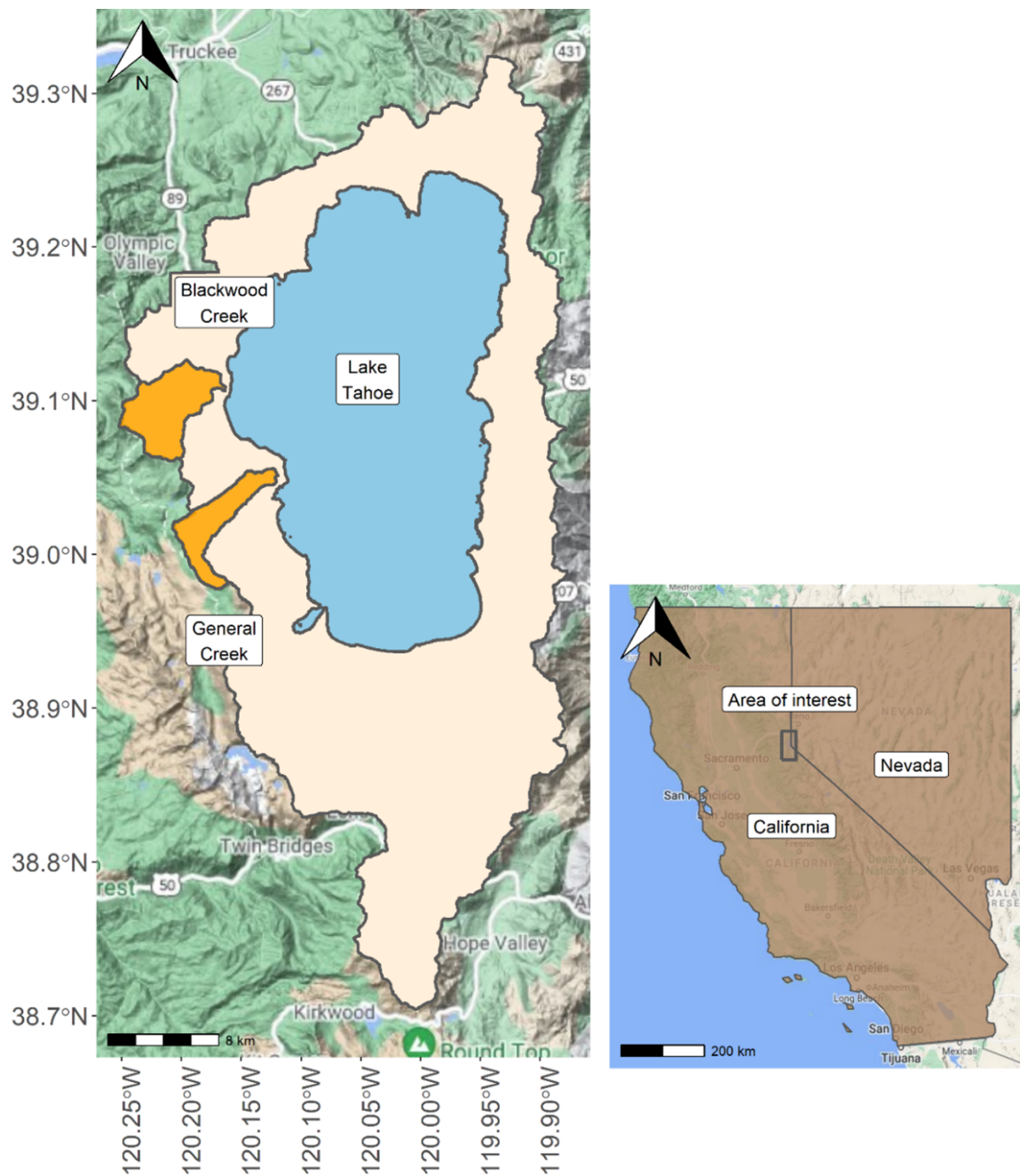
Figure 4.2: Location of the General Creek watershed and Blackwood Creek watershed in the Lake Tahoe Basin for which the WEPP-WQ was set up.
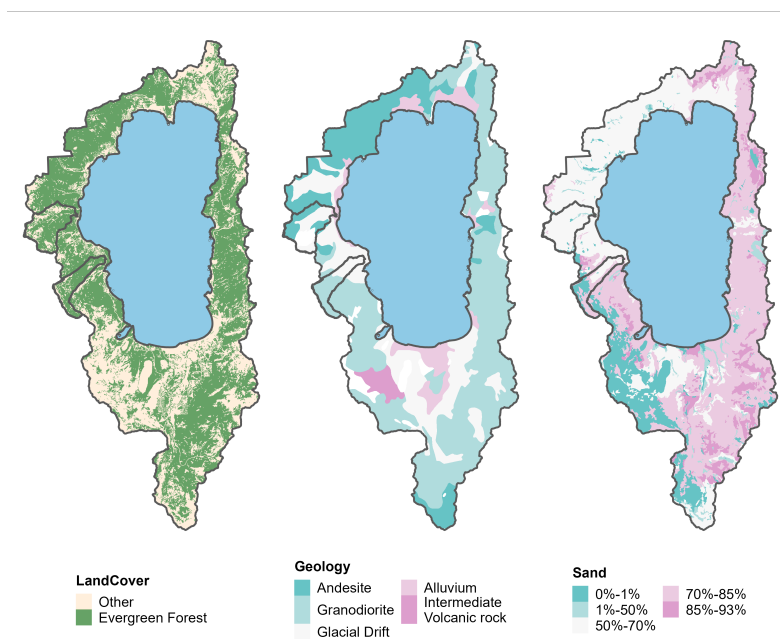
Figure 4.3: Land cover type, geology type and sand (%) distribution in the Lake Tahoe Basin

yields (proportional to the total hillslope area of the watershed) to the observations at the watershed outlet. It was assumed dissolved reactive P concentration would be minimally affected by instream processing and therefore could calibrated against observed dissolved reactive P loading at the watershed outlet. It was also assumed that the simulated timing and magnitude of particulate P loading from the daily model could be compared to the relative timing and magnitude of observed particulate P loading at the watershed outlet. Model performance for both watersheds was assessed using streamflow data measured at the USGS gauging stations and the observed annual average flow-adjusted loads of TP, SRP, and PP from a previous study [Coats et al., 2016]. Model performance was assessed using three goodness-of-fit statistics namely Nash-Sutcliffe efficiency (NSE), Pearson's coefficient of determination (R^2), and Bias. The NSE, R^2, and Bias were calculated using equations 4.9, 4.10, and 4.11 respectively employing the 'hydroGOF' R package [Mauricio Zambrano-Bigiarini, 2020].

$$NSE = 1 - \left[\frac{\sum\limits_{i=1}^{n}(x_i - y_i)^2}{\sum\limits_{i=1}^{n}(x_i - \overline{x})^2} \right] \qquad (4.9)$$

where n is the total number of observations (daily/monthly/WY), x_i is the observed value and y_i is the corresponding simulated value. $\overline{x}$ is the mean simulated value for the length of the data. The NSE range lies between $-\infty$ to 1 and generally the NSE value between 0 to 1 is considered an acceptable level of model performance [Moriasi et al., 2007]. In essence, closer the NSE value to 1 better the model performance.

$$R^2 = \left[\frac{\sum\limits_{i=1}^{n}(x_i - \overline{x})(y_i - \overline{y})}{\sqrt{\sum_{i=1}^{n}(x_i - \overline{x})^2}\sqrt{\sum_{i=1}^{n}(y_i - \overline{y})^2}} \right]^2 \qquad (4.10)$$

The value of R^2, an indicator of how closely the simulated value fits against the observation, ranges between 0 and 1. The closer the value of R^2 to 1, the better the fit between the simulated and observed data. Since the absolute magnitude of particulate P transport at the outlet could not be compared due to the current limitation in the model, only the R^2 statistic was used to assess the ability of the model to simulate particulate P

$$PBias = \frac{\sum\limits_{i=1}^{n}(y_i - x_i) * 100}{\sum_{i=1}^{n}(x_i)} \qquad (4.11)$$

PBias indicates the mean deviation of the simulated value compared to the observation. The positive values of Bias indicate that the simulated values are overestimated compared to the observed values and vice-a-versa.

4.4 Results

4.4.1 WEPP-WQ sensitivity analyses using single hillslope

The sensitivity of nine output variables consisting of five soil pools, phosphorus plant uptake, and losses via runoff and sediments to the changes in input parameters over the input parameter range is displayed in Figure 4.4. Figure 4.5 shows the ranked sensitivity of these nine output variables to the change in input parameters calculated using the sensitivity index. TotalSoilP (mg/kg) pool which represents the total soil phosphorus in the soil profile was directly related and most sensitive to PSP (Figure 4.4). Overall, the sensitivity of TotalSoilP to input parameters was ranked in the order proceeding from greatest to least sensitive PSP > LabileP > orgP_L1 > PHOSKD > beinp > UPB > laimx > PPERCO > OrgN_L1. LabileP pool was most sensitive to PSP, followed by initial LabileP concentrations in the topsoil layer, PHOSKD, and beinp. Similar to TotalSoilP, LabileP was also inversely related to the PSP (Figure 4.4). Overall sensitivity ranking of LabileP to changes in input parameters was in the order PSP > LabilP > PHOSKD > beinp > UPB > PPERCO > orgN_L1 > orgP_L1 > laimx (Figure 4.5).

Puptake was most sensitive to LabileP, PSP, and beinp. The order of this sensitivity to the input parameters was LabileP > PSP > beinp > PHOSKD > laimx > UPB > PPERCO > orgN_L1 > orgP_L1. Overall P loss from the hillslope via Prunoff was most sensitive to PSP and LabileP, and P loss via Psediments was most sensitive to PSP, beinp, and LabileP. Generally, the larger the PSP, the smaller were the P losses via runoff and sediments. In contrast, the larger the LabileP pool, the greater were the P losses via runoff and sediments. P losses via sediments were also inversely related to the beinp, with smaller beinp yielding more sediment-bound P losses. The sensitivity of Prunoff to the parameters was in the order PSP > LabileP > PHOSKD, beinp > laimx > UPB > PPERCO > orgN_L1 > orgP_L1 (Figure 4.5). Similarly, the order of
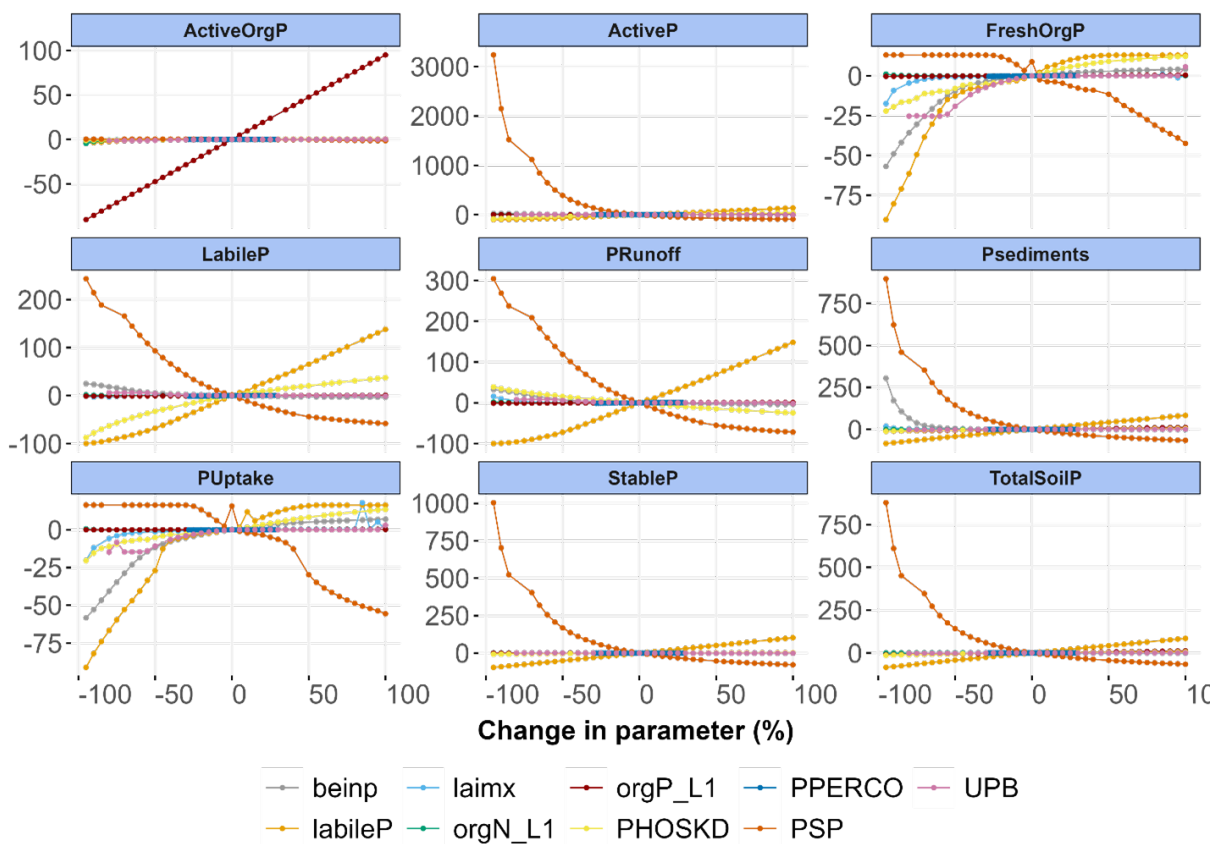
Figure 4.4: Sensitivity of each output variable (listed as subplot header) to change in input parameters (represented by each curve on the chart).
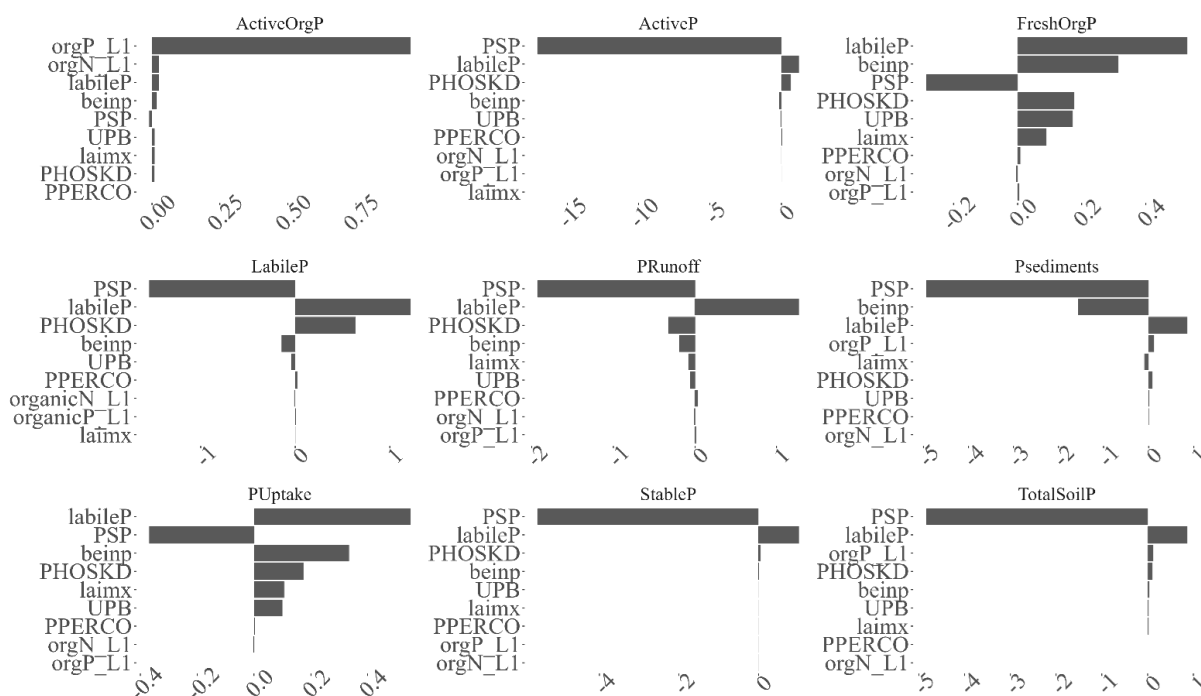
Figure 4.5: Sensitivity of each output variable (subplot headers) to changes in input parameters ranked using the sensitivity index.

sensitivity of Psediments to the parameters was PSP > beinp > labileP > orgP_L1 > laimx > PHOSKD > UPB > PPERCO > orgN_L1 (Figure 4.5).

4.4.2 Watershed-scale assessment

The WEPP-WQ model was applied to two watersheds, namely Blackwood Creek and General Creek watersheds, in the wetter western part of Lake Tahoe Basin with varying soils originating from different parent materials. P-related sensitive parameters identified using the single hillslope sensitivity analysis were used for calibrating the watershed scale model. However, not all parameters identified as sensitive during the analysis were used for calibrating soluble P yield. Parameters that were calibrated for simulating soluble P in both watersheds include initial concentrations of LabileP in the topsoil layer, PSP, PHOSKD, and UPB. Values used in the model for each watershed are presented in Table

4.2.

Table 4.2: Summary of P-related calibrated WEPP-WQ parameters for both simulated watersheds and their default range.

Calibrated Parameters				
Watershed	PSP	UPB	PHOSKD (m^3 Mg^{-1})	Initial LabileP (mg P kg^{-1})
Blackwood Creek	0.374	20.26	200	0.956
General Creek	0.401	20.11	176.45	0.57
Default range	0.01-0.7	0-100	100-200	

4.4.3 Streamflow

The goodness of fit statistics for simulated and observed streamflow are presented in Table 4.3 for daily, monthly, and water year (WY) intervals. The simulated WY trends of water yield compared well with those of observed yield in both General Creek and Blackwood Creek watersheds (Figure 4.6). Average daily and monthly NSE values across both watersheds were > 0.5 and R^2 was ≥ 0.5 with a small PBias of $\leq \pm 6\%$ indicating a satisfactory model performance on both daily and monthly time frames. PBias of $< \pm 6\%$ indicates a slight but acceptable overestimation or underestimation of the simulated streamflow. The comparison of observed and simulated streamflow on the WY time frame indicates a very good model performance with NSE ≥ 0.94, $R^2 \geq 0.94$, and PBias $\leq \pm 6\%$.

4.4.4 Sediment Yield

Generally, the sediment yield from Blackwood creek can be one or more orders of magnitude larger than that from the General Creek watershed (Figure 4.7). This is mainly associated with the difference in the amount of runoff in both watersheds with Blackwood Creek generating significantly larger runoff than General Creek watershed (Figure 4.8). The goodness-of-fit statistics between the simulated and observed sediment yield
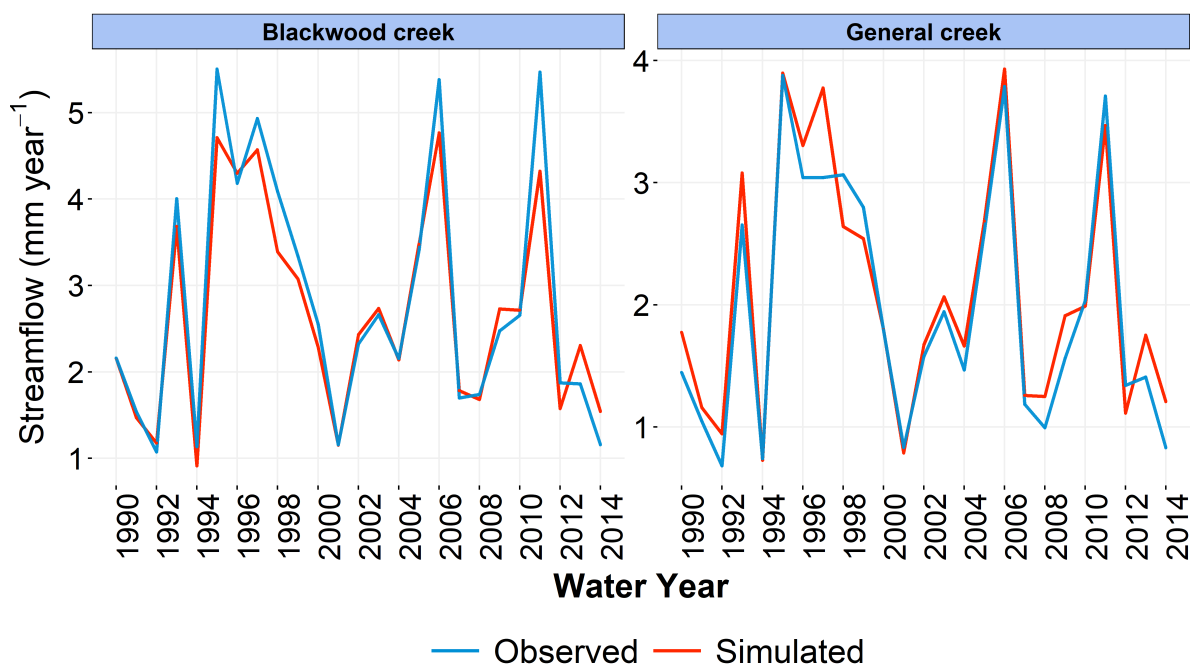
Figure 4.6: Goodness-of-fit between the observed and simulated WY streamflow.

Table 4.3: Goodness-of-fit statistics for the WEPP-WQ model streamflow simulations in the Blackwood Creek watershed and General Creek watershed. D = daily, M = monthly, WY = Water Year statistics.

Watershed		Blackwood Creek	General Creek
Begin		1/1/1990	
End		9/30/2014	
	D	0.53	0.48
NSE	M	0.62	0.56
	WY	0.92	0.92
	D	-4.90	5.80
PBias (%)	M	-4.70	6.10
	WY	-4.90	5.90
	D	0.53	0.49
R^2	M	0.62	0.56
	WY	0.95	0.94

indicated a large underestimation of sediment yield in both watersheds. The goodness-of-fit statistics for the same are presented in Table 4.4. This underestimation was mainly
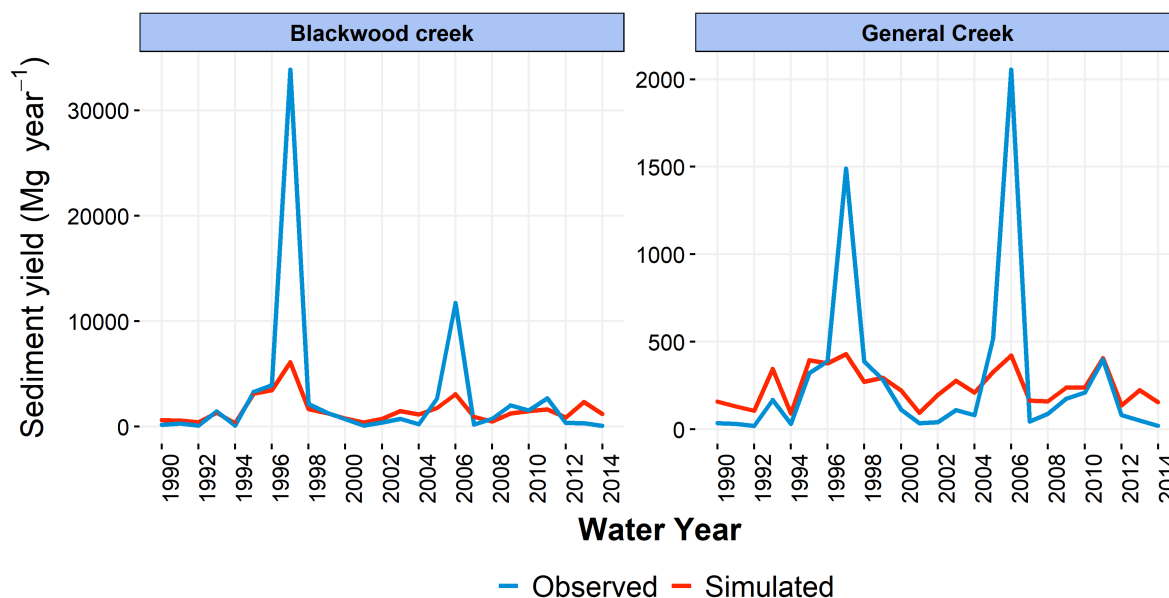
Figure 4.7: Goodness-of-fit between the observed and simulated WY sediment yield.

associated with the 1997 and 2006 WYs that experienced relatively wetter winters with rain-on-snow events leading to significantly high flow events. The goodness-of-fit statistics showed marked improvement in model performance when these two WYs were not considered in the calculation of statistics. The improvements in NSE were from 0.25 to 0.6, PBias were from -45.90 to 14.40 for the Blackwood Creek watershed indicating a satisfactory model performance. Similarly, satisfactory performance was observed for the General Creek watershed with NSE improving from 0.25 to 0.45.

4.4.5 Phosphorus Yield

Overall, the WEPP-WQ model was able to satisfactorily match the annual trends in soluble P delivery. The general trends in the simulated soluble (SRP), particulate (PP), and total P (TP) yields along with the corresponding observed P is displayed in in Figure 4.9. The goodness-of-fit statistics between observed and simulated P are presented in Table 4.5. Daily NSE for SRP was -0.6 for Blackwood Creek and -5.99 for General Creek. Daily PBias for SRP was -4.4% for Blackwood Creek and 24.60% for General Creek
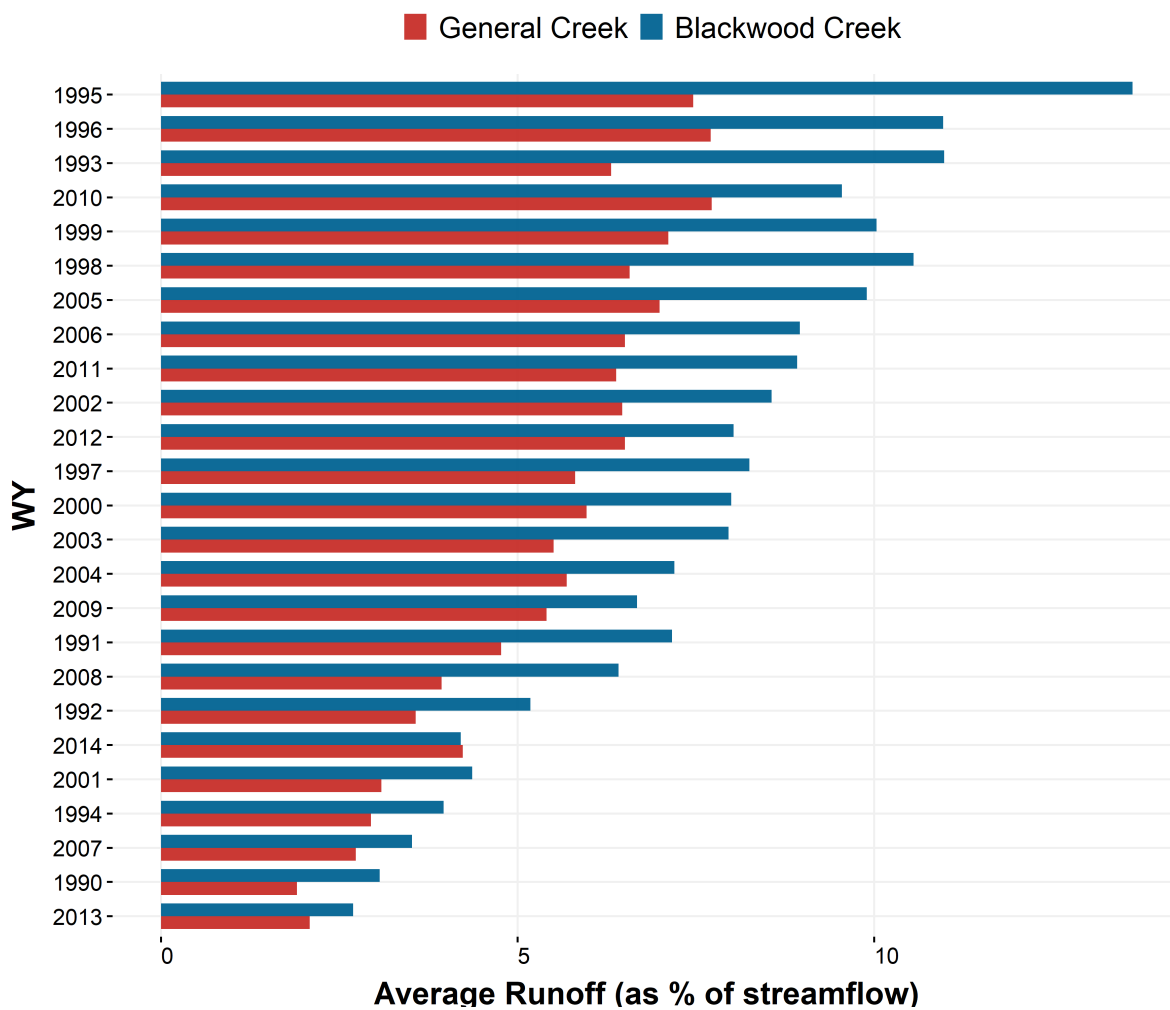
Figure 4.8: Average WY runoff as a fraction of streamflow in the General Creek watershed and Blackwood Creek watershed.

Table 4.4: Goodness-of-fit statistics for the WEPP-WQ model sediment concentration (SSC) simulations in the Blackwood Creek watershed and General Creek watershed. Values in parenthesis show goodness-of-fit without considering WY 1997 and 2006 for calculating statistics.

Parameter	SSC	
Watershed	Blackwood Creek	General Creek
Begin	01/01/1990	
End	9/30/2014	
NSE	0.25 (0.61)	0.25 (0.44)
PBias (%)	-45.90 (14.20)	-15.4 (43.17)
R^2	0.74 (0.64)	0.48 (0.69)

watershed. This indicates model underestimation bias in the Blackwood Creek watershed and overestimation bias in the General Creek watershed, and relatively unsatisfactory model performance to simulate daily SRP. However, the model performance improved at monthly and WY times frame for both watersheds. For the Blackwood Creek watershed, the NSE values were 0.46 for monthly predictions and 0.63 for WY predictions with PBias of $\sim$ -5% indicating a slight overestimation but a satisfactory model performance. Across both the watersheds the average R^2 was 0.37 for daily, 0.57 for monthly, and 0.64 for WY comparisons indicating a satisfactory capture of trends between the observed and simulated SRP.

4.5 Discussion

Sensitivity analysis revealed that PSP, initial LabileP pool, PHOSKD, and UPB were highly sensitive parameters to simulate total soil phosphorus pool and P losses from the profile. Many other studies have documented these four parameters as important and sensitive parameters for simulating P and have used them as key calibration parameters to better represent P export from the watersheds [Merriman et al., 2018, Santhi et al.,
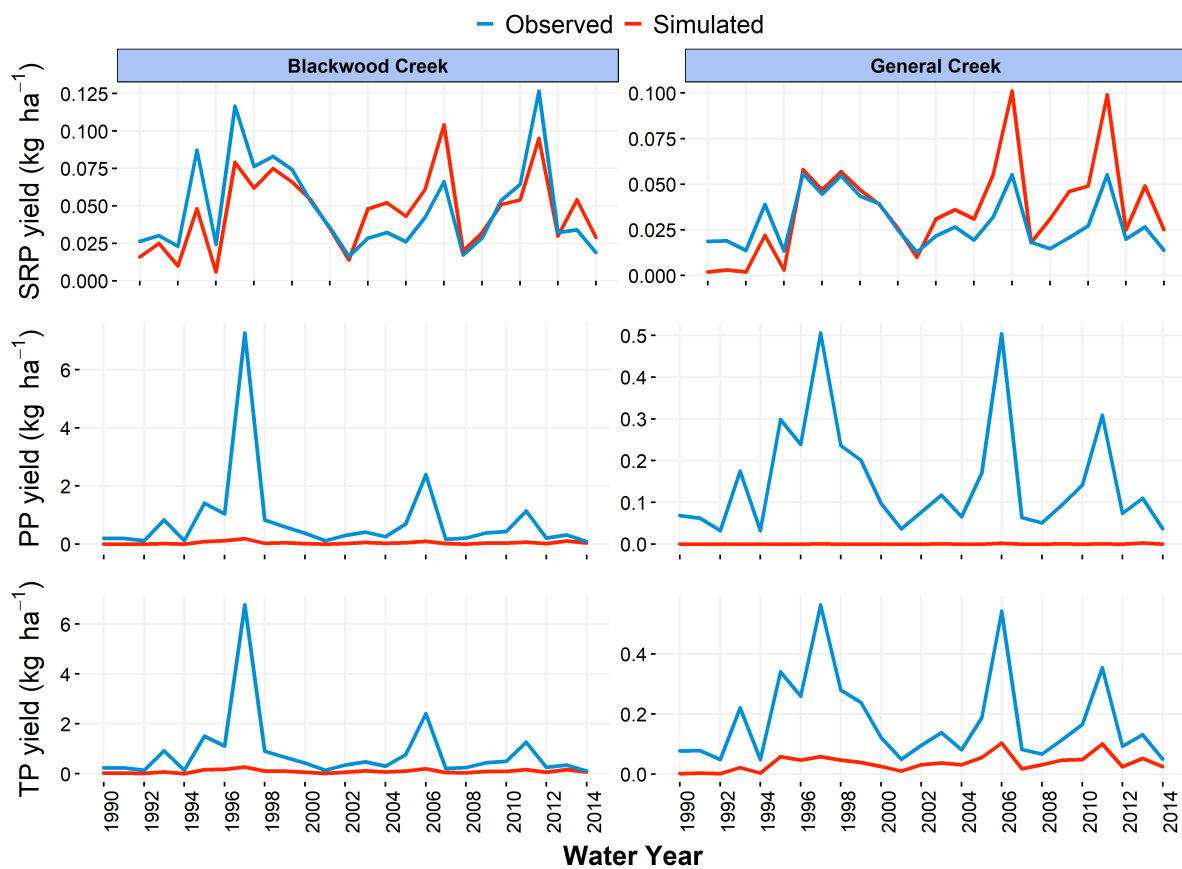
Figure 4.9: Goodness-of-fit between the observed and simulated WY SRP, PP and TP.

Table 4.5: Goodness-of-fit statistics for the WEPP-WQ model phosphorus simulations in the Blackwood Creek watershed and General Creek watershed.

Watershed		Blackwood Creek			General Creek		
Begin		01/01/1990					
End		9/30/2014					
Parameter		SRP	PP	TP	SRP	PP	TP
	D	-0.60	0.03	0.04	-5.99	-0.01	0.09
NSE	M	0.46	0.00	0.02	-1.67	-0.15	0.10
	WY	0.63	-0.24	-0.24	-0.52	-1.33	-0.72
	D	-4.40	-94.41	-89.00	24.60	-99.80	-79.20
PBias (%)	M	-5.00	-94.41	-89.10	23.60	-99.80	-79.40
	WY	-4.40	-94.41	-89.00	24.70	-99.80	-79.20
	D	0.39	0.29	0.26	0.34	0.24	0.20
R^2	M	0.58	0.33	0.29	0.55	0.16	0.42
	WY	0.64	0.65	0.59	0.64	0.17	0.63

2001, White and Chaubey, 2005]. In particular, PSP largely affected the simulated Labile and the total soil phosphorus pools. This consequently affected the phosphorus losses via plant uptake and in dissolved as well as particulate forms. This is reasonable because PSP in the model represents the percent of any added phosphorus that remains labile after equilibrium conditions are established [Vadas et al., 2006] and therefore maintains the inorganic P pool in the model. For instance, 37% of any added P in Blackwood Creek and 40% in General Creek remained labile and the rest was added to the Active P pool. Because the initialization of the Active P and Stable P pools is proportional to the Labile P pool (see Figure 4.1), the total soil phosphorus pool in the soil is sensitive to the initialized labile phosphorus pools as well as the PSP. Along with PSP, the P loss from the soil profile was also sensitive to the initial labile P pool in the topsoil layer as well as the PHOSKD. The calibrated value of initial labile P concentrations was substantially higher in the andesitic Blackwood Creek watershed as compared to the granitic General Creek watershed. Similarly, the linear partition coefficient PHOSKD value for andesitic Blackwood Creek watershed were relatively higher compared to the granitic General Creek watershed. This is consistent with the findings of isotherm experiments reported in chapter 3. Although in chapter 3 P isotherms were based on Langmuir and Fruendlich relationships, by focusing only on the lower dissolved P concentrations, the linear PHOSKD value for andesitic meadows was $\sim$ 200 L/kg and for granitic meadows was $\sim$ 110 L/kg. Relatively higher calibrated PHOSKD and lower calibrated PSP values in andesitic watersheds would suggest a soil having higher total phosphorus but lower water-extractible phosphorus and this is consistent with the findings of [Heron et al., 2021]. Heron et al. [2021] reported the high TP forest soils had less labile P compared to the low TP forest soils which also had less Fe and Al hydroxides. In addition to these parameters, P loss from soil profile via plant uptake was sensitive to the UPB value. The values of these four parameters determined via calibration in this study agree with those

reported in the literature that used the SWAT model to simulate phosphorus losses [Merriman et al., 2018, Santhi et al., 2001, White and Chaubey, 2005]. In a forested watershed context, plant residue decomposition and atmospheric depositions can be two pathways by which P gets added to the soil. Therefore, P cycling between vegetation and soil could also be sensitive to the residue decay constant and the senescence fraction variables in the WEPP-WQ model. In, this study, these two variables were not evaluated for their effect on simulating P and should be investigated for their effects in the future study.

Based on the criteria of Foglia et al. [2009], agreement of simulated streamflow to the observed streamflow generally ranged from 'good' to 'very good' at both the watersheds for varying time frames. While the overall streamflow for the simulation period was modeled quite well, the peak flows during the extremely wet winters of WY 1997 and WY 2006 were underestimated. One likely source of this peak flow underestimation could be the uncertainty associated with the precipitation input data itself. Brooks et al. [2016] have shown that WEPP can capture the 1997 peak flows in Lake Tahoe Basin watersheds with an accurate precipitation input that represents rainfall distribution more precisely. The underestimated peak flows also caused the underestimation of simulated sediments in both the watersheds during WY 1997 and WY 2006. These peak flows were associated with the early winter extreme rain on snow events. For instance, the 1997 wetter winter was regarded as a 100-year-flood event [Tetra Tech Inc., 2007] and caused a 40-year-sediment event in the Blackwood Creek watershed [Simon et al., 2003]. Such rain on snow events are a frequent occurrence in the Lake Tahoe Basin [McCabe et al., 2007, Roberts et al., 2018].

Generally, Blackwood Creek delivered a larger sediment load compared to General Creek. The contribution of channels and hillslopes to sediment yield varied largely between the two modeled watersheds (Figure 4.10). Channels contributed a significantly large fraction of sediment in the General Creek watershed with minimal sediment from

the hillslopes. In the case of Blackwood Creek, hillslopes contributed a relatively larger fraction of the sediment yield. These findings on sediment yield are in agreement with the findings reported in other studies [Brooks et al., 2016, Simon et al., 2003]. Except for the two wetter WY's, the simulated sediment yields agreed well with the observed data. The channel-derived sediments from Blackwood Creek per km of the channel are reported to be 14 times that derived from General Creek [Simon et al., 2003]. Simon et al. [2003] reported that the lower 8.5 km of General Creek erode on an average 3975 kg/y/km of fine sediments. In addition, sediment resuspended into the stream/water column can be a potential source of P affecting the long-term observed P seasonality [Stutter et al., 2021]. Inamdar et al. [2020] have reported that the redox conditions and the stream water P concentrations can govern whether the resuspended sediment acts as source or sink of P. Inamdar et al. [2020] suggest that under low stream water P conditions or under anoxic conditions developed by reductive dissolution of iron oxides, resuspended sediment in the soil column could release P acting as a net source.

Overall, SRP magnitude and seasonality were generally adequately captured by the model in both the watersheds. Although the PP magnitude was underpredicted in both the watersheds there was good agreement between the simulated and observed seasonality and timing of PP yield from both the watersheds (Figure 4.9, Table 4.5). The seasonality and timing of PP yield seem to be much better captured in the Blackwood Creek watershed whereas the same appears to be much more channel-sediment driven in the General Creek watershed. This is because the WEPP-WQ simulations indicate that Blackwood Creek watershed has significant hillslope contributions to the sediment yield (Figure 4.10) whereas the hillslope contributions to the sediment yield are negligible from the General Creek watershed. Such hillslope contributions to the total sediment from the Blackwood Creek watershed were also reported by Brooks et al. [2016]. It is therefore reasonable to partly associate the better capture of overall seasonality and timing of PP yield in the
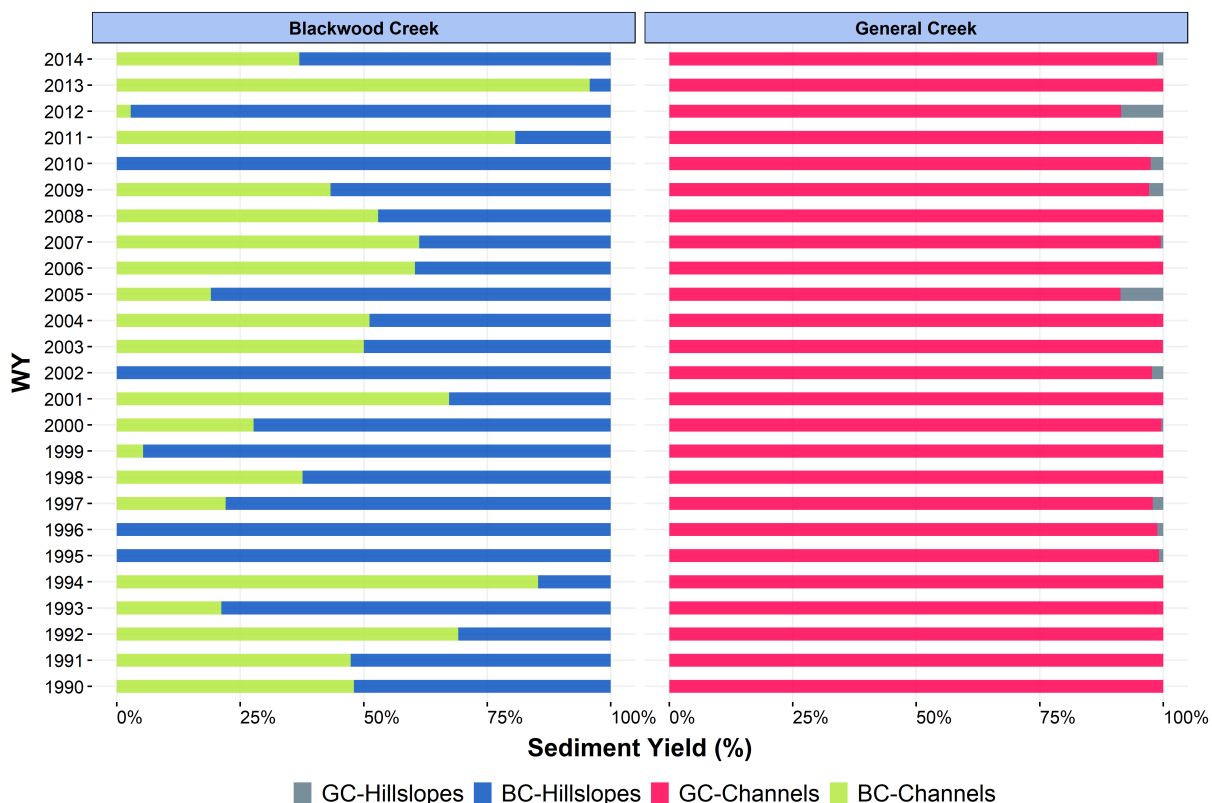
Figure 4.10: WY contribution from hillslopes and channels to the sediment yield from Blackwood and General Creek watersheds.

Blackwood Creek watershed to the fine sediment loading from the upland. In the case of simulated PP yield from the General Creek watershed, the slight capture of seasonality and timing coincides with the wet years when hillslopes did contribute some sediment (Figure 4.8, Figure 4.9).

Based on a simple mass balance analysis using the particulate P concentrations used by Dobre et al. [2022] it appears the absolute magnitude of particulate P is underpredicted by WEPP-WQ from Blackwood Creek watershed. Table 4.6 lists the absolute magnitudes of P export for each watershed based on both WEPP-WQ and P loading estimates based on the Dobre et al. [2022] approach. Dobre et al. [2022] reported the average P concentration on sediments to be 1300 mg/kg at the outlet of General Creek watershed and 1100 mg/kg at the outlet of Blackwood Creek watershed. WEPP-WQ simulated the sediment

contributions to overall export to be 239 Mg yr^{-1} and 355.5 Mg yr^{-1} from channels in Blackwood Creek watershed and General Creek watershed, respectively. Since the P algorithms in WEPP-WQ do not simulate P cycling in streams then it implies none of this sediment that has been eroded in the stream carries any phosphorus. By assuming this in stream channel sediment in General creek has a particulate P concentration of 1300 mg/kg [Dobre et al., 2022] the simulated TP load closely matches the observed TP load at the General Creek watershed outlet. When this same approach is applied to Blackwood creek using a PP concentration of 1100 mg/kg [Dobre et al., 2022] the simulate TP load at the outlet is much lower than the observed TP load even when excluding the 1997 and 2006 WY's. This suggests that the simulated PP load from upland hillslopes in Blackwood creek is underpredicted. The concentration of P on the sediments calculated as the ratio of predicted average particulate P yield to the total sediment yield is about 14 times smaller (78.4 mg kg^{-1}) than the concentrations suggested by Dobre et al. [2022]. This underprediction of upland PP load appears to be a model structure problem and associated with how the soil P pools are initialized in the model. Specifically, to generate more PP load with the same amount of eroded sediment the particulate P concentration, particularly the stable P pool, of the eroded sediment must increase. Interestingly, as currently structured the stable inorganic P pool is fixed based on the presumed equilibrium of 4 times the active P pool. Further, the active P pool is a function of PSP (see Figure 4.1; Eq 4.1) and the magnitude of the labile pool. Heron [2019] reported TP in the soils of andesitic forest in Lake Tahoe in the range of 1080-1130 mg/kg. To initialize the model to represent the total soil P concentration in this range requires a very small PSP value (e.g., 0.0045 as against the calibrated 0.374) which is three orders of magnitude smaller that calibrated value based on agreement between observed and simulate soluble P. Sensitivity analysis has shown that P losses via runoff are highly sensitive to PSP and making the PSP value substantially smaller (0.0045) in Blackwood Creek watershed will result

unreasonably large soluble P concentration and significantly larger SRP load than that has been observed. The other alternative to dropping PSP to increase the concentration of the stable P pool would be to assume a much large, fixed ratio between the stable and active P pools in the soil. The stable P pool would likely need to be orders of magnitude larger than the active P rather than the default 4-fold increase in order for the total P concentration in these soils to be in range with the values reported by [Heron, 2019]. It is possible that the 4-fold factor implemented into the WEPP-WQ based on SWAT water quality codes are a reasonable assumption for agricultural dominated soils but needs to be revised for forest soils. The reason the total P from General creek based on the Dobre et al. [2022] presumed particulate concentration in the eroded stream channel sediments is not greatly different as observed in the Blackwood creek simulation is very likely due to the fact that according to the model very little of the sediment delivered to the stream was derived from the upland hillslopes.

Table 4.6: Account of P load associated with the channel sediment load that is currently not captured by WEPP-WQ. *Calculated PP load assuming P concentrations reported by Dobre et al, (2022). **Sum of TP load modeled by WEPP-WQ and PP load associated with channel sediments. ***Sum of calibrated initial LabileP and proportional active and stable inorganic P.

	Units	General Creek	Blackwood Creek
Observed TP load	kg yr^{-1}	322.4	2221.9
Observed TP load excluding WY 1997 & 2006	kg yr^{-1}	262.9	1351.2
Modeled sediment load from channels	Mg yr^{-1}	239.5	355.5
P concentration on sediments*	mg kg^{-1}	1300.0	1100.0
PP load unaccounted from channel sediments *	kg yr^{-1}	311.3	391.1
Modeled TP from hillslopes	kg yr^{-1}	76.8	243.9
TP load including P associated with channel sediment load**	kg yr^{-1}	388.2	635.0
Initial TP pool in the model***	mg kg^{-1}	4.82	8.95

Despite the current limitation with accounting for P loading from stream sediments, there are some advantages of using WEPP-WQ over the simpler algorithm currently implemented in the WEPPcloud [Dobre et al., 2022]. First, WEPP-WQ P algorithms cycle P though the soil profile and interact with the vegetation growth and flow pathways.

This is in contrast with the simplistic approach currently implemented in WEPPcloud that uses fixed concentrations of P in different flow pathways to simulate P. Second, because there's interaction between soil P, vegetation growth and flow pathways WEPP-WQ can be an improved choice to model impacts of various managements on dissolved P transport. However, there are also some drawbacks of the current WEPP-WQ approach. Like the WEPPcloud P approach, WEPP-WQ does not provide fractions of P transported with runoff, lateral, and baseflow components. However, WEPP-WQ does simulate P percolating to the soil layer below using the PPERCO parameter. This in the future can be linked with the lateral flow and deep seepage to inform on the fractions of P transported with runoff, lateral, and baseflow components. In addition, there are several factors that need to be addressed for WEPP-WQ to be complete watershed scale water quality model. These are discussed later in this section.

In the context of targeting management, about 3% of the hillslope area in the General Creek watershed contributes 98% of sediment and particulate phosphorus losses compared to the 15% in the Blackwood Creek watershed (Figure 4.11). Similarly, 98% runoff and dissolved phosphorus occur from 25% of the hillslope area in the General Creek watershed and 31% of the hillslope area in Blackwood Creek watersheds (Figure 4.11). Much of these areas that generate sediment, phosphorus, and runoff are located upland in the General Creek watershed (Figure 4.12) and are either rock outcrops or very gravelly loamy sands at varying gradients. It is unlikely that much of this sediment and P will reach the watershed outlet. In Blackwood Creek watersheds, the hotspots of runoff, sediment, and phosphorus are located across the watersheds with some hillslopes located relatively closer to the watershed outlet (Figure 4.13). Much of these hillslopes are rock outcrops or sandy soils of type Melody, Ellispeak, Waca, Montrose, and Keenridge. These findings are consistent with those reported by Brooks et al. [2016] and therefore these areas could be important hotspots for the management of sediment and phosphorus losses.
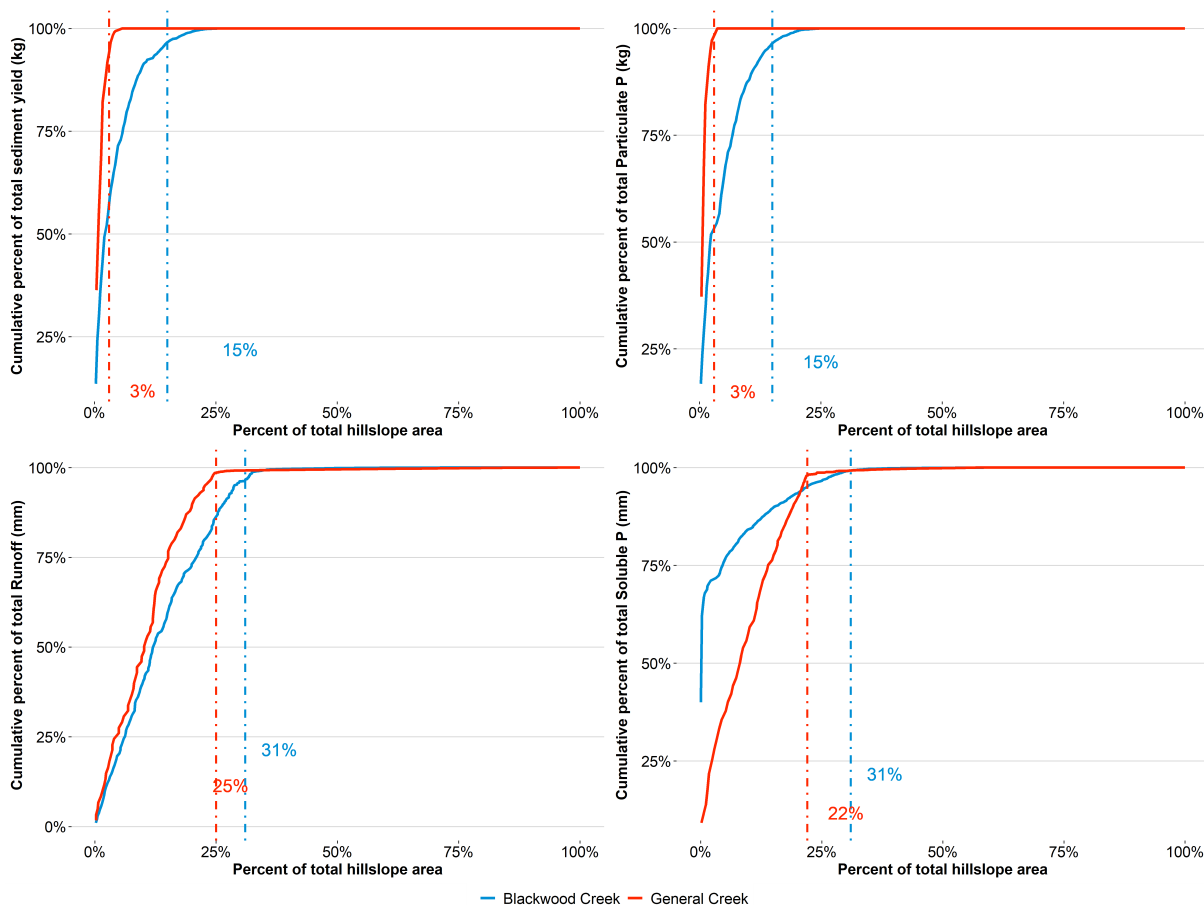
Figure 4.11: Cumulative curves of sediment, runoff, SRP, PP yields showing percent of total hillslope area contributing to the significant yields.

Multiple themes need to be addressed in the future before WEPP-WQ becomes a complete watershed-scale water quality model. These include (i) routing of phosphorus from hillslopes to the watershed outlet, (ii) accounting for phosphorus associated with sediments yield from channels, as well as the instream adsorption and release dynamics based on the redox conditions in the water column (iii) and incorporating P yield via different pathways such as baseflow, lateral flow, and runoff. Another factor that could be considered in the future study is informing the labile P initialization of the model by using soil test phosphorus data. To be able to better capture PP load associated with the upland erosion, the initialization of stable P pool needs to be further investigated. This
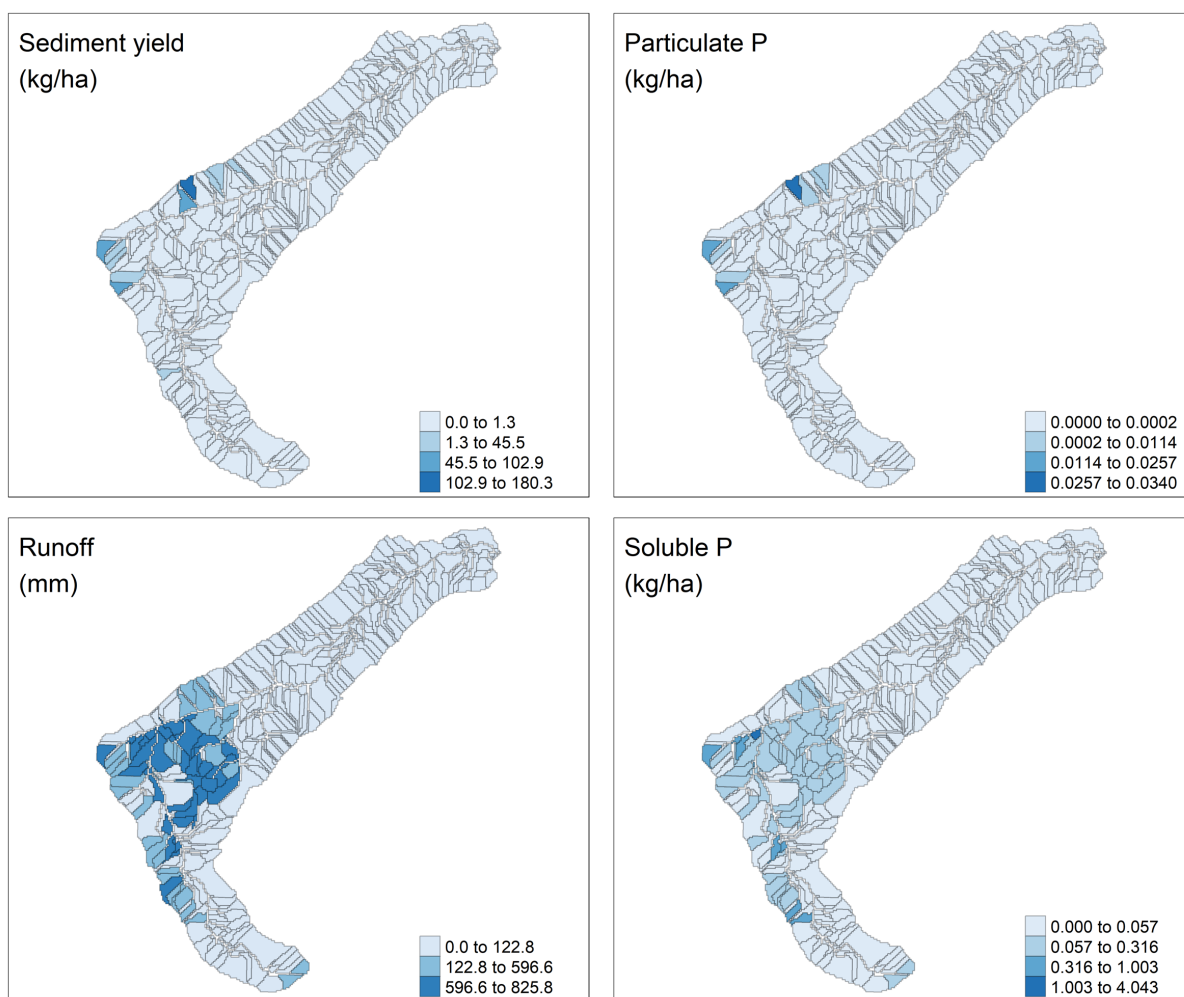
Figure 4.12: Hillslope-scale hotspots of simulated average Runoff, sediment yield, and P (soluble and particulate) in the General Creek watershed.

will not only help initialize a more representative soil phosphorus pool in the watershed but also remove the need to calibrate the initial soil phosphorus concentration. While all these updates will make WEPP-WQ a more comprehensive water quality model, this study has presented enough evidence to suggest that the model adequately captures the processes and loss of dissolved phosphorus via surface pathways. The model structure for soil P pool initialization needs to be further investigated for improving the PP load simulation associated with the upland sediment load. In its present state with the ability to achieve satisfactory model performance by calibrating minimal parameters for calibrating
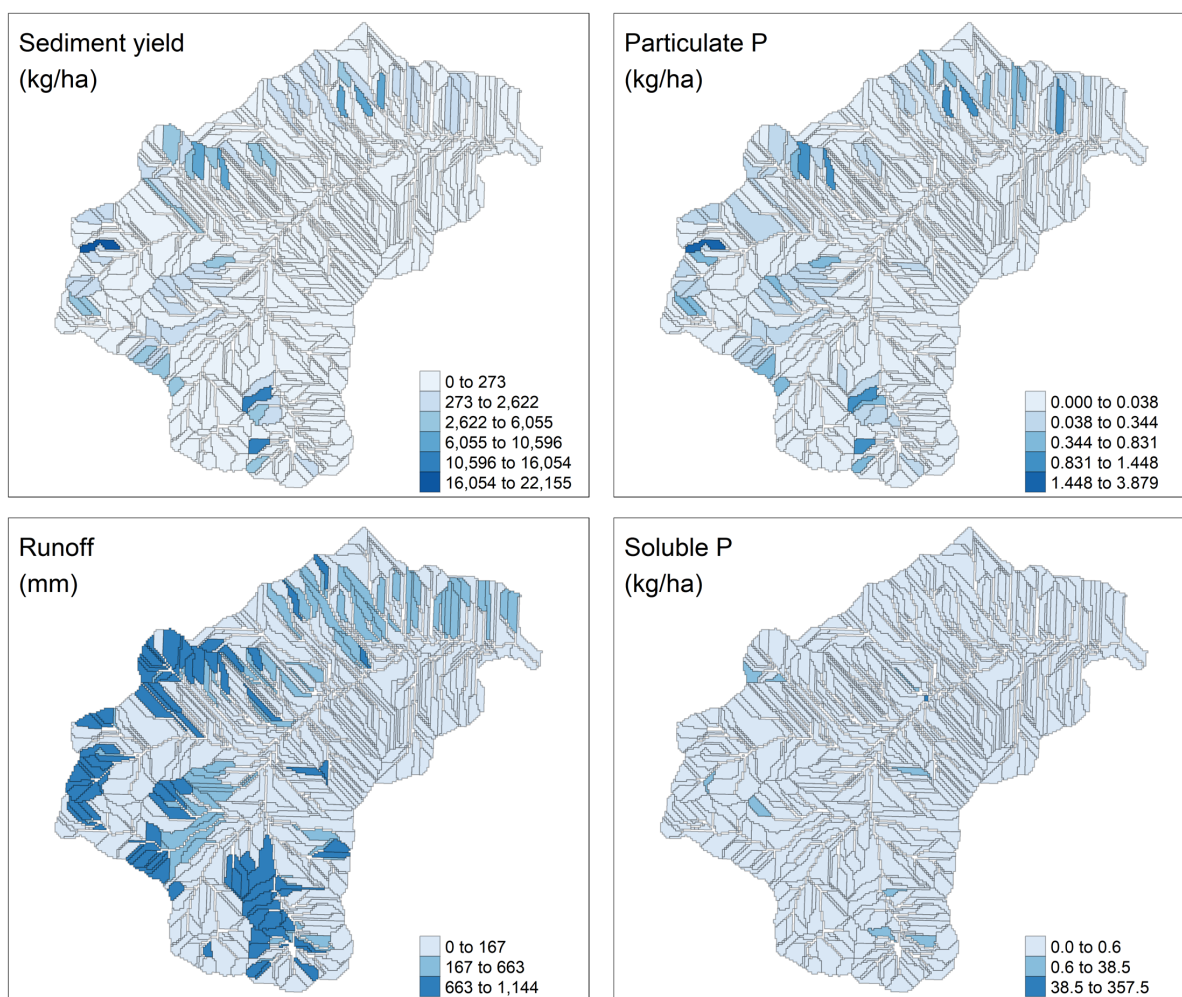
Figure 4.13: Hillslope-scale hotspots of simulated average Runoff, sediment yield, and P (soluble and particulate) in the Blackwood Creek watershed.

water, sediment, and dissolved phosphorus yields and with future developments of channel nutrient routines, WEPP-WQ presents a strong case for a process-based yet parsimonious water quality model. Currently, it can be a useful tool to inform management when used to assess the edge-of-the-hillslope effects of management on dissolved phosphorus losses.

4.6 Conclusions

In this study, the process-based coupled Water Erosion Prediction Project and Water Quality (WEPP-WQ) model was evaluated for the parameter sensitivities for simulating dissolved and particulate phosphorus and its prediction capabilities for simulating phosphorus yield from large, forested watersheds. Model sensitivity to phosphorus parameters was determined by varying each parameter one a time while keeping the rest of the parameter's constant. Parameter sensitivity analysis showed that the P sorption parameter (PSP), P soil partitioning parameter (PHOSKD), initial labile phosphorus pool in the topsoil layer (LabileP), and P uptake distribution parameter (UPB) are some of the relatively important and sensitive parameters for simulating phosphorus with WEPP-WQ. The relative differences between calibrated values obtained for these parameters in watersheds with differing soil type are well supported by the findings of isotherm experiments in this chapter as well as the findings reported byHeron et al. [2021]. This study was one of the first times WEPP-WQ was applied to large watersheds and demonstrated the application of WEPP-WQ to the large, forest-dominated watershed with varying soil types. WEPP-WQ performance was adequate to predict dissolved phosphorus yields in the modeled watersheds. While WEPP-WQ does not account for the P contributions associated with the channel processes, the seasonality and relative trends of particulate phosphorus were correctly predicted. A simple analysis of TP load using a fixed P concentration associated with detached channel sediments, showed that the absolute magnitude of predicted particulate phosphorus from upland sources is underpredicted by the model. This underprediction may be due to the assumed relative distribution of P in active and stable pools that may not be appropriate for forested soils or due to the underestimation of P enrichment ratio or a combination of both. Further investigation of model structure is needed to identify appropriate soil P pool initialization. Significant development

and testing are needed for WEPP-WQ to be fully ready for use. Model structure, soil P pool initialization, correct P enrichment ratio estimations, sensitivity of parameters like plant residue decay and senescence to P cycling, in-stream P processes, and routing of P from hillslopes to watershed outlet are some of the areas that the future testing and investigations should focus on. Target analysis with the model indicate in the Lake Tahoe watersheds that much of the P load comes from a small fraction of the total hillslope area and much is delivered in infrequent major rain/snow events. This has important implications for management. Modeling dissolved P with WEPP-WQ could be a better approach compared to the current P approach implemented in WEPPcloud that does not incorporate P-cycling. WEPP-WQ is likely better able to capture changes in disturbance on P pools and dissolved P. Overall, this study shows that WEPP-WQ, with its current dissolved phosphorus routines, can be an effective, process-based, and yet parsimonious edge-of-the-hillslope effects tool for informing land and water management decisions.

References

J. K. Agee and C. N. Skinner. Basic principles of forest fuel reduction treatments. In *Forest Ecology and Management*, volume 211, pages 83–96. Elsevier, jun 2005. ISBN 0378-1127. doi: 10.1016/j.foreco.2005.01.034. URL `https://www.sciencedirect.com/science/article/pii/S0378112705000411?via{\%}3Dihub{\#}bib13`.

L. Andersson, J. Rosberg, B. C. Pers, J. Olsson, and B. Arheimer. Estimating catchment nutrient flow with the HBV-NP model: Sensitivity to input data. *Ambio*, 34(7):521–532, nov 2005. ISSN 00447447. doi: 10.1579/0044-7447-34.7.521. URL `https://bioone.org/journals/ambio-a-journal-of-the-human-environment/volume-34/issue-7/0044-7447-34.7.521/Estimating-Catchment-Nutrient-Flow-with-the-HBV-NP-Model/10.1579/0044-7447-34.7.521.fullhttps://bioone.org/journals/ambio-a-journal-of-the-human-env`.

J. G. Arnold, R. Srinivasan, R. S. Muttiah, and J. R. Williams. Large area hydrologic modeling and assessment part I: Model development. *Journal of the American Water Resources Association*, 34(1):73–89, feb 1998. ISSN 1093474X. doi: 10.1111/j.1752-1688.1998.tb05961.x. URL `https://onlinelibrary.wiley.com/doi/full/10.1111/j.1752-1688.1998.tb05961.xhttps://onlinelibrary.wiley.com/doi/abs/10.1111/j.1752-1688.1998.tb05961.xhttps://onlinelibrary.wiley.com/doi/10.1111/j.1752-1688.1998.tb05961.x`.

B. J. Bentz, J. Régnière, C. J. Fettig, E. M. Hansen, J. L. Hayes, J. A. Hicke, R. G. Kelsey, J. F. Negrón, and S. J. Seybold. Climate Change and Bark Beetles of the Western United States and Canada: Direct and Indirect Effects. *BioScience*, 60(8): 602–613, 2010. doi: 10.1525/bio.2010.60.8.6. URL `www.biosciencemag.org`.

J. Boll, E. S. Brooks, B. Crabtree, S. Dun, and T. S. Steenhuis. Variable Source Area Hydrology Modeling with the Water Erosion Prediction Project Model. *Journal of the*

American Water Resources Association, 51(2):330–342, apr 2015. ISSN 1093474X. doi: 10.1111/1752-1688.12294. URL `http://doi.wiley.com/10.1111/1752-1688.12294http://dx.doi.org/10.1111/1752-1688.12294`.

E. S. Brooks, M. Dobre, W. J. Elliot, J. Q. Wu, and J. Boll. Watershed-scale evaluation of the Water Erosion Prediction Project (WEPP) model in the Lake Tahoe basin. *Journal of Hydrology*, 533:389–402, feb 2016. ISSN 00221694. doi: 10.1016/j.jhydrol.2015.12.004.

R. Coats, M. Larsen, A. Heyvaert, J. Thomas, M. Luck, and J. Reuter. Nutrient and sediment production, watershed characteristics, and land use in the Tahoe Basin, California-Nevada. *Journal of the American Water Resources Association*, 44(3):754–770, jun 2008. ISSN 1093474X. doi: 10.1111/j.1752-1688.2008.00203.x.

R. Coats, J. Lewis, N. Alvarez, and P. Arneson. Temporal and Spatial Trends in Nutrient and Sediment Loading to Lake Tahoe, California-Nevada, USA. *JAWRA Journal of the American Water Resources Association*, 52(6):1347–1365, dec 2016. ISSN 1752-1688. doi: 10.1111/1752-1688.12461. URL `https://onlinelibrary.wiley.com/doi/full/10.1111/1752-1688.12461https://onlinelibrary.wiley.com/doi/abs/10.1111/1752-1688.12461https://onlinelibrary.wiley.com/doi/10.1111/1752-1688.12461`.

A. S. Collick, T. L. Veith, D. R. Fuka, P. J. Kleinman, A. R. Buda, J. L. Weld, R. B. Bryant, P. A. Vadas, M. J. White, R. D. Harmel, and Z. M. Easton. Improved Simulation of Edaphic and Manure Phosphorus Loss in SWAT. *Journal of Environmental Quality*, 45(4):1215–1225, jul 2016. ISSN 1537-2537. doi: 10.2134/jeq2015.03.0135.

B. J. Collins, C. C. Rhoades, M. A. Battaglia, and R. M. Hubbard. The effects of bark beetle outbreaks on forest development, fuel loads and potential fire behavior in

salvage logged and untreated lodgepole pine forests. *Forest Ecology and Management*, 284:260–268, nov 2012. ISSN 03781127. doi: 10.1016/j.foreco.2012.07.027. URL `https://www.sciencedirect.com/science/article/pii/S037811271200432X`.

S. A. Covert, P. R. Robichaud, W. J. Elliot, and T. E. Link. Evaluation of runoff prediction from WEPP-based erosion models for harvested and burned forest watersheds. *Transactions of the American Society of Agricultural Engineers*, 48(3):1091–1100, may 2005. ISSN 00012351. doi: 10.13031/2013.18519. URL `https://elibrary.asabe.org/azdez.asp?JID=3{\&}AID=18519{\&}CID=t2005{\&}v=48{\&}i=3{\&}T=1http://elibrary.asabe.org/abstract.asp?aid=18519{\&}confalias={\&}t=1{\&}redir={\&}redirType=https://doi.org/10.13031/2013.18519`.

M. Devak and C. T. Dhanya. Sensitivity analysis of hydrological models: Review and way forward. *Journal of Water and Climate Change*, 8(4):557–575, dec 2017. ISSN 20402244. doi: 10.2166/wcc.2017.149. URL `http://iwaponline.com/jwcc/article-pdf/8/4/557/239262/jwc0080557.pdf`.

M. Dobre, A. Srivastava, R. Lew, C. Deval, E. S. Brooks, W. J. Elliot, and P. Robichaud. WEPPcloud: An online watershed-scale hydrologic modeling tool. Part II. Model performance assessment and applications to forest management and wildfires. *Journal of Hydrology*, (this issue), 2022.

J. E. Doherty. *Calibration and Uncertainty Analysis for Complex Environmental Models.* Watermark Numerical Computing, 2015. ISBN 978-0-9943786-0-6.

S. Dun, J. Q. Wu, W. J. Elliot, P. R. Robichaud, D. C. Flanagan, J. R. Frankenberger, R. E. Brown, and A. C. Xu. Adapting the Water Erosion Prediction Project (WEPP) model for forest applications. *Journal of Hydrology*, 366(1-4):46–54, mar 2009. ISSN 00221694. doi: 10.1016/j.jhydrol.2008.12.019.

W. Elliot, E. Brooks, D. E. Traeumer, and M. Dobre. Extending WEPP Technology to Predict Fine Sediment and Phosphorus Delivery from Forested Hillslopes. In *SEDHYD 2015 Interagency Conference*, page 12, Reno, NV, 2015. URL `https://www.fs.fed.us/rm/pubs{\_}journals/2015/rmrs{\_}2015{\_}elliot{\_}w002.pdf`.

D. C. Flanagan, J. E. Gilley, and T. G. Franti. Water Erosion Prediction Project (WEPP): Development history, model capabilities, and future enhancements. *Transactions of the ASABE*, 50(5):1603–1612, 2007. ISSN 21510032.

D. C. Flanagan, J. R. Frankenberger, and J. C. A. II. WEPP: Model Use, Calibration, and Validation. *Transactions of the ASABE*, 55(4):1463–1477, 2012. doi: 10.13031/2013.42254. URL `https://elibrary.asabe.org/azdez.asp?JID=3{\&}AID=42254{\&}CID=t2012{\&}v=55{\&}i=4{\&}T=1http://elibrary.asabe.org/abstract.asp?aid=42254{\&}confalias={\&}t=1{\&}redir={\&}redirType=https://doi.org/10.13031/2013.42254`.

L. Foglia, M. C. Hill, S. W. Mehl, and P. Burlando. Sensitivity analysis, calibration, and testing of a distributed hydrological model using error-based weighting and one objective function. *Water Resources Research*, 45 (6):6427, jun 2009. ISSN 00431397. doi: 10.1029/2008WR007255. URL `https://onlinelibrary.wiley.com/doi/full/10.1029/2008WR007255https://onlinelibrary.wiley.com/doi/abs/10.1029/2008WR007255https://agupubs.onlinelibrary.wiley.com/doi/10.1029/2008WR007255`.

D. A. Haith and L. L. Shoenaker. GENERALIZED WATERSHED LOADING FUNCTIONS FOR STREAM FLOW NUTRIENTS. *JAWRA Journal of the American Water Resources Association*, 23(3):471–478, jun 1987. ISSN 17521688. doi: 10.1111/j.1752-1688.1987.tb00825.x. URL `http://doi.wiley.com/10.1111/j.1752-1688.1987.tb00825.x`.

L. K. Hatch, J. E. Reuter, and C. R. Goldman. Stream phosphorus transport in the Lake Tahoe basin, 1989-1996. *Environmental Monitoring and Assessment*, 69(1):63–83, 2001. ISSN 01676369. doi: 10.1023/A:1010752628576.

T. Heron. *Environmental Factors Influencing Phosphorus Availability and Speciation in Forest and Meadow Soils of the Lake Tahoe Basin.* PhD thesis, University of Idaho, 2019.

T. Heron, D. G. Strawn, M. Dobre, B. J. Cade-Menun, C. Deval, E. S. Brooks, J. Piaskowski, C. Gasch, and A. Crump. Soil Phosphorus Speciation and Availability in Meadows and Forests in Alpine Lake Watersheds With Different Parent Materials. *Frontiers in Forests and Global Change*, 3:159, feb 2021. ISSN 2624893X. doi: 10.3389/ffgc.2020.604200.

S. Inamdar, N. Sienkiewicz, A. Lutgen, G. Jiang, and J. Kan. Streambank legacy sediments in surface waters: Phosphorus sources or sinks? *Soil Systems*, 4(2):1–20, 2020. ISSN 25718789. doi: 10.3390/soilsystems4020030.

R. Johanson, J. Imhoff, J. Little, and A. Donigian. Hydrological Simulation Program-Fortran (HSPF): user's manual. Technical report, U.S. Environmental Protection Agency, Athens, GA., 1984.

C. A. Johnston, G. Pinay, C. Arens, and R. J. Naiman. Influence of Soil Properties on the Biogeochemistry of a Beaver Meadow Hydrosequence. *Soil Science Society of America Journal*, 59(6):1789–1799, nov 1995. ISSN 0361-5995. doi: 10.2136/sssaj1995. 03615995005900060041x. URL `https://onlinelibrary.wiley.com/doi/full/` `10.2136/sssaj1995.03615995005900060041xhttps://onlinelibrary.wiley.` `com/doi/abs/10.2136/sssaj1995.03615995005900060041xhttps://acsess.` `onlinelibrary.wiley.com/doi/10.2136/sssaj1995.03615995005900060041x.`

J. M. Laflen and S. Forest. WEPP-Predicting water erosion using a process-based model. *Journal of Soil and Water Conservation*, 52(2):96–102, 1997. URL `http://www.jswconline.org/content/52/2/96.full.pdf+html`.

R. Lew, M. Dobre, A. Srivastava, E. S. Brooks, W. J. Elliot, P. R. Robichaud, and D. C. Flanagan. WEPPcloud: An online watershed-scale hydrologic modeling tool. Part I. Model description. *Journal of Hydrology*, page 127603, feb 2022. ISSN 00221694. doi: 10.1016/j.jhydrol.2022.127603.

Mauricio Zambrano-Bigiarini. *hydroGOF: Goodness-of-fit functions for comparison of simulated and observed hydrological time series*, 2020. URL `https://github.com/hzambran/hydroGOF`.

G. J. McCabe, M. P. Clark, and L. E. Hay. Rain-on-snow events in the western United States. *Bulletin of the American Meteorological Society*, 88(3):319–328, mar 2007. ISSN 00030007. doi: 10.1175/BAMS-88-3-319. URL `https://journals.ametsoc.org/view/journals/bams/88/3/bams-88-3-319.xml`.

K. R. Merriman, A. M. Russell, C. M. Rachol, P. Daggupati, R. Srinivasan, B. A. Hayhurst, and T. D. Stuntebeck. Calibration of a field-scale soil and water assessment tool (SWAT) model with field placement of best management practices in Alger Creek, Michigan. *Sustainability (Switzerland)*, 10(3):851, mar 2018. ISSN 20711050. doi: 10.3390/su10030851. URL `https://www.mdpi.com/2071-1050/10/3/851/htmhttps://www.mdpi.com/2071-1050/10/3/851`.

D. N. Moriasi, J. G. Arnold, M. W. Van Liew, R. L. Bingner, R. D. Harmel, and T. L. Veith. Model evaluation guidelines for systematic quantification of accuracy in watershed simulations. *Transactions of the ASABE*, 50(3):885–900, 2007. ISSN 21510032.

D. G. Neary, G. G. Ice, and C. R. Jackson. Linkages between forest soils and water

quality and quantity. *Forest Ecology and Management*, 258(10):2269–2281, 2009. ISSN 03781127. doi: 10.1016/j.foreco.2009.05.027.

S. Neitsch, J. Arnold, J. Kiniry, and J. Williams. Soil & Water Assessment Tool Theoretical Documentation Version 2009, 2011. ISSN 2151-0040. URL `http://oaktrust.library.tamu.edu/bitstream/handle/1969.1/128050/TR-406{\_}SoilandWaterAssessmentToolTheoreticalDocumentation.pdf?sequence=1`.

P. W. Gassman, J. R. Williams, X. Wang, A. Saleh, E. Osei, L. M. Hauck, R. C. Izaurralde, and J. D. Flowers. Invited Review Article: The Agricultural Policy/Environmental eXtender (APEX) Model: An Emerging Tool for Landscape and Watershed Environmental Analyses. *Transactions of the ASABE*, 53(3):711–740, 2010. ISSN 2151-0040. doi: 10.13031/2013.30078. URL `https://ageconsearch.umn.edu/bitstream/49156/2/09-TR49.pdfhttp://elibrary.asabe.org/abstract.asp??JID=3{\&}AID=30078{\&}CID=t2010{\&}v=53{\&}i=3{\&}T=1`.

A. Pandey, V. M. Chowdary, B. C. Mal, and M. Billib. Application of the WEPP model for prioritization and evaluation of best management practices in an Indian watershed. *Hydrological Processes*, 23(21):2997–3005, oct 2009. ISSN 08856087. doi: 10.1002/hyp.7411. URL `www.interscience.wiley.com`.

S. S. Rájan and R. L. Fox. Phosphate adsorption by soils 1. influence of time and ionic environment on phosphate adsorption. *Communications in Soil Science and Plant Analysis*, 3(6):493–504, 1972. ISSN 15322416. doi: 10.1080/00103627209366406. URL `https://www.tandfonline.com/doi/abs/10.1080/00103627209366406`.

D. C. Roberts, A. L. Forrest, G. B. Sahoo, S. J. Hook, and S. G. Schladow. Snowmelt Timing as a Determinant of Lake Inflow Mixing. *Water Resources Research*, 54

(2):1237–1251, feb 2018. ISSN 19447973. doi: 10.1002/2017WR021977. URL `https://onlinelibrary.wiley.com/doi/full/10.1002/2017WR021977https://onlinelibrary.wiley.com/doi/abs/10.1002/2017WR021977https://agupubs.onlinelibrary.wiley.com/doi/10.1002/2017WR021977`.

C. Santhi, J. G. Arnold, J. R. Williams, W. A. Dugas, R. Srinivasan, and L. M. Hauck. Validation of the SWAT model on a large river basin with point and nonpoint sources. *Journal of the American Water Resources Association*, 37(5):1169–1188, 2001. ISSN 1093474X. doi: 10.1111/J.1752-1688.2001.TB03630.X/FORMAT/PDF.

M. R. Savabi, D. C. Flanagan, J. R. Frankenberger, R. K. Hubbard, D. D. Bosch, and T. L. Potter. Development of A WEPP-water quality (WEPP-WQ) model. In *ASABE - International Symposium on Erosion and Landscape Evolution 2011*, pages 815–820. American Society of Agricultural and Biological Engineers, 2011. ISBN 9781618397966. doi: 10.13031/2013.39201. URL `https://elibrary.asabe.org/azdez.asp?JID=1{\&}AID=39201{\&}CID=isel2011{\&}v={\&}i={\&}T=1http://elibrary.asabe.org/abstract.asp?aid=39201{\&}t=1{\&}redir={\&}redirType=https://doi.org/10.13031/2013.39201`.

T. Schoennagel, J. K. Balch, H. Brenkert-Smith, P. E. Dennison, B. J. Harvey, M. A. Krawchuk, N. Mietkiewicz, P. Morgan, M. A. Moritz, R. Rasker, M. G. Turner, and C. Whitlock. Adapt to more wildfire in western North American forests as climate changes. *Proceedings of the National Academy of Sciences*, 114(18):4582–4590, 2017. ISSN 0027-8424. doi: 10.1073/pnas.1617464114. URL `http://www.ncbi.nlm.nih.gov/pubmed/28416662http://www.pubmedcentral.nih.gov/articlerender.fcgi?artid=PMC5422781http://www.pnas.org/lookup/doi/10.1073/pnas.1617464114`.

A. N. Sharpley, S. C. Chapra, R. Wedepohl, J. T. Sims, T. C. Daniel, and K. R. Reddy. Managing Agricultural Phosphorus for Protection of Surface Waters: Issues and Op-

tions. *Journal of Environmental Quality*, 23(3):437–451, may 1994. ISSN 0047-2425. doi: 10.2134/jeq1994.00472425002300030006x. URL `https://onlinelibrary.wiley.com/doi/abs/10.2134/jeq1994.00472425002300030006x`.

A. Simon, E. Langendoen, R. Bingner, R. Wells, A. Heins, N. Jokay, and I. Jaramillo. Lake Tahoe Basin Framework Implementation Study: Sediment Loadings and Channel Erosion. Technical report, USDA-Agricultural Research Service Channel and Watershed Processes Research Unit National Sedimentation Laboratory, Oxford, Mississippi, 2003. URL `https://www.ars.usda.gov/ARSUserFiles/60600505/TechnicalReports/NSLTechnicalReport39.pdf`.

R. K. Singh, R. K. Panda, K. K. Satapathy, and S. V. Ngachan. Simulation of runoff and sediment yield from a hilly watershed in the eastern Himalaya, India using the WEPP model. *Journal of Hydrology*, 405(3-4):261–276, aug 2011. ISSN 00221694. doi: 10.1016/j.jhydrol.2011.05.022.

A. Srivastava, M. Dobre, J. Q. Wu, W. J. Elliot, E. A. Bruner, S. Dun, E. S. Brooks, and I. S. Miller. Modifying WEPP to improve streamflow simulation in a pacific northwest watershed. *Trans. ASABE*, 56(2):603–611, 2013. URL `https://www.fs.fed.us/rm/pubs{\_}other/rmrs{\_}2013{\_}srivastava{\_}a001.pdf`.

A. Srivastava, J. Q. Wu, W. J. Elliot, E. S. Brooks, and D. C. Flanagan. MODELING STREAMFLOW IN A SNOW-DOMINATED FOREST WATERSHED USING THE WATER EROSION PREDICTION PROJECT (WEPP) MODEL. *American Society of Agricultural and Biological Engineers*, 60(4):1171–1187, 2017. doi: 10.13031/trans.12035. URL `https://elibrary.asabe.org/azdez.asp?search=0{\&}JID=3{\&}AID=48344{\&}CID=t2017{\&}v=60{\&}i=4{\&}T=2`.

A. Srivastava, D. C. Flanagan, J. R. Frankenberger, and B. A. Engel. Updated

climate database and impacts on WEPP model predictions. *Journal of Soil and Water Conservation*, 74(4):334–349, jul 2019. ISSN 19413300. doi: 10.2489/ jswc.74.4.334. URL `https://www.jswconline.org/content/74/4/334https://www. jswconline.org/content/74/4/334.abstract`.

A. Srivastava, E. S. Brooks, M. Dobre, W. J. Elliot, J. Q. Wu, D. C. Flanagan, J. A. Gravelle, and T. E. Link. Modeling forest management effects on water and sediment yield from nested, paired watersheds in the interior Pacific Northwest, USA using WEPP. *Science of the Total Environment*, 701:134877, jan 2020. ISSN 18791026. doi: 10.1016/j.scitotenv.2019.134877.

M. Stutter, S. Richards, A. Ibiyemi, and H. Watson. Spatial representation of in-stream sediment phosphorus release combining channel network approaches and in-situ experiments. *Science of The Total Environment*, 795:148790, nov 2021. ISSN 0048-9697. doi: 10.1016/J.SCITOTENV.2021.148790.

Tetra Tech Inc. Watershed Hydrologic Modeling and Sediment and Nutrient Loading Estimation for the Lake Tahoe Total Maximum Daily Load. Technical report, Tetra Tech, Inc., Fairfax, VA, 2007. URL `https://www.waterboards.ca.gov/lahontan/water{\_ }issues/programs/tmdl/lake{\_}tahoe/docs/peer{\_}review/tetra2007. pdfftp://swrcb2a.waterboards.ca.gov/pub/rwqcb6/LakeTahoeWatershedModel/ LakeTahoeWatershedModelingReport.pdf`.

P. A. Vadas, T. Krogstad, and A. N. Sharpley. Modeling Phosphorus Transfer between Labile and Nonlabile Soil Pools. *Soil Science Society of America Journal*, 70(3):736–743, may 2006. ISSN 1435-0661. doi: 10.2136/sssaj2005.0067. URL `https://onlinelibrary.wiley.com/doi/full/10.2136/sssaj2005.0067https: //onlinelibrary.wiley.com/doi/abs/10.2136/sssaj2005.0067https://acsess. onlinelibrary.wiley.com/doi/10.2136/sssaj2005.0067`.

A. J. Wade, P. Durand, V. Beaujouan, W. W. Wessel, K. J. Raat, P. G. Whitehead, D. Butterfield, K. Rankinen, and A. Lepisto. A nitrogen model for European catchments: INCA, new model structure and equations. *Hydrology and Earth System Sciences*, 6(3):559–582, 2002. ISSN 10275606. doi: 10.5194/hess-6-559-2002.

L. Wang. *CLIMATE CHANGE IMPACTS ON THE SOIL EROSION AND NUTRIENT LOSSES IN THE GREAT LAKES REGION*. PhD thesis, jan 2015. URL `https://docs.lib.purdue.edu/open{\_}access{\_}dissertations/1459`.

A. L. Westerling, H. G. Hidalgo, D. R. Cayan, and T. W. Swetnam. Warming and Earlier Spring Increase Western U.S. Forest Wildfire Activity. *Science*, 313(5789):940 LP – 943, aug 2006. doi: 10.1126/science.1128834. URL `http://science.sciencemag.org/content/313/5789/940.abstract`.

K. L. White and I. Chaubey. Sensitivity analysis, calibration, and validations for a multisite and multivariable SWAT model. *Journal of the American Water Resources Association*, 41(5):1077–1089, oct 2005. ISSN 1093474X. doi: 10.1111/j.1752-1688.2005.tb03786.x. URL `https://onlinelibrary.wiley.com/doi/full/10.1111/j.1752-1688.2005.tb03786.xhttps://onlinelibrary.wiley.com/doi/abs/10.1111/j.1752-1688.2005.tb03786.xhttps://onlinelibrary.wiley.com/doi/10.1111/j.1752-1688.2005.tb03786.x`.

R. A. Young, C. A. Onstad, D. D. Bosch, and W. P. Anderson. AGNPS - A Non-Point Source Pollution Model for Evaluating Agricultural Watersheds. *Journal of Soil Water Conservation*, 44(2):168–173, 1989.

CHAPTER 5

Pi-VAT: A web-based visualization tool for decision support using spatially complex water quality model outputs.

5.1 Abstract

Effective watershed management and protection of water resources from non-point source pollution require identification, prioritization, and targeting of pollutant source areas. Process-based hydrology and water quality models are powerful heuristic tools for land and water resources managers. However, because of their complexity, such models are often under-utilized as management prioritization and planning tools. In this paper, we present a prioritization, interactive visualization, and analysis tool (Pi-VAT) that is programmed to synthesize multi-scenario, multi-watershed outputs from process-based geospatial models. We demonstrate the utility of Pi-VAT to examine simulated hydrologic, sediment, and water quality response at the hillslope/hydrologic response unit (HRU) scale. We apply Pi-VAT to output from multiple watersheds and for multiple management scenarios and treatments from two geospatial models for watershed management: Water Erosion Prediction Project (WEPP) and Soil & Water Assessment Tool (SWAT). Pi-VAT was developed using the Shiny web application framework for the R programming language. In a matter of minutes, Pi-VAT can synthesize overwhelming amounts of output from process-based models into information useful for land and water resources managers. We illustrate the use of Pi-VAT to interactively identify, quantify, and visualize areas

that are most susceptible to disturbance under different scenarios and provide a synthesis approach based on land use, soil type, and slope steepness. This approach guides land and water resources managers in prioritizing the areas of the watershed that provide the maximum reduction in pollutant loads while treating the least amount of area. Pi-VAT provides a flexible reactive platform for the development of decision support tools based on process-based models intended for watershed management and research applications.

Keywords: *Decision-support tools, Targeted management, Prioritization, Process-based models, WEPP, SWAT.*

5.2   Introduction

Water quality concerns from non-point source pollution (NPS) are a challenge for land and water resources managers. Effective management of NPS requires strategic targeting and prioritization of watershed areas for implementing best management practices (BMPs) [Diebel et al., 2008]. Such targeting and prioritization typically consist of the identification of pollutant source areas and subsequent management to reduce water quality degradation [Daggupati et al., 2011, Easton et al., 2017].

Process-based hydrology and water quality simulation models have shown the capability to evaluate the potential effects of land management and climate scenarios on water quantity and quality. For example, a review of various process-based distributed watershed models by Wellen et al. [2015] reported that 83% of the reviewed scientific studies (257) published between the year 1992 and 2010 used one of these five models: Soil and Water Assessment Tool (SWAT), Integrated Catchment Model (INCA), Annualized/Agricultural Non-Point Source pollution model (AGNPS/AnnAGNPS), Hydrological Simulation Program - FORTRAN (HSPF), and Hydrologiska Byråns Vattenbalansavdelning (HBV). Such models can provide a link between management decisions and watershed response and provide a scientific basis for management decisions [Rode et al., 2010]. The

utility of these process-based models is not only to provide spatially explicit predictions of runoff and erosion but also to provide a deeper understanding of the key factors and dominant hydrologic processes and flow paths that drive the detachment and transport of sediment and associated pollutants [Brooks et al., 2015]. Characteristically, such models have been successfully applied, predominantly by the scientific community for a management scenario-oriented impact assessment on water quality and quantity, to identify priority source areas, and to formulate management plans. For instance, the utility of the SWAT model has been widely demonstrated in the scenario-based evaluation of the efficacy of site-specific BMPs on water quality as well as in the targeting of BMPs placement for improving water quality [Briak et al., 2019, Daggupati et al., 2011, Easton et al., 2010, Liu et al., 2019, Merriman et al., 2019, Park et al., 2014, Xu et al., 2019]. Similarly, the WEPP model has been successfully used for guiding watershed managers in the selection and placement of the BMPs in forested watersheds [Efta and Chung, 2014, Robichaud et al., 2007]. It has also been applied for investigating the effectiveness of conservation management practices and targeted management in agricultural watersheds [Brooks et al., 2015, Pandey et al., 2009, Singh et al., 2011]. Other models recognized in Wellen et al. [2015] were used to investigate sediment and nutrients response under alternative management scenarios as well as to identify priority areas for erosion control measures and to assess the BMPs effectiveness on nutrient loading [Abdelwahab et al., 2014, Ahn and Kim, 2016, Bastrup-Birk and Gundersen, 2004, Gudino-Elizondo et al., 2019, Luo et al., 2015, Zhang et al., 2020].

Despite this demonstrated usefulness, the use of process-based models by managers in "what if" scenario testing has been limited to date. Ease of use, extensive model setup and training requirements often form barriers to the adoption and effective use of process-based models in the planning process [Garen et al., 1999]. There is also a strong need to disseminate the information generated by these models to stakeholders and decision-

makers in a functional format. The recent evolution of web-based user interfaces for some models attempts to partly address these barriers. For example, SWATonline simplifies SWAT data querying as well as enables simple data visualizations [McDonald et al., 2019]; The Hydrologic and Water Quality System (HAWQS) makes it easier to set up and run the SWAT model at the hydrologic unit codes (HUCs) 8 to 12 or larger scale and provides users with summary visualization capabilities and the ability to download an entire project to be used on a local computer [Yen et al., 2016]. To enhance the use of process-based models in informed decision-making, an online watershed interface (WEPPcloud) has been developed to make use of the Water Erosion Prediction Project (WEPP) model across the US by watershed managers easier and more convenient [Dobre et al., 2022]. This interface was specifically developed for forestry applications as part of the Forest Service suite of models (https://forest.moscowfsl.wsu.edu/fswepp/) and its use recently has been extended to rangeland landscapes (WEPPcloud-RHEM) as well [Lew et al., 2022].

Web-based user interfaces make the models more accessible and easier to use, but do not necessarily provide the data summaries and visualizations in a functional format to compare multiple watershed simulations of different management options and facilitate 'what if' scenario testing. To develop an action plan and ensure appropriate and effective management practices are implemented, managers need to understand the key hydrologic drivers and factors (soil type, land use/land cover, slope, and climate) involved in the transport of the pollutant and the sensitivity of these factors to pollutant transport. The amount of simulated output generated by process-based models especially when using the model to assess multiple management options over multiple years in unique land types within a watershed can be overwhelming. End-user (e.g., watershed managers) would require extensive training in geospatial analysis and modeling to process the output. In essence, process-based models are very useful tools for ingesting 'Big Data' as model
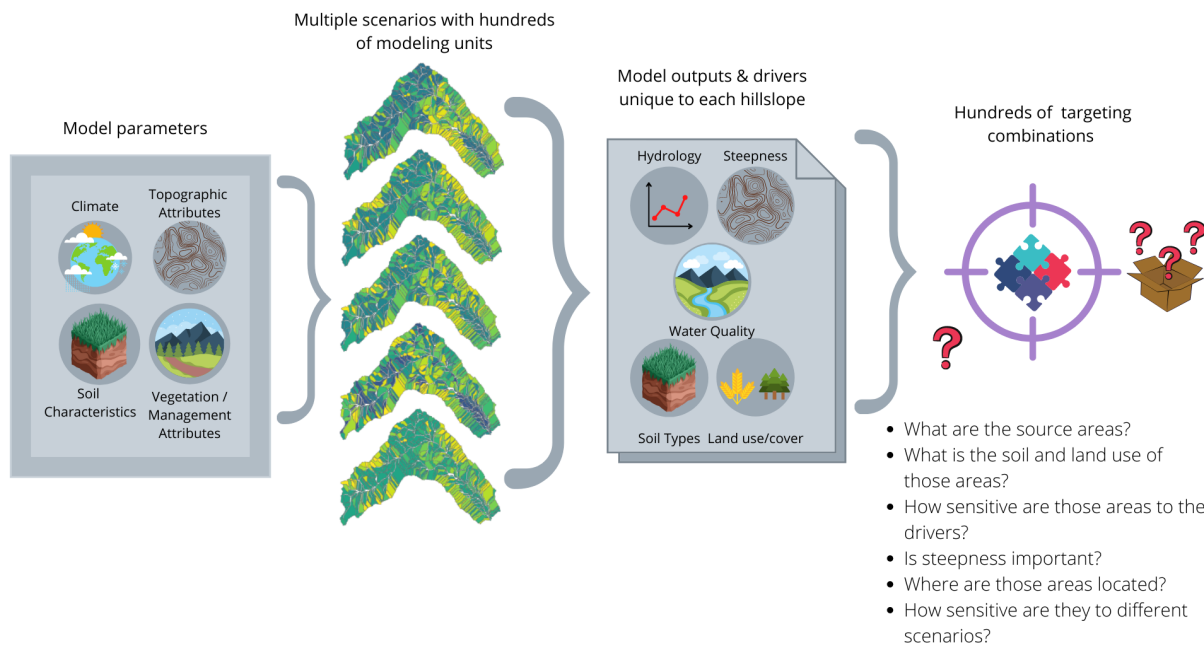
Figure 5.1: The 'what-if' scenario testing and comparative analysis require further synthesis of the enormous datasets and resulting targeting combinations generated by process-based models.

input, however, they can also generate an equal amount of 'Big Data' that can be equally daunting for end-users to synthesize and extract useful knowledge for identifying and spatially prioritizing BMPs. A multiple scenario simulation from a hillslope or HRU based geospatial model for even a relatively small watershed and short daily weather time series can easily generate hundreds to thousands of targeting combinations (Figure 5.1).

Integrating 'what-if' scenario information with decision support tools would enable watershed managers to harness the potential of sophisticated, process-based models and truly aid in decision-making. Brooks et al. [2015] emphasized the need to connect science and management by improving process-based planning tools such that crucial information is available to planners to target areas in the landscape. Brooks et al. [2015] demonstrated the use of a simplified web interface consisting of post-processing algorithms built on top of the WEPP model to effectively support BMP assessment and planning.

The number of commercial and open-source platforms for hosting online tools has led to an explosion in web-based applications and has provided an opportunity to develop geospatial decision support tools. For example, tools developed using Shiny, an open-source web application framework developed by the RStudio Team [R Core Team, 2021], have enabled the creation of interactive web applications that allow users to interact dynamically with the model simulations. Since its inception, the use of Shiny has increased steadily as evidenced by peer-reviewed papers through which specialists in academic fields disseminated knowledge to stakeholders [Kasprzak et al., 2020]. While Shiny has been used across a diverse range of academic fields, to our knowledge, few peer-reviewed papers in the earth and environmental sciences have used the Shiny web application framework. For instance, Klein et al. [2017] developed the webXTREME tool to facilitate agroclimatic risk evaluation under climate change. WebXTREME has provided an important link between scientists and decision-makers. Whateley et al. [2015] used Shiny to develop a web-based decision support tool that provides an interactive environment to water managers and stakeholders to explore water supply system vulnerabilities to climate change. This tool, targeted at small-scale water supply systems, provides an opportunity for more dynamic and collaborative water resources management.

The objectives of this work were to develop a stand-alone, post-processing, interactive analysis, and visualization tool that can ingest complex, spatially distributed output from geospatial hydrologic models, and to demonstrate its use as a decision support tool for scenario-oriented planning and management. We developed the Prioritization-Visualization and Analysis Tool (Pi-VAT) that synthesizes tabular and map-based outputs for multiple watersheds and scenarios. We demonstrate the utility of the tool with watershed case studies using outputs from two of the most well-known hydrologic management models: WEPP and SWAT. We describe its development and demonstrate its use in evaluating and guiding land and water resources management decisions in three

watershed case studies.

5.3 Methods

5.3.1 Interface implementation

Pi-VAT is an interactive tool developed for the identification and prioritization of pollutant hotspots and areas suitable for targeted management. Currently, Pi-VAT ingests output from two of the most widely used hydrologic models WEPP and SWAT using the Shiny web application framework for the R programming language [Beeley and Sukhdeve, 2018, Chang et al., 2021, R Core Team, 2021]. Pi-VAT is deployed on the shinyapps.io server and can be accessed at https://cdeval.shinyapps.io/Pi-VAT/. The Pi-VAT source code can be found on the GitHub page of the tool (https://github.com/devalc/Pi-VAT). Pi-VAT requires users to have pre-computed scenario runs using either online or offline WEPP or SWAT interfaces. Information on summarizing and preparing multiple pre-computed scenarios for use in Pi-VAT is provided on the Pi-VAT's GitHub page.

5.3.2 Main interface components

The Pi-VAT interface intuitively guides the user through a "what-if" analysis from data input to dynamic visualization (Figure 5.2). Each tab on the Pi-VAT user interface consists of two sections: the input/control panel and the visualization/summary panel as shown in Figure 5.3. The visualization/summary panel was implemented using the R wrappers for the Plotly, Leaflet, and DataTables [Cheng et al., 2021, Sievert, 2020, Xie et al., 2021] making it fully interactive. The input/control panel contains four main options (denoted by numbers in Figure 5.3) namely, data import options and three auto-populated drop-down menus for the watershed scenario, and the targeted water quality/quantity metric, respectively. The input panel provides users with the ability to upload output files from

the hydrologic model, select water quality/quantity metrics of interest, and control visualization and data summaries by using the control buttons.

We specifically included synthesis products based on feedback from watershed managers for scenario-testing watershed applications. Three of the most common suggestions are to provide the ability to (i) compare impacts from different management options within a single sub-watershed; (ii) identify priority watersheds or hillslopes to implement a particular management practice; (iii) assess trade-offs from the implementation of particular management practice. In the first case, the user needs to have the ability to visualize and compare multiple treatments in a single watershed. In the second case, the user needs to be able to summarize and visualize differences across unique spatial units. In the third case, a manager may also want to better understand the implications of management options from multiple responses (e.g., reduced runoff and increased subsurface lateral flow) to identify whether a management practice may result in a positive environmental impact from one perspective but at the cost of creating another environmental problem from another perspective. In addition, a manager may want to identify the most sensitive areas in the landscape which give the greatest benefit from the application of a particular management practice (e.g., sediment reduction per unit area of the watershed treated). Furthermore, a manager may also want to ascertain unique soil, landscape, and climatic characteristics that make this identified landscape area very sensitive to the particular treatment. Managers can also be constrained by specific regulatory policies which limit the application of practice to a specific region (e.g., no logging timber on slopes greater than 30%). In this case, the manager would like to focus the analysis on treatable areas within the watershed. These management challenges are common to nearly all watershed studies [Brooks et al., 2015, Mulla et al., 2008, Rittenburg et al., 2015] and therefore we developed the tool (Pi-VAT) to address these objectives.

Specifically, Pi-VAT provides the ability to graphically compare differences in the
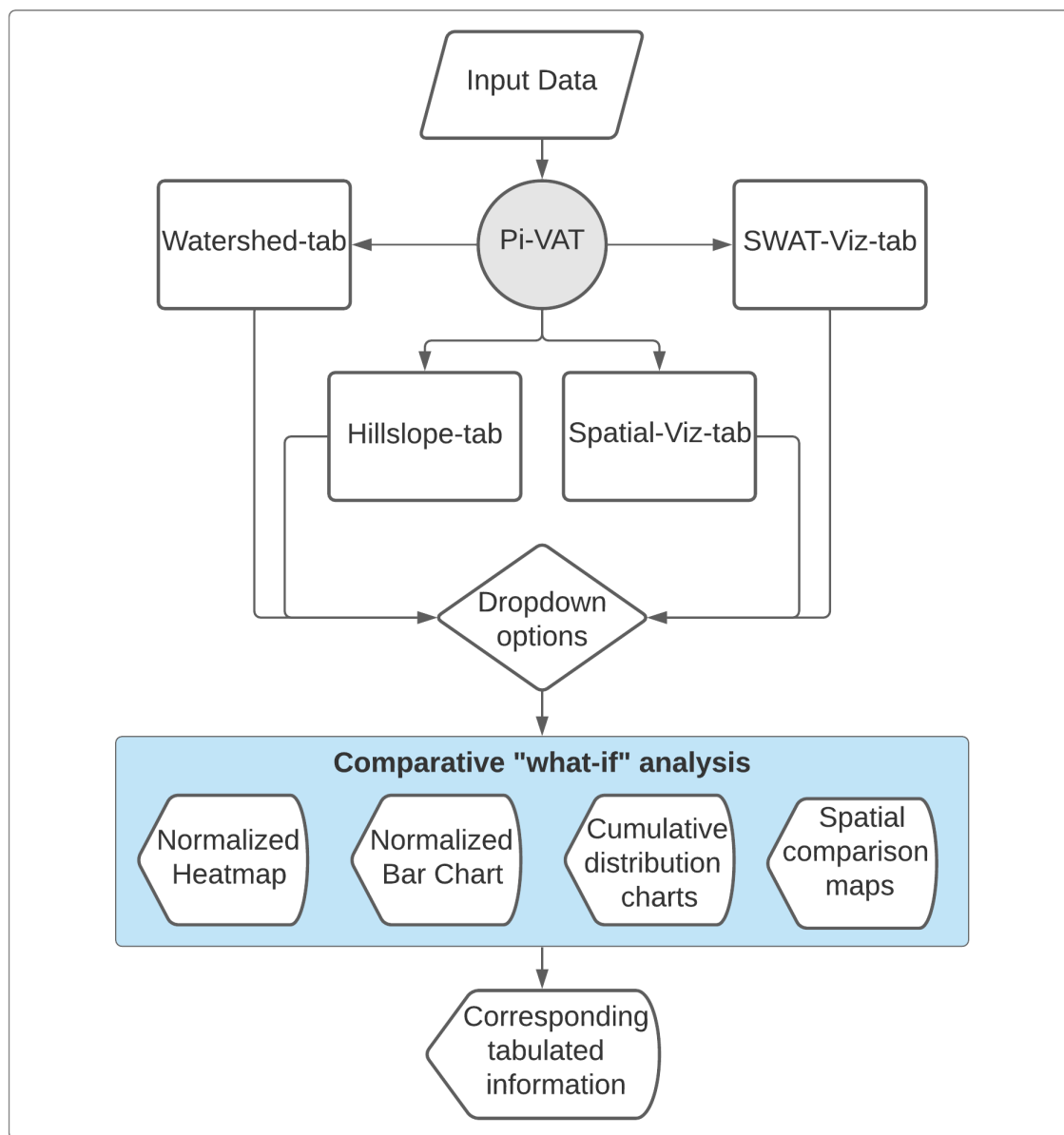
Figure 5.2: General flow diagram of the comparative 'what-if' analysis in the Pi-VAT interface.
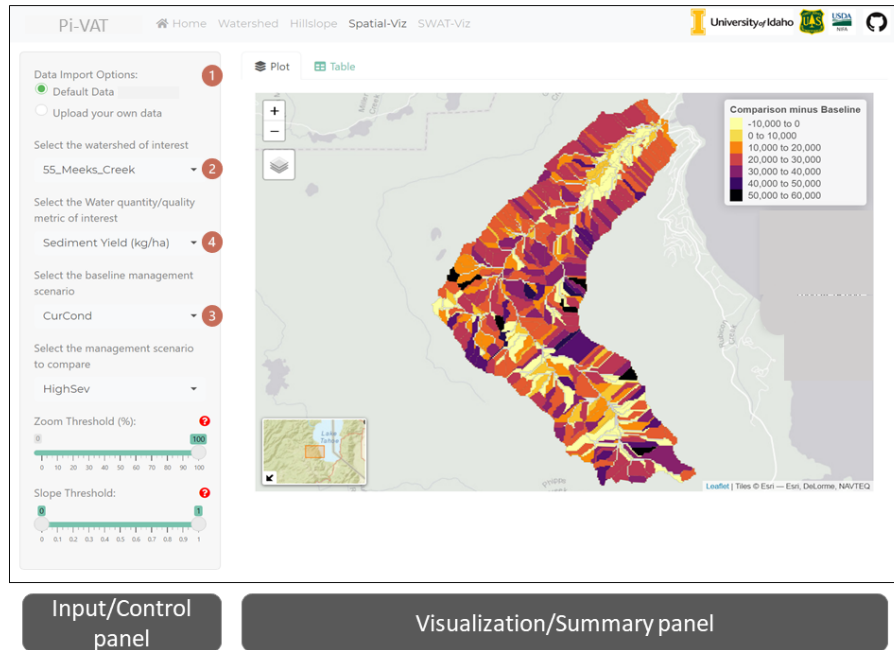
Figure 5.3: Example of the spatial visualization (Spatial-Viz) tab of the Pi-VAT interface.

magnitude of a certain simulated output (e.g., sediment yield) from multiple management scenarios on a single chart (Heatmap/Bar chart). For spatial analysis, the tool can map these differences in simulated output between two scenarios in a particular watershed. To identify watersheds sensitive to a particular management scenario, Pi-VAT also provides the option to generate charts and maps comparing the magnitude of a simulated output for a single management scenario across multiple watersheds. It provides the option to select and analyze single or multiple hydrologic response output variables. Pi-VAT also provides cumulative distribution figures which display the percent of the hydrologic or pollutant response output within a watershed vs the cumulative percent area from which the pollutant was generated within the watershed. Users can then use slider bars to filter the output and identify the areas which contribute the greatest source loading per unit area of the watershed. This is particularly useful where a manager might have limited financial resources which only allow the treatment of a small fraction of the watershed. Similar filter options have been implemented to narrow the analysis to a particular slope

steepness range. For example, Pi-VAT allows users to select and only display output from areas having a slope steepness greater than and/or less than a certain minimum and/or maximum slope. To assist users in the identification of key factors and hydrologic drivers, Pi-VAT continuously updates downloadable output tables based on user-selected options which include not only multiple output hydrologic response variables but also key soil, topographic, and climatic input factors.

5.3.3 Site Descriptions

We selected three case studies from three regions consisting of either a forest or an agricultural system: Lake Tahoe Basin (California/Nevada), Palouse (Washington), and WE-38 sub-watershed within the Mahantango Experimental Watershed (south-central Pennsylvania). We selected sub-watersheds in these regions based on the unique land uses and the associated land management and water quality concerns in each area. We first describe the sites, and in section 5.3.4 describe the modeling scenarios.

5.3.3.1 Lake Tahoe Basin

Lake Tahoe, despite being in an ultra-oligotrophic state [Coats et al., 2008, Hatch et al., 2001], has experienced long-term declining water clarity due to upland contributions of fine sediment and phosphorus [Sahoo et al., 2013]. Previous research suggests that the primary productivity of the lake has been increasing by about 5% per year [Coats et al., 2008], and in the last five decades the Secchi depth of Lake Tahoe has decreased by about 10 m [Kerlin, 2017]. Fire suppression in the Lake Tahoe basin during the 20th century has resulted in forest floor accumulation of duff and woody debris, which has increased the risk of frequent and more intense wildfires [Miller et al., 2010]. Land managers in the basin are interested in comparing the impacts of wildfires and timber harvest on water quality to identify sensitive areas in the landscape for targeted management. In this

case study, we used Pi-VAT to evaluate the effects of several forest treatments (thinning) and wildfire scenarios on sediment yield from multiple watersheds. We considered seven watersheds, with areas ranging between 4.1 km^2 and 110 km^2, and an average of 626 hillslopes in each watershed, and a total of 11 simulated scenarios ranging from forest treatments (such as thinning and prescribed fire) to wildfires. This amounts to 48,202 combinations of hillslopes along with the associated soils, land uses, and slope steepness that were evaluated for targeted management.

5.3.3.2   Palouse (Washington)

Conventional tillage management on the steep hillslopes of the dryland wheat-based cropping systems within the Inland Pacific Northwest 'Palouse' region has caused excessive soil erosion. Aggressive tillage with low residual ground cover has left a degraded landscape. In USDA (1978), it was estimated that the topsoil was completely removed from 10% of the cropland and one-fourth to three-fourths was lost from 60% of the region. Subsoil horizons in the region can often include dense subsoil, calcium carbonate (B_k), argillic (B_{tb}), and fragipan (Bt_{xb}) soil horizons that lead to perched water tables, subsurface lateral flow, and saturation excess runoff processes [Brooks et al., 2012, McDaniel et al., 2008]. Erosion rates can be reduced through the adoption of conservation tillage practices however the effectiveness varies by topography, soil type, and climate [Kok et al., 2009]. In this watershed case study, we examine the effects of tillage management on the sediment yield within the Thorn creek (109 km2) and Kamiache creek (40 km^2) watersheds located within the 381 to 457 mm mean annual precipitation zone in the Palouse. Soil and water conservation districts are interested in incentivizing conservation tillage practices on the hillslopes which contribute the greatest benefit to the cost ratio from the treatment application. These watersheds implement a three-year crop rotation consisting of winter wheat-spring barley-summer fallow. Each watershed has an average of 1,590

hillslopes and a total of three simulated management scenarios resulting in more than 9,540 combinations. Three types of tillage systems were compared: a conventional tillage system (CT) with a chisel plow, a minimum or mulch tillage (MT) scenario, and a no-till system (NT).

5.3.3.3 WE-38 Experimental Sub-Watershed

Managing the transport, delivery, and long-term legacy of excessive phosphorus loading from agriculturally dominated landscapes is a well-documented challenge particularly in the eastern US with a long history of dairy operations and impacts on soil chemistry [Kleinman et al., 2011, Sharpley et al., 1994, 2001, Stackpoole et al., 2019]. Accurately identifying nutrient source areas, dominant delivery mechanisms, and the impact of management strategies on phosphorus loading is, therefore, an essential step to avoid long-term water quality impairment in downstream water bodies. WE-38 is a 7.3 km^2 first-order upland agricultural experimental sub-watershed, located within the larger 420 km^2 Mahantango Creek Experimental Watershed. It was established in 1976 by the USDA-Agricultural Research Service to better understand the water quantity and water quality implications of agriculturally-based farming systems in Pennsylvania and particularly for better understanding nutrient loading to Chesapeake Bay [Buda et al., 2011]. WE-38 is known for its variable source area hydrology driven by topographic variability and perched water tables over fragipan subsoil horizons [Bryant et al., 2011]. In the case of the WE-38 sub-watershed, we use Pi-VAT to examine the effects of varying soil phosphorus content, manure application, and tillage and cropping management on phosphorus and nutrient losses [Collick et al., 2015]. We considered six sub-watersheds of WE-38 with a total of 1,286 HRUs and eight simulated management scenarios resulting in a 10,288 combination of HRUs that can be considered for targeted management.

5.3.4 Synthesis Approach

Our synthesis approach demonstrates the application of Pi-VAT for multi-watershed, multi-scenario simulated results from WEPP and SWAT with a focus on targeting and prioritizing management. We demonstrate the utility of the tool rather than assess the accuracy or validate the model predictions because several previous validation studies already have shown the accuracy of WEPP [Boll et al., 2015, Brooks et al., 2016, Elliot et al., 2015, Srivastava et al., 2017, 2020] and SWAT [Collick et al., 2015, Easton et al., 2009, 2010, Xu et al., 2019] model predictions. To demonstrate the utility of Pi-VAT, we used WEPP model output for the Lake Tahoe and Palouse case studies generated using the WEPPcloud interface. For the Lake Tahoe test case, we considered the current conditions (CurCond) scenario as the baseline scenario and for the Palouse test case, we considered conventional till (CT) as the baseline scenario. For the WE-38 case study, we used SWAT-VSA model output [Easton et al., 2008] and used the high rate, spring surface manure application scenario as the baseline scenario in the synthesis. From the target combinations described in each case study, we respond to land and water resources managers' desires to be able to identify which watershed and hillslopes to prioritize, and what treatment/management to implement to minimize water quality impacts. In the synthesis approach, we answer the following general targeting questions aimed at addressing the unique water quality problem in each case study described before:

1. Which watersheds are a major concern with respect to the pollutant of concern?

2. How sensitive is this watershed to the disturbances and changes in management practices?

3. What amount of the watershed needs to be treated to reduce the loading of the pollutant of concern?

4. Where are these source areas located in the watershed? How do they compare to the baseline scenario? What are the general driving factors in these areas?

5.4 Results

5.4.1 Lake Tahoe Basin

The Lake Tahoe Basin case study presents Pi-VAT usefulness for identifying critical source areas of sediment in forested environments with fire risk. A large percentage of total sediment yield and soil loss from both hillslopes and channels for the baseline scenario emerges from the Blackwood Creek watershed (41%) followed by the Ward Creek watershed (20%) (Figure 5.4a, b). The sediment yield and soil loss are generally larger in the cases of fire scenarios, whereas these increases in the case of thinning management scenarios are comparatively small (Figure 5.4c). The largest contribution of the total hillslope soil loss (54%) and the sediment yield (27%) across scenarios arises from the high severity (High-Sev) fire scenario (Figure 5.4d). In the case of the 85% thinning scenario (Thin85), this contribution of total hillslope soil loss and sediment yield across scenarios amounted to 2% and 4% respectively.

More than 80% of the total sediment yield in the Blackwood Creek watershed across three different scenarios comes from only 25% of the total hillslope area (Figure 5.5 a). In this 25% of the total hillslope area, the cumulative sediment yield increased from the baseline scenario by 195 Mg for the thinning scenario (Thinn85) and 1264 Mg for the low severity fire scenario (LowSev), respectively (Figure 5.5 c). The relative difference in sediment yield between the comparison scenario and the baseline scenario from all hillslopes in the Blackwood Creek watershed (Figure 5.5 b) and Figure 5.5 d shows the same for the top 25% of the total hillslopes contributing maximum sediment yield. Table 5.1 lists the top 15 hillslopes with a maximum increase in sediment yield relative to
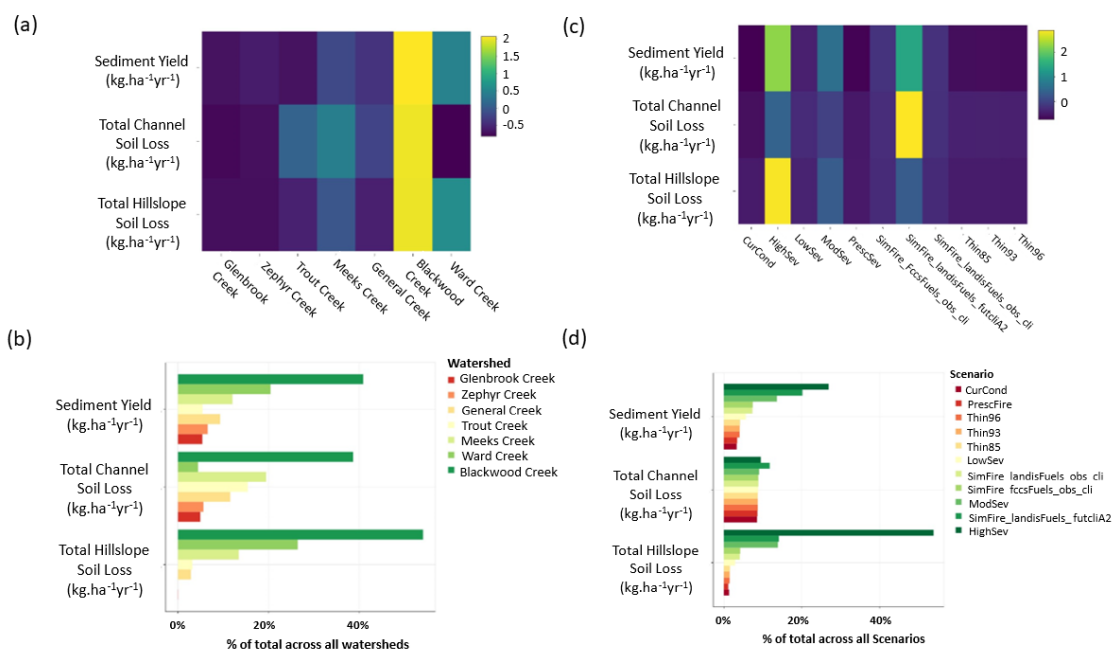
Figure 5.4: Example application of synthesis approach in the Lake Tahoe basin. Relative normalized response in water quality/quantity metrics from (a) different watersheds for the current conditions (CurCond) baseline scenario and (c) different scenarios for Blackwood Creek watershed. Percent of total water quality/quantity metrics across (b) all compared watersheds for the baseline scenario and (d) all compared scenarios for Blackwood Creek watershed.
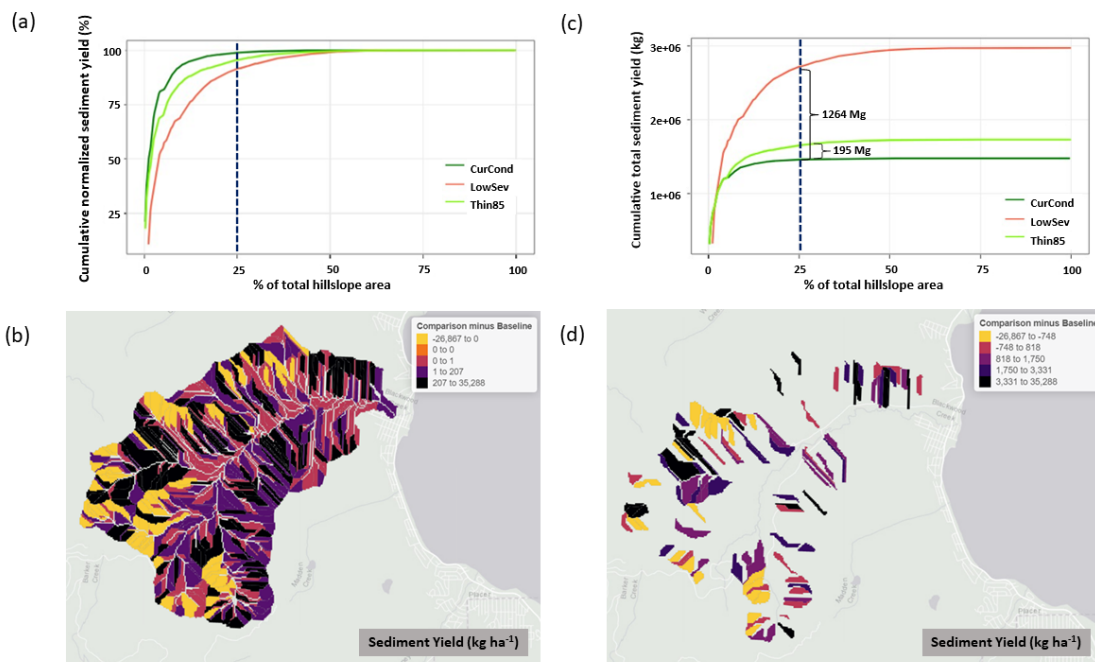
Figure 5.5: Example application of synthesis approach in the Blackwood Creek watershed (Lake Tahoe basin): (a) cumulative normalized sediment yield (%) vs total hillslope area (%) for three scenarios; (b) difference plot (LowSev minus CurCond) for sediment yield (kg ha^{-1}) from all hillslopes, where negative/positive values indicate a net decrease/increase in sediment yield (kg ha^{-1}) ; (c) cumulative total sediment yield (kg) vs total hillslope area (%) for different scenarios; and (d) difference plot (LowSev minus CurCond) for sediment yield (kg ha^{-1}) from the top 25% hillslopes with the largest contribution.

the baseline scenario. For each of these top 25% contributing hillslopes, appendix table 6.7 lists the sediment yield from the comparison scenario and its relative change from the baseline scenario along with the land use, soil characteristics, and slope description. Approximately 85% of these hillslopes have a steepness greater than 30%, and the majority of these soils are rock outcrop complexes or sandy loam soils.

Table 5.1: Hillslope characteristics along with the baseline sediment yield and the absolute change from the baseline (LowSev minus CurCond) for the top 15 hillslopes with maximum increases in the Blackwood Creek watershed. Negative values of absolute change indicate a net decrease in the sediment yield (kg ha^{-1}) whereas the positive values indicate a net increase in the sediment yield (kg ha^{-1}).

Hillslope-ID	Landuse	Soil	Slope Steepness (m/m)	Sediment Yield LowSev (kg ha^{-1})	Absolute Change from baseline (kg ha^{-1})
2211	Tahoe Low Severity Fire	Melody-Rock Outcrop complex, 30 to 50 percent slopes (SPM)	0.42	25851	25191
2212	Tahoe Low Severity Fire	Melody-Rock Outcrop complex, 30 to 50 percent slopes (SPM)	0.39	14939	14511
2143	Tahoe Low Severity Fire	Paige medial sandy loam, 30 to 50 percent slopes (SPM)	0.42	10831	10364
2961	Tahoe Low Severity Fire	Melody-Rock outcrop complex, 50 to 70 percent slopes (SPM)	0.47	10371	9917
1351	Tahoe Low Severity Fire	Melody-Rock outcrop complex, 50 to 70 percent slopes (SPM)	0.56	9393	9167
2373	Tahoe Low Severity Fire	Melody-Rock outcrop complex, 50 to 70 percent slopes (SPM)	0.47	8999	8624
741	Tahoe Low Severity Fire	Waca very gravelly medial coarse sandy loam, 30 to 50 percent slopes (SPM)	0.5	4206	4079
2391	Tahoe Low Severity Fire	Melody-Rock outcrop complex, 50 to 70 percent slopes (SPM)	0.47	3899	3751
2851	Tahoe Low Severity Fire	Melody-Rock Outcrop complex, 9 to 30 percent slopes (SPM)	0.21	3672	3570
871	Tahoe Low Severity Fire	Ellispeak-Waca complex, 9 to 30 percent slopes (ST-FSL)	0.28	3340	3273
1551	Tahoe Low Severity Fire	Melody-Rock outcrop complex, 50 to 70 percent slopes (SPM)	0.44	3203	3094
1561	Tahoe Low Severity Fire	Ellispeak-Waca complex, 30 to 50 percent slopes (ST-FSL)	0.35	3005	2928
2672	Tahoe Low Severity Fire	Ellispeak-Rock outcrop complex, 9 to 30 percent slopes (ST-FSL)	0.27	2692	2639
653	Tahoe Low Severity Fire	Kneeridge gravelly sandy loam, 5 to 15 percent slopes, very stony (SPM)	0.19	2602	2277
3221	Tahoe Low Severity Fire	Ellispeak-Rock outcrop complex, 50 to 70 percent slopes (ST-FSL)	0.48	2336	2237

5.4.2 Palouse

The Palouse case study presents Pi-VAT usefulness for identifying critical source areas of sediment of agricultural basins under different tillage intensities. Relatively large soil losses from both hillslopes and channels for the baseline scenario occur in the Thorn Creek watershed whereas relatively large sediment yield occurs from the Kamiache Creek watershed (Figure 5.6a). Pi-VAT visuals indicated that the majority of the sediment yield in the region (67%) was generated from the Kamiache Creek watershed with a much smaller percentage (33%) generated from the Thorn Creek watershed (Figure 5.6b). When compared across different management scenarios, the relative sediment yield and soil loss from the Kamiache Creek watershed occurs in the following order: CT > MT > NT (Figure 5.6c). The largest contribution (40%) of the total hillslope soil loss and the sediment yield across scenarios arises from the CT practices (Figure 5.6d), whereas the smallest contribution (25%) of the total hillslope soil loss and the sediment yield across scenarios arises from the NT practices (Figure 5.6d).

About 80-85% of the total sediment yield in the Kamiache Creek watershed across the three different scenarios comes from only 15% of the total hillslope area (Figure 5.7a). In this 15% of the total hillslope area, the cumulative sediment yield decreased by about 6 Mg and 11.5 Mg by switching from CT to MT and NT management practices, respectively (Figure 5.7c). Figure 5.7b shows the relative difference in sediment yield between the comparison scenario and the baseline scenario from all the hillslopes in the Kamiache Creek watershed, and Figure 5.7d shows the same for the top 15% of the total hillslopes contributing maximum sediment yield. Table 5.2 lists the top 15 hillslopes with a maximum increase in sediment yield relative to the baseline scenario. Appendix D table 6.8 lists the sediment yield from the comparison scenario and its relative change from the baseline scenario for these top 15% of the total contributing hillslopes. Generally, soil ero-
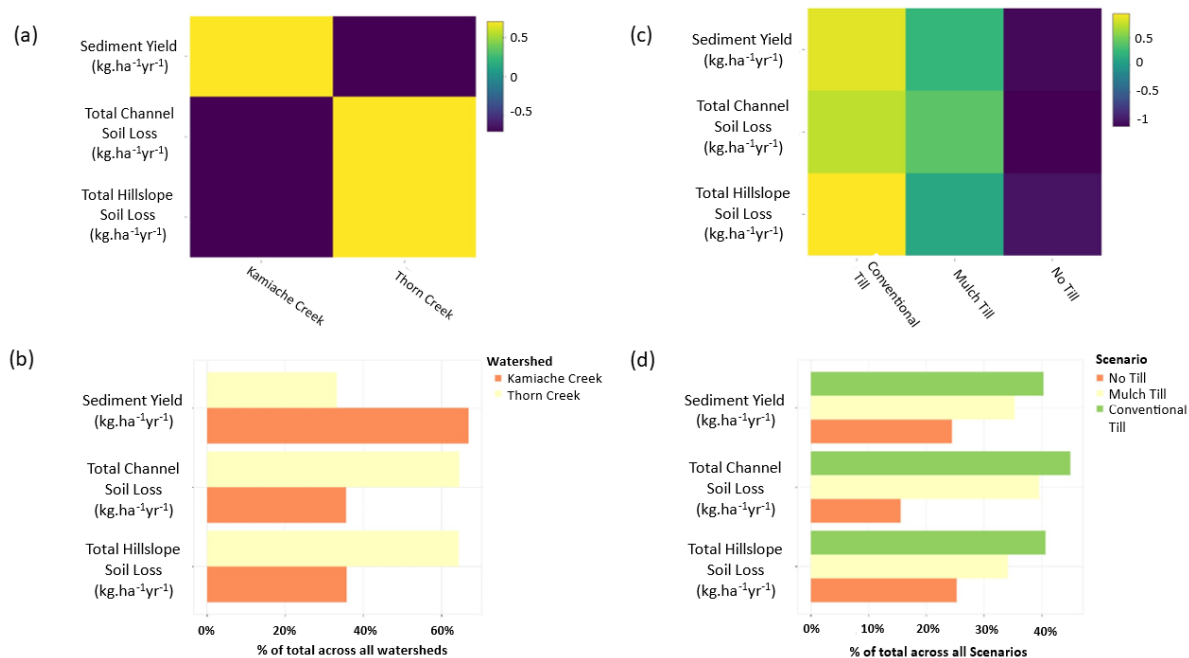
Figure 5.6: Example application of synthesis approach in the Palouse. Relative response in water quality/quantity metrics from: (a) different watersheds for the baseline scenario (CT); (c) different scenarios for Kamiache Creek watershed. Percent of total water quality/quantity metrics across all the compared: (b) watersheds for the baseline scenario; (d) scenarios for Kamiache Creek watershed.
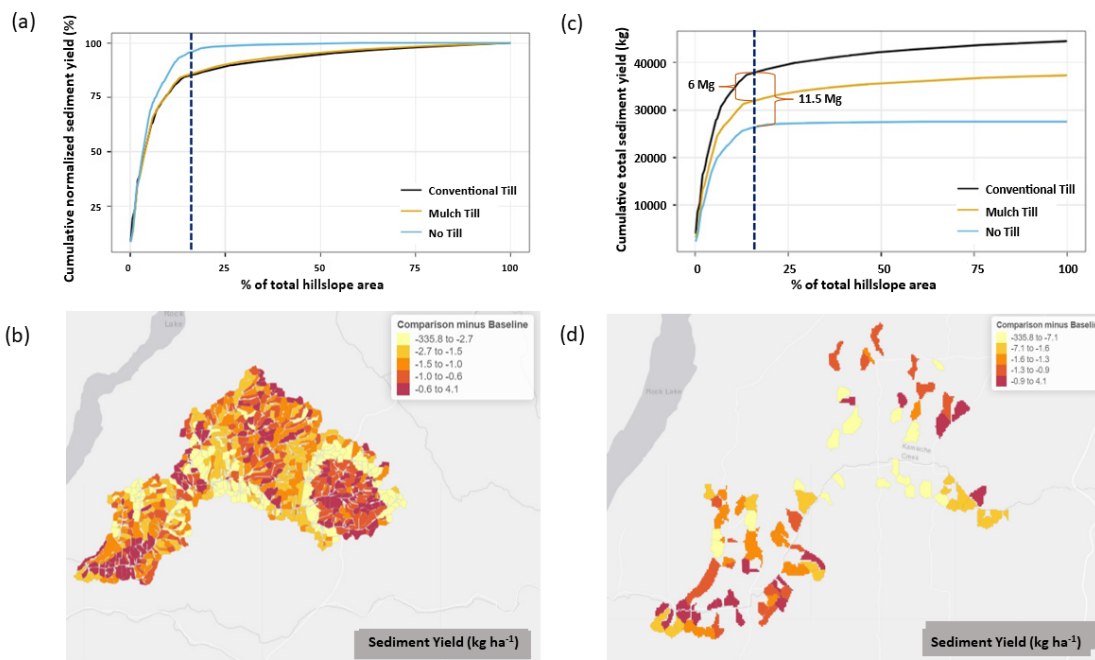
Figure 5.7: Example application of synthesis approach in Palouse: (a) cumulative normalized sediment yield (%) vs total hillslope area (%) for different scenarios in for Kamiache Creek watershed; (b) difference plot (CT minus NT) for sediment yield (kg ha^{-1}) from all hillslopes in the Kamiache Creek watershed; (c) cumulative total sediment yield (kg) vs total hillslope area (%) for different scenarios in for Kamiache Creek watershed; and (d) difference plot (CT minus NT) for sediment yield (kg ha^{-1}) from the top 15% hillslopes that have the largest contribution in the Kamiache Creek watershed.

sion increased with slope steepness and slope length and was greatest where conventional tillage practices were employed in winter wheat-spring barley, summer fallow rotations in Chard silt loams which have dense calcium carbonate Bk horizon at ~90 cm below the soil surface.

5.4.3 WE-38

The Pi-VAT analysis of WE-38 indicates a phosphorus response to management which is sensitive to treatment and the form of the phosphorus transported. Mineral and organic phosphorus (kg) transported with water out of the reach decreases in the following reach order number 6>1>2>3>4>5 (Figure 5.8a). However, when normalized by the area of

Table 5.2: Hillslope characteristics along with the baseline sediment yield and the absolute change from the baseline (CT minus NT) for the top 15 hillslopes with maximum change in the Kamiache Creek watershed. Negative values of absolute change indicate a net decrease in the sediment yield (kg ha^{-1}) whereas the positive values indicate a net increase in the sediment yield (kg ha^{-1}).

Hillslope	Land use Description	Soil Description	Slope Steepness (m/m)	Sediment Yield CT (kg ha^{-1})	Absolute Change from baseline (kg ha^{-1})
23	Barley Fallow Int Precip NT 1	Chard silt loam, 15 to 25 percent slopes (SIL)	0.17	101.4	4.08
63	Barley Fallow Int Precip NT 1	Chard silt loam, 15 to 25 percent slopes (SIL)	0.18	54.83	1.78
352	Barley Fallow Int Precip NT 1	Chard silt loam, 15 to 25 percent slopes (SIL)	0.1	18.08	1.23
62	Barley Fallow Int Precip NT 1	Chard silt loam, 15 to 25 percent slopes (SIL)	0.1	26	0.59
322	Barley Fallow Int Precip NT 1	Chard silt loam, 15 to 25 percent slopes (SIL)	0.15	14.52	0.24
1802	Barley Fallow Int Precip NT 1	Calouse silt loam, 7 to 25 percent slopes (SIL)	0.12	12.05	-0.31
2222	Barley Fallow Int Precip NT 1	Athena silt loam, 7 to 25 percent slopes (SIL)	0.11	25.45	-0.4
3671	Barley Fallow Int Precip NT 1	Athena silt loam, 7 to 25 percent slopes (SIL)	0.12	9	-0.66
932	Barley Fallow Int Precip NT 1	Athena silt loam, 7 to 25 percent slopes (SIL)	0.14	30.86	-0.71
3602	Barley Fallow Int Precip NT 1	Athena silt loam, 7 to 25 percent slopes (SIL)	0.12	21.39	-0.72
643	Barley Fallow Int Precip NT 1	Athena silt loam, 7 to 25 percent slopes (SIL)	0.1	14.32	-0.86
1283	Barley Fallow Int Precip NT 1	Athena silt loam, 7 to 25 percent slopes (SIL)	0.11	17.7	-0.9
683	Barley Fallow Int Precip NT 1	Athena silt loam, 7 to 25 percent slopes (SIL)	0.1	29.19	-0.91
992	Barley Fallow Int Precip NT 1	Athena silt loam, 7 to 25 percent slopes (SIL)	0.14	6.29	-0.93
3672	Barley Fallow Int Precip NT 1	Athena silt loam, 7 to 25 percent slopes (SIL)	0.16	24.09	-1.15

each subbasin, the largest transport of mineral P attached to the sediment and soluble P into the reach occurs from subbasin 3 in the business-as-usual ((high rate, spring surface manure application) scenario (Figure 5.8b and Figure 5.8d). Also, for the same scenario, the amount of mineral P attached to the sediment transported into the reach decreases by subbasin in the following subbasin order number 3>6>5>2>4>1, and for the transport of soluble P decreases by the subbasin order number 3>1>4>2>5>6 (Figure 5.8b and Figure 5.8d). The highest mineral phosphorus (20%) and organic phosphorus (18%) transported through stream reach 3 compared across all the scenarios occur for the business-as-usual scenario. Whereas adopting a low-rate spring injection manure application method, the mineral phosphorus and organic phosphorus transport through stream reach 3 reduces to 8% and 11%, respectively. Reductions in organic (a), sediment (b), and soluble (c) phosphorus losses from corn silage land within subbasin 3 by converting from business-as-usual manure application methods to the high-rate spring injection method are displayed in Figure 5.9. The reduction in phosphorus transport from an alternative or comparison management option/scenario relative to a baseline scenario along with the specific land use, soil type, and slope descriptions for organic, sediment, and soluble phosphorus output responses are listed in appendix D tables 6.9, 6.10,and 6.11, respectively.

5.5   Discussion

In each of the case studies, Pi-VAT was able to ingest large output files from multiple watersheds for multiple management scenarios. Synthesis results very clearly identify not only the greatest hydrologic response to treatment but also where the pollutant was generated, the type of pollutant which was most sensitive, and knowledge on key factors and characteristics (soil type or topographic) of the most sensitive landscape positions. This type of scenario comparison and detailed synthesis is cumbersome as these hydrologic models are developed to provide output for one scenario at a time. Comparison of
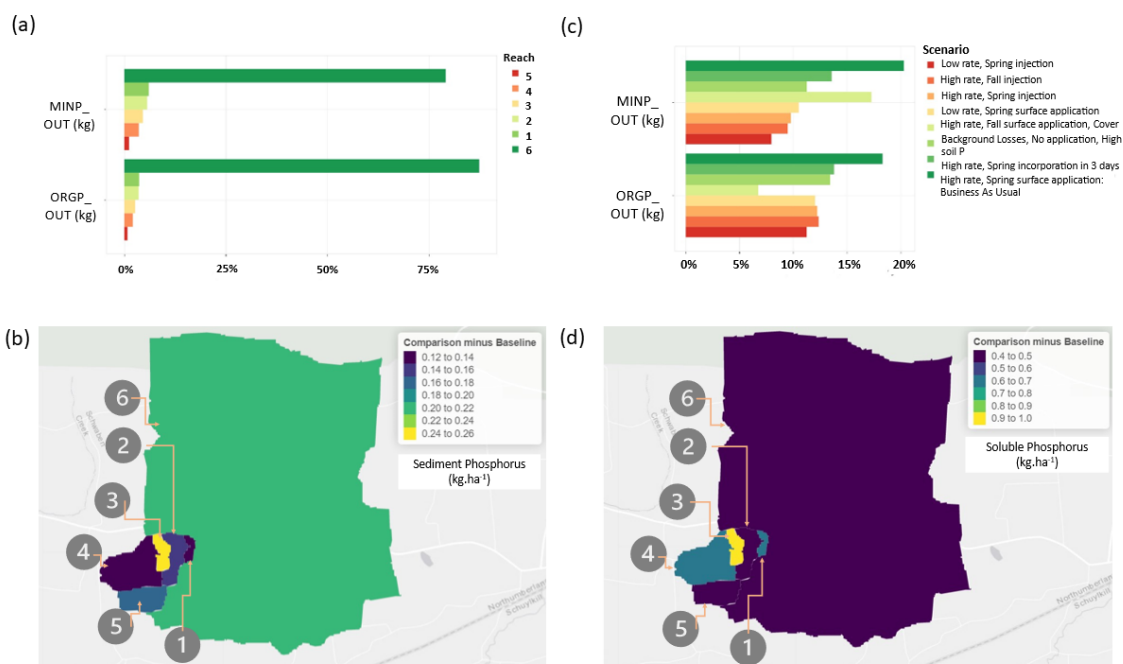
Figure 5.8: Example application of the synthesis approach using SWAT in WE-38 experimental watersheds: (a) Mineral and organic phosphorus (kg) leaving the main channel for each subbasin; Difference plots (high rate, spring surface manure application [business as usual] scenario minus the background losses from high soil P with no manure application scenario) for (b) sediment phosphorus (kg ha⁻¹) and (d) soluble phosphorus (kg ha⁻¹) from all subbasin in the WE-38 watershed. (c) Mineral and organic phosphorus (kg) leaving the main channel for subbasin 3 across different scenarios.
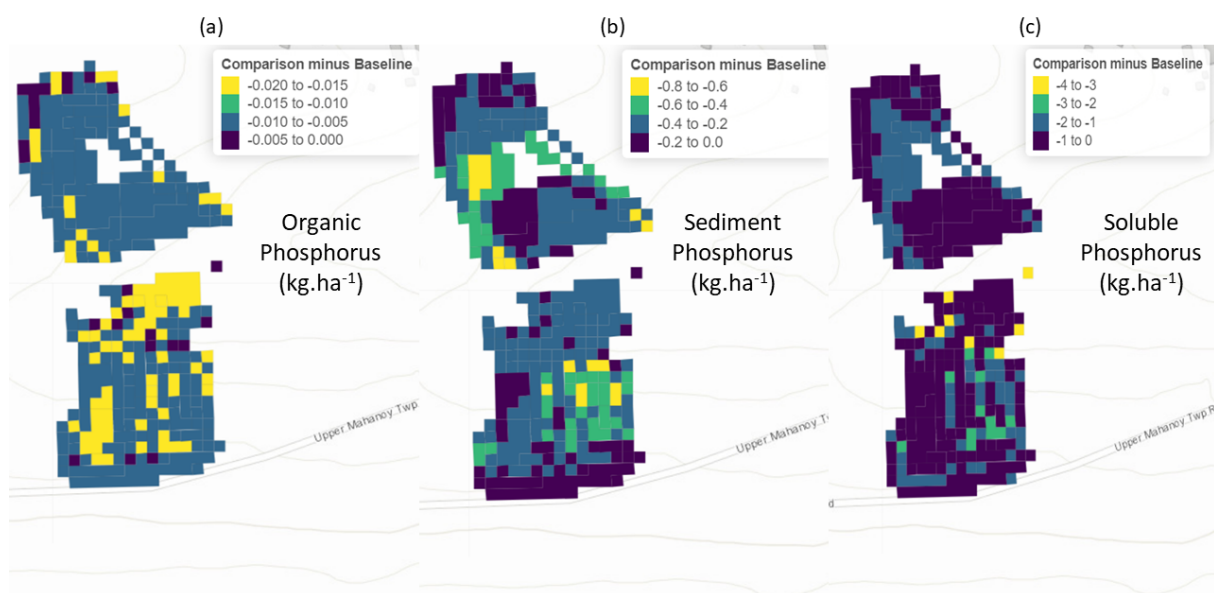
Figure 5.9: Difference plots (high rate, spring surface manure application [business-as-usual] scenario minus the high-rate spring manure injection scenario) for organic phosphorus (a), sediment phosphorus (b), and soluble phosphorus (c) from corn silage land cover in subbasin 3.

multiple scenarios in WEPP, for example, often requires a user to upload output files into spreadsheets or use programming languages such as R which is very time-consuming and complicated for typical land managers who would like this type of comparative analysis. Pi-VAT significantly reduced the time and complexity of such comparative analyses allowing the managers to carry out the 'what-if' analysis in a matter of minutes.

In all three case studies, we saw that the effectiveness of management practices was not equal across a landscape suggesting that targeted management strategies rather than blanketed management would be successful and will likely be cost-effective. This is a well-known and documented finding for large watershed management studies [Walter et al., 2000]. Here, however, we showed that Pi-VAT can quickly visualize this using modeling output especially when a land manager may be trying to convince stakeholders and investors of implementing a targeted management approach. Not only was Pi-VAT able to show where targeted responses to management will occur in these watersheds, but the tool also quickly provided the location and characteristics of the targeted locations as well as the hydrologic responses in the dominant hydrologic flow paths. In particular, for WE-38, we see that the phosphorus response to treatment varied by the delivered form of phosphorus. Pi-VAT was able to show that this varied response by the delivered form of phosphorus was also associated with the hydrologic pathways. For instance, the spatial patterns of sediment-bound phosphorus were similar to that of the runoff from the HRUs.

We demonstrated using Pi-VAT that comparative visualization and analysis can help identify pollutant source areas for prioritizing targeted management. For all three cases, Pi-VAT's comparative analysis was able to directly identify locations in the landscape where the greatest relative unit decrease in the response of the pollutant of concern occurred from the application of different management practices. For example, generally in the Lake Tahoe and Palouse analysis, we found that specific soil types with restrictive soil horizons were often the most sensitive to treatments. In the Lake Tahoe case study,

land types characterized as having steep slopes with rock outcrops and gravelly sandy loam soils had the potential to generate high to very high surface runoff. In addition, these land types were often identified as landscape positions having the greatest sensitivity to alternative management practices.

Given the abundance of process-based hydrology and water quality models coupled with the increased use of data-driven analytics, the broader opportunities for the hydrologic community to integrate models with decision tools are vast and yet unrealized [Guswa et al., 2014]. Such integration will enable land and water resources managers to harness the potential of these sophisticated models in decision-making. With the three case studies, we demonstrated the potential utility of Pi-VAT, as a standalone tool, in bridging the barriers in the use of two commonly employed sophisticated hydrology and water quality models (WEPP and SWAT) for management prioritization. By making the results available to managers in an interactive and functional format, Pi-VAT has the potential to assist watershed managers in using the physically based models more regularly alongside their current planning process and effectively communicating the implications of proposed managements.

5.6   Conclusions

Land and water resources managers are interested in the optimal use of conservation dollars to protect water resources from NPS sediments, nutrients, and other water quality issues associated with land management practices. This requires identifying, prioritizing, and targeting critical source areas for implementing conservation management practices. Process-based models that account for the relevant physical processes are powerful tools and can be effective for prioritization and targeted watershed management provided the outputs from these models are made available to the managers in a more functional format. We demonstrate the use of Pi-VAT to interactively identify, quantify and visualize the

areas that are most susceptible to disturbance and change in management. We provide a synthesis approach based on land use, soil type, and slope steepness such that the synthesized data and visuals can aid managers in identifying watersheds/subbasins of concern; evaluating the sensitivity of these watersheds/ subbasins to land management practices; quantifying and isolating source areas for treatment/management and understanding factors driving hydrologic and water quality response. We demonstrate the utility of Pi-VAT in facilitating a better understanding of the critical pollution source areas and in devising an action plan. The simplicity and accessibility of this web-based interactive tool along with compatibility to process both WEPP and SWAT-based outputs can greatly support watershed planning using complex process-based models. The tool was developed such that it can be potentially quickly modified to ingest output from any model that can provide tabular files from spatial modeling units represented by geospatial maps and therefore has the potential to be widely adopted as a decision support tool for multiple applications.

References

O. M. Abdelwahab, R. L. Bingner, F. Milillo, and F. Gentile. Effectiveness of alternative management scenarios on the sediment load in a Mediterranean agricultural watershed. *Journal of Agricultural Engineering*, 45(3):125–136, 2014. ISSN 22396268. doi: 10.4081/jae.2014.430.

S. R. Ahn and S. J. Kim. The effect of rice straw mulching and no-tillage practice in upland crop areas on nonpoint-source pollution loads based on HSPF. *Water (Switzerland)*, 8 (3), 2016. ISSN 20734441. doi: 10.3390/w8030106.

A. Bastrup-Birk and P. Gundersen. Water quality improvements from afforestation in an agricultural catchment in Denmark illustrated with the INCA model. *Hydrology and Earth System Sciences*, 8(4):764–777, 2004. ISSN 10275606. doi: 10.5194/hess-8-764-2004.

C. Beeley and S. R. Sukhdeve. *Web Application Development with R using Shiny*, volume 2. 2018. ISBN 9781783284474. URL `https://books.google.com/books?hl=en{\&}lr={\&}id=FWOdDAAAQBAJ{\&}oi=fnd{\&}pg=PP1{\&}ots=kF5if6rtzO{\&}sig={\_}bPSsZwkiNTAP1nEn6ICDq3PEeU{\#}v=onepage{\&}q{\&}f=false`.

J. Boll, E. S. Brooks, B. Crabtree, S. Dun, and T. S. Steenhuis. Variable Source Area Hydrology Modeling with the Water Erosion Prediction Project Model. *Journal of the American Water Resources Association*, 51(2):330–342, apr 2015. ISSN 1093474X. doi: 10.1111/1752-1688.12294. URL `http://doi.wiley.com/10.1111/1752-1688.12294http://dx.doi.org/10.1111/1752-1688.12294`.

H. Briak, R. Mrabet, R. Moussadek, and K. Aboumaria. Use of a calibrated SWAT model to evaluate the effects of agricultural BMPs on sediments of the Kalaya river basin (North of Morocco). *International Soil and Water Conservation Research*, 7

(2):176–183, 2019. ISSN 20956339. doi: 10.1016/j.iswcr.2019.02.002. URL `http://dx.doi.org/10.1016/j.iswcr.2019.02.002`.

E. S. Brooks, J. Boll, and P. A. McDaniel. Hydropedology in Seasonally Dry Landscapes: The Palouse Region of the Pacific Northwest USA. In *Hydropedology*, pages 329–350. Elsevier, jan 2012. ISBN 9780123869418. doi: 10.1016/B978-0-12-386941-8.00010-1.

E. S. Brooks, S. M. Saia, J. Boll, L. Wetzel, Z. M. Easton, and T. S. Steenhuis. Assessing BMP effectiveness and guiding BMP planning using process-based modeling. *Journal of the American Water Resources Association*, 51(2):343–358, 2015. ISSN 17521688. doi: 10.1111/1752-1688.12296.

E. S. Brooks, M. Dobre, W. J. Elliot, J. Q. Wu, and J. Boll. Watershed-scale evaluation of the Water Erosion Prediction Project (WEPP) model in the Lake Tahoe basin. *Journal of Hydrology*, 533:389–402, feb 2016. ISSN 00221694. doi: 10.1016/j.jhydrol.2015.12.004.

R. B. Bryant, T. L. Veith, G. W. Feyereisen, A. R. Buda, C. D. Church, G. J. Folmar, J. P. Schmidt, C. J. Dell, and P. J. Kleinman. U.S. Department of Agriculture Agricultural Research Service Mahantango Creek Watershed, Pennsylvania, United States: Physiography and history, aug 2011. ISSN 00431397. URL `http://www.ars.usda.gov/Research/docs`.

A. R. Buda, T. L. Veith, G. J. Folmar, G. W. Feyereisen, R. B. Bryant, C. D. Church, J. P. Schmidt, C. J. Dell, and P. J. Kleinman. U.S. Department of Agriculture Agricultural Research Service Mahantango Creek Watershed, Pennsylvania, United States: Long-term precipitation database, aug 2011. ISSN 00431397. URL `https://agupubs.onlinelibrary.wiley.com/doi/full/10.1029/2010WR010058https:`

//agupubs.onlinelibrary.wiley.com/doi/abs/10.1029/2010WR010058https:
//agupubs.onlinelibrary.wiley.com/doi/10.1029/2010WR010058.

W. Chang, J. Cheng, J. Allaire, C. Sievert, B. Schloerke, Y. Xie, J. Allen, J. McPherson,
A. Dipert, and B. Borges. Shiny - Web Application Framework for R. Technical report,
2021. URL https://cran.r-project.org/web/packages/shiny/shiny.pdf.

J. Cheng, B. Karambelkar, and Y. Xie. *leaflet: Create Interactive Web Maps with
the JavaScript 'Leaflet' Library*, 2021. URL https://cran.r-project.org/package=
leaflet.

R. Coats, M. Larsen, A. Heyvaert, J. Thomas, M. Luck, and J. Reuter. Nutrient and sedi-
ment production, watershed characteristics, and land use in the Tahoe Basin, California-
Nevada. *Journal of the American Water Resources Association*, 44(3):754–770, jun
2008. ISSN 1093474X. doi: 10.1111/j.1752-1688.2008.00203.x.

A. S. Collick, D. R. Fuka, P. J. Kleinman, A. R. Buda, J. L. Weld, M. J. White,
T. L. Veith, R. B. Bryant, C. H. Bolster, and Z. M. Easton. Predicting phosphorus
dynamics in complex terrains using a variable source area hydrology model. *Hydro-
logical Processes*, 29(4):588–601, feb 2015. ISSN 10991085. doi: 10.1002/hyp.10178.
URL https://onlinelibrary.wiley.com/doi/full/10.1002/hyp.10178https://
onlinelibrary.wiley.com/doi/abs/10.1002/hyp.10178https://onlinelibrary.
wiley.com/doi/10.1002/hyp.10178.

P. Daggupati, K. R. Douglas-Mankin, A. Y. Sheshukov, P. L. Barnes, and D. L. Devlin.
Field-level targeting using SWAT: Mapping output FROM HRUs to fields and assessing
limitations of GIS input data. *Transactions of the ASABE*, 54(2):501–514, 2011. ISSN
21510032. doi: 10.13031/2013.36453.

M. W. Diebel, J. T. Maxted, P. J. Nowak, and M. J. Vander Zanden. Landscape plan-

ning for agricultural nonpoint source pollution reduction I: A geographical allocation framework. *Environmental Management*, 42(5):789–802, 2008. ISSN 0364152X. doi: 10.1007/s00267-008-9186-3.

M. Dobre, A. Srivastava, R. Lew, C. Deval, E. S. Brooks, W. J. Elliot, and P. Robichaud. WEPPcloud: An online watershed-scale hydrologic modeling tool. Part II. Model performance assessment and applications to forest management and wildfires. *Journal of Hydrology*, (this issue), 2022.

Z. M. Easton, D. R. Fuka, M. T. Walter, D. M. Cowan, E. M. Schneiderman, and T. S. Steenhuis. Re-conceptualizing the soil and water assessment tool (SWAT) model to predict runoff from variable source areas. *Journal of Hydrology*, 348(3-4):279–291, jan 2008. ISSN 00221694. doi: 10.1016/j.jhydrol.2007.10.008.

Z. M. Easton, M. T. Walter, E. M. Schneiderman, M. S. Zion, and T. S. Steenhuis. Including Source-Specific Phosphorus Mobility in a Nonpoint Source Pollution Model for Agricultural Watersheds. *Journal of Environmental Engineering*, 135(1):25–35, jan 2009. ISSN 0733-9372. doi: 10.1061/(ASCE)0733-9372(2009) 135:1(25). URL `http://ascelibrary.org/doi/10.1061/{\%}28ASCE{\%}290733-9372{\%}282009{\%}29135{\%}3A1{\%}2825{\%}29`.

Z. M. Easton, D. R. Fuka, E. D. White, A. S. Collick, B. Biruk Ashagre, M. McCartney, S. B. Awulachew, A. A. Ahmed, and T. S. Steenhuis. A multi basin SWAT model analysis of runoff and sedimentation in the Blue Nile, Ethiopia. *Hydrology and Earth System Sciences*, 14(10):1827–1841, 2010. ISSN 10275606. doi: 10.5194/hess-14-1827-2010.

Z. M. Easton, P. J. Kleinman, A. R. Buda, D. Goering, N. Emberston, S. Reed, P. J. Drohan, M. T. Walter, P. Guinan, J. A. Lory, A. R. Sommerlot, and A. Sharpley. Short-

term Forecasting Tools for Agricultural Nutrient Management. *Journal of Environmental Quality*, 46(6):1257–1269, nov 2017. ISSN 1537-2537. doi: 10.2134/jeq2016.09.0377. URL `http://www.wheatscab.psu.edu/`.

J. A. Efta and W. Chung. Planning best management practices to reduce sediment delivery from forest roads using WEPP: Road erosion modeling and simulated annealing optimization. *Croatian Journal of Forest Engineering*, 35(2):167–178, sep 2014. ISSN 18455719.

W. Elliot, E. Brooks, D. E. Traeumer, and M. Dobre. Extending WEPP Technology to Predict Fine Sediment and Phosphorus Delivery from Forested Hillslopes. In *SEDHYD 2015 Interagency Conference*, page 12, Reno, NV, 2015. URL `https://www.fs.fed.us/rm/pubs{\_}journals/2015/rmrs{\_}2015{\_}elliot{\_}w002.pdf`.

D. Garen, D. Woodward, and F. Geter. A user agency's view of hydrologic, soil erosion and water quality modelling. *Catena*, 37(3-4):277–289, 1999. ISSN 03418162. doi: 10.1016/S0341-8162(99)00039-9.

N. Gudino-Elizondo, T. W. Biggs, R. L. Bingner, E. J. Langendoen, T. Kretzschmar, E. V. Taguas, K. T. Taniguchi-Quan, D. Liden, and Y. Yuan. Modelling runoff and sediment loads in a developing coastalwatershed of the US-Mexico border. *Water (Switzerland)*, 11(5):1–23, 2019. ISSN 20734441. doi: 10.3390/w11051024.

A. J. Guswa, K. A. Brauman, C. Brown, P. Hamel, B. L. Keeler, and S. S. Sayre. Ecosystem services: Challenges and opportunities for hydrologic modeling to support decision making. *Water Resources Research*, 50(5):4535–4544, may 2014. ISSN 19447973. doi: 10.1002/2014WR015497. URL `http://doi.wiley.com/10.1002/2014WR015497`.

L. K. Hatch, J. E. Reuter, and C. R. Goldman. Stream phosphorus transport in the Lake

Tahoe basin, 1989-1996. *Environmental Monitoring and Assessment*, 69(1):63–83, 2001. ISSN 01676369. doi: 10.1023/A:1010752628576.

P. Kasprzak, L. Mitchell, O. Kravchuk, and A. Timmins. Six Years of Shiny in Research - Collaborative Development of Web Tools in R. *R Journal*, 12:1–23, 2020. ISSN 20734859. doi: 10.32614/rj-2021-004.

K. Kerlin. Climate and Ecology Linked to Lake Tahoe Clarity Decline in 2016, 2017. URL `https://www.ucdavis.edu/news/climate-and-ecology-linked-lake-tahoe-clarity-decline-2016https://tahoe.ucdavis.eduresearch/SecchiData.pdf`.

T. Klein, A. Samourkasidis, I. N. Athanasiadis, G. Bellocchi, and P. Calanca. webXTREME: R-based web tool for calculating agroclimatic indices of extreme events. *Computers and Electronics in Agriculture*, 136:111–116, apr 2017. ISSN 01681699. doi: 10.1016/j.compag.2017.03.002.

P. J. A. Kleinman, A. N. Sharpley, R. W. McDowell, D. N. Flaten, A. R. Buda, L. Tao, L. Bergstrom, and Q. Zhu. Managing agricultural phosphorus for water quality protection: Principles for progress. *Plant and Soil*, 349(1-2):169–182, dec 2011. ISSN 0032079X. doi: 10.1007/s11104-011-0832-9. URL `http://link.springer.com/10.1007/s11104-011-0832-9`.

H. Kok, R. I. Papendick, and K. E. Saxton. STEEP: Impact of long-term conservation farming research and education in Pacific Northwest wheatlands. *Journal of Soil and Water Conservation*, 64(4):253–264, jul 2009. ISSN 00224561. doi: 10.2489/jswc.64.4.253. URL `www.swcs.org`.

R. Lew, M. Dobre, A. Srivastava, E. S. Brooks, W. J. Elliot, P. R. Robichaud, and D. C. Flanagan. WEPPcloud: An online watershed-scale hydrologic modeling tool. Part I.

Model description. *Journal of Hydrology*, page 127603, feb 2022. ISSN 00221694. doi: 10.1016/j.jhydrol.2022.127603.

Y. Liu, R. Wang, T. Guo, B. A. Engel, D. C. Flanagan, J. G. Lee, S. Li, B. C. Pijanowski, P. D. Collingsworth, and C. W. Wallace. Evaluating efficiencies and cost-effectiveness of best management practices in improving agricultural water quality using integrated SWAT and cost evaluation tool. *Journal of Hydrology*, 577(July):123965, 2019. ISSN 00221694. doi: 10.1016/j.jhydrol.2019.123965. URL `https://doi.org/10.1016/j.jhydrol.2019.123965`.

C. Luo, Z. Li, H. Li, and X. Chen. Evaluation of the annAGNPS model for predicting runoff and nutrient export in a typical small watershed in the hilly region of Taihu Lake. *International Journal of Environmental Research and Public Health*, 12(9):10955–10973, 2015. ISSN 16604601. doi: 10.3390/ijerph120910955.

P. A. McDaniel, M. P. Regan, E. Brooks, J. Boll, S. Barndt, A. Falen, S. K. Young, and J. E. Hammel. Linking fragipans, perched water tables, and catchment-scale hydrological processes. *Catena*, 73(2):166–173, apr 2008. ISSN 03418162. doi: 10.1016/j.catena.2007.05.011.

S. McDonald, I. N. Mohammed, J. D. Bolten, S. Pulla, C. Meechaiya, A. Markert, E. J. Nelson, R. Srinivasan, and V. Lakshmi. Web-based decision support system tools: The Soil and Water Assessment Tool Online visualization and analyses (SWATOnline) and NASA earth observation data downloading and reformatting tool (NASAaccess). *Environmental Modelling and Software*, 120, oct 2019. ISSN 13648152. doi: 10.1016/j.envsoft.2019.104499. URL `https://pubmed.ncbi.nlm.nih.gov/31534434/`.

K. R. Merriman, P. Daggupati, R. Srinivasan, and B. Hayhurst. Assessment of site-specific agricultural Best Management Practices in the Upper East River watershed, Wisconsin,

using a field-scale SWAT model. *Journal of Great Lakes Research*, 45(3):619–641, 2019. ISSN 03801330. doi: 10.1016/j.jglr.2019.02.004. URL `https://doi.org/10.1016/j.jglr.2019.02.004`.

W. W. Miller, D. W. Johnson, S. L. Karam, R. F. Walker, and P. J. Weisberg. A synthesis of sierran forest biomass management studies and potential effects on water quality. *Forests*, 1(3):131–153, 2010. ISSN 19994907. doi: 10.3390/f1030131.

D. J. Mulla, A. S. Birr, N. R. Kitchen, and M. B. David. Limitations of Evaluating the Effectiveness of Agricultural Management Practices at Reducing Nutrient Losses to Surface Waters. In J. Baker, editor, *In: Final Report Gulf Hypoxia and Local Water Quality Con- cerns Workshop, Upper Mississippi River Sub-Basin Nutrient Hypoxia Committee and ASABE, St. Joseph, Michigan*, pages 189–212. American Society of Agricultural and Biological Engineers, apr 2008. doi: 10.13031/2013.24253. URL `https://elibrary.asabe.org/azdez.asp?JID=6{\&}AID=24253{\&}CID=ghlw2008{\&}v={\&}i={\&}T=1http://elibrary.asabe.org/abstract.asp?aid=24253{\&}confalias={\&}t=1{\&}redir={\&}redirType=https://doi.org/10.13031/2013.24253`.

A. Pandey, V. M. Chowdary, B. C. Mal, and M. Billib. Application of the WEPP model for prioritization and evaluation of best management practices in an Indian watershed. *Hydrological Processes*, 23(21):2997–3005, oct 2009. ISSN 08856087. doi: 10.1002/hyp.7411. URL `www.interscience.wiley.com`.

J. Y. Park, Y. S. Yu, S. J. Hwang, C. Kim, and S. J. Kim. SWAT modeling of best management practices for Chungju dam watershed in South Korea under future climate change scenarios. *Paddy and Water Environment*, 12(SUPPL1):65–75, 2014. ISSN 16112504. doi: 10.1007/s10333-014-0424-4.

R Core Team. The R Project for Statistical Computing, 2021. URL `https://www.r-project.org/`.

R. A. Rittenburg, A. L. Squires, J. Boll, E. S. Brooks, Z. M. Easton, and T. S. Steenhuis. Agricultural BMP effectiveness and dominant hydrological flow paths: Concepts and a review. *Journal of the American Water Resources Association*, 51(2):305–329, apr 2015. ISSN 17521688. doi: 10.1111/1752-1688.12293. URL `https://onlinelibrary.wiley.com/doi/full/10.1111/1752-1688.12293https://onlinelibrary.wiley.com/doi/abs/10.1111/1752-1688.12293https://onlinelibrary.wiley.com/doi/10.1111/1752-1688.12293`.

P. R. Robichaud, W. J. Elliot, F. B. Pierson, D. E. Hall, C. A. Moffet, and L. E. Ashmun. Erosion Risk Management Tool (ERMiT) User Manual. Technical report, USDA-FS, Moscow, ID, 2007. URL `http://www.fs.fed.us/rm/publications`.

M. Rode, G. Arhonditsis, D. Balin, T. Kebede, V. Krysanova, A. Van Griensven, and S. E. Van Der Zee. New challenges in integrated water quality modelling. *Hydrological Processes*, 24(24):3447–3461, nov 2010. ISSN 08856087. doi: 10.1002/hyp.7766. URL `https://onlinelibrary.wiley.com/doi/full/10.1002/hyp.7766https://onlinelibrary.wiley.com/doi/abs/10.1002/hyp.7766https://onlinelibrary.wiley.com/doi/10.1002/hyp.7766`.

G. B. Sahoo, D. M. Nover, J. E. Reuter, A. C. Heyvaert, J. Riverson, and S. G. Schladow. Nutrient and particle load estimates to Lake Tahoe (CA-NV, USA) for Total Maximum Daily Load establishment. *Science of the Total Environment*, 444: 579–590, feb 2013. ISSN 00489697. doi: 10.1016/j.scitotenv.2012.12.019. URL `https://www.sciencedirect.com/science/article/pii/S0048969712015628{\#}!`

A. N. Sharpley, S. C. Chapra, R. Wedepohl, J. T. Sims, T. C. Daniel, and K. R. Reddy.

Managing Agricultural Phosphorus for Protection of Surface Waters: Issues and Options. *Journal of Environmental Quality*, 23(3):437–451, may 1994. ISSN 0047-2425. doi: 10.2134/jeq1994.00472425002300030006x. URL `https://onlinelibrary.wiley.com/doi/abs/10.2134/jeq1994.00472425002300030006x`.

A. N. Sharpley, R. W. Mcdowell, and P. J. A. Kleinman. Phosphorus loss from land to water: Integrating agricultural and environmental management. *Plant and Soil*, 237(2):287–307, 2001. ISSN 0032079X. doi: 10.1023/A:1013335814593. URL `http://link.springer.com/10.1023/A:1013335814593`.

C. Sievert. *Interactive Web-Based Data Visualization with R, plotly, and shiny*. Chapman and Hall/CRC, 2020. ISBN 9781138331457. URL `https://plotly-r.com`.

R. K. Singh, R. K. Panda, K. K. Satapathy, and S. V. Ngachan. Simulation of runoff and sediment yield from a hilly watershed in the eastern Himalaya, India using the WEPP model. *Journal of Hydrology*, 405(3-4):261–276, aug 2011. ISSN 00221694. doi: 10.1016/j.jhydrol.2011.05.022.

A. Srivastava, J. Q. Wu, W. J. Elliot, E. S. Brooks, and D. C. Flanagan. MODELING STREAMFLOW IN A SNOW-DOMINATED FOREST WATERSHED USING THE WATER EROSION PREDICTION PROJECT (WEPP) MODEL. *American Society of Agricultural and Biological Engineers*, 60(4):1171–1187, 2017. doi: 10.13031/trans.12035. URL `https://elibrary.asabe.org/azdez.asp?search=0{\&}JID=3{\&}AID=48344{\&}CID=t2017{\&}v=60{\&}i=4{\&}T=2`.

A. Srivastava, E. S. Brooks, M. Dobre, W. J. Elliot, J. Q. Wu, D. C. Flanagan, J. A. Gravelle, and T. E. Link. Modeling forest management effects on water and sediment yield from nested, paired watersheds in the interior Pacific Northwest, USA using

WEPP. *Science of the Total Environment*, 701:134877, jan 2020. ISSN 18791026. doi: 10.1016/j.scitotenv.2019.134877.

S. M. Stackpoole, E. G. Stets, and L. A. Sprague. Variable impacts of contemporary versus legacy agricultural phosphorus on US river water quality. *Proceedings of the National Academy of Sciences of the United States of America*, 116(41):20562–20567, oct 2019. ISSN 10916490. doi: 10.1073/pnas. 1903226116. URL `www.pnas.org/lookup/suppl/doi:10.1073/pnas.1903226116/-/DCSupplemental.www.pnas.org/cgi/doi/10.1073/pnas.1903226116`.

M. T. Walter, M. F. Walter, E. S. Brooks, T. S. Steenhuis, J. Boll, and K. Weiler. Hydrologically sensitive areas: Variable source area hydrology implications for water quality risk assessment. *Journal of Soil and Water Conservation*, 55(3):277–284, 2000. ISSN 00224561.

C. Wellen, A. R. Kamran-Disfani, and G. B. Arhonditsis. Evaluation of the current state of distributed watershed nutrient water quality modeling. *Environmental Science and Technology*, 49(6):3278–3290, mar 2015. ISSN 15205851. doi: 10.1021/es5049557. URL `https://pubs.acs.org/sharingguidelines`.

S. Whateley, J. D. Walker, and C. Brown. A web-based screening model for climate risk to water supply systems in the northeastern United States. *Environmental Modelling and Software*, 73:64–75, nov 2015. ISSN 13648152. doi: 10.1016/j.envsoft.2015.08.001.

Y. Xie, J. Cheng, and X. Tan. *DT: A Wrapper of the JavaScript Library 'DataTables'*, 2021. URL `https://cran.r-project.org/package=DT`.

Y. Xu, D. J. Bosch, M. B. Wagena, A. S. Collick, and Z. M. Easton. Meeting Water Quality Goals by Spatial Targeting of Best Management Practices under Climate

Change. *Environmental Management*, 63(2):173–184, 2019. ISSN 14321009. doi: 10.1007/s00267-018-01133-8. URL https://doi.org/10.1007/s00267-018-01133-8.

H. Yen, P. Daggupati, M. J. White, R. Srinivasan, A. Gossel, D. Wells, and J. G. Arnold. Application of large-scale, multi-resolution watershed modeling framework using the Hydrologic and Water Quality System (HAWQS). *Water (Switzerland)*, 8(4):1–23, 2016. ISSN 20734441. doi: 10.3390/w8040164.

T. Zhang, Y. Yang, J. Ni, and D. Xie. Best management practices for agricultural non-point source pollution in a small watershed based on the AnnAGNPS model. *Soil Use and Management*, 36(1):45–57, 2020. ISSN 14752743. doi: 10.1111/sum.12535.

CHAPTER 6

Summary and Conclusions

Effective watershed management and protection of water resources from non-point source pollution requires identification, prioritization, and targeting of pollutant source areas. Land and water resources managers are interested in the optimal use of conservation dollars to protect water resources from non-point source sediments, nutrients, and other water quality issues associated with land management practices. This necessitates that the watershed managers have a fair understanding of not just the pollutant source areas but also the impacts of different management strategies and climate scenarios on pathways and quantities of pollutants being exported from the watershed.

This study used a combination of long-term water quality monitoring data, laboratory flow-through leaching experiments, and water quality models to deliver an improved understanding of the source areas, fate, and transport of nutrients in forest-dominated watersheds. In addition, this study attempted to better integrate the science and learnings generated from watershed modeling into informed decision-making by developing a decision support tool with watershed managers as the target audience.

Specifically, in chapter 2 of this study, we shed light on the effect of contemporary forest management activities, including clear-cutting and thinning, on water yield and stream nitrogen and phosphorus dynamics using a quarter-century-long (1992–2016) monitoring data from a paired and nested watershed in the interior Pacific Northwest, US. We reported statistically significant increases in stream $NO_3 + NO_2$ loading from the paired and nested watersheds following timber harvest treatments. In the case of OP, we attributed an increase in nutrient load to increases in streamflow, as OP concentrations remained near minimum detectable concentrations. Downstream cumulative watersheds exhibited lower in-stream $NO_3 + NO_2$ concentrations likely due to dilution and nutrient assimilation effects. Interestingly, the $NO_3 + NO_2$ concentration, streamflow, and loads

of $NO_3 + NO_2$ and OP from the undisturbed control watershed also increased. However, these increases were relatively smaller than the harvested watersheds and likely driven by climate variability or subtle forest succession changes. Overall, this study showed that the contemporary forest management activities increased stream $NO_3 + NO_2$ concentrations and loads following timber harvest activities, but these effects are attenuated due to downstream uptake processes. Furthermore, relative to post-wildfire impacts, these nutrient increases are small and short-lived.

In chapter 3, the effects of parent material, ecosystem system types, and hydrologic pathways on phosphorus retention and release were investigated. Results showed that the phosphorus leaching in the forest-meadow systems of Lake Tahoe Basin occurs primarily in organic form. Leaching from granitic sites is larger than that from andesitic sites with granitic meadows leaching the largest amounts of phosphorus. The greatest risk of phosphorus leaching, translocation, and potential loss via subsurface pathways occurs in granitic soils with enriched phosphorus sources. Saturation excess runoff is an important pathway for phosphorus loss from meadow systems as demonstrated by the losses from the exfiltration pathway.

In chapter 4, a process based distributed parameter hydrologic model was applies, calibrated and assessed for its ability to predict P transport from two contrasting watershed in the Lake Tahoe Basin. The study reported the parameter sensitivity of the WEPP-WQ model to simulate phosphorus losses using a single hillslope as our modeling unit. Following that we assessed the ability of the minimally calibrated WEPP-WQ model to simulate phosphorus losses from large, and relatively undisturbed, forested watersheds in the Lake Tahoe Basin. Parameter sensitivity analysis showed that the P sorption parameter (PSP), P soil partitioning parameter (PHOSKD), initial labile phosphorus pool in the topsoil layer (LabileP), and P uptake distribution parameter (UPB) are some of the relatively important and sensitive parameters for simulating phosphorus loss. The

relative differences between calibrated values obtained for these parameters in watersheds with differing soil type are well supported by the findings of isotherm experiments in this chapter. Watershed scale modeling study also showed adequate capabilities of the existing phosphorus routines in WEPP to simulate soluble phosphorus losses from the watersheds. While WEPP-WQ does not account for the P contributions associated with the channel processes, the seasonality and relative trends of particulate phosphorus were correctly predicted. A simple analysis of TP load using a fixed P concentration associated with detached channel sediments, suggested that the absolute magnitude of predicted particulate phosphorus from upland sources is underpredicted by the model. This underprediction may be due to the assumed relative distribution of P in active and stable pools that may not be appropriate for forested soils or due to the underestimation of P enrichment ratio or a combination of both. Further investigation of model structure is needed to identify appropriate soil P pool initialization. Significant development and testing are needed for WEPP-WQ to be fully ready for use. Modeling dissolved P with WEPP-WQ could be a better approach compared to the current P approach implemented in WEPPcloud that does not incorporates P-cycling. WEPP-WQ is likely better able to capture changes in disturbance on P pools and dissolved P. Overall, this study shows that WEPP-WQ, with its current dissolved phosphorus routines, can be an effective, process-based, and yet parsimonious edge-of-the-hillslope effects tool for informing land and water management decisions. Improving the particulate P predictions and making WEPP-WQ a complete water quality prediction tool requires further developments and testing.

While process-based hydrology and water quality models are powerful heuristic tools for land and water resources managers, they are complex. Consequently, such models are often under-utilized as management prioritization and planning tools. In chapter 5 of this dissertation, we developed a prioritization, interactive visualization, and analysis tool (Pi-VAT) to assist watershed managers with synthesizing multi-scenario, multi-watershed

outputs from process-based geospatial models. Pi-VAT was applied to output from multiple watersheds and for multiple management scenarios and treatments from two geospatial models for watershed management: Water Erosion Prediction Project (WEPP) and Soil & Water Assessment Tool (SWAT). This chapter demonstrated the utility of Pi-VAT to examine simulated hydrologic, sediment, and water quality response at the hillslope/hydrologic response unit (HRU) scale. In a matter of minutes, Pi-VAT can synthesize overwhelming amounts of output from process-based models into information useful for land and water resources managers. Pi-VAT can be used to interactively identify, quantify, and visualize areas that are most susceptible to disturbance under different scenarios and provide a synthesis approach based on land use, soil type, and slope steepness. This approach guides land and water resources managers in prioritizing the areas of the watershed that provide the maximum reduction in pollutant loads while treating the least amount of area. Pi-VAT provides a flexible reactive platform for the development of decision support tools based on process-based models intended for watershed management and research applications.

Appendix A: Appendix for Chapter 2
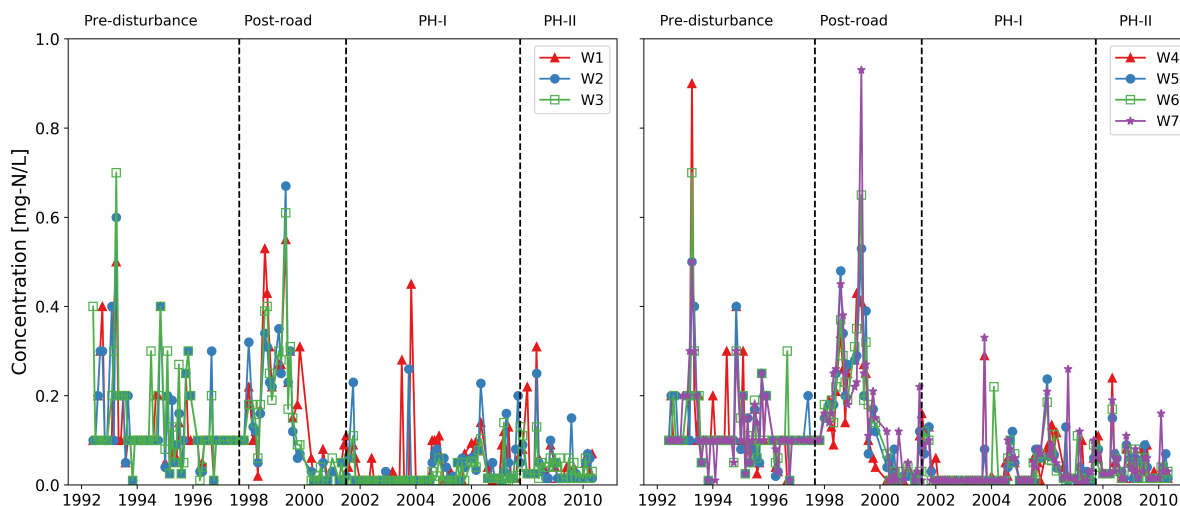
Figure 6.1: Observed monthly stream TKN concentrations (mg-N L^{-1}) in MCEW watersheds.
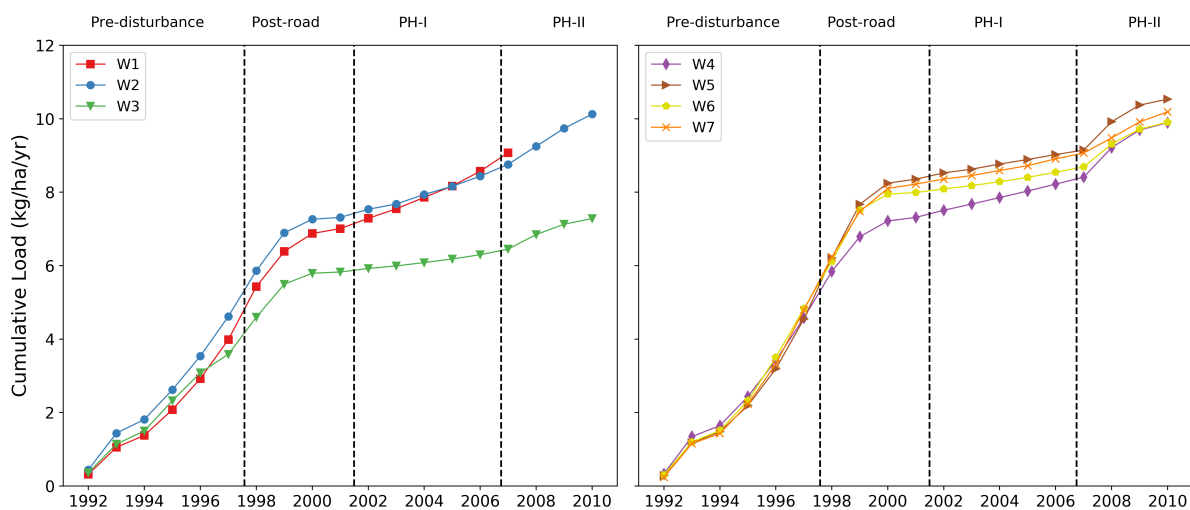
Figure 6.2: Observed monthly stream TKN loads (kg ha^{-1} yr^{-1}) in MCEW watersheds.
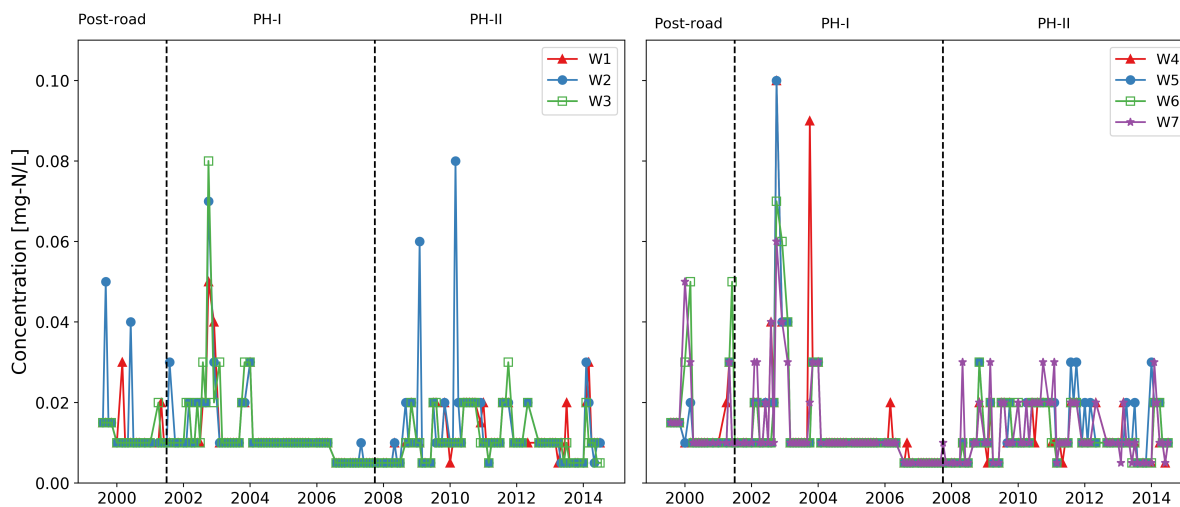
Figure 6.3: Observed monthly stream TAN concentrations (mg-NH$_3$ L^{-1}) in MCEW watersheds.
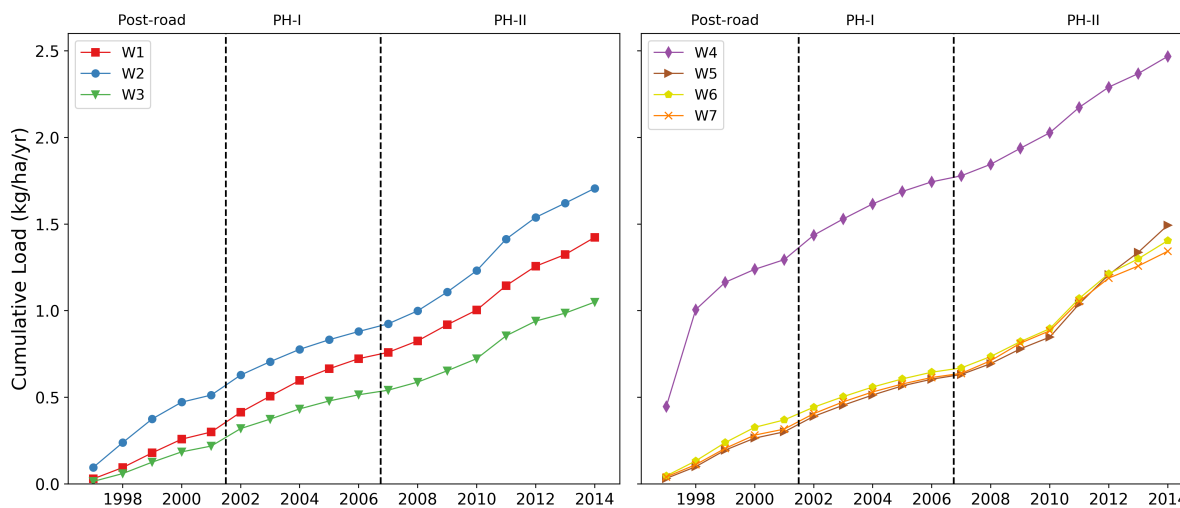
Figure 6.4: Observed monthly stream TAN loads (kg ha^{-1} yr^{-1}) in MCEW watersheds.

Table 6.1: Summary of regression models selected by LOADEST to estimate TKN daily loads for each watershed along with the model performance metrics

TKN						
Watershed No.	Treatment	No. of Obs	Model Number	AIC	R-squared(%)	Pbias
F1	Calibration	54	3	2.282	54.29	8.403
	Post-Road	33	3	3.153	46.5	-6.848
	Post-Harvest	63	3	3.043	41.57	-5.798
	Phase-II	28	9	2.174	85.51	-13.94
F2	Calibration	54	3	2.461	52.47	5.056
	Post-Road	33	9	2.787	71.19	-18.621
	Post-Harvest	63	7	2.73	51.82	-17.513
	Phase-II	28	1	2.461	62.23	-23.858
F3	Calibration	55	5	2.514	61.39	-3.975
	Post-Road	33	9	2.797	75.5	-20.158
	Post-Harvest	63	3	2.376	57.79	-14.58
	Phase-II	28	3	2.11	70.95	-9.841
F4	Calibration	54	3	2.453	66.25	-1.519
	Post-Road	33	3	2.865	64.06	-3.933
	Post-Harvest	62	1	2.877	25.3	-12.561
	Phase-II	28	3	2.093	78.21	-14.611
F5	Calibration	54	3	2.293	63.62	-5.471
	Post-Road	31	3	2.761	73.15	6.95
	Post-Harvest	63	4	2.715	38.26	-4.387
	Phase-II	26	3	2.032	80	4.396
F6	Calibration	54	3	2.185	66.29	-3.977
	Post-Road	32	9	2.565	79.28	-14.254
	Post-Harvest	63	3	2.789	30.14	-12.846
	Phase-II	26	3	1.831	81.86	-9.488
F7	Calibration	54	3	2.295	69.6	4.242
	Post-Road	31	3	3.087	56.01	-14.83
	Post-Harvest	63	7	2.838	36.74	-10.375
	Phase-II	26	1	2.342	68.23	-18.526

Table 6.2: Summary of regression models selected by LOADEST to estimate Nitrate-Nitrite daily loads for each watershed along with the model performance metrics

NO3+NO2						
Watershed No.	Treatment	No. of Obs	Model Number	AIC	R-squared(%)	Pbias
	Calibration	54	9	1.785	83.78	1.582
F1	Post-Road	34	1	3.004	64.52	24.84
	Post-Harvest	63	9	0.992	93.85	2.641
	Phase-II	96	9	0.959	89.67	-3.702
	Calibration	54	7	1.648	70.96	3.911
F2	Post-Road	34	5	3.36	52.49	-1.516
	Post-Harvest	63	9	1.492	86.15	-1.105
	Phase-II	96	9	1.313	86.88	-4.204
	Calibration	55	7	1.548	76.16	2.162
F3	Post-Road	34	3	3.147	57.1	1.332
	Post-Harvest	63	3	1.938	63.16	-0.511
	Phase-II	96	9	0.964	84.15	2.635
	Calibration	54	7	1.775	80.93	3.571
F4	Post-Road	33	3	3.185	58.94	11.051
	Post-Harvest	63	9	1.518	88.84	-0.083
	Phase-II	96	9	0.494	92.32	2.05
	Calibration	54	8	1.262	86.28	0.111
F5	Post-Road	32	3	3.171	50.55	-0.285
	Post-Harvest	63	1	1.718	69.06	4.11
	Phase-II	95	7	1.843	86.45	-9.925
	Calibration	54	8	1.828	80.4	-11.638
F6	Post-Road	32	3	3.508	47.03	14.382
	Post-Harvest	63	1	1.673	65.64	-0.213
	Phase-II	95	7	1.69	89.18	-3.675
	Calibration	54	7	1.452	83.29	6.506
F7	Post-Road	33	3	3.27	56.89	13.174
	Post-Harvest	63	9	1.726	85.51	-3.709
	Phase-II	94	9	1.296	89.72	9.069

Table 6.3: Summary of regression models selected by LOADEST to estimate TP daily loads for each watershed along with the model performance metrics

TP						
Watershed No.	Treatment	No. of Obs	Model Number	AIC	R-squared(%)	Pbias
F1	Calibration	54	1	2.082	63.89	7.807
	Post-Road	36	9	2.286	72.74	-1.231
	Post-Harvest	63	3	1.989	73.07	-14.621
	Phase-II	72	1	1.49	78.67	-11.97
F2	Calibration	54	1	2.02	62.9	6.28
	Post-Road	36	9	2.425	69.31	-3.836
	Post-Harvest	63	3	1.774	76.96	-9.797
	Phase-II	72	4	1.593	76.51	-2.148
F3	Calibration	55	1	2.077	70.71	5.57
	Post-Road	36	9	2.301	76.98	3.674
	Post-Harvest	63	4	2.121	75.79	-24.498
	Phase-II	72	4	1.596	75.92	-1.81
F4	Calibration	54	1	2.013	74.98	10.373
	Post-Road	35	3	2.678	54.9	-2.43
	Post-Harvest	63	4	2.268	58.13	-8.728
	Phase-II	72	7	1.628	74.94	-4.029
F5	Calibration	54	4	2.169	67.08	6.905
	Post-Road	35	1	2.535	47.93	-0.717
	Post-Harvest	63	1	2.601	49.17	-2.325
	Phase-II	71	8	1.57	78.37	-0.722
F6	Calibration	54	1	2.104	65.61	4.744
	Post-Road	35	1	2.394	49.5	-0.826
	Post-Harvest	63	2	2.212	61.8	-14.432
	Phase-II	70	3	1.701	71.58	1.942
F7	Calibration	54	1	2.19	65.23	6.703
	Post-Road	34	1	2.084	64.27	-2.722
	Post-Harvest	62	3	2.139	69.82	-15.351
	Phase-II	71	1	1.599	72.56	-1.361

Table 6.4: Summary of regression models selected by LOADEST to estimate OP daily loads for each watershed along with the model performance metrics

OP						
Watershed No.	Treatment	No. of Obs	Model Number	AIC	R-squared(%)	Pbias
F1	Calibration	52	3	0.984	86.75	-0.249
	Post-Road	35	3	1.342	80.16	-3.448
	Post-Harvest	63	7	1.531	76	0.099
	Phase-II	93	9	1.803	75.82	-0.712
F2	Calibration	53	3	1.319	79.35	2.247
	Post-Road	36	5	1.759	71.54	0.346
	Post-Harvest	63	9	1.389	80.57	-1.72
	Phase-II	93	7	1.842	69.46	0.82
F3	Calibration	54	5	1.12	87.87	-3.34
	Post-Road	36	7	1.668	88.07	1.15
	Post-Harvest	63	4	1.328	78.69	2.173
	Phase-II	93	7	1.431	78.2	0.019
F4	Calibration	53	1	1.555	79.74	-2.881
	Post-Road	35	7	1.699	83.62	0.936
	Post-Harvest	63	7	1.474	74.8	-0.431
	Phase-II	93	7	1.73	73.26	-1.632
F5	Calibration	53	7	1.276	83.7	0.841
	Post-Road	35	7	1.725	82.42	3.395
	Post-Harvest	63	9	1.509	79.44	-3.725
	Phase-II	91	7	1.705	74.12	-2.089
F6	Calibration	52	7	1.862	70.33	-7.149
	Post-Road	35	7	1.73	81.23	-3.936
	Post-Harvest	63	9	1.606	75.5	-2.877
	Phase-II	91	7	1.703	73.73	0.998
F7	Calibration	53	7	1.531	81.06	-0.662
	Post-Road	34	4	2.157	77.94	0.456
	Post-Harvest	63	7	1.645	71.03	1.248
	Phase-II	91	7	1.634	75.99	0.418

Table 6.5: Summary of regression models selected by LOADEST to estimate TAN daily loads for each watershed along with the model performance metrics

TAN						
Watershed No.	Treatment	No. of Obs	Model Number	AIC	R-squared(%)	Pbias
F1	Calibration	NA	NA	NA	NA	NA
	Post-Road	17	1	0.744	88.95	1.889
	Post-Harvest	63	9	0.673	89.06	3.733
	Phase-II	69	9	1.342	82.74	0.817
F2	Calibration	NA	NA	NA	NA	NA
	Post-Road	17	3	1.504	79.07	-2.272
	Post-Harvest	63	3	0.992	81.66	3.486
	Phase-II	69	9	1.841	70.05	0.428
F3	Calibration	NA	NA	NA	NA	NA
	Post-Road	17	1	-0.036	96.37	1.958
	Post-Harvest	63	9	0.96	85.76	1.924
	Phase-II	69	9	1.104	85.78	0.272
F4	Calibration	NA	NA	NA	NA	NA
	Post-Road	17	9	0.726	95.35	-2.777
	Post-Harvest	63	9	1.505	73.83	2.661
	Phase-II	69	9	1.289	81.71	0.238
F5	Calibration	NA	NA	NA	NA	NA
	Post-Road	17	2	0.703	92.62	-3.201
	Post-Harvest	63	9	1.121	83.92	1.962
	Phase-II	69	9	1.561	80.03	2.617
F6	Calibration	NA	NA	NA	NA	NA
	Post-Road	17	2	1.855	75.19	-2.891
	Post-Harvest	63	1	1.673	65.64	-0.213
	Phase-II	69	9	1.431	79.35	3.231
F7	Calibration	NA	NA	NA	NA	NA
	Post-Road	17	6	1.382	87.63	-2.124
	Post-Harvest	63	9	1.137	84.98	1.857
	Phase-II	69	9	1.689	78.14	-0.1

Table 6.6: Calibration phase correlations for streamflow, concentrations and yields between treatment control pairs in MCEW watersheds

Watershed-Pair		W1-W3	W2-W3	W4-W5	W6-W7
Streamflow		0.98	0.98	0.94	0.99
Concentrations	NO3+NO2	0.04	0.76	0.62	0.12
	TP	0.73	0.88	0.92	0.89
	OP	0.73	0.59	0.39	0.81
	TKN	0.66	0.72	0.78	0.87
	TAN	NA	NA	NA	NA
Yields	NO3+NO2	0.86	0.97	0.75	0.77
	TP	0.98	0.98	0.89	0.99
	OP	0.86	0.87	0.94	0.98
	TKN	0.72	0.7	0.9	0.98
	TAN	NA	NA	NA	NA
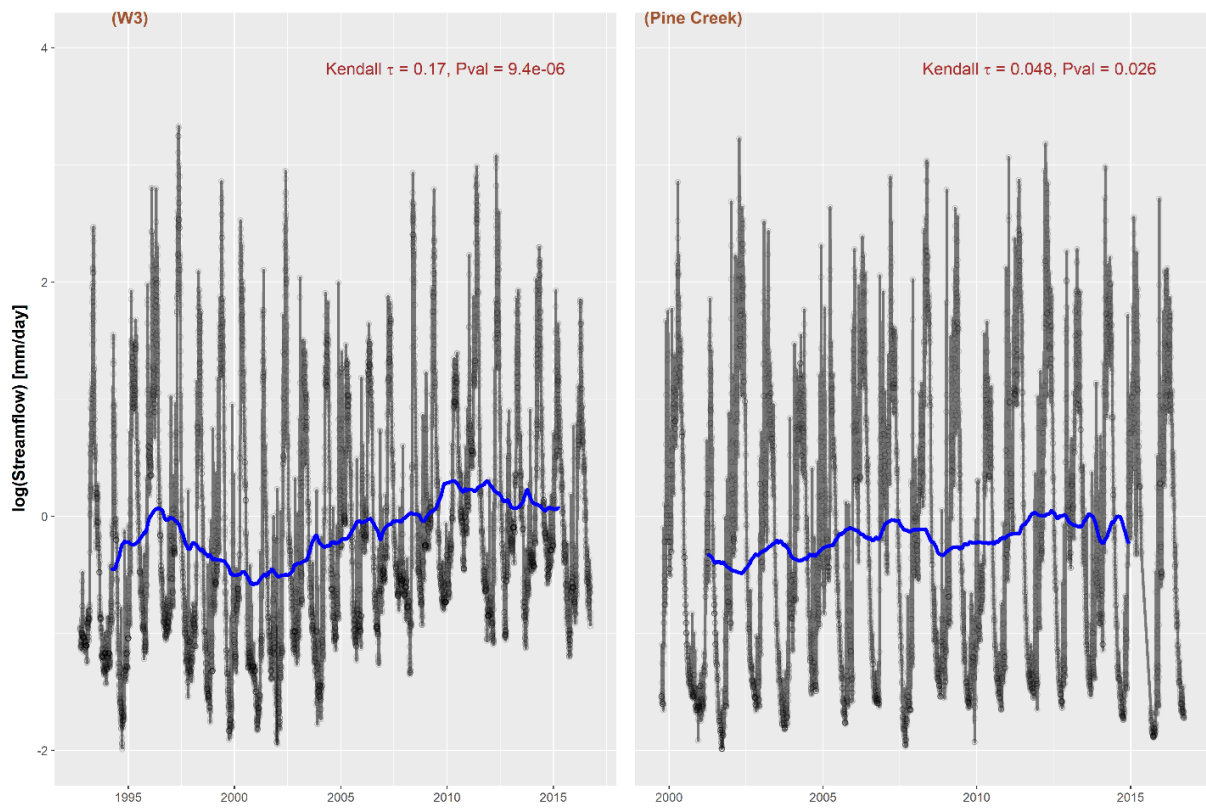
Figure 6.5: Long term daily mean streamflow and modified Mann-Kendall statistic at the MCEW control site (W3) and PC watersheds. The blue line shows the 3-year rolling mean.
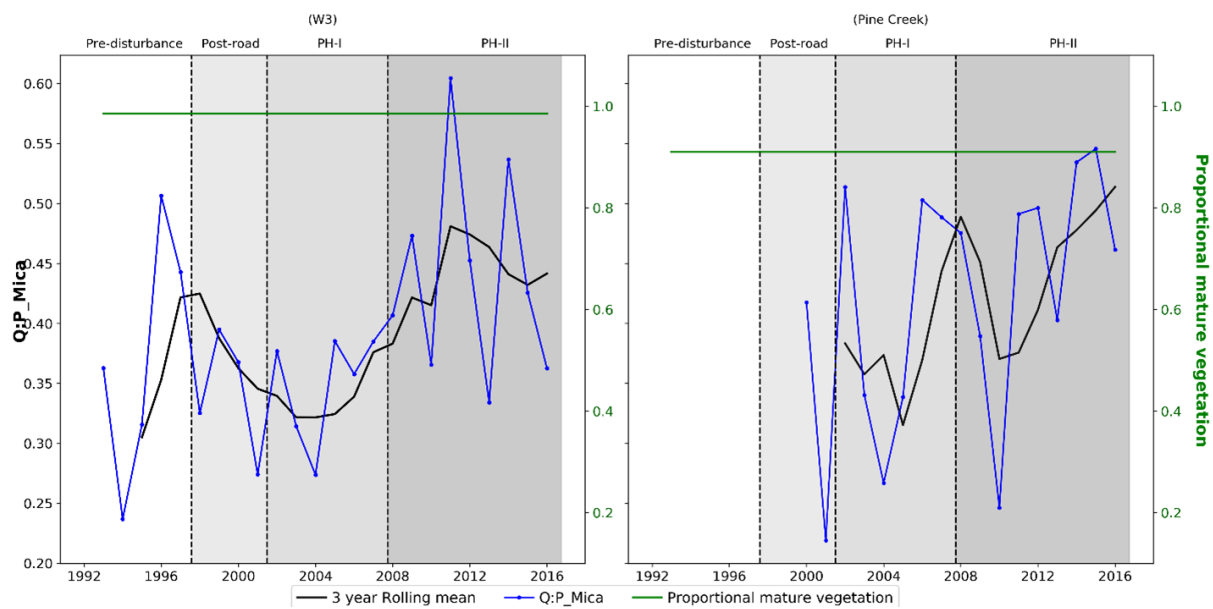
Figure 6.6: Annual streamflow index and proportional area covered with mature vegetation in the undisturbed site at MCEW (W3) and PC watersheds.
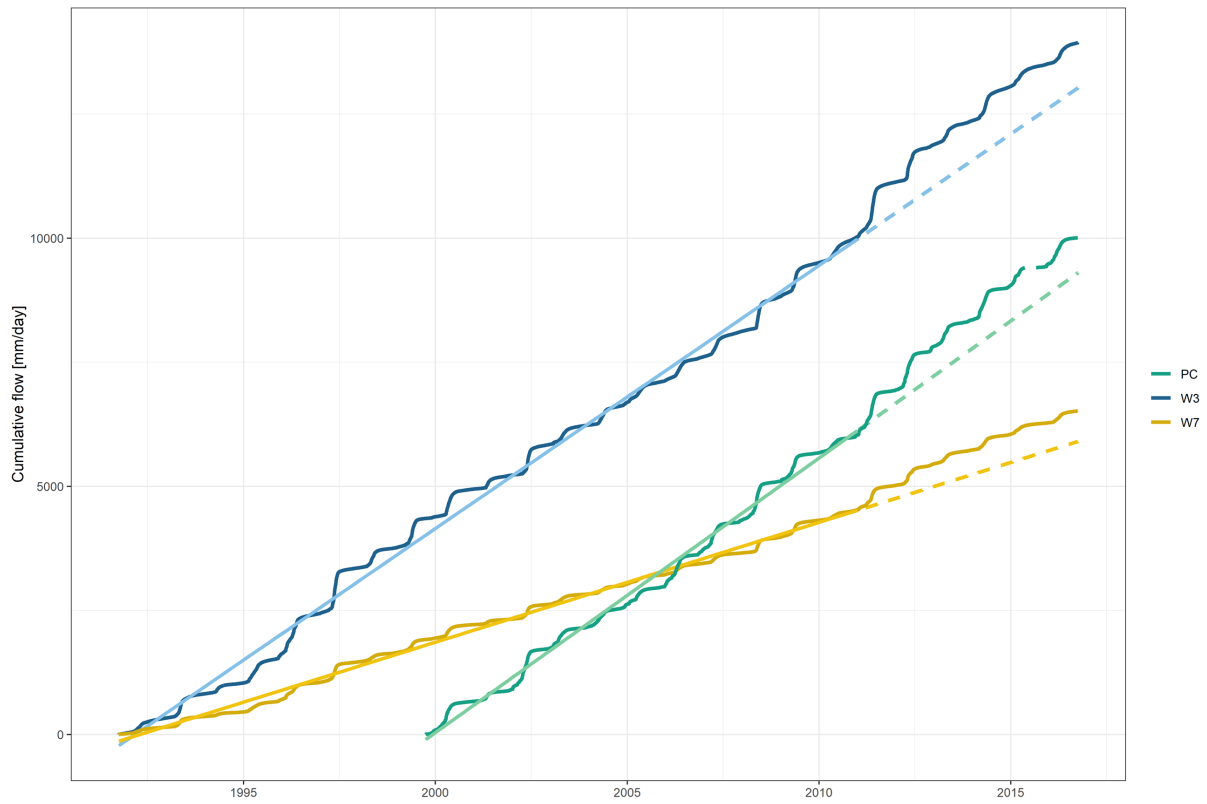
Figure 6.7: Cumulative flow (mm) with time from the W3, W7, and PC watersheds with long term linear trendline from 1990-2010 (solid line) and extrapolated to 2010-2016 (dashed line).

Appendix B: Appendix for Chapter 3
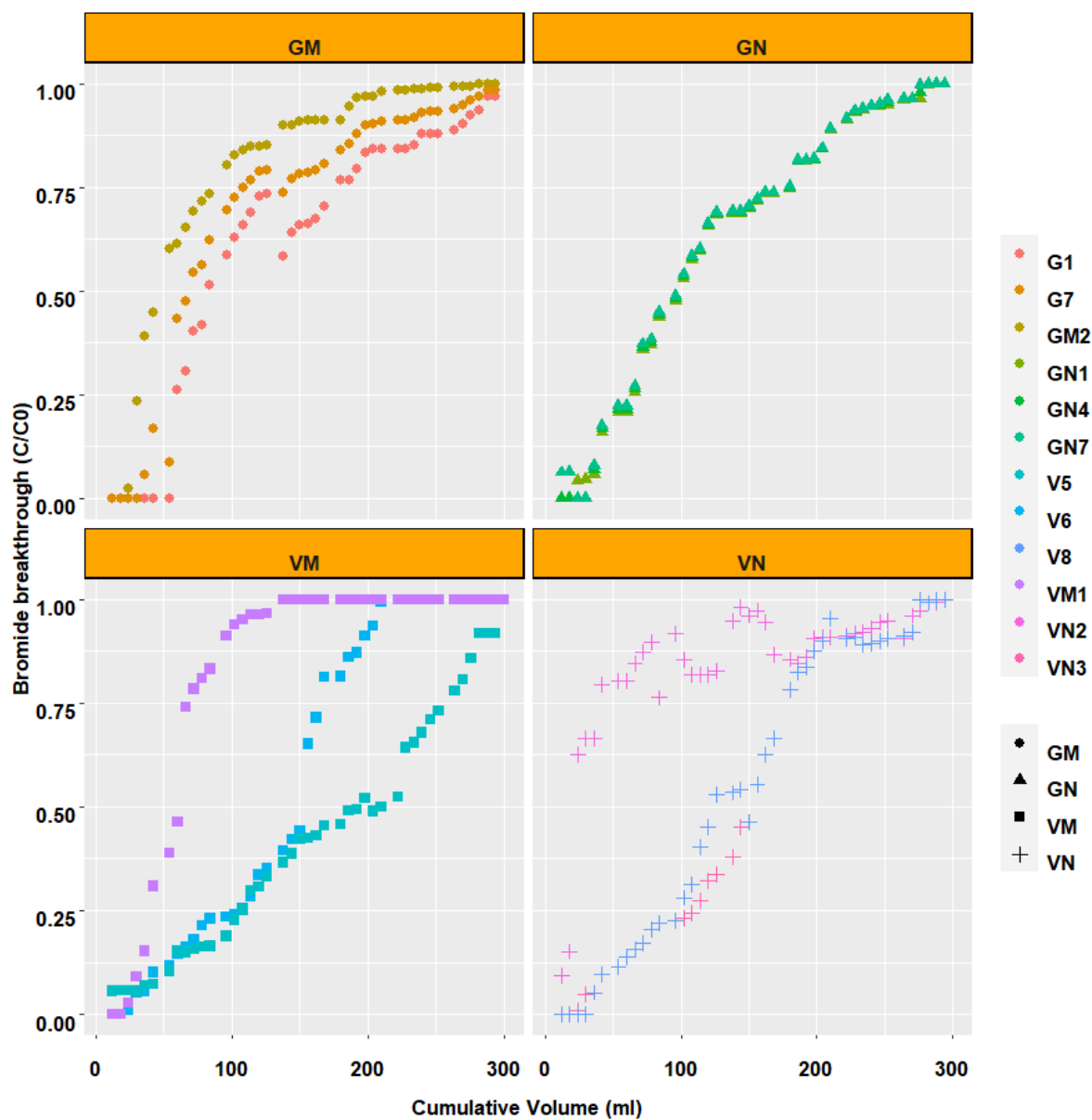
Figure 6.8: Bromide breakthrough curves (C/C$_0$) for each core used in the experiment
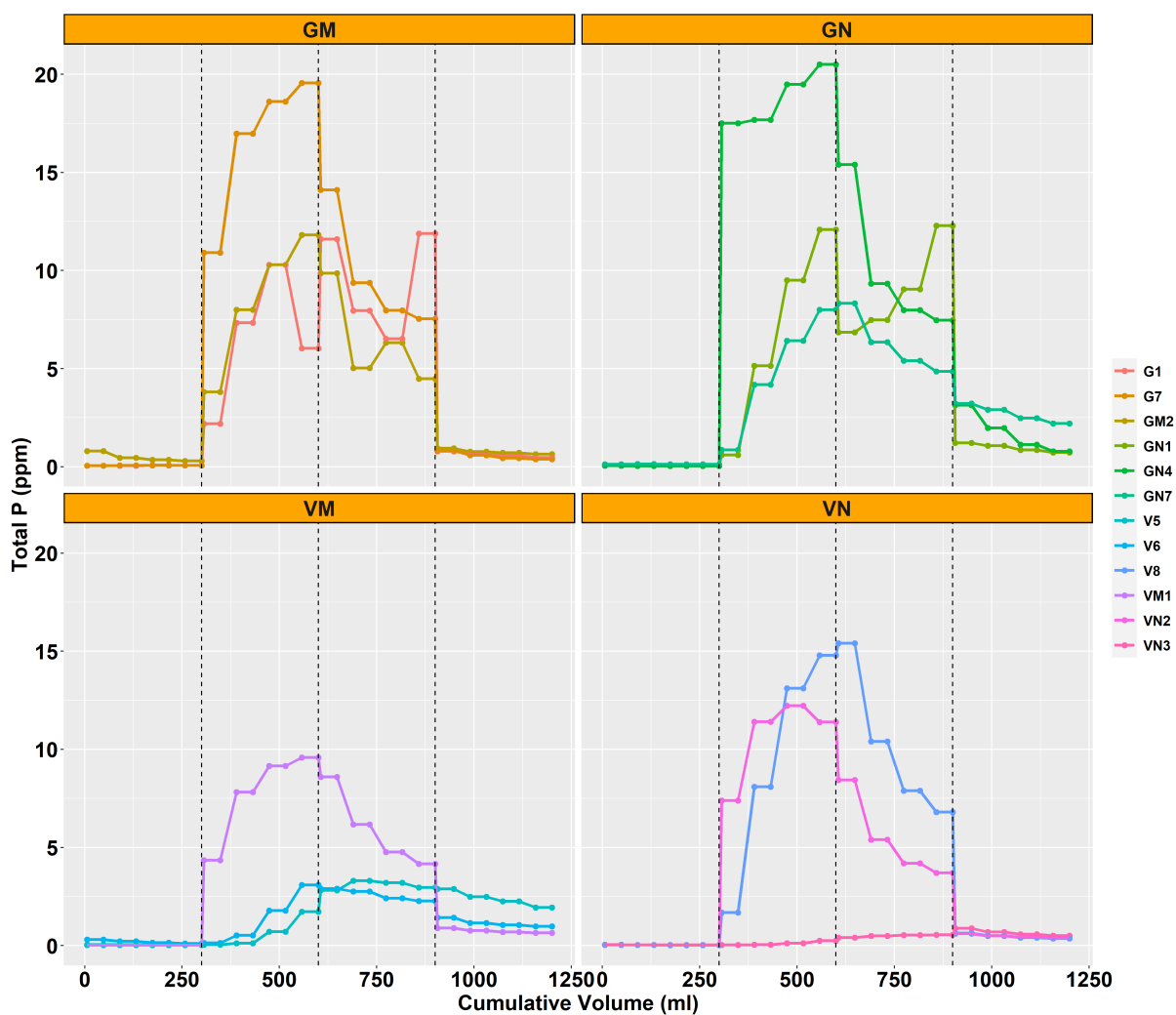
Figure 6.9: Total dissolved phosphorus concentrations (ppm) in the leachate of each core lined up sequentially by experiment sequence.
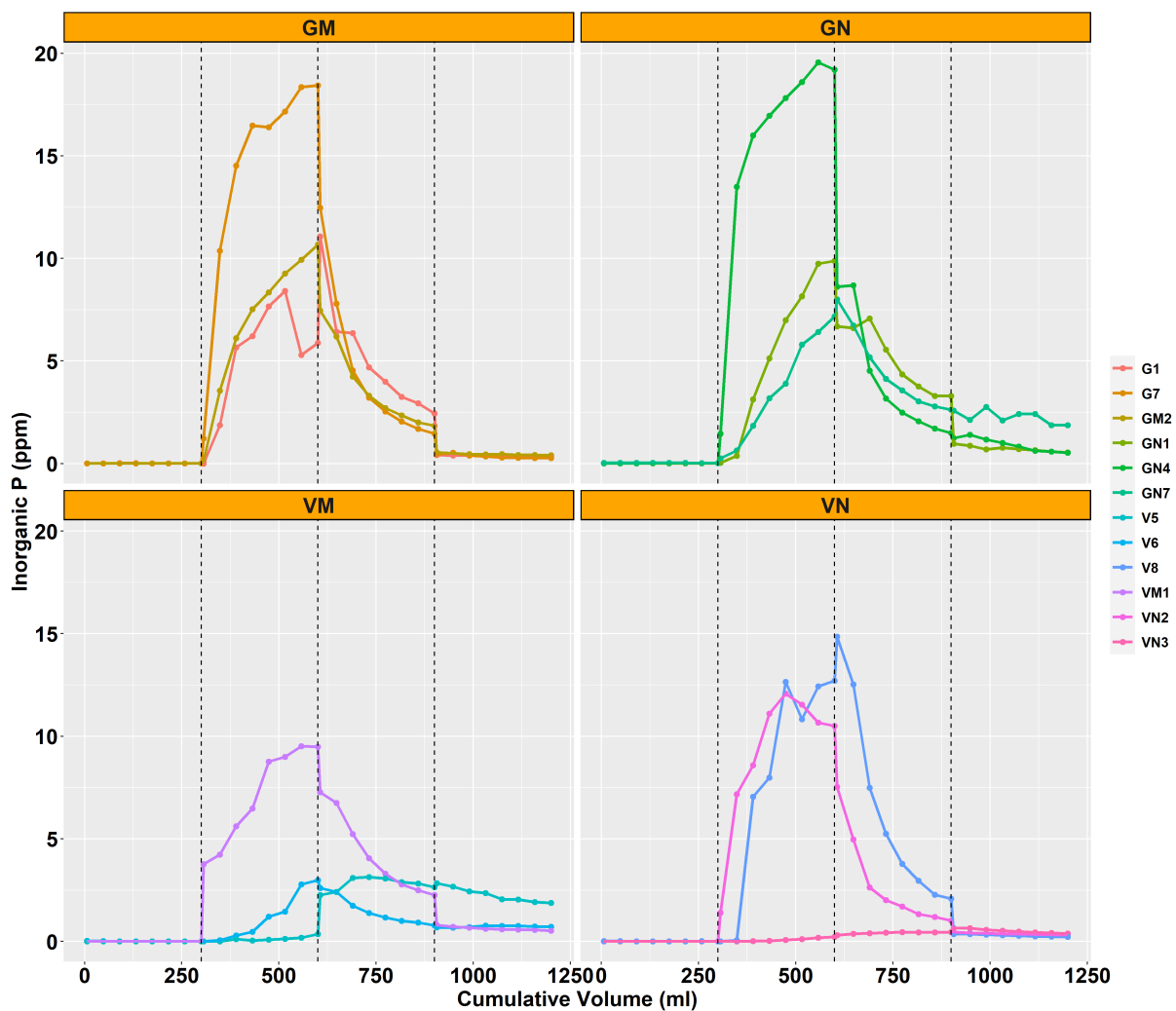
Figure 6.10: Dissolved inorganic phosphorus concentrations (ppm) in the leachate of each core lined up sequentially by experiment sequence.
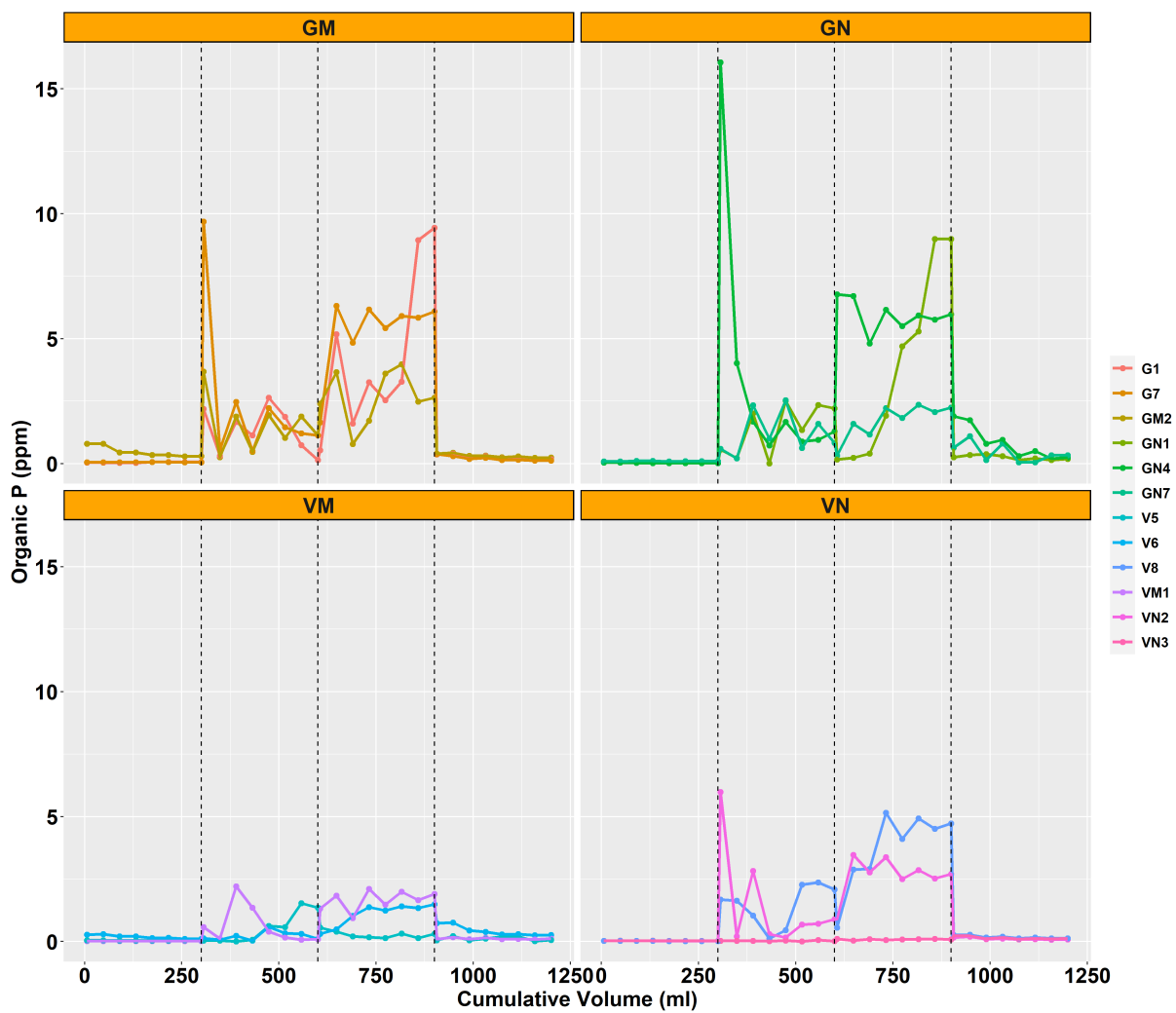
Figure 6.11: Dissolved organic phosphorus concentrations (ppm) in the leachate of each core lined up sequentially by experiment sequence.

Appendix C: Appendix for Chapter 4
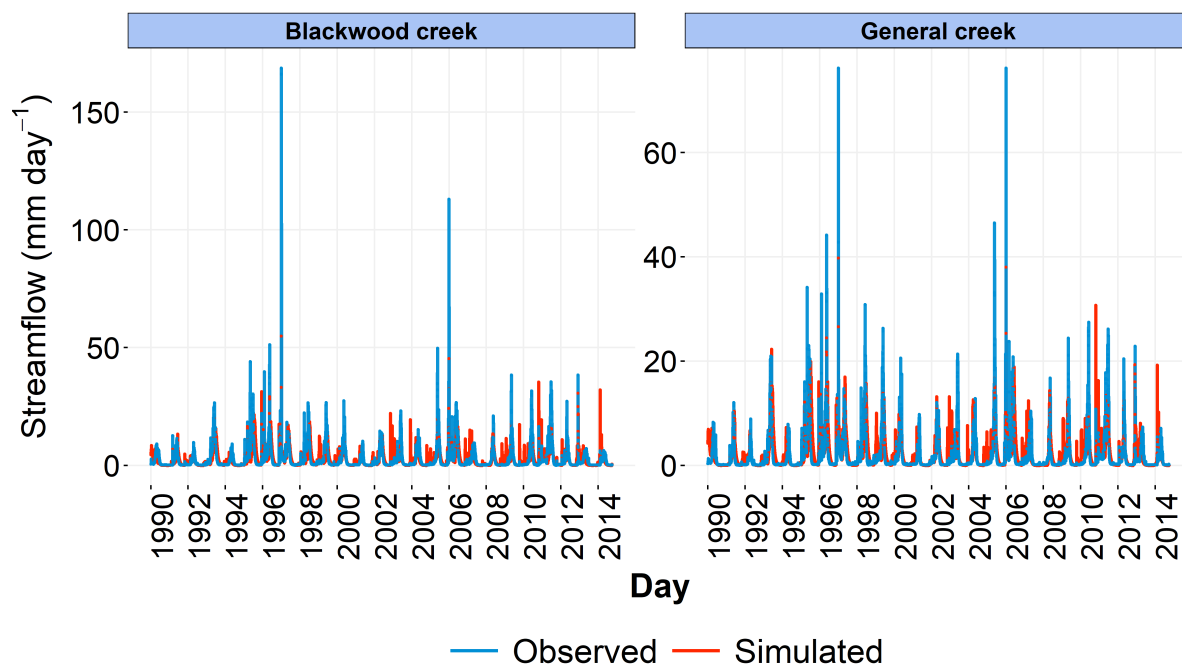
Figure 6.12: Observed and simulated daily streamflow in Blackwood Creek and General Creek watersheds
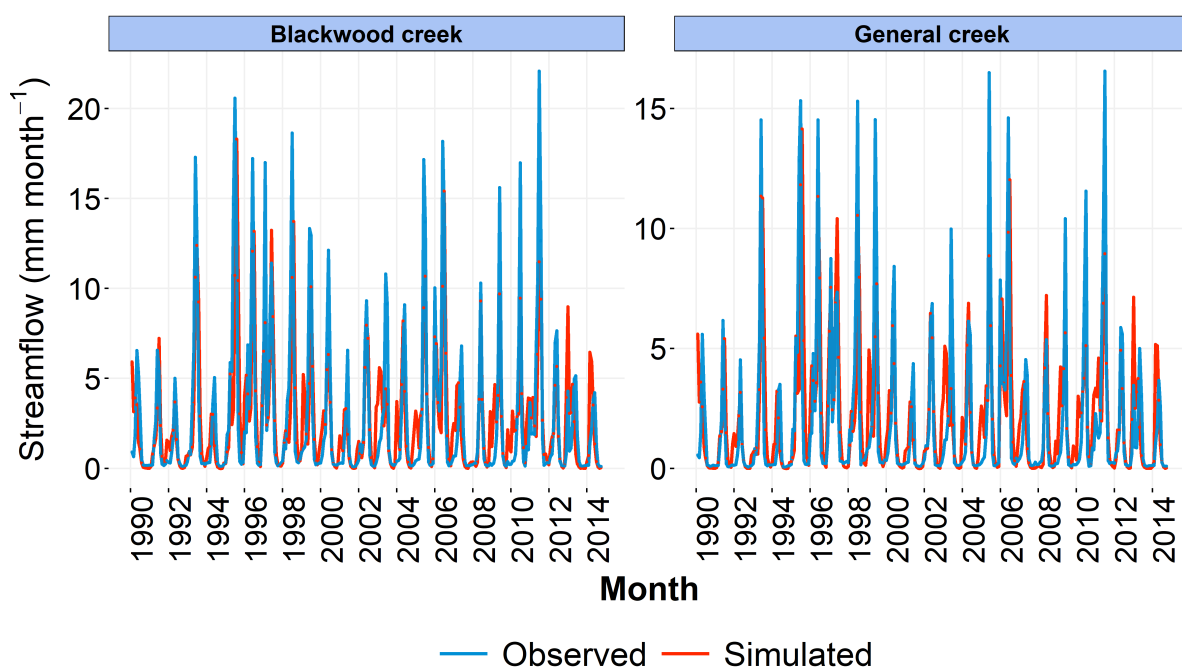
Figure 6.13: Observed and simulated monthly streamflow in Blackwood Creek and General Creek watersheds
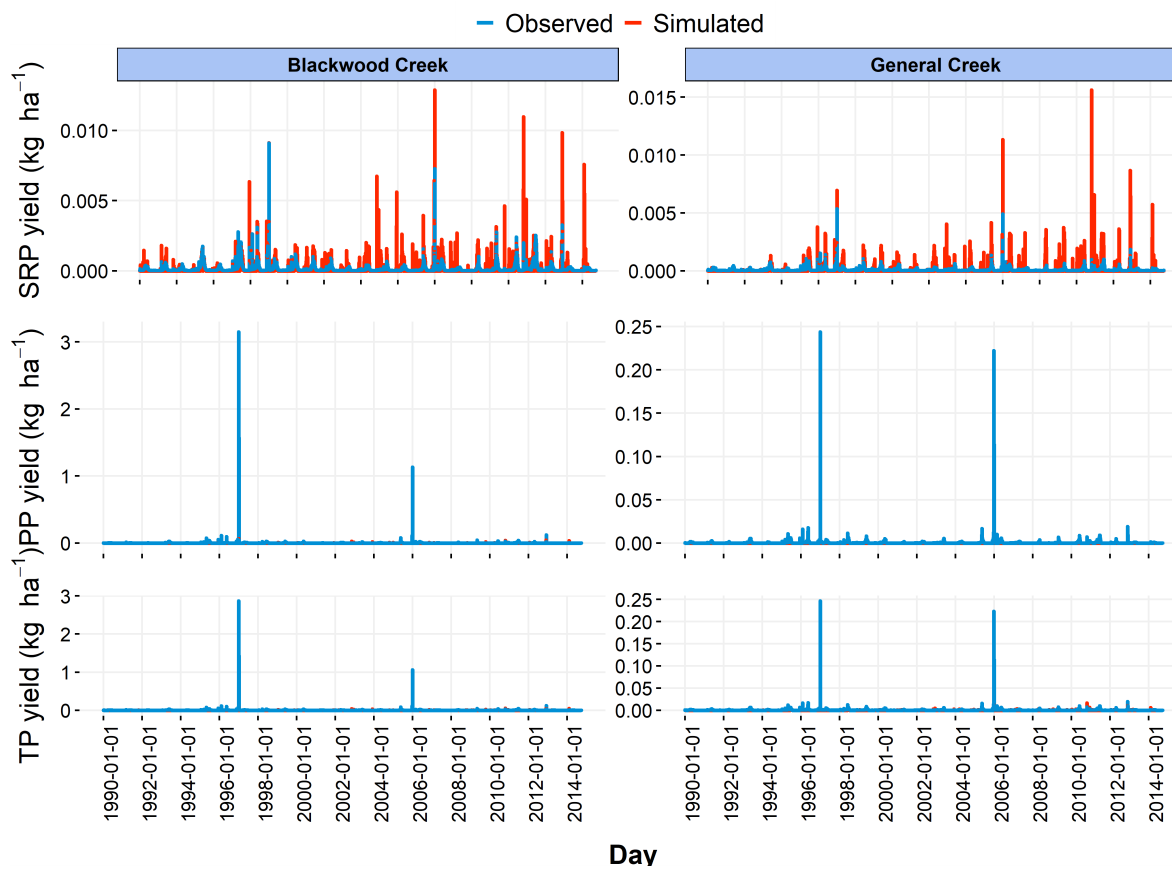
Figure 6.14: Observed and simulated daily P yields in Blackwood Creek and General Creek watersheds
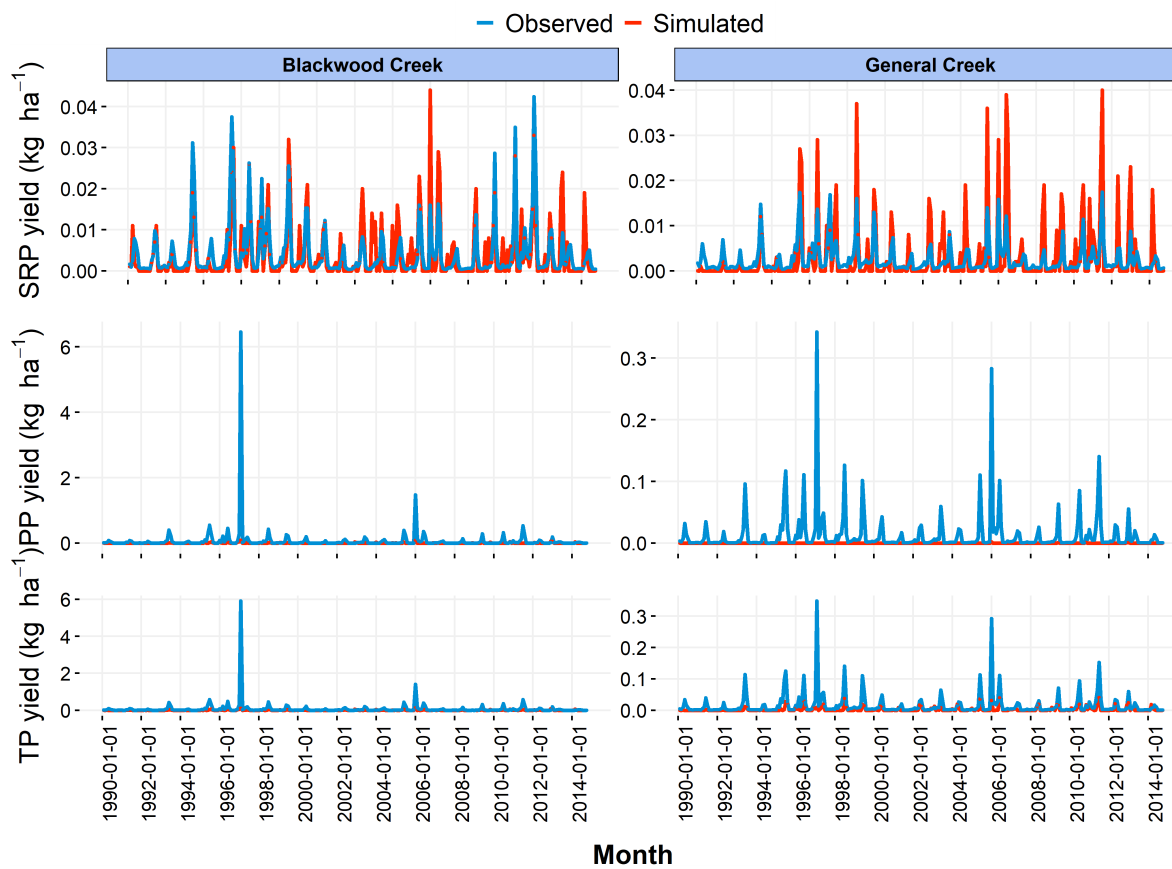
Figure 6.15: Observed and simulated monthly P yields in Blackwood Creek and General Creek watersheds

Appendix D: Appendix for Chapter 5

Table 6.7: Hillslope characteristics along with the baseline sediment yield and the absolute change from the baseline (LowSev minus CurCond) for the top 15 hillslopes with maximum increases in the Blackwood Creek watershed. Negative values of absolute change indicate a net decrease in the sediment yield (kg ha^{-1}) whereas the positive values indicate a net increase in the sediment yield (kg ha^{-1}).

HillslopeID	Landuse	Soil	Slope Steepness (m/m)	Sediment Yield LowSev (kg/ha)	Absolute Change from baseline (kg/ha)
2211	Tahoe Low Severity Fire	Melody-Rock Outcrop complex, 30 to 50 percent slopes (SPM)	0.42	25851	25191
2212	Tahoe Low Severity Fire	Melody-Rock Outcrop complex, 30 to 50 percent slopes (SPM)	0.39	14939	14511
2143	Tahoe Low Severity Fire	Paige medial sandy loam, 30 to 50 percent slopes (SPM)	0.42	10831	10364
2961	Tahoe Low Severity Fire	Melody-Rock outcrop complex, 50 to 70 percent slopes (SPM)	0.47	10371	9917
1351	Tahoe Low Severity Fire	Melody-Rock outcrop complex, 50 to 70 percent slopes (SPM)	0.56	9393	9167
2373	Tahoe Low Severity Fire	Melody-Rock outcrop complex, 50 to 70 percent slopes (SPM)	0.47	8999	8624

Table 6.7 continued from previous page

HillslopeID	Landuse	Soil	Slope Steepness (m/m)	Sediment Yield LowSev (kg/ha)	Absolute Change from baseline (kg/ha)
741	Tahoe Low Severity Fire	Waca very gravelly medial coarse sandy loam, 30 to 50 percent slopes (SPM)	0.5	4206	4079
2391	Tahoe Low Severity Fire	Melody-Rock outcrop complex, 50 to 70 percent slopes (SPM)	0.47	3899	3751
2851	Tahoe Low Severity Fire	Melody-Rock Outcrop complex, 9 to 30 percent slopes (SPM)	0.21	3672	3570
871	Tahoe Low Severity Fire	Ellispeak-Waca complex, 9 to 30 percent slopes (ST-FSL)	0.28	3340	3273
1551	Tahoe Low Severity Fire	Melody-Rock outcrop complex, 50 to 70 percent slopes (SPM)	0.44	3203	3094
1561	Tahoe Low Severity Fire	Ellispeak-Waca complex, 30 to 50 percent slopes (ST-FSL)	0.35	3005	2928
2672	Tahoe Low Severity Fire	Ellispeak-Rock outcrop complex, 9 to 30 percent slopes (ST-FSL)	0.27	2692	2639

Table 6.7 continued from previous page

HillslopeID	Landuse	Soil	Slope Steepness (m/m)	Sediment Yield LowSev (kg/ha)	Absolute Change from baseline (kg/ha)
653	Tahoe Low Severity Fire	Kneeridge gravelly sandy loam, 5 to 15 percent slopes, very stony (SPM)	0.19	2602	2277
3221	Tahoe Low Severity Fire	Ellispeak-Rock outcrop complex, 50 to 70 percent slopes (ST-FSL)	0.48	2336	2237
2131	Tahoe Low Severity Fire	Sky-Melody complex, 30 to 50 percent slopes (SPM)	0.36	2145	2003
1821	Tahoe Low Severity Fire	Sky gravelly sandy loam, 30 to 50 percent slopes (SPM)	0.36	2005	1862
2082	Tahoe Low Severity Fire	Waca very gravelly medial coarse sandy loam, 9 to 30 percent slopes (SPM)	0.41	1934	1830
1191	Tahoe Low Severity Fire	Sky-Melody complex, 30 to 50 percent slopes (SPM)	0.44	1905	1827

Table 6.7 continued from previous page

HillslopeID	Landuse	Soil	Slope Steepness (m/m)	Sediment Yield LowSev (kg/ha)	Absolute Change from baseline (kg/ha)
641	Tahoe Low Severity Fire	Waca very gravelly medial coarse sandy loam, 9 to 30 percent slopes (SPM)	0.35	1787	1738
2571	Tahoe Low Severity Fire	Waca very gravelly medial coarse sandy loam, 9 to 30 percent slopes (SPM)	0.3	1694	1639
3311	Tahoe Low Severity Fire	Ellispeak-Rock outcrop complex, 50 to 70 percent slopes (ST-FSL)	0.37	1496	1473
2791	Tahoe Low Severity Fire	Waca very gravelly medial coarse sandy loam, 30 to 50 percent slopes (SPM)	0.4	1551	1396
1421	Tahoe Low Severity Fire	Meiss-Waca-Cryumbrepts, wet complex, 30 to 75 percent slopes (SL)	0.37	1309	1249

Table 6.7 continued from previous page

HillslopeID	Landuse	Soil	Slope Steepness (m/m)	Sediment Yield LowSev (kg/ha)	Absolute Change from baseline (kg/ha)
2142	Tahoe Low Severity Fire	Waca very gravelly medial coarse sandy loam, 30 to 50 percent slopes (SPM)	0.4	1262	1206
1391	Tahoe Low Severity Fire	Rock outcrop, volcanic (BR)	0.42	1126	1117
1942	Tahoe Low Severity Fire	Waca very gravelly medial coarse sandy loam, 30 to 50 percent slopes (SPM)	0.35	1136	1067
1241	Tahoe Low Severity Fire	Sky-Melody Complex, 50 To 70 Percent Slopes (SPM)	0.58	946	895
1451	Tahoe Low Severity Fire	Sky-Melody complex, 30 to 50 percent slopes (SPM)	0.34	864	817
582	Tahoe Low Severity Fire	Waca very gravelly medial coarse sandy loam, 9 to 30 percent slopes (SPM)	0.33	875	794

Table 6.7 continued from previous page

HillslopeID	Landuse	Soil	Slope Steepness (m/m)	Sediment Yield LowSev (kg/ha)	Absolute Change from baseline (kg/ha)
2581	Tahoe Low Severity Fire	Waca very gravelly medial coarse sandy loam, 9 to 30 percent slopes (SPM)	0.29	806	793
931	Tahoe Low Severity Fire	Waca very gravelly medial coarse sandy loam, 30 to 50 percent slopes (SPM)	0.35	790	764
2721	Tahoe Low Severity Fire	Sky gravelly sandy loam, 9 to 30 percent slopes (SPM)	0.48	742	695
3401	Tahoe Low Severity Fire	Ellispeak-Rock outcrop complex, 50 to 70 percent slopes (ST-FSL)	0.48	696	689
1121	Tahoe Low Severity Fire	Waca very gravelly medial coarse sandy loam, 9 to 30 percent slopes (SPM)	0.35	690	668

Table 6.8: Hillslope characteristics along with the baseline sediment yield and the absolute change from the baseline (CT minus NT) for the top 15 hillslopes with maximum change in the Kamiache Creek watershed. Negative values of absolute change indicate a net decrease in the sediment yield (kg ha^{-1}) whereas the positive values indicate a net increase in the sediment yield (kg ha^{-1}).

Hillslope	Land use Description	Soil Description	Slope Steepness (m/m)	Sediment Yield Conventional till (kg/ha)	Absolute Change from baseline (kg/ha)
23	Barley Fallow Int Precip NT 1	Chard silt loam, 15 to 25 percent slopes (SIL)	0.17	101.4	4.08
63	Barley Fallow Int Precip NT 1	Chard silt loam, 15 to 25 percent slopes (SIL)	0.18	54.83	1.78
352	Barley Fallow Int Precip NT 1	Chard silt loam, 15 to 25 percent slopes (SIL)	0.1	18.08	1.23
62	Barley Fallow Int Precip NT 1	Chard silt loam, 15 to 25 percent slopes (SIL)	0.1	26	0.59
322	Barley Fallow Int Precip NT 1	Chard silt loam, 15 to 25 percent slopes (SIL)	0.15	14.52	0.24
1802	Barley Fallow Int Precip NT 1	Calouse silt loam, 7 to 25 percent slopes (SIL)	0.12	12.05	-0.31

Table 6.8 continued from previous page

Hillslope	Land use Description	Soil Description	Slope Steepness (m/m)	Sediment Yield Conventional till (kg/ha)	Absolute Change from baseline (kg/ha)
2222	Barley Fallow Int Precip NT 1	Athena silt loam, 7 to 25 percent slopes (SIL)	0.11	25.45	-0.4
3671	Barley Fallow Int Precip NT 1	Athena silt loam, 7 to 25 percent slopes (SIL)	0.12	9	-0.66
932	Barley Fallow Int Precip NT 1	Athena silt loam, 7 to 25 percent slopes (SIL)	0.14	30.86	-0.71
3602	Barley Fallow Int Precip NT 1	Athena silt loam, 7 to 25 percent slopes (SIL)	0.12	21.39	-0.72
643	Barley Fallow Int Precip NT 1	Athena silt loam, 7 to 25 percent slopes (SIL)	0.1	14.32	-0.86
1283	Barley Fallow Int Precip NT 1	Athena silt loam, 7 to 25 percent slopes (SIL)	0.11	17.7	-0.9
683	Barley Fallow Int Precip NT 1	Athena silt loam, 7 to 25 percent slopes (SIL)	0.1	29.19	-0.91

Table 6.8 continued from previous page

Hillslope	Land use Description	Soil Description	Slope Steepness (m/m)	Sediment Yield Conventional till (kg/ha)	Absolute Change from baseline (kg/ha)
992	Barley Fallow Int Precip NT 1	Athena silt loam, 7 to 25 percent slopes (SIL)	0.14	6.29	-0.93
3672	Barley Fallow Int Precip NT 1	Athena silt loam, 7 to 25 percent slopes (SIL)	0.16	24.09	-1.15
72	Barley Fallow Int Precip NT 1	Athena silt loam, 0 to 8 percent slopes (SIL)	0.13	75.79	-1.19
433	Barley Fallow Int Precip NT 1	Athena silt loam, 7 to 25 percent slopes (SIL)	0.13	25	-1.22
1792	Barley Fallow Int Precip NT 1	Athena silt loam, 7 to 25 percent slopes (SIL)	0.15	17.18	-1.23
3702	Barley Fallow Int Precip NT 1	Athena silt loam, 25 to 40 percent slopes (SIL)	0.12	18.67	-1.32
152	Barley Fallow Int Precip NT 1	Athena silt loam, 7 to 25 percent slopes (SIL)	0.2	7.86	-1.39

Table 6.8 continued from previous page

Hillslope	Land use Description	Soil Description	Slope Steepness (m/m)	Sediment Yield Conventional till (kg/ha)	Absolute Change from baseline (kg/ha)
141	Barley Fallow Int Precip NT 1	Athena silt loam, 7 to 25 percent slopes (SIL)	0.15	49.35	-1.4
682	Barley Fallow Int Precip NT 1	Athena silt loam, 7 to 25 percent slopes (SIL)	0.1	62.08	-1.42
3701	Barley Fallow Int Precip NT 1	Athena silt loam, 25 to 40 percent slopes (SIL)	0.14	47.26	-1.48
192	Barley Fallow Int Precip NT 1	Athena silt loam, 7 to 25 percent slopes (SIL)	0.15	27.05	-1.49
1672	Barley Fallow Int Precip NT 1	Athena silt loam, 7 to 25 percent slopes (SIL)	0.15	7.25	-1.52
3611	Barley Fallow Int Precip NT 1	Athena silt loam, 7 to 25 percent slopes (SIL)	0.15	70.11	-1.54
653	Barley Fallow Int Precip NT 1	Athena silt loam, 7 to 25 percent slopes (SIL)	0.12	79.18	-1.55

Table 6.8 continued from previous page

Hillslope	Land use Description	Soil Description	Slope Steepness (m/m)	Sediment Yield Conventional till (kg/ha)	Absolute Change from baseline (kg/ha)
3641	Barley Fallow Int Precip NT 1	Athena silt loam, 7 to 25 percent slopes (SIL)	0.14	98.38	-1.56
162	Barley Fallow Int Precip NT 1	Athena silt loam, 7 to 25 percent slopes (SIL)	0.13	27.88	-1.61
3601	Barley Fallow Int Precip NT 1	Athena silt loam, 7 to 25 percent slopes (SIL)	0.18	104.34	-1.66
2223	Barley Fallow Int Precip NT 1	Athena silt loam, 7 to 25 percent slopes (SIL)	0.12	6.78	-1.67
3743	Barley Fallow Int Precip NT 1	Athena silt loam, 25 to 40 percent slopes (SIL)	0.18	38.89	-1.95
3731	Barley Fallow Int Precip NT 1	Athena silt loam, 25 to 40 percent slopes (SIL)	0.14	82.52	-2.07
201	Barley Fallow Int Precip NT 1	Athena silt loam, 7 to 25 percent slopes (SIL)	0.12	5.8	-2.28

Table 6.8 continued from previous page

Hillslope	Land use Description	Soil Description	Slope Steepness (m/m)	Sediment Yield Conventional till (kg/ha)	Absolute Change from baseline (kg/ha)
2263	Barley Fallow Int Precip NT 1	Athena silt loam, 7 to 25 percent slopes (SIL)	0.13	18.47	-2.35
2193	Barley Fallow Int Precip NT 1	Athena silt loam, 7 to 25 percent slopes (SIL)	0.19	19.82	-3
101	Barley Fallow Int Precip NT 1	Athena silt loam, 7 to 25 percent slopes (SIL)	0.15	193.06	-7.12
923	Barley Fallow Int Precip NT 1	Athena silt loam, 7 to 25 percent slopes (SIL)	0.1	11.15	-15.8
1641	Barley Fallow Int Precip NT 1	Athena silt loam, 7 to 25 percent slopes (SIL)	0.13	12.64	-18.8
3391	Barley Fallow Int Precip NT 1	Athena silt loam, 7 to 25 percent slopes (SIL)	0.13	51.82	-32.17
1653	Barley Fallow Int Precip NT 1	Athena silt loam, 7 to 25 percent slopes (SIL)	0.09	8.34	-36.09

Table 6.8 continued from previous page

Hillslope	Land use Description	Soil Description	Slope Steepness (m/m)	Sediment Yield Conventional till (kg/ha)	Absolute Change from baseline (kg/ha)
1623	Barley Fallow Int Precip NT 1	Athena silt loam, 7 to 25 percent slopes (SIL)	0.1	34.64	-51.8
3441	Barley Fallow Int Precip NT 1	Athena silt loam, 7 to 25 percent slopes (SIL)	0.17	40.74	-93.74
92	Barley Fallow Int Precip NT 1	Athena silt loam, 7 to 25 percent slopes (SIL)	0.15	138.27	-103.45
3431	Barley Fallow Int Precip NT 1	Athena silt loam, 7 to 25 percent slopes (SIL)	0.17	61.16	-186.98

Table 6.9: Change in organic phosphorus transport from an alternative or comparison management option/scenario relative to a baseline scenario along and the corresponding land use, soil type, and slope descriptions

HRU	LULC	SUBBASIN	LU_CODE	SOIL CODE	MEAN SLOPE (%)	AREA	Organic Phosphorus business-as-usual (kg ha^{-1})	Absolute Change from baseline (kg ha^{-1})
30012	CSIL	3	AAKE	11000.2TI02A0Bd22-2bc	19.72	0.04	0.05	-0.02
30011	CSIL	3	AAKE	11000.1TI01A0Bd22-2bc	20.14	0.03	0.03	-0.02
30036	CSIL	3	AAKN	11000.1TI01A0Bd22-2bc	18.34	0.05	0.03	-0.02
30010	CSIL	3	AAKD	11001.0TI10A0Bd22-2bc	6.52	0.26	0.02	-0.02
30002	CSIL	3	AAKD	11000.2TI02A0Bd22-2bc	9.28	0.06	0	-0.02
30017	CSIL	3	AAKE	11000.7TI07A0Bd22-2bc	10.84	0.06	0	-0.02
30026	CSIL	3	AAKF	11000.7TI07A0Bd22-2bc	8.81	0.13	0	-0.02
30033	CSIL	3	AAKG	11000.5TI05A0Bd22-2bc	8.56	0.07	0	-0.02
30040	CSIL	3	AAKN	11000.6TI06A0Bd22-2bc	10.2	0.03	0	-0.02
30047	CSIL	3	AAKQ	11000.6TI06A0Bd22-2bc	10.5	0.03	0	-0.02
30072	CSIL	3	AADX	11000.1TI01A0Bd22-2bc	16.97	0.08	0	-0.02
30015	CSIL	3	AAKE	11000.5TI05A0Bd22-2bc	15.63	0.08	0.1	-0.01
30038	CSIL	3	AAKN	11000.3TI03A0Bd22-2bc	18.58	0.02	0.1	-0.01
30039	CSIL	3	AAKN	11000.4TI04A0Bd22-2bc	13.67	0.03	0.1	-0.01

Table 6.9 continued from previous page

HRU	LULC	SUBBASIN	LU_CODE	SOIL CODE	MEAN SLOPE (%)	AREA	Organic Phosphorus business-as-usual (kg ha⁻¹)	Absolute Change from baseline (kg ha⁻¹)
30014	CSIL	3	AAKE	11000.4TI04A0Bd22-2bc	14.04	0.03	0.08	-0.01
30016	CSIL	3	AAKE	11000.6TI06A0Bd22-2bc	12.92	0.02	0.08	-0.01
30045	CSIL	3	AAKQ	11000.2TI02A0Bd22-2bc	9.14	0.02	0.08	-0.01
30046	CSIL	3	AAKQ	11000.3TI03A0Bd22-2bc	17.48	0.02	0.08	-0.01
30053	CSIL	3	AAKR	11000.5TI05A0Bd22-2bc	10.36	0.07	0.08	-0.01
30023	CSIL	3	AAKF	11000.4TI04A0Bd22-2bc	15.65	0.01	0.07	-0.01
30025	CSIL	3	AAKF	11000.6TI06A0Bd22-2bc	11.12	0.08	0.07	-0.01
30054	CSIL	3	AAKR	11000.6TI06A0Bd22-2bc	10.11	0.15	0.07	-0.01
30005	CSIL	3	AAKD	11000.5TI05A0Bd22-2bc	7.87	0.03	0.06	-0.01
30013	CSIL	3	AAKE	11000.3TI03A0Bd22-2bc	17.85	0.05	0.06	-0.01
30037	CSIL	3	AAKN	11000.2TI02A0Bd22-2bc	7.68	0.01	0.06	-0.01
30044	CSIL	3	AAKQ	11000.1TI01A0Bd22-2bc	18.13	0.07	0.06	-0.01
30052	CSIL	3	AAKR	11000.4TI04A0Bd22-2bc	9.84	0.02	0.06	-0.01
30004	CSIL	3	AAKD	11000.4TI04A0Bd22-2bc	9.39	0.03	0.04	-0.01
30021	CSIL	3	AAKF	11000.2TI02A0Bd22-2bc	9.34	0.06	0.04	-0.01

Table 6.9 continued from previous page

HRU	LULC	SUBBASIN	LU_CODE	SOIL CODE	MEAN SLOPE (%)	AREA	Organic Phosphorus business-as-usual (kg ha⁻¹)	Absolute Change from baseline (kg ha⁻¹)
30022	CSIL	3	AAKF	11000.3TI03A0Bd22-2bc	8.16	0.05	0.04	-0.01
30051	CSIL	3	AAKR	11000.3TI03A0Bd22-2bc	11.37	0.02	0.04	-0.01
30078	CSIL	3	AADX	11000.7TI07A0Bd22-2bc	10.03	0.06	0.04	-0.01
30020	CSIL	3	AAKF	11000.1TI01A0Bd22-2bc	16.67	0.04	0.03	-0.01
30024	CSIL	3	AAKF	11000.5TI05A0Bd22-2bc	19.24	0.02	0.03	-0.01
30043	CSIL	3	AAKN	11000.9TI09A0Bd22-2bc	11.87	0.02	0.03	-0.01
30077	CSIL	3	AADX	11000.6TI06A0Bd22-2bc	6.54	0.15	0.03	-0.01
30003	CSIL	3	AAKD	11000.3TI03A0Bd22-2bc	5.06	0.03	0.02	-0.01
30030	CSIL	3	AAKG	11000.2TI02A0Bd22-2bc	11.87	0.04	0.02	-0.01
30031	CSIL	3	AAKG	11000.3TI03A0Bd22-2bc	14.38	0.09	0.02	-0.01
30050	CSIL	3	AAKR	11000.1TI01A0Bd22-2bc	16.42	0.08	0.02	-0.01
30076	CSIL	3	AADX	11000.5TI05A0Bd22-2bc	7.75	0.06	0.02	-0.01
30019	CSIL	3	AAKE	11000.9TI09A0Bd22-2bc	10.73	0.09	0.01	-0.01
30028	CSIL	3	AAKF	11000.9TI09A0Bd22-2bc	8.9	0.02	0.01	-0.01
30029	CSIL	3	AAKG	11000.1TI01A0Bd22-2bc	21.76	0.21	0.01	-0.01

Table 6.9 continued from previous page

HRU	LULC	SUBBASIN	LU_CODE	SOIL CODE	MEAN SLOPE (%)	AREA	Organic Phosphorus business-as-usual (kg ha^{-1})	Absolute Change from baseline (kg ha^{-1})
30035	CSIL	3	AAKG	11000.7TI07A0Bd22-2bc	7.27	0.02	0.01	-0.01
30042	CSIL	3	AAKN	11000.8TI08A0Bd22-2bc	10.18	0.21	0.01	-0.01
30049	CSIL	3	AAKQ	11000.8TI08A0Bd22-2bc	10.59	0.13	0.01	-0.01
30074	CSIL	3	AADX	11000.3TI03A0Bd22-2bc	7.51	0.08	0.01	-0.01
30075	CSIL	3	AADX	11000.4TI04A0Bd22-2bc	8.2	0.05	0.01	-0.01
30001	CSIL	3	AAKD	11000.1TI01A0Bd22-2bc	18.13	0.04	0	-0.01
30008	CSIL	3	AAKD	11000.8TI08A0Bd22-2bc	10.39	0.07	0	-0.01
30009	CSIL	3	AAKD	11000.9TI09A0Bd22-2bc	8.02	0.06	0	-0.01
30018	CSIL	3	AAKE	11000.8TI08A0Bd22-2bc	12.81	0.1	0	-0.01
30027	CSIL	3	AAKF	11000.8TI08A0Bd22-2bc	9.02	0.06	0	-0.01
30034	CSIL	3	AAKG	11000.6TI06A0Bd22-2bc	8.17	0.05	0	-0.01
30041	CSIL	3	AAKN	11000.7TI07A0Bd22-2bc	9.95	0.08	0	-0.01
30048	CSIL	3	AAKQ	11000.7TI07A0Bd22-2bc	9.28	0.2	0	-0.01
30079	CSIL	3	AADX	11000.8TI08A0Bd22-2bc	7.48	0.01	0	-0.01
30081	CSIL	3	AANT	11000.2TI02A0Bd22-2bc	17.68	0.01	0	-0.01

Table 6.9 continued from previous page

HRU	LULC	SUBBASIN	LU_CODE	SOIL CODE	MEAN SLOPE (%)	AREA	Organic Phosphorus business-as-usual (kg ha⁻¹)	Absolute Change from baseline (kg ha⁻¹)
30006	CSIL	3	AAKD	11000.6TI06A0Bd22-2bc	8.49	0.02	0.06	0
30007	CSIL	3	AAKD	11000.7TI07A0Bd22-2bc	8.65	0.06	0.03	0
30032	CSIL	3	AAKG	11000.4TI04A0Bd22-2bc	13.14	0.03	0.03	0
30073	CSIL	3	AADX	11000.2TI02A0Bd22-2bc	15.23	0.12	0	0
30080	CSIL	3	AANT	11000.1TI01A0Bd22-2bc	13.69	0.02	0	0

Table 6.10: Change in sediment phosphorus transport from an alternative or comparison management option/scenario relative to a baseline scenario along and the corresponding land use, soil type, and slope descriptions

HRU	LULC	SUB BASIN	LU CODE	SOIL CODE	MEAN SLOPE (%)	AREA	Sediment Phosphorus business-as-usual (kg ha-1)	Absolute Change from baseline (kg ha-1)
30038	CSIL	3	AAKN	11000. 3TI03A0Bd22-2bc	18.58	0.02	1.26	-0.73
30015	CSIL	3	AAKE	11000. 5TI05A0Bd22-2bc	15.63	0.08	1.32	-0.68
30039	CSIL	3	AAKN	11000. 4TI04A0Bd22-2bc	13.67	0.03	1.21	-0.62
30053	CSIL	3	AAKR	11000. 5TI05A0Bd22-2bc	10.36	0.07	1.01	-0.61
30045	CSIL	3	AAKQ	11000. 2TI02A0Bd22-2bc	9.14	0.02	0.99	-0.58
30014	CSIL	3	AAKE	11000. 4TI04A0Bd22-2bc	14.04	0.03	0.99	-0.57

Table 6.10 continued from previous page

HRU	LULC	SUB BASIN	LU CODE	SOIL CODE	MEAN SLOPE (%)	AREA	Sediment Phosphorus business-as-usual (kg ha-1)	Absolute Change from baseline (kg ha-1)
30046	CSIL	3	AAKQ	11000. 3TI03A0Bd22-2bc	17.48	0.02	1.02	-0.54
30013	CSIL	3	AAKE	11000. 3TI03A0Bd22-2bc	17.85	0.05	0.77	-0.53
30052	CSIL	3	AAKR	11000. 4TI04A0Bd22-2bc	9.84	0.02	0.75	-0.52
30037	CSIL	3	AAKN	11000. 2TI02A0Bd22-2bc	7.68	0.01	0.72	-0.51
30012	CSIL	3	AAKE	11000. 2TI02A0Bd22-2bc	19.72	0.04	0.59	-0.51
30025	CSIL	3	AAKF	11000. 6TI06A0Bd22-2bc	11.12	0.08	0.95	-0.49
30054	CSIL	3	AAKR	11000. 6TI06A0Bd22-2bc	10.11	0.15	0.92	-0.49

Table 6.10 continued from previous page

HRU	LULC	SUB BASIN	LU CODE	SOIL CODE	MEAN SLOPE (%)	AREA	Sediment Phosphorus business-as-usual (kg ha-1)	Absolute Change from baseline (kg ha-1)
30023	CSIL	3	AAKF	11000. 4TI04A0Bd22-2bc	15.65	0.01	0.82	-0.49
30044	CSIL	3	AAKQ	11000. 1TI01A0Bd22-2bc	18.13	0.07	0.69	-0.48
30016	CSIL	3	AAKE	11000. 6TI06A0Bd22-2bc	12.92	0.02	1.02	-0.47
30021	CSIL	3	AAKF	11000. 2TI02A0Bd22-2bc	9.34	0.06	0.5	-0.42
30051	CSIL	3	AAKR	11000. 3TI03A0Bd22-2bc	11.37	0.02	0.47	-0.41
30036	CSIL	3	AAKN	11000. 1TI01A0Bd22-2bc	18.34	0.05	0.36	-0.4
30010	CSIL	3	AAKD	11001. 0TI10A0Bd22-2bc	6.52	0.26	0.23	-0.4

Table 6.10 continued from previous page

HRU	LULC	SUB BASIN	LU CODE	SOIL CODE	MEAN SLOPE (%)	AREA	Sediment Phosphorus business-as-usual (kg ha-1)	Absolute Change from baseline (kg ha-1)
30040	CSIL	3	AAKN	11000. 6TI06A0Bd22-2bc	10.2	0.03	0.07	-0.4
30047	CSIL	3	AAKQ	11000. 6TI06A0Bd22-2bc	10.5	0.03	0.07	-0.38
30011	CSIL	3	AAKE	11000. 1TI01A0Bd22-2bc	20.14	0.03	0.32	-0.37
30005	CSIL	3	AAKD	11000. 5TI05A0Bd22-2bc	7.87	0.03	0.71	-0.36
30020	CSIL	3	AAKF	11000. 1TI01A0Bd22-2bc	16.67	0.04	0.32	-0.36
30033	CSIL	3	AAKG	11000. 5TI05A0Bd22-2bc	8.56	0.07	0.06	-0.36
30006	CSIL	3	AAKD	11000. 6TI06A0Bd22-2bc	8.49	0.02	0.77	-0.35

Table 6.10 continued from previous page

HRU	LULC	SUB BASIN	LU CODE	SOIL CODE	MEAN SLOPE (%)	AREA	Sediment Phosphorus business-as-usual (kg ha-1)	Absolute Change from baseline (kg ha-1)
30022	CSIL	3	AAKF	11000. 3TI03A0Bd22-2bc	8.16	0.05	0.49	-0.34
30017	CSIL	3	AAKE	11000. 7TI07A0Bd22-2bc	10.84	0.06	0.06	-0.34
30026	CSIL	3	AAKF	11000. 7TI07A0Bd22-2bc	8.81	0.13	0.06	-0.34
30050	CSIL	3	AAKR	11000. 1TI01A0Bd22-2bc	16.42	0.08	0.3	-0.33
30072	CSIL	3	AADX	11000. 1TI01A0Bd22-2bc	16.97	0.08	0.06	-0.33
30078	CSIL	3	AADX	11000. 7TI07A0Bd22-2bc	10.03	0.06	0.47	-0.3
30004	CSIL	3	AAKD	11000. 4TI04A0Bd22-2bc	9.39	0.03	0.47	-0.29

Table 6.10 continued from previous page

HRU	LULC	SUB BASIN	LU CODE	SOIL CODE	MEAN SLOPE (%)	AREA	Sediment Phosphorus business-as-usual (kg ha-1)	Absolute Change from baseline (kg ha-1)
30043	CSIL	3	AAKN	11000. 9TI09A0Bd22-2bc	11.87	0.02	0.33	-0.29
30019	CSIL	3	AAKE	11000. 9TI09A0Bd22-2bc	10.73	0.09	0.18	-0.29
30002	CSIL	3	AAKD	11000. 2TI02A0Bd22-2bc	9.28	0.06	0.05	-0.29
30081	CSIL	3	AANT	11000. 2TI02A0Bd22-2bc	17.68	0.01	0.04	-0.27
30024	CSIL	3	AAKF	11000. 5TI05A0Bd22-2bc	19.24	0.02	0.42	-0.26
30077	CSIL	3	AADX	11000. 6TI06A0Bd22-2bc	6.54	0.15	0.36	-0.26
30009	CSIL	3	AAKD	11000. 9TI09A0Bd22-2bc	8.02	0.06	0.05	-0.26

Table 6.10 continued from previous page

HRU	LULC	SUB BASIN	LU CODE	SOIL CODE	MEAN SLOPE (%)	AREA	Sediment Phosphorus business-as-usual (kg ha-1)	Absolute Change from baseline (kg ha-1)
30076	CSIL	3	AADX	11000. 5TI05A0Bd22-2bc	7.75	0.06	0.27	-0.23
30028	CSIL	3	AAKF	11000. 9TI09A0Bd22-2bc	8.9	0.02	0.14	-0.23
30001	CSIL	3	AAKD	11000. 1TI01A0Bd22-2bc	18.13	0.04	0.04	-0.23
30003	CSIL	3	AAKD	11000. 3TI03A0Bd22-2bc	5.06	0.03	0.29	-0.22
30049	CSIL	3	AAKQ	11000. 8TI08A0Bd22-2bc	10.59	0.13	0.13	-0.22
30035	CSIL	3	AAKG	11000. 7TI07A0Bd22-2bc	7.27	0.02	0.12	-0.22
30042	CSIL	3	AAKN	11000. 8TI08A0Bd22-2bc	10.18	0.21	0.17	-0.21

Table 6.10 continued from previous page

HRU	LULC	SUB BASIN	LU CODE	SOIL CODE	MEAN SLOPE (%)	AREA	Sediment Phosphorus business-as-usual (kg ha-1)	Absolute Change from baseline (kg ha-1)
30079	CSIL	3	AADX	11000. 8TI08A0Bd22-2bc	7.48	0.01	0.03	-0.21
30032	CSIL	3	AAKG	11000. 4TI04A0Bd22-2bc	13.14	0.03	0.31	-0.2
30008	CSIL	3	AAKD	11000. 8TI08A0Bd22-2bc	10.39	0.07	0.03	-0.2
30030	CSIL	3	AAKG	11000. 2TI02A0Bd22-2bc	11.87	0.04	0.2	-0.19
30029	CSIL	3	AAKG	11000. 1TI01A0Bd22-2bc	21.76	0.21	0.17	-0.19
30031	CSIL	3	AAKG	11000. 3TI03A0Bd22-2bc	14.38	0.09	0.21	-0.18
30027	CSIL	3	AAKF	11000. 8TI08A0Bd22-2bc	9.02	0.06	0.05	-0.18

Table 6.10 continued from previous page

HRU	LULC	SUB BASIN	LU CODE	SOIL CODE	MEAN SLOPE (%)	AREA	Sediment Phosphorus business-as-usual (kg ha-1)	Absolute Change from baseline (kg ha-1)
30075	CSIL	3	AADX	11000. 4TI04A0Bd22-2bc	8.2	0.05	0.13	-0.15
30048	CSIL	3	AAKQ	11000. 7TI07A0Bd22-2bc	9.28	0.2	0.04	-0.15
30018	CSIL	3	AAKE	11000. 8TI08A0Bd22-2bc	12.81	0.1	0.03	-0.15
30074	CSIL	3	AADX	11000. 3TI03A0Bd22-2bc	7.51	0.08	0.09	-0.14
30034	CSIL	3	AAKG	11000. 6TI06A0Bd22-2bc	8.17	0.05	0.04	-0.14
30007	CSIL	3	AAKD	11000. 7TI07A0Bd22-2bc	8.65	0.06	0.39	-0.12
30041	CSIL	3	AAKN	11000. 7TI07A0Bd22-2bc	9.95	0.08	0.02	-0.1

Table 6.10 continued from previous page

HRU	LULC	SUB BASIN	LU CODE	SOIL CODE	MEAN SLOPE (%)	AREA	Sediment Phosphorus business-as-usual (kg ha-1)	Absolute Change from baseline (kg ha-1)
30073	CSIL	3	AADX	11000. 2TI02A0Bd22-2bc	15.23	0.12	0.02	-0.08
30080	CSIL	3	AANT	11000. 1TI01A0Bd22-2bc	13.69	0.02	0	-0.01

Table 6.11: Change in soluble phosphorus transport from an alternative or comparison management option/scenario relative to a baseline scenario along and the corresponding land use, soil type, and slope descriptions

HRU	LULC	SUBBASIN	LU_CODE	SOIL_CODE	MEAN SLOPE (%)	AREA	Soluble Phosphorus business-as-usual (kg ha⁻¹)	Absolute Change from baseline (kg ha⁻¹)
30080	CSIL	3	AANT	11000.1TI01A0Bd22-2bc	13.69	0.02	4.16	-3.85
30007	CSIL	3	AAKD	11000.7TI07A0Bd22-2bc	8.65	0.06	3.8	-3.63
30006	CSIL	3	AAKD	11000.6TI06A0Bd22-2bc	8.49	0.02	1.99	-2.31
30016	CSIL	3	AAKE	11000.6TI06A0Bd22-2bc	12.92	0.02	1.98	-2.29
30025	CSIL	3	AAKF	11000.6TI06A0Bd22-2bc	11.12	0.08	1.98	-2.29
30046	CSIL	3	AAKQ	11000.3TI03A0Bd22-2bc	17.48	0.02	1.55	-1.92
30024	CSIL	3	AAKF	11000.5TI05A0Bd22-2bc	19.24	0.02	1.64	-1.9
30005	CSIL	3	AAKD	11000.5TI05A0Bd22-2bc	7.87	0.03	1.62	-1.9
30054	CSIL	3	AAKR	11000.6TI06A0Bd22-2bc	10.11	0.15	1.59	-1.89
30039	CSIL	3	AAKN	11000.4TI04A0Bd22-2bc	13.67	0.03	1.57	-1.88
30015	CSIL	3	AAKE	11000.5TI05A0Bd22-2bc	15.63	0.08	1.56	-1.88
30078	CSIL	3	AADX	11000.7TI07A0Bd22-2bc	10.03	0.06	1.22	-1.59
30004	CSIL	3	AAKD	11000.4TI04A0Bd22-2bc	9.39	0.03	1.23	-1.58
30032	CSIL	3	AAKG	11000.4TI04A0Bd22-2bc	13.14	0.03	1.25	-1.57

Table 6.11 continued from previous page

HRU	LULC	SUBBASIN	LU_CODE	SOIL_CODE	MEAN SLOPE (%)	AREA	Soluble Phosphorus business-as-usual (kg ha⁻¹)	Absolute Change from baseline (kg ha⁻¹)
30053	CSIL	3	AAKR	11000.5TI05A0Bd22-2bc	10.36	0.07	1.18	-1.57
30023	CSIL	3	AAKF	11000.4TI04A0Bd22-2bc	15.65	0.01	1.21	-1.56
30045	CSIL	3	AAKQ	11000.2TI02A0Bd22-2bc	9.14	0.02	1.21	-1.54
30038	CSIL	3	AAKN	11000.3TI03A0Bd22-2bc	18.58	0.02	1.21	-1.52
30014	CSIL	3	AAKE	11000.4TI04A0Bd22-2bc	14.04	0.03	1.24	-1.51
30031	CSIL	3	AAKG	11000.3TI03A0Bd22-2bc	14.38	0.09	0.9	-1.27
30077	CSIL	3	AADX	11000.6TI06A0Bd22-2bc	6.54	0.15	0.9	-1.26
30003	CSIL	3	AAKD	11000.3TI03A0Bd22-2bc	5.06	0.03	0.91	-1.25
30022	CSIL	3	AAKF	11000.3TI03A0Bd22-2bc	8.16	0.05	0.9	-1.24
30037	CSIL	3	AAKN	11000.2TI02A0Bd22-2bc	7.68	0.01	0.89	-1.24
30044	CSIL	3	AAKQ	11000.1TI01A0Bd22-2bc	18.13	0.07	0.89	-1.24
30013	CSIL	3	AAKE	11000.3TI03A0Bd22-2bc	17.85	0.05	0.91	-1.22
30052	CSIL	3	AAKR	11000.4TI04A0Bd22-2bc	9.84	0.02	0.9	-1.22
30051	CSIL	3	AAKR	11000.3TI03A0Bd22-2bc	11.37	0.02	0.61	-0.96
30030	CSIL	3	AAKG	11000.2TI02A0Bd22-2bc	11.87	0.04	0.64	-0.95

Table 6.11 continued from previous page

HRU	LULC	SUBBASIN	LU_CODE	SOIL_CODE	MEAN SLOPE (%)	AREA	Soluble Phosphorus business-as-usual (kg ha⁻¹)	Absolute Change from baseline (kg ha⁻¹)
30076	CSIL	3	AADX	11000.5TI05A0Bd22-2bc	7.75	0.06	0.64	-0.95
30043	CSIL	3	AAKN	11000.9TI09A0Bd22-2bc	11.87	0.02	0.63	-0.95
30021	CSIL	3	AAKF	11000.2TI02A0Bd22-2bc	9.34	0.06	0.62	-0.95
30012	CSIL	3	AAKE	11000.2TI02A0Bd22-2bc	19.72	0.04	0.62	-0.93
30075	CSIL	3	AADX	11000.4TI04A0Bd22-2bc	8.2	0.05	0.39	-0.7
30029	CSIL	3	AAKG	11000.1TI01A0Bd22-2bc	21.76	0.21	0.39	-0.69
30042	CSIL	3	AAKN	11000.8TI08A0Bd22-2bc	10.18	0.21	0.39	-0.69
30020	CSIL	3	AAKF	11000.1TI01A0Bd22-2bc	16.67	0.04	0.39	-0.68
30036	CSIL	3	AAKN	11000.1TI01A0Bd22-2bc	18.34	0.05	0.39	-0.68
30050	CSIL	3	AAKR	11000.1TI01A0Bd22-2bc	16.42	0.08	0.39	-0.68
30011	CSIL	3	AAKE	11000.1TI01A0Bd22-2bc	20.14	0.03	0.38	-0.68
30049	CSIL	3	AAKQ	11000.8TI08A0Bd22-2bc	10.59	0.13	0.21	-0.46
30074	CSIL	3	AADX	11000.3TI03A0Bd22-2bc	7.51	0.08	0.21	-0.46
30019	CSIL	3	AAKE	11000.9TI09A0Bd22-2bc	10.73	0.09	0.2	-0.46
30028	CSIL	3	AAKF	11000.9TI09A0Bd22-2bc	8.9	0.02	0.2	-0.46

Table 6.11 continued from previous page

HRU	LULC	SUBBASIN	LU_CODE	SOIL_CODE	MEAN SLOPE (%)	AREA	Soluble Phosphorus business-as-usual (kg ha^{-1})	Absolute Change from baseline (kg ha^{-1})
30035	CSIL	3	AAKG	11000.7TI07A0Bd22-2bc	7.27	0.02	0.2	-0.46
30010	CSIL	3	AAKD	11001.0TI10A0Bd22-2bc	6.52	0.26	0.2	-0.44
30018	CSIL	3	AAKE	11000.8TI08A0Bd22-2bc	12.81	0.1	0.06	-0.26
30027	CSIL	3	AAKF	11000.8TI08A0Bd22-2bc	9.02	0.06	0.06	-0.26
30034	CSIL	3	AAKG	11000.6TI06A0Bd22-2bc	8.17	0.05	0.06	-0.26
30041	CSIL	3	AAKN	11000.7TI07A0Bd22-2bc	9.95	0.08	0.06	-0.26
30048	CSIL	3	AAKQ	11000.7TI07A0Bd22-2bc	9.28	0.2	0.06	-0.26
30073	CSIL	3	AADX	11000.2TI02A0Bd22-2bc	15.23	0.12	0.06	-0.26
30009	CSIL	3	AAKD	11000.9TI09A0Bd22-2bc	8.02	0.06	0.05	-0.24
30079	CSIL	3	AADX	11000.8TI08A0Bd22-2bc	7.48	0.01	0.04	-0.23
30008	CSIL	3	AAKD	11000.8TI08A0Bd22-2bc	10.39	0.07	0.03	-0.19
30001	CSIL	3	AAKD	11000.1TI01A0Bd22-2bc	18.13	0.04	0.03	-0.17
30002	CSIL	3	AAKD	11000.2TI02A0Bd22-2bc	9.28	0.06	0.03	-0.17
30017	CSIL	3	AAKE	11000.7TI07A0Bd22-2bc	10.84	0.06	0.03	-0.17
30026	CSIL	3	AAKF	11000.7TI07A0Bd22-2bc	8.81	0.13	0.03	-0.17

Table 6.11 continued from previous page

HRU	LULC	SUBBASIN	LU_CODE	SOIL_CODE	MEAN SLOPE (%)	AREA	Soluble Phosphorus business-as-usual (kg ha^{-1})	Absolute Change from baseline (kg ha^{-1})
30033	CSIL	3	AAKG	11000.5TI05A0Bd22-2bc	8.56	0.07	0.03	-0.17
30040	CSIL	3	AAKN	11000.6TI06A0Bd22-2bc	10.2	0.03	0.03	-0.17
30047	CSIL	3	AAKQ	11000.6TI06A0Bd22-2bc	10.5	0.03	0.03	-0.17
30072	CSIL	3	AADX	11000.1TI01A0Bd22-2bc	16.97	0.08	0.03	-0.17
30081	CSIL	3	AANT	11000.2TI02A0Bd22-2bc	17.68	0.01	0.03	-0.17